Decision events in the Germinal Centre: the role of ACKR4

LAURA GARCIA-IBANEZ

A thesis submitted to

The University of Birmingham

for the degree of

Doctor of Philosophy

COLLEGE OF MEDICAL AND DENTAL SCIENCES

UNIVERSITY OF BIRMINGHAM

DECEMBER 2016

Abstract

Murine atypical chemokine receptor 4, ACKR4, which binds to chemokines CCL19, CCL21 and CCL25, is expressed specifically in germinal centre (GC) B cells and in a layer of stromal cells surrounding the splenic marginal zone. Although ACKR4 is unable to signal as classical GPCRs, it creates gradients of its ligands.

It is shown here that ACKR4 deficiency in the stroma causes infiltration of naïve B cells into the GC area. ACKR4 deficiency in the B cells causes dysregulation of the intragerminal centre distribution, with enlarged light zones and reduced dark zones when compared to ACKR4-competent mice. This skewed GC distribution is caused by the inability of ACKR4-deficient B cells to downregulate c-Myc, as they receive increased signalling though the CCR7- p-Akt - c-Myc signalling pathway.

Moreover, ACKR4-deficient mice contain elevated numbers of memory B cells (MBC) in the distant lymphoid organs. MBCs are retained in the draining lymph node (drLN) by the presence of a CCL19/21 gradient towards the subcapsular sinus (SCS). When this gradient is absent, as occurs in ACKR4-deficient mice, MBCs escape the drLN easier through the SCS and appear in other sites in elevated numbers.

Together, this shows a new role for ACKR4 in the GC response and in the migration of GC-derived MBCs out of the follicle and the drLN.

Acknowledgements

First, I would like to thank Dr. Kai-Michael Toellner for the opportunity to work in this project, for all his guidance and support during these years. Secondly, I would like to thank all present and past members of the Toellner group, especially Dr. Sarah Cook, Dr. Yang Zhang and Dr. Lingling Zhang for their help, support and useful advice. More importantly, thank you for becoming my friends.

To Dr. Geoffrey Brown, for giving me the opportunity to be part of DECIDE and for valuable advice during these three years. To all the DECIDE crew, for sharing the journey together and for the all the fun. Special thanks to Louise Woodall and Audrey Nganwa for their help.

To Prof. Antal Rot for giving me the opportunity to work in this project and for helpful discussions and advice.

To the fourth floor of the IBR for helpful discussion and help with reagents, guidance, and suggestions. Thank you to BMSU for their assistance. An important mention to all the office group, especially Coral, Claire, Ciaran, Tom, Charlie, Marisol, Ali, Lingling, Anna and Alan, for making me laugh and having good times, I will miss you all. You made the office an enjoyable place to work.

To my family and friends, you know who you are, thank you for being with me all this time despite the distance, with considerate words and encouragement, even when you did not understand me. Thank you for visiting me in rainy England.

Thank you all for making this journey more enjoyable and satisfying, because a thesis is not just this book, it is everything that surrounds it.

Abbreviations

7-AAD	7-amino-actinomycin D
aa	Aminoacid
ACKR	Atypical chemokine receptor
ACKR4	Atypical chemokine receptor 4
AF	Alexa Fluor
Ag	Antigen
AID	Activation-induce cytidine deaminase
AP	Alkaline phosphatase
APC	Allophycocyanin // Antigen-presenting cell
B cell	Bursa of Fabricius cell
BAFF	B cell activating factor
Bcl-6	B cell lymphoma protein 6
BCR	B cell receptor
BEC	Blood endothelial cell
BLAST	Basic local alignment search tool
BM	Bone marrow
b.p.	*Bordetella pertussis*
BrdU	Bromodeoxyuridine
BSA	Bovine serum albumin
Btk	Bruton's tyrosine kinase
BV	Brilliant Violet
CCL19	Chemokine C-C motif ligand 19
CCL21	Chemokine C-C motif ligand 21
CCR7	C-C chemokine receptor 7
CD	Cluster of differentiation
CGG	Chicken gamma globulin
cTEC	Cortical thymic epithelial cell
CSR	Class-switch recombination
CXCL12	C-X-C motif chemokine 12
CXCL13	C-X-C motif chemokine 13
CXCR4	C-X-C chemokine receptor type 4
CXCR5	C-X-C chemokine receptor type 5
Cy5	indotricarbocyanine
DAB	3,3 diaminobenzidine tetrahydrochloride
DLBCL	Diffuse large B cell lymphoma
DC	Dendritic cell
distLN	Distant lymph node
DZ	Dark zone
EBI2	Epstein-Barr virus induced molecule-2
EBV	Epstein-Barr virus
EDTA	Ethylenediaminetetraacetic acid
EdU	5-ethynyl-2′-deoxyuridine
ELISA	Enzyme-linked immunosorbent analysis
eYFP	Enhanced yellow fluorescent protein
FITC	Fluorescein isothiocyanate
FCS	Foetal calf sera
fl	Floxed gene
FRC	Fibroblastic reticular cell
GAG	Glycosaminoglycan
GC	Germinal centre
GFP	Green fluorescent protein
GPCR	G protein–coupled receptor
HEV	High endothelial venule
IFN	Interferon
Ig	Immunoglobulin
IL	Interleukin
i.p.	Intraperitoneal
i.v.	Intravenous
kDa	Kilo Dalton
KO ko	Knock-out
LEC	Lymphatic endothelial cell
LPS	Lipopolysaccharide
LTa	Lymphotoxin alpha
LZ	Light zone
LN	Lymph node
MBC	Memory B cell
MFI	Median fluorescence intensity
MHC	Major histocompatibility complex
mTEC	Medullary thymic epithelial cell
mTmG	Membrane Tomato-membrane GFP
MZ	Marginal zone

NF-κB	Nuclear factor kappa-light-chain-enhancer of activated B cells
NKT	Natural killer cell
NP	4-Hydroxy-3-nitrophenyl acetyl
PALS	Periarteriolar lymphoid sheath
Pax5	Paired box protein 5
PB	Plasmablast
PBS	Phosphate buffer saline
PBMC	Peripheral blood mononuclear cell
PC	Plasma cell
PE	Phycoerythrin
PFA	Paraformaldehyde
pLN	Popliteal lymph node
PTK	Protein tyrosine kinase
QM	Quasi monoclonal
RGS	Regulator of G protein signalling
S1PR2	Sphingosine-1-phosphate receptor 2
SA	Streptavidin
SAP	SLAM-associated protein
s.c.	Subcutaneous
SCS	Subcapsular sinus
SHM	Somatic hypermutation
SLO	Secondary lymphoid organ
SRBC	Sheep red blood cell
Syk	Spleen tyrosine kinase
Tfh	T follicular helper cell
Tfr	T follicular regulatory cell
TI	T cell independent
TM	Transmembrane
UI	Unimmunised
WT wt	Wild type

Table of Contents

List of Figures and Tables

Chapter 1. Introduction

1.1. Overview: The B lymphocyte

The immune system has developed to protect the host against pathogenic microbes and also to eliminate harmful or allergenic substances. There are two players: the innate immune response and the adaptive immune response. The innate immune response constitutes the first and more rapid response from the host. The adaptive immune response follows the innate response and has specificity for the antigens. Antigen-specific receptors are expressed in the surface of B and T lymphocytes.

B cell antigen-specific receptors are encoded by genes that are assembled by somatic rearrangements of germ-line gene elements to form immunoglobulin receptors. B cells are characterised by expression of surface bound immunoglobulins (antibody). In mice, B cells constitute 15% of peripheral leukocytes in blood and home to the peripheral lymphoid organs. In response to antigens, with or without the help of T lymphocytes, antigen-specific B cells undergo clonal expansion and differentiate into other types of B cells such as plasmablasts, plasma cells, germinal centre B cells or memory B cells, depending on the signals they receive.

Germinal centres (GCs) are the hallmark of T-dependent responses and constitute a place where B cell proliferation, hypermutation, class-switch recombination and selection take place. GC B cells can further differentiate into plasma cells, which produce high-affinity antibodies, or memory B cells, which are in charge of maintaining long-term protection.

The signals that cause the post-GC differentiation are far from being fully understood. In this thesis, I aim to elucidate the role of atypical chemokine receptor 4, which is specifically expressed in GC B cells, in this process.

1.2 Secondary lymphoid organs

Secondary lymphoid organs (SLO) include lymph nodes (LN), spleen and Peyer's patches and they are highly organised and compartmentalised structures that facilitate the encounter of cells of the immune system with antigens.

Lymph nodes are subdivided into cortical, paracortical and medullary areas (Malhotra, Fletcher et al. 2013). Each of them is composed of specific areas of the LN lobules surrounded by sinuses, containing motile lymphocytes in search of antigens. This arrangement creates a very effective and efficient venue for antigen surveillance, lymphocyte production, antibody secretion and lymph filtration (Willard-Mack 2006).

The spleen is the largest filter of the blood and is organised as a tree of branching arterial vessels. It is surrounded by a capsule of connective tissue (dense fibrous tissue, elastic fibres and smooth muscle) (Mebius and Kraal 2005). Its interior is divided into red pulp and white pulp. Blood enters the spleen at the hilus *via* the splenic artery which divides into trabecular arteries, central arterioles entering the red pulp and even smaller arterioles in the white pulp (Cesta 2006).

The red pulp filters the blood to remove old erythrocytes and recycle the iron and platelets. In rodents, it is a place for haematopoiesis, especially during the foetal and neonatal stages (Cesta 2006). Antibodies are produced in the red pulp, because plasmablasts (PB) and plasma cells (PC) are situated there. The white pulp is

subdivided into the periarteriolar lymphoid sheath (PALS), the follicles and the marginal zone (MZ). It is composed of lymphocytes, macrophages, dendritic cells (DC), PCs, arterioles and capillaries (Cesta 2006). While the inner PALS around the arterial vessels contains mainly T lymphocytes, stroma and DCs; follicles are populated by the B lymphocyte compartment (Mebius and Kraal 2005).

The recirculation of B and T lymphocytes between blood, SLOs and lymph is crucial for immune vigilance. B and T lymphocytes enter into LNs from the blood through high endothelial venules (HEV) and the spleen *via* the marginal sinus. B and T lymphocytes migrate to particular regions within SLOs as to the chemokine receptors they express and the availability of chemokines within a particular area. B cells migrate to the follicles expressing CXCR5, which binds to CXCL13, produced by $CD35^{+}$ follicular dendritic cells (FDCs) and follicular stroma (Ansel, Ngo et al. 2000). CCL19 and CCL21, produced by stromal cells, attract T cells and DCs through receptor CCR7 to the T zone (Forster, Schubel et al. 1999). Deficiency in CXCR5 and CCR7 leads to absence of peripheral lymph nodes. These mice also present an altered architecture to mesenteric LN and spleen; in particular, B cells fail to migrate into the white pulp and develop as small unorganised lymphocyte clusters rather than in B cell follicles (Ohl, Henning et al. 2003). B cell follicles in the spleen are surrounded by the MZ. The MZ is a transit area and contains particular cells (Mebius and Kraal 2005) like the MZ macrophages and MZ B cells that, although they can move into the follicle, they constitute a unique population. The main function of the MZ is to screen the systemic circulation for antigens and pathogens and it plays an essential part in antigen processing (Cesta 2006). PBs and PCs upregulate the chemokine receptor CXCR4, that binds CXCL12, which is expressed in the red pulp of the spleen and the medullary

cords of the LNs, and downregulate CXCR5 and CCR7, enabling movement into the red pulp and association with the vessels (Hargreaves, Hyman et al. 2001).

If the lymphocytes do not encounter antigenic stimuli, they will leave the SLOs after a characteristic residence time, different for each population. $CD4^+$ T cells have the shortest residence times (4-6h), followed by $CD8^+$ T cells (6-10h), while B cells present a longer residency, of 12-24 h. DC replacement is slower than T and B lymphocytes, at a rate of 30% per day (Tomura, Yoshida et al. 2008).

See Figure 1.1.

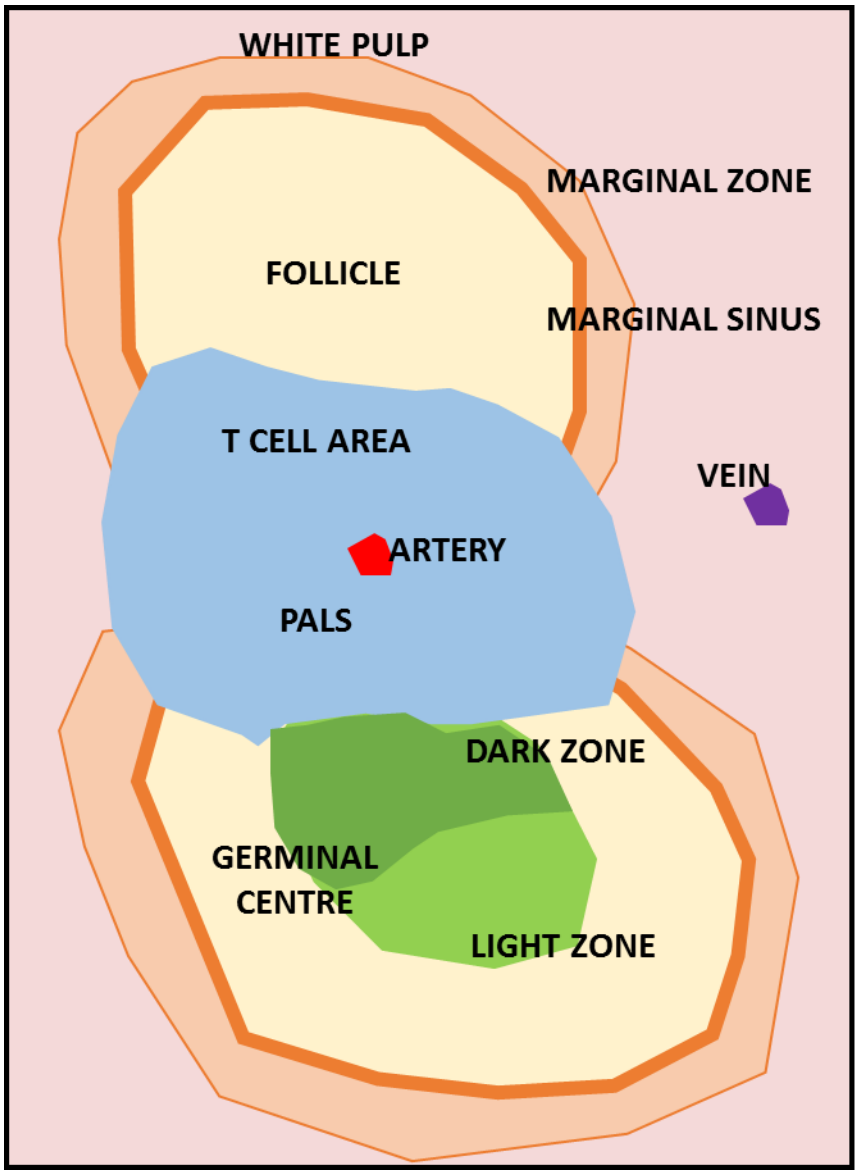

Figure 1.1: The structure of the murine spleen. White pulps are discrete areas within the red pulp in the spleen. In the middle of the white pulp, also known as periarteriolar lymphoid sheath (PALS), there is the central arteriole. Surrounding the arteriole there is a central T cell area with several B cell follicles adjacent to it, Follicles are surrounded by the marginal zone.

1.3 Early B cell development

In the adult, early B cell development takes place in the bone marrow (BM). A number of factors determine commitment to the B cell lineage. Expression of the transcription factor Pax5 is important to B cell development (Nutt, Heavey et al. 1999) and develop through various checkpoints of immunoglobulin (Ig) rearrangements (Rolink, Schaniel et al. 2001) (See Fig. 1.2). Immature B cells express IgM and then migrate to the spleen to undergo further antigen-driven maturation (Cancro and Kearney 2004). Immature B cells travel through different states, named early transitional (T1) and late transitional (T2) and then become either mature follicular or mature marginal zone B cells (Loder, Mutschler et al. 1999). Some of the immature B cells will express an immunoglobulin receptor that recognises self-antigen and there is a need to eliminate these cells. The elimination of autoreactive B cell clones takes place both in the BM and in the periphery by negative selection. Moreover, positive selection, dictated by the strength of signalling *via* the B cell receptor (BCR) mediates B cell survival, maturation, lineage commitment (Cancro and Kearney 2004).

There are 2 types of mature B cells, namely B1 B cells and B2 B cells. B1 B cells are a self-replicating population (Hardy and Hayakawa 2001). They are the dominant population of B cells in the peritoneal cavity, infrequent in the spleen and almost absent in the lymph nodes. B1 B cells express a high level of surface-IgM, low levels of B220 and IgD and do not express CD23 (Fagarasan, Watanabe et al. 2000). B1 B cells can recognise self-antigens and common bacterial antigens and without the help of T cells produce low-affinity antibodies that have a wide ranging specificity (Fagarasan, Watanabe et al. 2000). B1 B cells have been further subdivided in the basis of their expression of CD5. B1a are $CD5^+$ whilst B1b are $CD5^-$.

B2 B cells are recirculating and they express high levels of CD23, B220 and IgD and a low level of IgM. Most of the B2 B cells constitute the follicular B cell population. Follicular B cells home to B cell follicles in SLOs, while marginal zone B cells are sessile, express high levels of CD21 and CD1d and home to the MZ sinus. The decision to become a follicular or a MZ B cell lies on signalling through the BCR, Notch2, BAFF-R, the canonical NF-κB pathway and signals that are involved in migration and anatomical retention (Pillai and Cariappa 2009). In particular, it has also been shown that mice deficient for BAFF and APRIL do not generate marginal zone or follicular B cells, whilst B1 B cells are unaffected (Schneider, Takatsuka et al. 2001). In the spleen, both follicular and marginal zone B cells can respond to T-dependent antigens, while only marginal zone B cells can respond to T-independent antigens (Pillai and Cariappa 2009). However, B2 B cells can respond to T-independent antigens in the bone marrow (Pillai and Cariappa 2009).

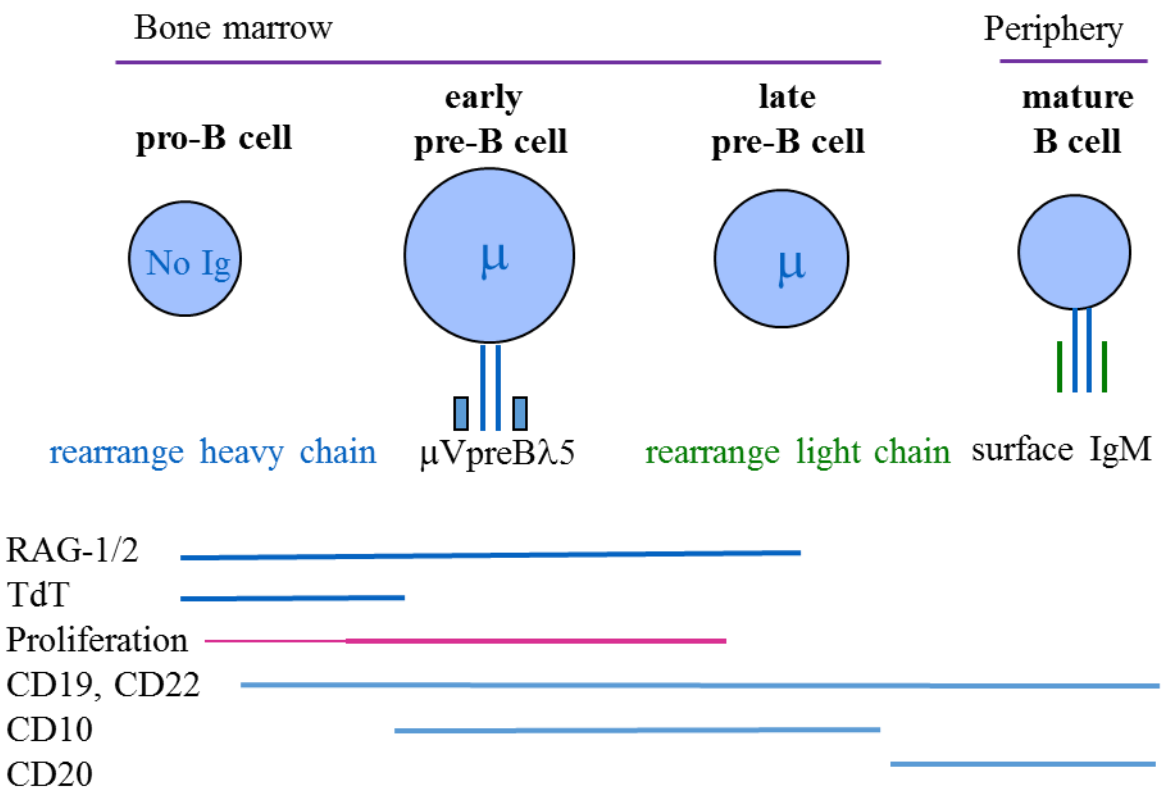

Figure 1.2: **Early B cell development.** B cell development takes place in the bone marrow in adult mice and consist of a series of sequential recombinations at IgH (heavy chain) and IgL (light chain) chain loci to create a diverse repertoire of B cell receptors. Mature B cells migrate to the periphery.

1.4 The types of B cell responses

Very early studies of B cell responses revealed that antigens can be classified as either T-dependent (TD) or T-independent (TI) depending on the nature of the antigen and of the B cell population recruited to the response (Feldmann and Easten 1971, Lewis, Ranken et al. 1976).

1.4.1 Thymus-dependent (TD) responses

TD responses need T cells for full activation and expansion of B cells (Gershon and Kondo 1970). These responses are elicited by protein antigens that are specifically

recognised by the BCR in the presence of cognate T cell help. Once B cells have recognised the antigen, it is processed and presented as peptides on the major histocompatibility complex (MHC) class II molecule to T cells in the B cell follicle-T zone border. Activated B and T cells form stable contacts through the interaction of CD40-CD40L and both these cells secrete cytokines (Noelle and Snow 1990). Immunoglobulin class-switching starts occurring at this point and B cells differentiate into extrafollicular PCs, early MBCs or GC B cells (Smith, Hewitson et al. 1996, Toellner, Gulbranson-Judge et al. 1996, Garside, Ingulli et al. 1998).

1.4.2 Thymus-independent (TI) responses

TI antigens induce antibody production by B cells without the involvement of T cell help. TI antigens are further classified in TI type I (TI-I) or TI type 2 (TI-II) as to whether these responses can occur in mice deficient in the Bruton's tyrosine kinase (Btk) and they differ in the mechanisms of B cell activation (Mosier, Mond et al. 1977).

TI-I antigens do stimulate an antibody response in the absence of Btk. They activate B cells directly through Toll-like receptors (TLR), causing extensive proliferation and differentiation of B cells. Lipopeptides, lipopolysaccharide, some viral-coating particles and bacterial nucleic acids are examples of this type of antigens (Bekeredjian-Ding and Jego 2009). TI-I responses occur faster than TD responses and cause the generation of extrafollicular PCs and MBCs (Martin, Oliver et al. 2001).

TI-II antigens are highly repetitive structures that are present in the surface of bacteria or viruses. The epitopes cause multiple BCR-crosslinking and provide the B cell with a persistent signal transmitted through Btk. B cells proliferate and form robust PC

responses in the extrafollicular foci. TI-II antigens do not cause memory B cell (MBC) generation (Garcia de Vinuesa, O'Leary et al. 1999). During TI-II responses, germinal centres (GC) have been reported to be generated very quickly at a high concentration of antigen but these are non-productive. These GCs abort at the point at which centrocytes would be selected, showing that T cells are not required until this point in GC biology. TI-II GCs are located in the follicles and contain mature FDCs. However, there is no somatic hypermutation happening within these GCs (de Vinuesa, Cook et al. 2000, Lentz and Manser 2001).

Recently, it has been shown that B cells can receive help from natural killer cells (NKT) in a TD manner and from other cells such as neutrophils in a TI manner. These new findings have led to a re-classification of the B cell responses to take into account help from the above cells (Vinuesa and Chang 2013).

1.5 The activation and differentiation of B cells

Naïve B cells and naïve T cells recognising the same antigen have to interact, but the chance of these cells encountering one another in the 3D space is remote. So, primed B cells upregulate chemokine receptors that are responsible for their migration to the zones where T cells are situated (MacLennan, Toellner et al. 2003). Upon encounter with antigen in the blood or in the splenic marginal zone, naïve B cells upregulate CCR7 expression 2-3 folds, which attracts them to the border of the T-zone and B follicles (Reif, Ekland et al. 2002). Increased expression of CCR7 is sufficient to direct B cells to the T zone and overexpression of CXCR5 is enough to prevent this movement to the T zone (Reif, Ekland et al. 2002). CXCR5 expression remains unchanged and this

new balance between CCR7 and CXCR5 expression makes B cells less prone to be directed by CXCL13 into the B cell follicle (Okada and Cyster 2006).

T-B interaction is a multistage process and requires integrin-mediated adhesion for the initial contact, and SLAM-associated protein (SAP) and CD84 are implicated in sustaining the contact (Cannons, Qi et al. 2010). CD40-CD40L interactions are essential for TD responses and their disruption aborts GC formation, MBC differentiation and the generation of long-lived PC (Erickson, Durell et al. 2002).

Activated B cells at the B-T zone border transform into large B-blasts that will follow one of three different pathways (Sagaert, Sprangers et al. 2007). Most of them will rapidly proliferate into short-living PCs that will be in charge of producing low-affinity antibodies to provide a first-line of defence. Some activated B cells will become early recirculating MBCs. The rest of the B-blasts will re-enter the follicle accompanied by some T cells and differentiate into GC B cells. This decision-making is controlled by the strength of binding of the BCR to the antigen. Strong binding will select B cells to contribute to the extrafollicular response, while weaker unions will lead them to the GC pathway (Paus, Phan et al. 2006), Moreover, antigen affinity has been shown to regulate proliferation and survival of extrafollicular switched plasmablasts (Chan, Gatto et al. 2009).

1.5.1 The non- GC or extrafollicular pathway

The non-GC pathway occurs in the medullary cords in the lymph nodes and in foci in the red pulp of the spleen (MacLennan, Toellner et al. 2003). Some antigens, such as polysaccharides, provoke antibody responses without T cell help in the extrafollicular

sites and these responses last for months, contrary to extrafollicular PCs generated after TD antigens (Hsu, Toellner et al. 2006).

B-blasts primed to become plasma cells leave the T zone to the extrafollicular site and there, without any help from T cells and in association with $CD11c^{high}$ dendritic cells, differentiate into plasma cells. This differentiation is associated with the upregulation of Blimp-1 expression (Shaffer, Lin et al. 2002). Ig class switch recombination (CSR) occurs in B-blasts rather than in plasmablasts (Marshall, Zhang et al. 2011). Some of these recently formed plasma cells will make contact with stromal cells to prolong their life span (MacLennan, Toellner et al. 2003). CD154-deficiency (CD40L), a key ligand of CD40, has been shown to be required for extrafollicular TD antibody responses as well as for GC responses (Cunningham, Serre et al. 2004). miR-182 is upregulated in activated B cells and its expression is important for normal antibody responses immediately after T-dependent immunisation and essential for antibody responses in T-independent type II antigens (Li, Ou et al. 2016).

Discriminating *in vivo* antibody responses as either T-dependent or T-independent is not entirely natural for the reason that bacteria and virus will elicit both types of responses. The extrafollicular response, as to expansion, differentiation and isotype switching of B cells can take place in the absence of T cells and such, has important consequences as to the generation of autoreactive B cells. In particular, TLR-ligands have a greater ability to cause autoreactive B cell activation in the absence of T cells (Sweet, Ols et al. 2011).

1.5.2 The GC or follicular pathway

The B and T cells that migrate back into the follicle upregulate CXCR5 and they are attracted by CXCL13 expressing cells, such as FDCs. CXCR5-deficient mice have an

aberrant distribution of B cell follicles, which form a ring around the T zone. Even so, the role of CXCR5 in T-B collaborations is contradictory (Junt, Fink et al. 2005). Upon immunisation with T-dependent antigen, CXCR5-deficient mice produced normal levels of switched Ig isotypes (Forster, Mattis et al. 1996) and GCs are formed in the proximity of the arterioles. These GCs contain FDC but do not segregate into LZ/DZ and B cells are highly proliferative. Affinity maturation and hypermutation occurrs normally in these ectopic GCs (Voigt, Camacho et al. 2000). However, the role of CXCR5 is antigen dose-dependent. When the availability of the Ag was limited, CXCR5-deficiency reduced the responsiveness of B cells to viruses (Junt, Fink et al. 2005).

At the T-B interface, B cells proliferate for 1 or 2 days. After that, activated B cells migrate to the perimeter of follicle which is next to the marginal zone. In this location, activated B cells proliferate but they do not hypermutate and they undergo little switching (Coffey, Alabyev et al. 2009). EBI2 (Epstein-Barr virus induced molecule-2 or GPR183) controls movement of B cells to the outer follicle; EBI2-deficient B cells are unable to move to the outer follicle at day 2 after activation, while its overexpression is sufficient to localise B cells in the outer follicle (Pereira, Kelly et al. 2009).

Seeding of the GCs is as yet unclear, but Bcl-6, a transcriptional repressor, has to be expressed. One of the targets of Bcl-6 is EBI2 (Basso and Dalla-Favera 2010). EBI2 is strongly downregulated in all GC B cells as compared to naïve B cells and it has been shown that LZ B cells express ~4-fold higher levels of EBI2 than DZ B cells (Gatto, Wood et al. 2011). When antigen-specific EBI2-deficient B cells were transferred into WT hosts, they gave rise to slightly elevated levels of LZ B cells and affinity maturation was not affected (Gatto, Wood et al. 2011).

GC B cells upregulate S1PR2 (sphingosine-1-phosphate receptor 2), a G-protein coupled receptor (GPCR) that plays an important role in GC positioning and GC homeostasis (Green, Suzuki et al. 2011). S1PR2 inhibits the migration of cells out of the GCs, helping to confine them to the GC niche, due to its coupling to Gα12 and Gα13 (Green, Suzuki et al. 2011). Its ligand, S1P, is present in a decaying gradient in the follicle (Green and Cyster 2012). Schwickert and colleagues (Schwickert, Victora et al. 2011) have shown that low-affinity B cells can seed the GC, but they fail to expand and become activated when high-affinity B cells are present, which prevents low-affinity B cells from reaching an intermediary pre-GC stage (upregulation of Fas, Gl-7 and CCR6).

Fully formed GCs, the hallmarks of T-dependent antibody responses, are highly specialised structures, characterised by high mitotic and apoptotic activity (Nieuwenhuis and Opstelten 1984) and are the place where high affinity antibodies are produced (MacLennan 1994). Class-switch recombination and hypermutation require Activation-induce cytidine deaminase (AID) (Muramatsu, Kinoshita et al. 2000). AID is a member of the RNA-editing deaminase family and it is expressed only in GC B cells and B cells that are induced to switch *in vitro*. AID has also been shown to be involved in a rare human immunodeficiency, the hyper-IgM syndrome (Revy, Muto et al. 2000), which is characterised by absence of IgG, IgA and IgE antibodies while IgM levels are normal. These patients are highly susceptible to infections.

Somatic hypermutation creates a huge number of point mutations in the VDJ exons, producing sequence variants that through selection and continued evolution may give rise to higher affinity antibodies. This process is named affinity maturation. These point mutations appear due to the repair of double-strand breaks by homologous recombination (Papavasiliou and Schatz 2000). Class-switch recombination (CSR)

replaces the Ig heavy chain constant region (C_H) from Cμ to other C_H genes, causing switching from IgM isotype to IgG, IgE or IgA (Muramatsu, Kinoshita et al. 2000).

GCs are divided into two anatomically distinct regions: the light zone (LZ), situated towards the marginal zone, where smaller, non-dividing B cells (centrocytes), antigen-specific T cells called Tfh cells (follicular helper cells), tingible body macrophages and follicular dendritic cells (FDCs) with antigen deposited on their surface stay; and the dark zone (DZ), where large, mitotically active B cells (centroblasts) stay (MacLennan 1994). Although initial studies suggested that centroblasts are larger than centrocytes, it has been shown that LZ and DZ B cells are the same size and cellular complexity (Victora and Nussenzweig 2012). The gene expression profiles of these two populations are different. The phenotype of DZ B cells is $CXCR4^{hi}C83^{lo}CD86^{lo}$ and that of LZ B cells is $CXCR4^{lo}CD83^{hi}CD86^{hi}$ (Victora, Schwickert et al. 2010). See Figure 1.3.

GC dark and light zone organisation is mediated by CXCR4 and CXCR5 (Allen, Ansel et al. 2004), whereby centroblasts express high levels of CXCR4 and CXCL12 is found mainly in the DZ and CXCL13 in the LZ. GC B cells cycle between the dark zone and the light zone. CXCR4-deficient GC B cells are restricted to the LZ, carry less mutations and are outcompeted by WT cells overtime (Bannard, Horton et al. 2013), suggesting that in order to facilitate more effective rounds of mutation and selection there is a need for spatial separation.

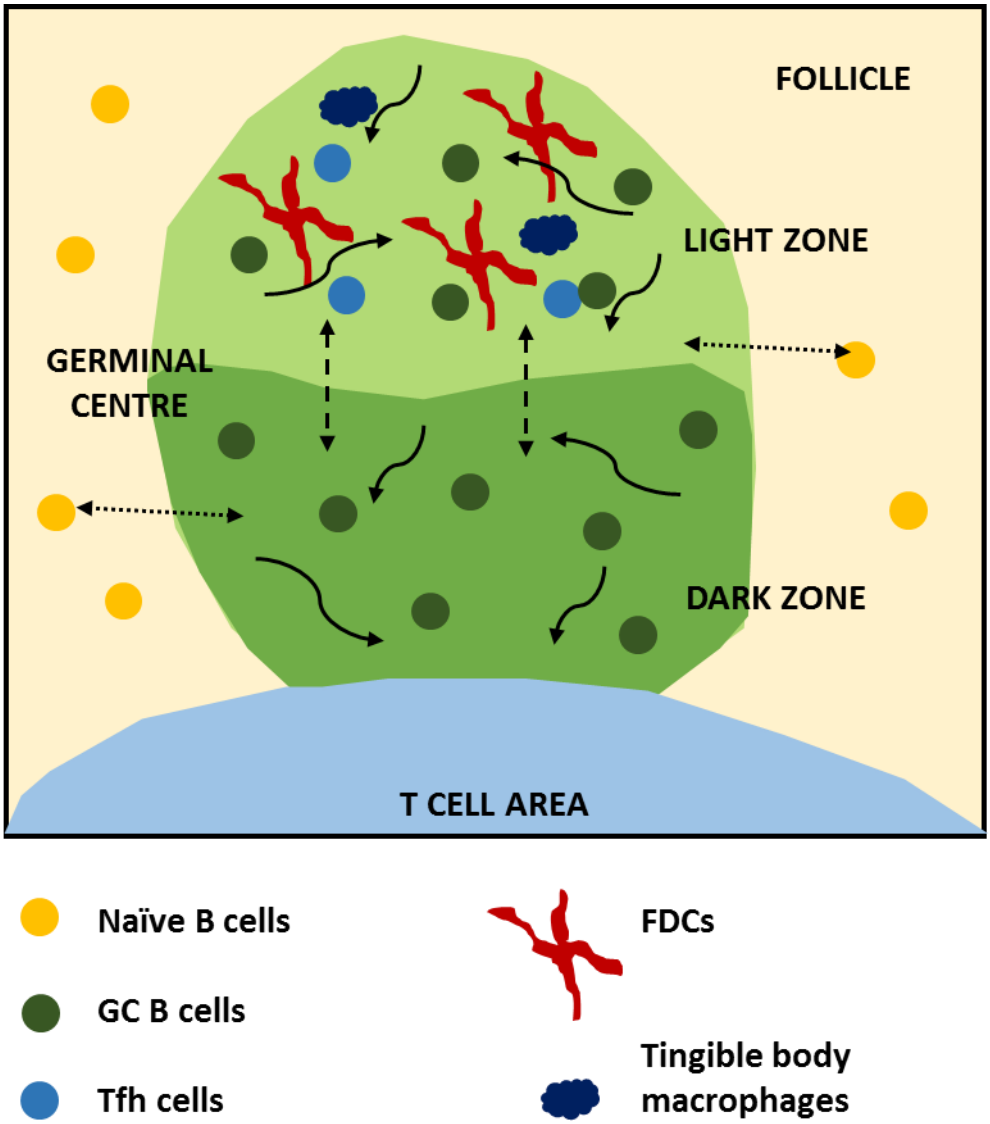

Figure 1.3: The morphology of the germinal centre. GCs form in the centre of follicles and are divided in the light zone and the dark zone, which sits adjacent to the T zone. FDCs, tingible body macrophages and Tfh cells are localised in the LZ. Selection occurs in the LZ and cells proliferate in the DZ.
Black arrows indicate previously described movements of cells within the GCs. Curved continuous arrows denote recirculation of cells in the DZ or in the LZ. Straight discontinuous arrows indicate migration from LZ to DZ or vice-versa. Straight dotted arrows indicate migration of naïve B cells to and from the GC area.

Thanks to the use of two-photon microscopy it has been possible to observe B cell motility *in vivo*, specifically bi-directional B cell migration between compartments within the GC (Allen, Okada et al. 2007, Schwickert, Lindquist et al. 2007). The findings from these studies have led to the cyclic re-entry model. Other two-photon microscopy studies combined with mathematical modelling have shown that GC B cells recirculate mostly intra-zonally within the LZ or the DZ, implying that inter-zonal migration is not necessary for consecutive rounds of mutation and selection (Hauser, Junt et al. 2007). However, re-analysis of the multi-photon microscopy data demonstrated that the intra-zonal pattern of migration is improbable and a new model was predicted (Figge, Garin et al. 2008). This new model stated that GC B cells in the LZ and DZ perform random walk migration but centroblasts and centrocytes acquire sensitivity to CXCL12 and CXCL13 respectively (Figge, Garin et al. 2008, Meyer-Hermann, Figge et al. 2009). The application of mathematical models has also revealed that chemokine-induced receptor downregulation, receptor-mediated chemotaxis and the presence of a simple fixed spatial distribution of the relevant chemokines is sufficient to induce complex migratory patterns (Chan, Billard et al. 2013).

GC are continually visited by follicular naïve B cells (Schwickert, Lindquist et al. 2007) but while the movement of naïve B cells is considered random, the migration of GC B cells is directed (O'Connor, Hauser et al. 2011). Interestingly, GC B cells present a varied morphology, some of the cells are polarised cells and only the ones that are dividing have a rounded shape (Hauser, Shlomchik et al. 2007). Cell division has classically been considered to be restricted to the DZ (Nieuwenhuis and Opstelten 1984), but several studies, especially in murine models, have observed that the onset of proliferation is triggered in the LZ (Allen, Okada et al. 2007) (Hauser, Junt et al. 2007). A new technique that combined transgenic photoactivatable fluorescent protein traced

with multi-photon microscopy has helped to show that the final stages of cell division are only occurring in the DZ. GC B cells enter the S phase in the LZ and transit to G2/M phases in the DZ. Genes for the G2/M phases such as Ccnb2 are enriched in the DZ (Victora, Schwickert et al. 2010).

Photoactivatable fluorescent protein traced with multi-photon microscopy has also revealed that there is increased movement from DZ to LZ and the decision to return to the DZ is controlled by T helper cells. This help from T cells is the limiting factor as to GC selection of high-affinity B cells (Victora, Schwickert et al. 2010). T cells select high-affinity B cells based on the amount of peptide-MHC presented in the LZ and induce them to cycle to the DZ (Victora, Schwickert et al. 2010). T cell selection triggers c-Myc expression in the LZ and subsequent cell-cycle entry. c-Myc is essential for the formation and maintenance of the GCs (Calado, Sasaki et al. 2012, Dominguez-Sola, Victora et al. 2012).

A second model for high-affinity B cell selection has been described. In this model, GC B cells compete for the limiting amount of antigen presented on the FDC network through their BCRs. The high-affinity clones then divide more than those with lower affinity BCR (Victora and Nussenzweig 2012). However, this model was dismissed by the antibody feedback model, as the amount of antigen in the GC is not limited (Zhang, Meyer-Hermann et al. 2013). By injecting monoclonal antibodies of defined affinity, the authors demonstrated that the antibodies produced outside the GC, whose affinity increase over time, are able to restrict the access of GC B cells to antigen presented on FDC and, therefore, influence B cell selection (Zhang, Meyer-Hermann et al. 2013). Evolution towards higher affinity antibody is achieved by a slow but consistent increase in the selection stringency and this constant increase explains the termination of the GC reaction, when the restriction of access to antigen is too high to allow for GC B cell

survival (Zhang, Meyer-Hermann et al. 2013, Zhang, Garcia-Ibanez et al. 2016). Although the BCR is essential for GC B cell survival and selection, its specific role in the GC reaction still has to be determined. Within the GC microenvironment, proliferating B cells undergo SHM that introduces mutations into the Ig gene region that encodes for the antigen-binding site (Sagaert, Sprangers et al. 2007). Most of these mutations do not improve the affinity of the receptor and so they don't interact correctly with the antigen presented by the FDCs, and therefore such cells do not receive appropriate survival signals. Further, self-reactive B cells may appear as consequence of SHM.

GC B cells express a variety of pro-apoptotic factors such as Fas, which is required for the elimination of low-affinity clones (Peperzak, Vikstrom et al. 2012). Autoreactive and low-affinity clones die *via* apoptosis and are quickly eliminated by tingible body macrophages. The impairment of the clearance of the apoptotic bodies results in autoantibody production, loss of B cell tolerance and autoimmunity (Rahman 2011).

After successfully completing a round of affinity maturation GC B cells may undergo further rounds or differentiate into post-GC cells. Bcl-6, as previously mentioned, is expressed in GC B cells and downregulates the signals implicated in B-cell activation, survival and differentiation at the end of the GC reaction (Basso, Saito et al. 2010). When high-affinity B cells interact with T cells through CD40-mediated signalling, Bcl-6 is downregulated to release the inactivation of the signals that regulate post-GC differentiation, such as Blimp-1 (Basso, Saito et al. 2010).

1.6 The chemokine superfamily

Chemokines regulate *in vivo* leukocyte migration. They also have a role during morphogenesis and the repair of tissue damage (Bajoghli 2013). In humans, there are 48 genes that encode chemokines, but taking into account polymorphisms, differential splicing and N- and C-terminal enzymatic processing, there are more than one hundred different chemokines (Ulvmar, Hub et al. 2011). Chemokines transmit their signals through one or more of 18 distinct heptahelical G-protein coupled receptors (GPCRs). Some receptors bind a single ligand and some of them are very promiscuous, binding up to ten ligands, but with different affinities and outcomes downstream (Rot and von Andrian 2004). There is functional redundancy in the chemokine system.

1.6.1 The chemokines

Chemokines are secreted proteins of small size, between 8 and 14 kDa and are defined on the basis of their amino acid composition rather than their function. Specifically, the presence of a highly-conserved tetra-cysteine motif is used to define chemokine families (Baggiolini, Dewald et al. 1997). Their monomeric structures are very similar and comprise of a NH_2-terminal loop, three antiparallel β-strands connected by loops, and a COOH-terminal α-helix (Baggiolini, Dewald et al. 1997). Chemokines are divided into four different groups depending on the position of the N-terminal cysteine residues. 'CXC' and 'CC' are the two main groups. The chemokines belonging to the 'CXC' group have an amino acid between the two first cysteines, also called α-chemokines; and the ones belonging to the 'CC' group, also called β-chemokines, do not (Zlotnik and Yoshie 2000). A third and fourth groups have been described, the 'C' group, or γ-chemokines, that lacks two out of four of the canonical cysteines; and the 'CX3C'

group, or δ-chemokines, that has 3 residues in between the two first cysteines (Zlotnik and Yoshie 2000).

Most chemokines have arisen from gene duplication from a single ancestral gene and they are clustered in specific chromosomal locations (Zlotnik and Yoshie 2000). Chemokines can also be divided in homeostatic and inflammatory. The former are constitutively present in the tissue while the later are dramatically upregulated by inflammatory and immune stimuli.

1.6.2 The chemokine receptors

Chemokine receptors are G- protein coupled receptors (GPCRs) with seven transmembrane domains. Neurotransmitters, peptides, chemokines, lipid-derived messengers, divalent cations, hormones, and ligands for light and odour perception transduce signals into intracellular pathways through GPCRs (Khoja, Wang et al. 2000).

There are 19 different GPCRs for chemokines in humans. Five structural motifs are conserved within the transmembrane (TM) domain. They are: TD(X)YLLNLA (X2)DLLF(X2)TLP(X)W in TM2, the NH_2- and COOH-terminal extensions of the DRYLAIVHA-motif in TM3 and the second intracellular loop, PLL(X)M(X2)CY in TM5, W(X)PYN in TM6, and HCC(X)NP(X)IYAF(X)G(X2)FR in TM7. Moreover, all of the receptors have two conserved cysteines, one in the NH_2-terminal domain and the other in the third extracellular loop that are assumed to form a disulphide bond critical for the conformation of the ligand-binding pocket (Baggiolini, Dewald et al. 1997). Chemokine receptors are coupled to Gα proteins and their activation leads to inhibition of production of cyclic adenosine monophosphate (cAMP). Other signalling pathways

are also implicated in the signalling from these receptors such as those involving MAPK and PI3K (Rollins 1997).

1.6.3 The atypical chemokine receptors

Atypical chemokine receptors (ACKRs) are also heptaspanning membrane receptors, homologous to chemokine GPCRs, but unable to provoke any classical GPCR downstream signalling (Ulvmar, Hub et al. 2011). This is due to the absence of one of the conserved domains, the DRYLAIV motif in the second intracellular loop, which impedes the ability to couple to G-proteins (Mantovani, Bonecchi et al. 2006).

As atypical receptors are unable to signal through the classical GPCRs pathways they have been excluded the standard nomenclature system, and a different standardised nomenclature has not been assigned (Bachelerie, Graham et al. 2014). In 2014, a committee representing scientists working in the field voted to adopt a unique designation, 'ACKR', an acronym for atypical chemokine receptor and this named system was approved by several committees (Bachelerie, Graham et al. 2014). There are four members in the ACKR family: ACKR1, (previously known as DARC, Duffy antigen, Fy antigen or CD234); ACKR2, (also known as D6, CCR9, CCR10, CCBP2 or CMKBR9); ACKR3, (previously CXCR7, RDC1 or CMKOR1); and ACKR4, (known as CCRL1, CCX-CKR or CCR11).

In general, ACKRs mediate internalisation and subcellular localisation of chemokines. Internalised chemokines can be directed to two different fates. On the one hand, they can be targeted to the lysosome, leading to chemokine degradation, and for this reason ACKRs are also called "scavenging decoys" (Ulvmar, Hub et al. 2011). The free receptor cycles back to the cell membrane to continue eliminating more extracellular

chemokines (revised in (Nibbs and Graham 2013)). On the other hand, ACKRs can transcytose chemokines, carrying them through biological barriers and concentrating them in micro-anatomical domains (Ulvmar, Hub et al. 2011). Both fates are able to form gradients of chemokines, either soluble or immobilised. These gradients may be directing cell responses to chemokines *in vivo*. ACKRs, as conventional chemokine receptors, dimerise. They can homodimerise (ACKR3) as well as heterodimerise (ACKR3-CXCR4). Some of them can even hetero-oligomerise (ACKR1-CCR5). Dimerization provides an additional way of control of chemokine activity (revised in (Nibbs and Graham 2013)).

1.7 The atypical chemokine receptor 4 (ACKR4)

The project described in this thesis is focused on the role of ACKR4 during the GC response.

ACKR4 was identified by homology searches using BLAST, looking for nucleotide sequences corresponding to the conserved motif in chemokine receptors in the human EST database (Khoja, Wang et al. 2000). Deposit H67224, with a length of 328 nucleotides and coming from olfactory epithelium, had a 95% homology to the consensus sequence. The full-length amino acid sequence consists of 350 aa (approximately 45 kDa). ACKR4 is a glycosylated seven transmembrane polypeptide with numerous intracellular serine and threonine residues (Khoja, Wang et al. 2000). ACKR4 lacks a signal sequence at the amino terminus. The BLAST program revealed an 86% amino acid sequence homology to bovine gustatory receptor-PPR1 (GenBank Accession No. S63848). ACKR4 and PPR1 are orthologous. ACKR4 also presents a 37%, 33% and 32% identity to the chemokines receptors CCR7, CCR9 and CCR6

respectively, meaning that ACKR4 resembles CCRs receptors more than CXCRs (Khoja, Wang et al. 2000, Schweickart, Epp et al. 2001). ACKR4 is mapped to chromosome 6 (Khoja, Wang et al. 2000). The canonical DRYLAIVHA transmembrane motif is replaced by DRYWAITKA in mouse and DRYVAVTKV in human (Townson and Nibbs 2002). Bioinformatic modelling of the ACKR4 structure has been provided by Behjati and colleagues (Behjati, Torktaz et al. 2012).

In mice, two distinct transcripts originate from two independently regulated promoters. The first one is abundantly expressed in heart (muscle cells) and lung; the rarer one is only expressed in brain and testes. Apart from heart and lung, ACKR4 mRNA transcripts have been detected in human DC, T cells, spleen and lymph nodes (Gosling, Dairaghi et al. 2000). In the adult thymus it is expressed in perivascular thymic epithelial cells (TECs) of the corticomedullary junction and the medulla and in the subcapsular epithelial layers (Heinzel, Benz et al. 2007).

Ligand profiles were determined by use of stalkokines (immobilized chemokines constructed on stalks) as bait for adhesion of cells expressing ACKR4 and further determined using radiolabelled ligand binding (Gosling, Dairaghi et al. 2000). High affinity ligands for ACKR4 (IC_{50}< 15 nM) are those in the β-chemokine group and include CCL19 (ELC or MIP-3β), CCL21 (6Ckine) and CCL25 (TECK). CCR7 is the canonical receptor for the first two ligands and CCR9 for the third high affinity ligand. Lower affinity ligands (IC_{50}< 150 nM) are CXCL13 (BLC) and vMIP-II (Gosling, Dairaghi et al. 2000). CCL19, CCL21 and CCL25 bind both in human and in mice, while CXCL13 has only been described to bind in humans (Gosling, Dairaghi et al. 2000). The binding of these chemokines to the receptor does not induce the classical calcium response (Heinzel, Benz et al. 2007) and, in transfected HEK293 cells, the

binding of ligand does not result in ligand-induced MAP kinase phosphorylation (Townson and Nibbs 2002).

ACKR4 is able to efficiently internalise, retain and degrade CCL19 with a higher capacity than CCR7 because ACKR4 is not desensitized by ligand stimulation, increasing its internalization and degrading capacity with the ligand concentration (Comerford, Milasta et al. 2006). This internalisation is independent of β-arrestins and clathrin-coated pits, as it is not impaired in Eps15 and Rab5 mutants (Comerford, Milasta et al. 2006). ACKR4 is internalised *via* caveolae (caveolin and cholesterol dependent) (Comerford, Milasta et al. 2006). The degrading capacity of ACKR4 for CCL19 and CCL21 has been shown *in vivo*, as in ACKR4$^{-/-}$ mice, CCL19 and CCL21 levels are increased in the serum as compared to WT mice (Comerford, Nibbs et al. 2010). In a more recent study (Watts, Verkaar et al. 2013), it has been shown that although ACKR4 does not cause constitutive β-arrestin relocalisation like other ACKRs (Nibbs and Graham 2013), the stimulation of ACKR4 with any of its ligands induces β-arrestin2 translocation, which does not take place in the absence of chemokines. From this result is not possible to exclude the role of β-arrestins in ACKR4-mediated endocytosis. After this internalisation, the receptor cycles back to the surface of the cell (Nibbs and Graham 2013). See Figure 1.4.

In non-inflammatory circumstances, ACKR4 is involved in the steady-state homing of CD11c^{+}MHCII^{high} dendritic cells to skin-draining lymph nodes *via* afferent lymphatics but not in the homing of dendritic cells that enter *via* the blood (Heinzel, Benz et al. 2007). In inflamed skin, ACKR4-expression by keratinocytes and by dermal lymphatic endothelial cells scavenges CCL19 *in situ* facilitating skin-derived CCR7^{+} APC emigration to draining lymph nodes (Bryce, Wilson et al. 2016).

ACKR4 is also implicated in the immigration of embryonic thymic precursors to the thymic anlage *in vivo*, as its overexpression impairs colonisation of the thymus by haematopoietic precursors (Heinzel, Benz et al. 2007). Despite this, thymocyte numbers reached normal levels in the new born mice when ACKR4 was overexpressed, ruling out a function for ACKR4 in the later stages of thymus development (Heinzel, Benz et al. 2007). However, an independent study provided contradictory results. Bunting et al. have shown that ACKR4 controls cortical and medullary size, leading to altered thymocyte development with the production of elevated numbers of $CD4^+$ T cells and a reduced transition from immature to mature phenotype in the single-positive T cells (Bunting, Comerford et al. 2013). ACKR4 expression in the thymus has been characterised by using ACKR4-GFP reporter mice both at the neonatal and adult stages. ACKR4 is expressed in both subpopulations of cTECs and mTECs and can be used to subdivide these populations (Ribeiro, Meireles et al. 2014). A third study was in agreement with the first study. Although ACKR4 is expressed in key thymic microenvironments in the thymic cortex and in stromal cells surrounding pericytes of vessels, the study found that ACKR4 does not affect thymus size, cellularity, T cell development or thymic output (Lucas, White et al. 2015).

$ACKR4^{-/-}$ mice develop spontaneous autoimmune lesions in the submandibular gland and in the liver that resemble Sjögren syndrome (Bunting, Comerford et al. 2013). Moreover, ACKR4-deficiency accelerates the onset of EAE (experimental autoimmune encephalomyelitis) induced by immunisation and EAE is more severe than in WT counterparts after immunisation (Comerford, Nibbs et al. 2010). This is associated with the increase of CCL21 in the central nervous system. Also, in this model, the balance between Th1 and Th17 responses was biased towards a Th17 response in the $ACKR4^{-/-}$

mice, due to increased CCL19/CCL21-driven IL-23 production (Comerford, Nibbs et al. 2010).

ACKR4 has been described recently to be expressed by a layer of lymphatic endothelial cells of the ceiling of the lymph node subcapsular sinus in steady state conditions (Ulvmar, Werth et al. 2014). This expression scavenges chemokines and creates functional CCL21 gradients that guide $CCR7^{+}$ dendritic cell entrance via afferent lymphatics towards the T cell areas (Ulvmar, Werth et al. 2014).

Interestingly, in *Salmonella Typhimurium*-infected pigs, ACKR4 expression, together with CCR9 and CCL25 expression, are downregulated in the gut wall and Peyer's patch, opening the possibility for a bacterial strategy to reduce lymphocyte homing to the intestines and therefore, for a role for ACKR4 in gut-lymphocyte homing (Meurens, Berri et al. 2009).

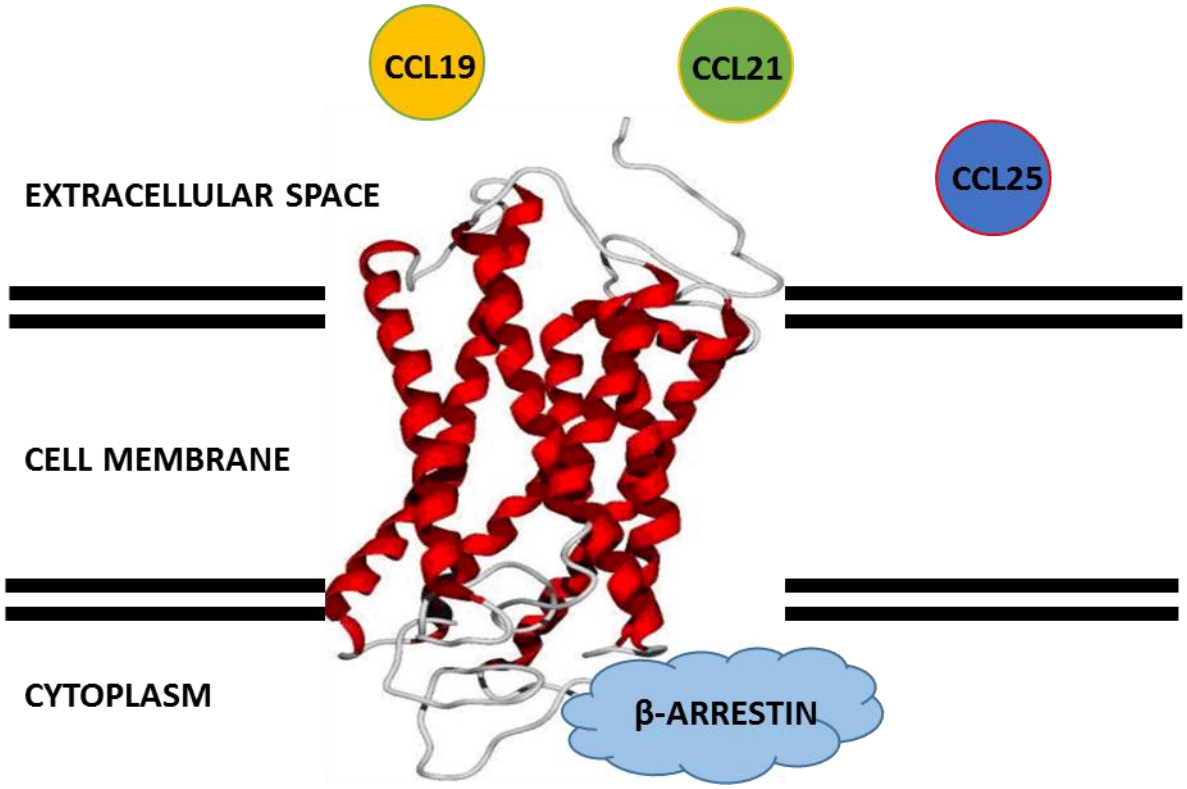

Figure 1.4: ACKR4 structure. ACKR4 is a seven-transmembrane receptor. It binds with high-affinity to CCL19, CCL21 and CCL25. Due to a mutation in the third intracellular loop, ACKR4 is unable to signal through GPCRs. Instead, when it is bound to its ligands causes β-arrestin translocation and the whole complex is internalised for ligand degradation and receptor recirculation back to the cell membrane.
ACKR4 model taken from (Behjati, Torktaz et al. 2012)

1.8 The C-C chemokine receptor type 7 (CCR7)

CCR7, a seven-transmembrane-spanning receptor which signals through heterotrimeric G proteins, is the canonical receptor for the two homeostatic chemokines CCL19 and CCL21 (Rot and von Andrian 2004). CCR7 is expressed by B and T lymphocytes and was first described as a gene that is induced in B lymphocytes by Epstein-Barr virus (EBV) infection, so it was previously known as EBI1 (EBV-induced gene 1) (Birkenbach, Josefsen et al. 1993). CCR7 has a high homology to IL-8 receptors, both at the RNA and protein level (Birkenbach, Josefsen et al. 1993). Murine CCR7 has an 86% protein homology to the human receptor (Schweickart, Raport et al. 1994). CCR7 is encoded by the region 17q12-q21.2 of the human chromosome and CCL19 (ELC) and CCL21 (SLC) form a mini-cluster at human chromosome 9p13. Both ligands cause calcium mobilization and induction of chemotaxis when bound to CCR7 (Yoshida, Imai et al. 1997, Yoshida, Nagira et al. 1998).

CCR7 is constitutively ubiquitylated and this ubiquitylation is essential for ligand-independent basal receptor trafficking and for the ligand-induced recycling *via* the trans-Golgi network and plays a pivotal role in immune migration (Schaeuble, Hauser et al. 2012). CCR7 is sialylated and reduction of this sialylation decreases CCL19-dependent downstream signalling (Su, Chang et al. 2014). This sialylation occurs in human CCR7 at the N-terminus and at the extracellular loop 3 and different cells carry different levels of sialylation which can be regulated by glycosidases that are secreted by mature DCs (Hauser, Kindinger et al. 2016).

CCR7 has been shown to control a variety of process within the immune system. CCR7 is involved in regulation of lymphocyte homing to SLO, in establishment of the peripheral tolerance and in autoimmunity (Forster, Davalos-Misslitz et al. 2008). CCR7

controls T cell entrance to lymph nodes *via* HEVs, as lymph nodes and Peyer patches from $CCR7^{-/-}$ mice lack T cells, although they can home to the spleen where they accumulate in the red pulp (Forster, Schubel et al. 1999). When DCs mature as a consequence of antigen encounter they upregulate CCR7 and other molecules and migrate from peripheral tissues to lymph nodes where they can stimulate T cells and initiate T-dependent responses (Yanagihara, Komura et al. 1998). $CCR7^{-/-}$ DCs fail to migrate to the draining lymph nodes from skin, intestine and lungs (Hintzen, Ohl et al. 2006, Worbs, Bode et al. 2006).

CCR7 together with CXCR5, as previously mentioned, are in charge of white pulp organisation. CCR7 guides cells to the T cell zones and CXCR5 guides cells to the B cell follicles (Ohl, Henning et al. 2003). Activated B cells downregulate CXCR5 and upregulate CCR7, allowing their migration to the T-B border (Reif, Ekland et al. 2002). Similarly, Tfh cells upregulate CXCR5 and downregulate CCR7 which permits their migration inside the follicle and subsequently, help during GC responses (Hardtke, Ohl et al. 2005). CCR7-upregulation in activated B cells and consecutive interaction with T cells has been shown to be essential for the production of antiviral neutralising antibodies to vesicular stomatitis virus when there is limited antigen availability (Scandella, Fink et al. 2007).

CCR7-deficient mice develop generalised autoimmune phenotypes and organs such as pancreas, stomach, kidneys and salivary and lachrymal glands are affected. Moreover, CCR7-deficient mice are also more susceptible to induced diabetes (Davalos-Misslitz, Rieckenberg et al. 2007). Additionally, CCR7-deficient mice develop persistent GCs in response to TI-II antigens and these GCs are located in the periarteriolar area and contain a ring of FDCs around them and T cells. However, affinity maturation, class-

switching, MBC generation and Treg distribution was seen to be normal (Achtman, Hopken et al. 2009).

CCR7-expression by tumours has been correlated with a bad prognosis and increased metastases to lymph nodes. The tumours include breast tumours, melanoma, colorectal cancer, gastric carcinoma, non-small cell lung cancer, cervical cancer, T-cell leukaemia and chronic lymphocytic leukaemia (Mburu, Wang et al. 2006, Ben-Baruch 2008). This increased metastases is thought to be caused by CCL21-CCR7-dependent induction of actin polymerisation, migration adhesion and invasion of CCR7-expressing tumour cells (Ben-Baruch 2008).

1.9 The chemokines CCL19 and CCL21

CCL19 and CCL21 bind to the chemokine receptors CCR7 and ACKR4. CCL19 and CCL21 are produced constitutively by a variety of stromal cell in the SLOs. CCL19-expressing cells include FRCs, mature DCs and mTECs; while CCL21-expressing cells include HEVs, LECs, FRCs and mTECs (Comerford, Harata-Lee et al. 2013).

Although CCL19 and CCL21 bind CCR7 with similar affinity, they are very different in structure, function and regulation (Comerford, Harata-Lee et al. 2013). CCL19 and CCL21 only share a 25% similarity in amino acid sequence. However, their tertiary structure contains conserved characteristics: a disordered N terminus, followed by a core domain containing an N-loop, a 3-stranded β-sheet and a C-terminal helix. The N-terminal domain has been shown to be important for stabilisation of the active receptor conformation and even if these regions from CCL19 and CCL21 only share one aa, swapping them does not cause a difference in signalling (Ott, Lio et al. 2006).

CCL21 contains a unique 30 aa length carboxyl-terminal extension with 2 extra cysteine residues and 12 of these residues are basic (Nagira, Imai et al. 1997). In humans, there is only one gene encoding CCL21. In mice, there have been identified two different isoforms of CCL21 with one aa variance at position 65. CCL21a (CCL21-Ser) is mainly expressed by mTECs and HEVs in SLOs and FRCs in T cell areas, while CCL21b (CCL21-Leu) is expressed mainly by LECs in peripheral tissues (Comerford, Harata-Lee et al. 2013). The carboxi-terminal extension allows CCL21 to bind to the matrix glycosaminoglycans and this is required for efficient presentation at the surface of endothelial cells (Yoshida, Nagira et al. 1998).

CCL19-deficient mice have only minor defects, which means that CCL21 is sufficient for most of the CCR7-dependent processes (Hauser and Legler 2016). Mice of the mutant strain *plt* (paucity of lymph node T cells), which are a result of a recessive spontaneous mutation, lack the gene for CCL21-Ser and for CCL19, while they express CCL21-Leu (Vassileva, Soto et al. 1999, Luther, Tang et al. 2000, Nakano and Gunn 2001). These mice have reduced numbers of naïve T cells in SLOs due to a defect in homing. DC numbers and migration towards T zones after stimuli are also impaired in these mice. However, DCs exhibit normal emigration from skin epidermis (Gunn, Kyuwa et al. 1999).

Both CCL19 and CCL21 induce G protein activation and calcium mobilisation to the same extent (Kohout, Nicholas et al. 2004). Moreover, both are able to cause polarisation of the actomyosin cytoskeleton, triggering chemotactic movement (Hauser and Legler 2016). Both ligands activate GRK6 (G-protein coupled kinases), but only CCL19 can activate GRK3. Cell polarisation is caused by small GTPases such as Rac,

RhoA and Cdc42 and it includes lamellipodia formation and stabilisation and uropod definition (Hauser and Legler 2016).

CCL19 efficiently stimulates CCR7 phosphorylation in several Ser and Thr in the region 373-378 of the carboxyl terminus and internalisation, which causes receptor desensitisation by β-arrestin recruitment. Although CCL21 is also able to cause ERK1/2 activation, CCL19 causes increased activation (Kohout, Nicholas et al. 2004). Receptor desensitisation by CCL19 may indicate that CCL19-mediated responses have a shorter time-span that those provoked by CCL21 binding (Forster, Davalos-Misslitz et al. 2008). As CCL21 is immobilised, it can cause integrin activation leading to cell adhesion. When DCs contact with CCL21, they are able to trim CCL21-anchoring residues, releasing a soluble form of CCL21, whose behaviour resembles that of CCL19 (Schumann, Lammermann et al. 2010). DCs subjected to immobilised CCL21 and soluble CCL19 use CCL21 for adhesive random migration while following CCL19-gradients. So, immobilised and soluble chemokines are able to shape the migration together (Schumann, Lammermann et al. 2010).

The observation that some ligands can induce more β-arrestin mobilisation than others gave rise to the notion that has been denominated 'phosphorylation barcode theory'. According to this theory, each ligand stabilises ligand-specific receptor conformations, which leads to specific recruitment of GRKs that provoke a definite phosphorylation pattern in the C-terminus end of the receptor. This phosphorylation pattern defines the strength and stability of β-arrestin union that will subsequently determine if the GPCR is desensitised or desensitised and internalised (Hauser and Legler 2016). CCL19 and CCL21 binding to CCR7 also cause the stabilisation of different conformational states. CCL21 modifies CCR7 conformation towards an active state of TM6, while CCL19

stabilises more varied conformations and may have an effect specifically in TM7 (Hauser and Legler 2016).

1.10 General aims of this thesis

The principal aim of this thesis is to broaden the knowledge about the signals that determine the pathway that a GC B cell will follow. The signals that help in the decisions that have to be made in the GC are just starting to be understood. Interactions with FDCs and Tfh cells have been shown to have a role in the post-GC differentiation as PCs or MBCs.

Chapter 3 characterises the role of atypical chemokine receptor 4 (ACKR4), which is differentially expressed in the GC B cells, in the B cell responses, taking advantage of the ACKR4$^{-/-}$ mouse model.

Chapter 4 studies the role of chemokines CCL19 and CCL21, through their receptors CCR7 and ACKR4, in memory B cell generation and migration.

Chapter 2. Materials and methods

2.1 Mice

Mice were bred and maintained under specific pathogen-free conditions at the Biomedical Services Unit, University of Birmingham, UK. All animal experiments preformed were approved by the institutional ethics committee and the Home Office, UK. Mice were used between 6 and 12 weeks old.

2.1.1 WT mice

C57BL/6 mice (wild type, WT) were purchased from Harlan laboratories. These mice were only used as host mice in B cell transfer experiments.

2.1.2 ACKR4$^{-/-}$ mice

ACKR4 knock-out (ACKR4$^{-/-}$) mice were a kind gift from R. Nibbs (University of Glasgow) and they were generated as described by Comerford and colleagues (Comerford, Nibbs et al. 2010). Briefly, the open reading frame of ACKR4 was replaced with a knock-out cassette that contained a floxed phosphoglycerine kinase promoter driven neomycin resistance gene and injected in mouse ES cells. Positive clones were identified and injected into blastocysts to generate chimeric mice. This offspring was crossed with ZP3-Cre transgenic mice and female offspring carrying both transgenes identified. Recombination occurred during oogenesis of the offspring from those females. Mice lacking ZP3-Cre and carrying the targeted version of ACKR4 were identified. They were then backcrossed for at least ten generations to C57BL/6.

2.1.3 ACKR4-GFP mice

ACKR4-GFP mice have been previously described by Heinzel and co-workers (Heinzel, Benz et al. 2007). Shortly, 578 bp of ACKR4 coding sequence (nucleotides 45-622 of the mRNA) were replaced in frame by an eGFP together with a neomycin resistance cassette, which was electroporated into ES cells. Specific integration was confirmed by Southern blotting and targeted ES cell were injected into C57BL/6 blastocysts and later backcrossed onto the C57BL76 background.

2.1.4 Quasi-monoclonal mice

Quasi-monoclonal (QM) mice were first described by Cascalho and colleagues (Cascalho, Ma et al. 1996). These mice have a rearranged V(D)J segment at the immunoglobulin (Ig) heavy chain locus, being the other allele and the kappa light chain allele non-functional. This heavy chain paired with any lambda chain is specific for the hapten (4-hydroxy-3-nitrophenyl) acetyl) NP. Somatic hypermutation and secondary rearrangements change the specificity of approximately 20% of the B cells antigen receptors. For the purposes of this project, QM mice have been considered as those with a rearranged V(D)J segment at the immunoglobulin (Ig) heavy chain locus in both alleles and both alleles from the kappa light chain are non-functional. QM mice were crossed onto an $eYFP^{+}$ strain (QM-$eYFP^{+}$) and onto the $ACKR4^{-/-}$ strain (QM-$eYFP^{+}$ $ACKR4^{-/-}$). QM mice were crossed onto a Tdtomato strain (QM-$TdTomato^{+}$) and onto the $ACKR4^{-/-}$ strain (QM-$TdTomato^{+}$ $ACKR4^{-/-}$).

2.1.5 Cγ1-Cre mice

Cγ1-Cre mice have been previously described by Casola and co-workers (Casola, Cattoretti et al. 2006). In these mice, the expression of Cre recombinase is induced by the transcription of the Ig γ1 constant region gene segment (Cγ1), providing conditional gene targeting in the majority of the GC B cells that are generated after immunisation with TD antigens (Casola, Cattoretti et al. 2006). An internal ribosome entry site (IRES) followed by the Cre-coding sequence has been incorporated into the 3' region of the Cγ1 locus between the last membrane-coding exon and the polyadenylation site. This approach creates two independent transcripts, the Cγ1 and the Cre. The carrying of two copies of the Cγ1-Cre only increases slightly the efficiency of Cre-mediated recombination.

2.1.6 $CCR7^{-/-}$ mice

$CCR7^{-/-}$ mice were a kind gift from A. Rot (University of York, UK) and were generated as described in (Forster, Schubel et al. 1999). Briefly, a vector was constructed carrying a neomycin resistant gene to target the Ccr7 gene by deleting large parts of exon 3. Blastocysts were injected and heterozygous animals were crossed. About a quarter of the offspring carry the disrupted locus of both alleles. $CCR7^{-/-}$ mice were crossed onto the QM and Tdtomato strain (QM-$TdTomato^{+}$ $CCR7^{-/-}$).

2.2 Immunisations

2.2.1 T-dependent antigens

To study the primary response to thymus dependent antigens (TD), mice were immunised intraperitoneally (i.p.) with 50 μg NP-CGG ((4-hydroxy-3-nitrophenyl) acetyl Chicken γ- globulin) alum-precipitated. NP was conjugated to CGG at a ratio of NP_{18}-CGG, a kind gift from Ms Chandra Raykundalia. NP-CGG is presented as a 5 mg/ml solution and an equivalent volume of 9% $AlK(SO_4)_2$ is added. The pH is adjusted to 6.5 with NaOH 10 M and material is left spinning in dark for 30 min to allow maximum precipitation. The precipitate is washed twice in PBS (Sigma-Aldrich, UK) and the pellet resuspended in PBS to a final concentration of 250 μg/ml.

When the primary response was studied in the popliteal lymph node (pLN), mice were immunised subcutaneously in one or both footpads with 20 μg NP-CGG alum precipitated prepared as the paragraph before. The pellet is resuspended to a final concentration of 1000 μg/ml. In order to study the secondary response to TD antigens, mice were primed i.p. with 50 μg alum–precipitated CGG (Rockland antibodies & assays, USA). CGG is precipitated in alum. CGG is presented as a 5 mg/ml solution and it is precipitated as NP-CGG. The pellet is resuspended to a final concentration of 250 μg/ml. $1x10^5$ chemically inactivated *Bordetella pertussis* (b.p.) bacteria (LEE laboratories, BC, USA) were added as an adjuvant in all primary immunisations.

Mice were challenged 5 weeks after priming with 50 μg of NP-CGG in 200 μl of PBS i.p. If the boosting was in the footpad, 20 μg of NP-CGG diluted in 20 μl of PBS were injected per leg in anesthetised mice.

Sheep red blood cells (SRBC) were also used as a TD antigen. $2x10^8$ SRBCs (TCS Biosciences, UK) in PBS were injected i.v. (intravenously) in the lateral tail vein. SRBCs were prepared by washing with PBS 3 times, followed by centrifugation and resuspension in PBS to a volume of 200 µl per mouse.

2.2.2 T-independent antigens

To study the response to thymus independent type II (TI-II) antigens, mice were injected i.p. with 30 µg of NP-Ficoll (Biosearch Technologies, CA) diluted in 200 µl of PBS.

2.3 Immunohistology

Spleens were snap-frozen and stored at -80˚C. Lymph nodes were snap-frozen in OCT tissue-freezing solution (Leica Microsystems, UK) and stored at -80˚C. Spleen and lymph node cryosections (Bright Instruments, Huntingdon, UK) of 6 µm were placed onto either multispot slides (Hendley-Essex, UK) or Surgipath X-tra Adhesive Clipped Corned slides (Leica Biosystems). Slides were fixed in acetone (Acros Organics, USA) at 4˚C for 20 min, air dried and stored at -20˚C in polyethylene bags until further use.

If the tissues were $eYFP^+$, they had to be fixated prior to freezing. First, for 8 h in 1% paraformaldehyde (PFA, TAAB Laboratories, UK) and then 24 h in 30% sucrose (Sigma-Aldrich) at 4ºC. Before staining, frozen slides were allowed to reach room temperature under a fan before opening the polyethylene bag.

2.3.1 Immunofluorescence

Slides were rehydrated in PBS. Once they were hydrated they should not be let to dry. Slides were blocked using 10% horse serum in PBS-10% BSA (Sigma-Aldrich) for 15 min and permeabilised with 0.2% Triton X-100 (Sigma-Aldrich) in PBS for 10 min. Antibodies were diluted at the optimal dilution in PBS-10% BSA and incubated in a humid dark chamber for 1 h (Table i). Secondary and tertiary antibodies were incubated for 45 min with 5 min wash in PBS between incubations (Table ii). Slides were mounted in ProLong Gold antifade reagent (Invitrogen, USA) and let dry in a dark chamber for 24 h. Slides were stored at -20ºC in dark until observation.

2.3.1a CCL21 staining

In order to achieve optimal staining of CCL21 gradients, CCL21 staining has to be performed in fresh tissue. Briefly, spleen and lymph nodes were dissected and snap-frozen in OCT immediately. Tissues had to be cut on the same day and stained without fixation. Image analysis gave better results when realised on the same day.

2.3.2 Immunohistochemistry

Slides were rehydrated in 5 mM Tris Buffered Saline pH 7.6 (TBS) prior to incubation. Antibodies were diluted at the optimal concentration in TBS (Table i) and incubated for 1 h. Secondary antibodies conjugated to biotin or horseradish peroxidase were applied with 10% normal mouse serum for 45 min. The biotinylated secondary antibodies were detected using biotin-conjugated StreptABComplex-alkaline phosphatase complex (Dako, Glostrup, Denmark). Slides were developed sequentially. First, 3,3

diaminobenzidine tetrahydrochloride (DAB) (Sigma-Aldrich) was used as a substrate for HRP enzyme. Slides were washed between the additions of substrates. Then, fast blue substrate (Sigma-Aldrich) was used as substrate for alkaline phosphate enzyme. Both substrates were made up freshly before use. Slides were washed in TBS and in distilled water and mounted in glycerol gelatin (Sigma-Aldrich).

Table i: Primary antibodies

Target	Isotype	Clone	Dilution	Manufacturer
CXCR4	Rat anti-mouse	2B11	1/100	BD Pharmingen
LYVE-1	Rabbit anti-mouse	14917	1/200	Abcam
Ki67	Rabbit anti-mouse	15580	1/300	Abcam
CD138	Biotin anti-mouse	281-2	1/100	BD Pharmingen
PNA	Biotin anti-mouse	B-1075	1/200	Vector Laboratories
CCXCKR (ACKR4)	Goat anti-mouse	C-16	1/50	Santa Cruz Biotech
IgD	Rat anti-mouse	11-26c	1/500	BD Pharmingen
CD3	Hamster anti-mouse	145-2C11	1/500	BD Pharmingen
NP	Sheep anti-mouse		1/3000	In house
c-myc	Rabbit anti-mouse	Y69	1/200	Abcam
CCL21	Goat anti-mouse	AF457	1/20	R&D Systems
CCR7	Rat anti-mouse	4B12	1/50	eBioscience

Table ii: Secondary and tertiary antibodies

Target	Conjugation	Dilution	Manufacturer
Rat anti-mouse CD4	APC	1/100	eBioscience
Rat anti-mouse IgD	APC	1/100	eBioscience
Rat anti-mouse IgD	BV421	1/100	Biolegend
Donkey anti-rat IgG	Cy3	1/200	Jackson ImmunoResearch
Donkey anti-rabbit IgG	FITC	1/200	Jackson ImmunoResearch
Donkey anti-rabbit IgG	DyLight 405	1/200	Jackson ImmunoResearch
Biotin anti-hamster IgG	Biotin	1/200	Vector Laboratories
Donkey anti-goat IgG	AF 488	1/200	Jackson ImmunoResearch
SA	AF 647	1/200	Jackson ImmunoResearch
SA	AF 488	1/200	Jackson ImmunoResearch

2.3.3 Slide observation

Fluorescent slides were observed in a Leica DM6000 (Leica Microsystems) controlled by LAS-AT software (Leica Microsystems) and pictures taken with a Leica DF350FX camera. Non-fluorescent slides were observed using a Leica DM6000 and pictures taken with a 5.ORTV camera with Q capture software. Whole spleen or whole lymph node section images were obtained with the Zeiss AxioScan Z1 equipment (Carl Zeiss, Germany) and processed with software ZEN, blue edition (Carl Zeiss).

2.4 Enzyme-linked immunosorbent analysis (ELISA)

Blood was collected by cardiac puncture from anaesthetised mice by isoflurane inhalation. Sera were obtained after clotting and centrifugation of blood samples. It was stored at -20˚C until analysis. Microtiter plates (Thermo Fisher Scientific, USA) were coated (5 µg/ml) overnight at 4ºC. NP_{15}-BSA-coupled microtiter plates were used to detect NP-specific antibody. NP_2-BSA-coupled microtiter plates were used to measure the high-affinity antibody fraction. CGG-coupled microtiter plates were used to measure antibodies coming from the memory response. Plates were washed in wash buffer and blocked with 200 µl of blocking buffer for 1 h at 37ºC. Serial tripling dilutions (1/30 dilution at start) of serum samples were added into the plates and incubated for 1 h at 37ºC. After this incubation, plates were washed and secondary AP-conjugated antibodies were added, specific for IgG, IgG1, IgG3 and IgM (Southern Biotech, USA) (Table iii). In adoptive transfer experiments, to detect antibodies produced from transferred cells, biotin-conjugated IgM^a and $IgG1^a$ (BD Pharmingen, USA) followed by incubation with streptavidin-conjugated Alkaline Phosphatase (Vector Laboratories,

USA) were used. Plates were incubated with secondary antibodies for 45 min at 37ºC and washed again.

ELISA plates were developed using SIGMAFAST^{TM} (Sigma-Aldrich). Shortly, one p-nitrophenyl phosphate (pNPP) tablet (1.0 mg/ml) and one Tris Buffer tablet (0.2 M Tris buffer and 5 mM magnesium chloride) were dissolved in 20 ml of ddH_2O. Plate's absorbance is read at 405 nm using Synergy HT Microplate Reader (BioTek, USA). Table iv provides a list of the reagents used.

Negative and positive controls were included in each plate and antibody titres were calculated as a relative measure. Relative affinity was calculated as the fraction of NP_2 and NP_{15} relative antibody titres (NP_2/NP_{15}).

Table iii: Antibodies used in ELISA

Target	Clone	Dilution	Manufacturer
Goat anti-mouse IgM-AP	1020	1/2000	Southern Biotech
Goat anti-mouse IgG3-AP	1100	1/1000	Southern Biotech
Goat anti-mouse IgG1-AP	1070	1/1000	Southern Biotech
Goat anti-mouse IgG-AP	1030	1/1000	Southern Biotech
Biotin mouse anti-mouse IgMa	DS-1	1/500	BD Pharmingen
Biotin mouse anti-mouse IgMb	AF6-78	1/500	BD Pharmingen

Table iv: Reagents used in ELISA

Reagent's name	Reagent's ingredients
Coating buffer	Na_2CO_3 1.95g, $NaHCO_3$ 2.93g in 1 litre dH_2O, pH=9.6
Blocking/Dilution buffer	0.1M PBS + 0.05% Tween (Sigma)
Wash buffer	0.1M PBS + 1% BSA (Sigma)
Developing solution	2 tablets (1 silver, 1 gold) in 20 ml ddH_2O

2.5 Flow cytometry

Spleens and lymph nodes were mashed and the cell suspensions were filtered using a 70 µm cell strainer (Thermo Fisher Scientific) in RPMI 1641 culture media (Sigma-Aldrich) supplemented with 5% foetal calf sera (FCS, Thermo Fisher Scientific, Gibco) and 1% penicillin/streptomycin (penicillin 10000 units/ml and streptomycin 10000 µg/ml, Invitrogen) and stained for surface markers in a 96 well plate (Corning, USA).

Bone marrow was extracted from femur and tibia bones. The cell suspension was filtered and stained for surface markers in a 96 well plate.

Blood was collected by cardiac puncture from anaesthetised mice by isoflurane inhalation and incubated with Ethylenediaminetetraacetic acid (EDTA, Sigma-Aldrich) to avoid clotting. Red blood cells were lysated by several incubations with ACK lysing buffer (Gibco). Cells were stained for surface markers in a U-bottom 96 well plate (Thermo Fisher Scientific).

Fc gamma II and III receptors were blocked (20 min at 4˚C) using an anti-CD16/32 antibody diluted in FACS buffer (PBS supplemented with 1% FBS plus 5 mM EDTA). Surface antibodies were incubated diluted at the optimal concentrations (20 min at 4˚C) in FACS buffer and washed twice with FACS buffer prior to analysis (Table v).

If required, 10000 counting beads (Spherotech, Inc) were added to the samples before analysis. Samples were analysed using CyAN FACS Analyser (Beckman Coulter) with the software Summit v4.3 (Beckman Coulter, USA) or with BD LSRFortessa Analyzer (BD Biosciences, USA) with the software BD FACSDiva (BD Biosciences). Data were analysed offline with FlowJo (FlowJo LLC, USA).

2.5.1 Proliferation measure by injection of EdU

Mice were injected intraperitoneally with 2 mg of the thymidine analog 5-ethynyl-2'-deoxyuridine (EdU, Life Technologies) dissolved in PBS. EdU incorporation was analysed using the kit Click-iT Edu Alexa Fluor 647 for Flow cytometry (Life Technologies) following manufacturer's instructions. This protocol is based on aldehyde fixation and detergent permeabilisation for antibody labelling. Once the cell suspension has been stained with surface antibodies (except BV510, PE and PE-conjugated), they were washed with PBS-1% BSA. Then, they were incubated with Click-iT fixative and washed again. Afterwards, cells were incubated with Click-iT saponin-based permeabilisation and wash reagent. Following this incubation, cells were stained with Click-iT reaction cocktail (Table vi). Cells were washed again and incubated with the remaining surface markers.

2.5.2 phospho-Akt staining by flow cytometry

First, the cell suspension was stained with surface antibodies as described above. Cells were fixed in 4% freshly prepared PFA in PBS for 15 min at RT. Then, they were centrifuged and 1 ml of ice-cold acetone was added and incubated for 20 min on ice. After removing of the acetone by pipetting and wash with FACS buffer, the cell suspension was stained with anti-p-Akt-biotin in FACS buffer for 1 h at RT. Finally, cell suspension was stained using streptavidin and analysed in a flow cytometer.

As this method destroys many antibody-epitopes, it was important to check if the other markers used are still working. B220 staining was found to be altered and appropriate controls were included.

Table v: Antibodies and chemicals used in FACS

Target	Clone	Conjugation	Dilution	Manufacturer
CD16/32	93	Purified	1/200	eBioscience
CXCR4 (CD184)	2B11	biotin	1/100	BD Pharmingen
PDL2 (CD273)	TY25	biotin	1/200	Biolegend
B220 (CD45R)	RA3-6B2	FITC	1/200	BD Pharmingen
B220 (CD45R)	RA3-6B2	eFluor 450	1/100	eBioscience
B220 (CD45R)	RA3-6B2	BV510	1/200	Biolegend
CD86	GL1	PE-Cy5	1/300	eBioscience
CD86	GL1	BV650	1/200	Biolegend
CD80	16-10A1	PE-Cy5	1/300	eBioscience
Fas (CD95)	Jo2	PE-Cy7	1/200	BD Pharmingen
CD73	eBioTY	PE-Cy7	1/300	eBioscience
CD38	90	APC	1/1000	eBioscience
CD38	90	FITC	1/100	eBioscience
Syndecan-1 CD138	281-2	BV421	1/300	Biolegend
GL7	GL-7	eFluor 450	1/200	eBioscience
NP		PE		In house
phospho-Akt (S473)	D9E	biotin	1/100	Cell Signalling
Annexin V		APC	1/20	BD Pharmingen
7-AAD			1/20	eBioscience
SA		FITC	1/200	BD Pharmingen
SA		PE-Cy5	1/200	BD Pharmingen
SA		BV650	1/200	BD Horizon

Table vi: Reagents included in Click-iT EdU reaction cocktail

Reagent	Amount for 1 sample (µl)
PBS	43.8
$CuSO_4$	1
AF 647 azide	0.25
1x Click-iT EdU buffer	5
Click-iT Wash buffer	10

2.6 Adoptive transfer

B cells were isolated from the spleen of unimmunised QM mice using the MACS system (Miltenyi Biotec GmbH, Germany). First, spleens were mashed and filter as described in section 2.5. Red cells were lysed by incubation with ACK lysis buffer (Gibco) for 1 min. Splenocytes were counted and re-suspended to a concentration of

$3x10^7$ cells in 270 µl MACS buffer (degassed PBS without calcium and magnesium, 0.5% BSA (Sigma-Aldrich), 2 mM EDTA (Sigma-Aldrich)). 30 µl $CD43^+$ microbeads (Miltenyi Biotec) were added and incubated at 4ºC for 15 min. Then, splenocytes were washed and re-suspended in 500 µl MACS buffer before being applied to the LS column (Miltenyi Biotec) under the magnetic field. After pass through of 9 ml of MACS buffer, a purity of >90% B cells was generated. Eluted cells were counted using a haemocytometer after trypan blue (Sigma-Aldrich) dead-cell exclusion. The number of NP^+B220^+ cells was determined using flow cytometry.

For TI responses studied in the spleen, a total of $2x10^5$ NP^+B220^+ B cells were injected i.v. in 200 µl RPMI in the lateral tail vein. For TD responses studied in the pLN, a total of $2x10^5$ of NP^+B220^+ B cells were injected i.v. in 200 µl RPMI in the lateral tail vein. In co-transfer experiments, a mix of $1x10^5$ of NP^+B220^+ B cells of each genotype respectively were injected i.v. One day after adoptive transfer mice were immunised with NP-CGG or NP-Ficoll, as described in the immunisations section.

2.7 Fluorescence-activated cell sorting (FACs)

Spleens, draining and distal lymph nodes were mashed, filtered and stained in a 100 µl volume. Fc gamma II and III receptors were blocked (30 min at 4˚C) using an anti-CD16/32 antibody diluted in FACS buffer. Surface antibodies were incubated (30 min at 4˚C) in FACS buffer and washed twice with FACS buffer. Dead cells were excluded by Hoechst 33342 inclusion. Cells were sorted in MoFlo high-speed cell sorter (Beckman Coultier). Sorted cells were checked for purity using flow cytometry, immediately pelleted and frozen at -80ºC.

2.8 mRNA detection

2.8.1 Total mRNA extraction

RNA was extracted from sorted cells (previously stored at -80˚C) using the RNeasy Mini kit or Micro kit (Qiagen, Crawley, UK) depending on the amount of cells, after homogenization of tissue using a QIAshredder column (Qiagen), following manufacturer's instructions. mRNA was eluted in 15 or 30 µl of RNase free water and stored at -80ºC until further requirement.

2.8.2 Production of cDNA

cDNA was obtained by addition of random oligo-dN6 (1 µg/µl) (Promega Biosciences, USA) to the mRNA, denatured at 70˚C for 10 min and instantly cooled on ice. Reverse transcription mix was added to retrotranscribe the previously denatured mRNA.

12 µl 5X first strand buffer (Invitrogen)

6 µl DTT 0.1 M (Promega)

3 µl dNTPs 10 mM (Invitrogen)

3 µl Moloney murine leukaemia virus (M-MLV) reverse transcriptase (Invitrogen)

1.5 µl RNasin RNase inhibitor (Promega)

1.5 µl RNase free water (Qiagen)

This mix was heated for 1 h at 41ºC and after for 10 min at 90ºC. cDNA was stored at -20˚C until further use.

2.8.3 Semi-quantitative real time PCR

PCR was carried out in 384 well plates (Applied Biosystems, USA) with 1 µl of cDNA plus the optimal concentration of primers and probes, previously determined, and Taqman Universal PCR Master Mix (Applied Biosystems). The plate was covered with clear adhesive foil (Applied Biosystems) and centrifuged for a few seconds to eliminate any air bubble. Amplification of the internal housekeeping gene (β2-microglobulin, NED labelled) was done at the same time as the target gene. Ccr7 was FAM labelled. Ackr4 was detected using SYBR Green PCR Master mix (Thermo Fisher Scientific).

PCRs were run using an ABI 7900 real-time PCR machine (Applied Biosystems):

2 min at 50ºC

10 min at 95ºC

Followed by 40 cycles of:

15 s at 95ºC

1 min 60ºC

SDS 2.2.2 (Applied Biosystems) software with manual determination of the threshold was used for the analysis of the fluorescence signals. The relative quantity of the fluorescent signals was made as described elsewhere (Livak and Schmittgen 2001) using the $2^{-\Delta\Delta Ct}$ method.

Target		**Nucleotide sequence**	**Concentration**
Ccr7	Forward	GGTGGCTCTCCTTGTCATTTTC	50 nM
	Reverse	GTGGTATTCTCGCCGATGTAGTC	50 nM
	Probe	TGCTTCTGCCAAGATGAGGTCACCG	150 nM
β2-micro globulin	Forward	CTGCAGAGTTAAGCATGCCAGTAT	60 nM
	Reverse	ATCACATGTCTCGATCCCAGTAGA	80 nM
	Probe	CGAGCCCAAGACC	125 nM
Ackr4	Forward	TGGATCCAAGATAAAGGCGGGGTGT	20 nM
	Reverse	TGACTGGTTCAGCTCCAGAGCCATG	20 nM

2.9 *In vitro* cell culture

B cells were isolated from spleen as described in section 2.6 and labelled with CellTrace Violet Cell Proliferation kit (Invitrogen) following the manufacturers' instructions. B cells were seeded in triplicates at $1x10^5$ cells/well into sterile flat-bottomed 96 well plates (Corning) and grown in 150 µl pre-warmed RPMI 1641 media supplemented with 10% FCS, 1% pen/strep, 10 mM HEPES, 50 µM 2-mercaptoethanol and 1 mM sodium pyruvate (all from Sigma-Aldrich). At selected time points after stimulation, cell were harvested by centrifugation and further analysed by flow cytometry.

2.9.1 NP-Ficoll-CCL19 stimulation

Cells were isolated from QM mice. NP^+B220^+cells were quantified by flow cytometry and seeded at $1x10^5$ NP^+B220^+cells in 200 µl of culture media per well. Cells were stimulated with 2 ng/well NP-Ficoll and if necessary, with 200 ng/well mouse recombinant CCL19 (R&D Systems). p-Akt status was analysed 30 min after stimulation.

2.10 Image analysis

The images obtained from the microscope were analysed offline with the software Fiji (Fiji Is Just ImageJ). All analyses were performed blindly for the genotype of the sample. All images were analysed using the same parameters for contrast and brightness.

2.10.1 Migration of NP^+ B cells to the B-T zone interphase

The region of interest (B follicle – T zone interphase) was marked manually with a thickness of 5-6 cells and converted into a mask. The original image was separated into Blue and Brown channels using the tool "Colour deconvolution" of ImageJ. The blue channel image, which corresponded with the NP staining, was thresholded with the "Default" method and the positive area for NP inside the mask area was measured. The fraction of positive area was represented graphically (Fig. 2.1).

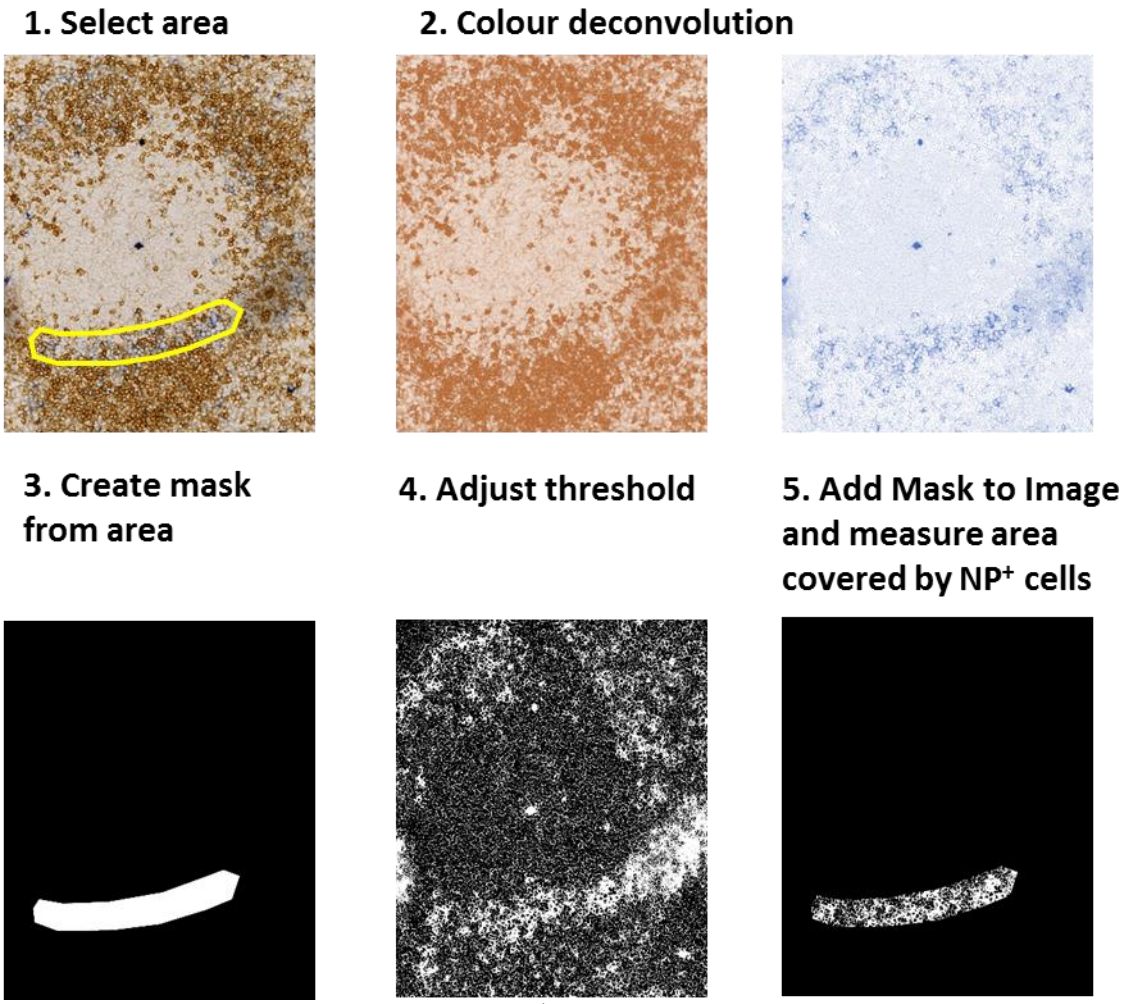

Figure 2.1: Technique for quantifying NP^+ cells at the T-B border. Representative example of a spleen section 4h post NP-Ficoll immunisation where NP^+ cells at the T zone-B follicle border were quantified. ImageJ was used to separate the blue and brown colours using colour deconvolution. The region of interest was drawn in the original image and converted into a Mask. The blue channel was thresholded using the "Default" Thresholding method and added using "Image calculator" to the Mask. The positive area in the resulting image was measured using "Analyze particles" and the % of the selected area covered by NP^+ cells calculated.

2.10.2 Infiltration of IgD^+ cells in the GC area

GC areas were marked manually in the original images and these areas were converted into masks. Using the tool "Colour deconvolution" from ImageJ, the original image was separated into blue and brown channels. The brown channel image, which corresponded with the IgD staining, was thresholded using the "Default" thresholding method. The particles in the area of the mask from the Thresholded image were measured and the % of GC covered by IgD^+ cells was calculated (Fig. 2.2).

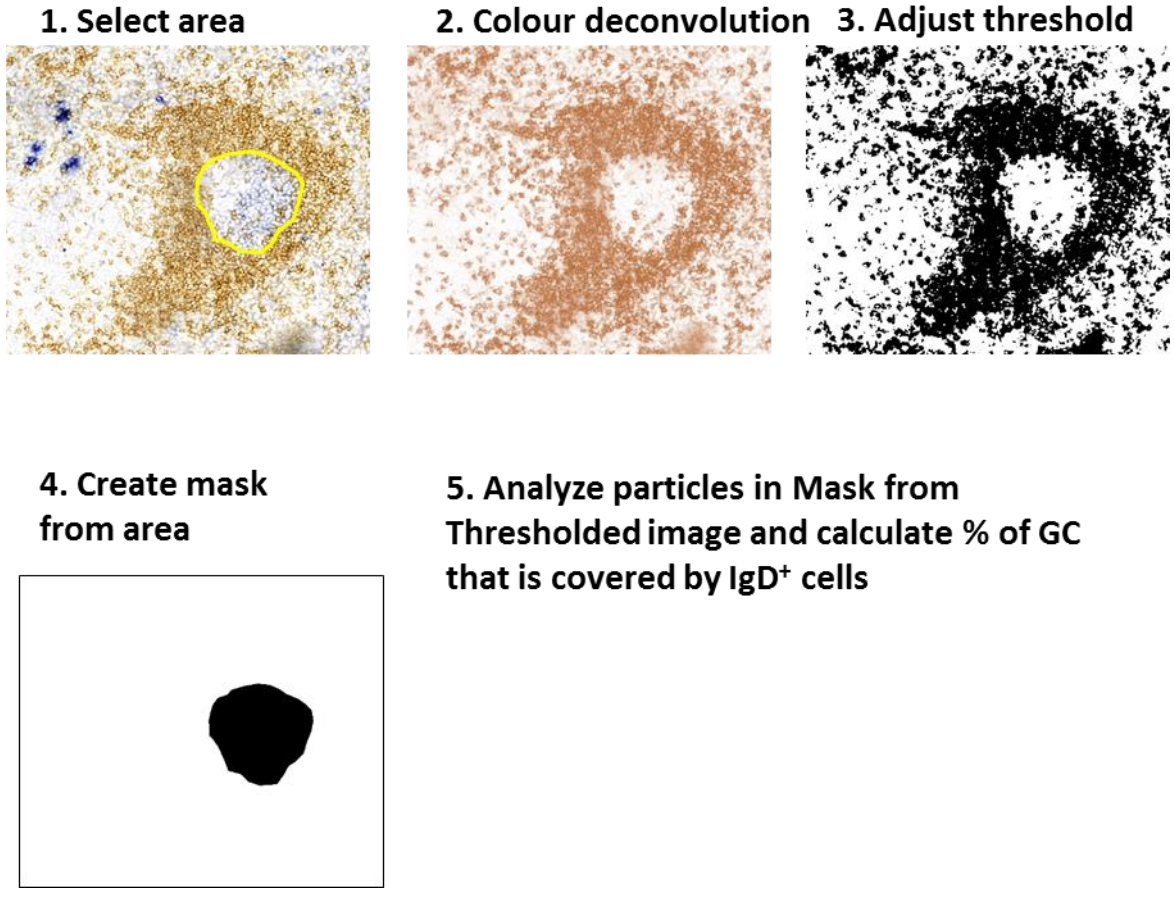

Figure 2.2: Technique for quantifying IgD^+ cells in the GC area. Representative example of a spleen section 8 days post immunisation with NP-CGG where IgD^+ cells invading the GC area were quantified. ImageJ was used to separate the blue and brown colours using colour deconvolution. The region of interest was drawn in the original image and converted into a Mask. The brown channel was thresholded using the "Default" Thresholding method and added using "Image calculator" to the Mask. The positive area of the resulting image between the mask and the brown thresholded image was measured using "Analyze particles" and the % of GC covered by IgD^+ cells calculated.

2.10.3 PNA/IgD ratio

The fraction of GC that was covered by naïve B cells was measured in immunofluorescence staining images from splenic sections of mice transferred with $eYFP^+$ antigen-specific B cells 4 days post-immunisation with NP-Ficoll. GCs were identified as regions positive for PNA. The area positive for PNA and negative for IgD in the GC were selected manually by drawing around the significant area. PNA^+ areas and IgD^- areas were selected independently in each specific fluorescence channel. The areas of interest were measured using the option "Analyze; Measure". Afterwards, the area in pixels was transformed to area in μm^2. The ratio was calculated as the fraction of (PNA^+ area/ IgD^- area *100).

2.10.4 DZ/LZ ratio

To investigate the intragerminal centre distribution, the fraction of GC that formed the DZ was analysed. Splenic sections from $ACKR4^{+/+}$ and $ACKR4^{-/-}$ mice at different time points post-immunisation were stained for PNA, CXCR4 and IgD. GCs were identified as regions positive for PNA and negative for IgD and selected manually by drawing around the area. DZ/LZ distribution was determined by the $CXCR4^+$ staining. DZ areas positive for CXCR4 were selected manually. The fraction of GC covered by the DZ was calculated as ($CXCR4^+$ area/ PNA^+ area *100).

2.10.5 $CXCR4^+$ cells in GC-T zone interphase

In order to investigate the possibility of increased PC output from the GC, splenic sections from $ACKR4^{+/+}$ and $ACKR4^{-/-}$ mice at different time points post-immunisation

were stained for PNA, CXCR4 and IgD. For this quantification only the GCs that were orientated appropriately were analysed. GCs had to be adjacent to the T zone, with a clear separation between LZ and DZ, denoted with CXCR4 staining. T cell areas were distinguished as IgD^- areas in the centre between IgD^+ follicles. $CXCR4^+$ plasmablasts that were positioned on the GC-T zone interphase were counted manually. The GC-T zone interphase was identified by the region were GCs were adjacent to the T zone with no IgD^+ B cells in the middle and its length was measured using the tool "Analyze: Measure". Numbers of $CXCR4^+$ plasmablasts were represented in relation to the length of the interphase.

2.10.6 Counts of $CD3^+$ cells in GC areas

In order to investigate the possibility of enlarged LZ areas due to increased numbers of T cells, the numbers of T cells per GC were analysed. Splenic sections from $ACKR4^{+/+}$ and $ACKR4^{-/-}$ mice at different time points post-immunisation were stained for PNA, CD3 and IgD. GCs were identified as regions positive for PNA staining. $CD3^+$ cells inside each GC were counted manually at 20x magnification. $CD3^+$ cell numbers were divided by PNA^+ area, in order to represent the number of positive cells per unit of area.

2.10.7 Counts of c-Myc^+ cells in GC areas

To explore the possibility of enlarged LZ areas due to increased expression of c-Myc by GC B cells, the numbers of GC B cells expressing c-Myc were analysed. Splenic sections from $ACKR4^{+/+}$ and $ACKR4^{-/-}$ mice at different time points post-immunisation were stained for PNA, c-Myc and IgD. GCs were identified as regions positive for

PNA staining. c-Myc$^+$ cells inside each GC were counted manually at 20x magnification. c-Myc$^+$ cell numbers were divided by PNA$^+$ area, in order to represent the number of positive cells per unit of area.

2.10.8 Counts of GFP$^+$ MBCs in different distLN areas

The distribution of GFP$^+$ MBCs within the distant lymph nodes of Cγ1-Cre mTmG ACKR4$^{+/+}$ and Cγ1-Cre mTmG ACKR4$^{-/-}$ mice was analysed 8 days post-immunisation. GFP$^+$ cells were counted manually from digital images of axillary lymph nodes stained for IgD and Lyve-1. The total area of the axillary LN and of the different areas were measured (vessels, follicles and T zone). The number of GFP$^+$ MBCs was represented in relation to the area there were in.

2.10.9 Counts of GFP$^+$ MBCs in SCS

The number of GFP$^+$ MBCs that have migrated to the SCS was investigated in popliteal lymph node sections from Cγ1-Cre mTmG ACKR4$^{+/+}$ and Cγ1-Cre mTmG ACKR4$^{-/-}$ mice at different time points post-immunisation stained for IgD and Lyve-1. GFP$^+$ cells in the SCS were counted manually. The portion of the SCS analysed had to be intact, this is that the floor and ceiling LECs were present, marked by Lyve-1 staining and TdTomato expression, respectively. The length of the intact SCS was measured using the tool "Analyze: Measure". The number of GFP$^+$ MBCs was represented in relation to the length of the SCS measured.

2.11 CCL19 injection

Recombinant mouse CCL19 (R&D systems) was injected in the same footpad where antigen was injected at a concentration of 3 μg/ 20 μl PBS, 24 h or 6 h before lymph nodes were taken.

2.12 Statistical analysis

All statistical tests were performed using GraphPad Prism 6 software. Two-tailed Mann-Whitney non-parametric test was used to calculate significance.

In Chapter 4, where 2 parameters coming from the same individual mouse are compared, Wilcoxon matched-pairs signed rank test (paired non-parametric test) was used to calculate significance.

P values <0.05 were considered significant (*).

*p<0.05, ** p< 0.01, *** p<0.001, ****p<0.0001

Chapter 3. The role of ACKR4 in the murine splenic B cell responses

3.1 Introduction and objectives

3.1.1 Migration of GC B cells

GC B cells are type of antigen-specific B cell that, although they are considered to be mature, they must differentiate further into high-affinity plasma cells or memory B cells. These cells have very distinct characteristics and a specific transcriptional programme. The signals that regulate this differentiation are far from being fully understood. In order for this differentiation to occur, GC B cells must migrate within the GC microenvironments and respond to different signals from FDCs and Tfh cells, which include cytokines and chemokines.

Originally, GC B cells were considered to be a stage of non-migratory antigen-activated cells as they were unable to recognise and bind to HEVs, which normally mediate the entrance of lymphocytes to lymphoid tissues (Reichert, Gallatin et al. 1983). GC B cells are irresponsive *in vitro* to signals such as CXCL12, CCL19 and CXCL13, which drive migration of other B cells such as naïve and MBCs (Bleul, Schultze et al. 1998, Roy, Kim et al. 2002). Today, we know that GC B cells constitute a highly migratory population although they are confined to the local GC microenvironment. Two-photon microscopy imaging of the GC *in vivo* has allowed investigation of the movement of B cells within the GC (Allen, Okada et al. 2007, Hauser, Junt et al. 2007, Schwickert, Lindquist et al. 2007) and, together with mathematical modelling, demonstrated that GC B cells actively undergo chemotaxis to maintain GC zoning (LZ/DZ). Additionally, chemokine sensitivity is quickly downregulated (Figge, Garin et al. 2008).

Responsiveness to CXCL12 *via* CXCR4 is required for DZ/LZ segregation in the GC, while responsiveness to CXCL13 *via* CXCR5 helps to guide GC B cells towards the LZ (Allen, Ansel et al. 2004). CXCR4-deficient GC B cells are prevented from entering the DZ; but in the LZ cell-cycle progression occurs normally, they accumulate less mutations and PC development is normal. However, when GC B cells are restricted to the LZ there is increased generation of MBCs (Bannard, Horton et al. 2013). Therefore, responsiveness of GC B cells to chemokines and cytokines needs to be coordinated in order to balance proliferation versus differentiation.

Moreover, once GC B cells differentiate to leave the GC and become PCs or MBCs, their responsiveness to chemokines needs to change so they are able to migrate to their respective niches.

3.1.1a Regulation of chemokine receptor signalling

Chemokine receptor signalling needs to be tightly regulated. Limitation and desensitization/resensitization of chemokine receptor signalling is important for the transzone migration frequencies, the re-entry into the cell cycle and the closure of the response in the GC (Meyer-Hermann, Mohr et al. 2012).

GC B cells regulate their responsiveness to chemokines CXCL12 and CXCL13 by two Regulator of G protein signalling (RGS) molecules, the sensitizer RGS1 and the desensitizer RGS13. CD40 stimulation augments RGS13 while engagement of the B cell receptor (BCR) enhances the expression of RGS1 (Shi, Harrison et al. 2002). Mice deficient in RGS1, a GTPase that activates proteins for Gα subunits, have GCs in steady-state conditions and immunisation of these mice leads to exacerbated GC

formation and abnormal trafficking of plasma cells (Moratz, Hayman et al. 2004). As compared to WT B cells, a higher percentage of unstimulated RGS1-deficient B cells migrate towards CXCL12 (Moratz, Hayman et al. 2004). Despite the abnormalities in mice deficient in RGS1, affinity maturation is not altered (Moratz, Hayman et al. 2004). LZ GC B cells express high levels of RGS13 which desensitises chemokine signalling from CXCR4 and CXCR5 (Mountz, Wang et al. 2011). Furthermore, GC B cells also regulate their responsiveness in regard to fluctuating levels of chemokines in the GC zones, for example CXCL13 is expressed in the LZ and CXCL12 in the DZ (Allen, Ansel et al. 2004).

Atypical chemokine receptors (ACKRs) also provide a way to regulate responsiveness to chemokines, as they are able to internalise chemokines to influence gradients (Ulvmar, Hub et al. 2011). The aim of this project has been to elucidate the role of atypical chemokine receptor 4 (ACKR4) which is able to regulate the responsiveness of cells to CCL19, CCL21 and CCL25, during the GC response.

3.1.2 c-Myc in B cells and in the germinal centre

In the case of human hepatocellular carcinoma, tumours that express ACKR4 have been shown to be less malignant. ACKR4 inhibited tumour progression by scavenging CCL19 and CCL21, reducing their binding to CCR7 and, therefore, the signalling driven by CCR7. CCR7 signals through the Akt-GSK3β pathway, and its downregulation leads to downregulation of c-Myc (Shi, Yang et al. 2015). In this Chapter, findings are presented as to the link between ACKR4 and c-Myc in the GC response.

The c-Myc oncogene was identified more than three decades ago and aberrant c-Myc has been associated with many cancers (Nie, Hu et al. 2012). As to B cells, c-Myc has also been found to be linked to chromosomal translocations in human GC-derived B cell lymphomas (Klein and Dalla-Favera 2008), such as in Burkitt lymphoma, where it collaborates with PI3K for its development (Sander and Rajewsky 2012). c-Myc is a transcription factor which acts as master regulator of cellular proliferation and apoptosis in haematopoietic and non-haematopoietic cells (Calado, Sasaki et al. 2012). The structure of c-Myc is a basic-loop-helix-leucine zipper and c-Myc binds to DNA in a sequence specific manner (E-boxes) when bound to Max (Perez-Roger, Kim et al. 1999). Expression of c-Myc is associated with cell activation and is induced during the transition from G0-G1 to the S-phase of the cell cycle (Nie, Hu et al. 2012). c-Myc does not act as a global transcriptional amplifier but activates and represses transcription of discrete gene sets which then leads to changes in the cellular state that can increase the global production of RNA (Sabo, Kress et al. 2014).

In the mouse, germline inactivation of c-Myc causes embryonic lethality at E10 (de Alboran, O'Hagan et al. 2001). Therefore, to study the role of cMyc in mature B cells, c-Myc has been specifically deleted in CD19 B cells using the LoxP/Cre system. Using this system, it has been shown that c-Myc is required for normal B cell activation and proliferation, as c-Myc deficient B cells express low levels of CD95 (Fas) and CD95L (FasL) after activation (de Alboran, O'Hagan et al. 2001). c-Myc deficient B cells express normal surface levels of activation markers and are more resistant to CD95 and staurosporine-induced and spontaneous cell death (de Alboran, Baena et al. 2004). The early stages of B cell differentiation *in vivo* require c-Myc which endows B cell identity *via* direct transcriptional regulation of Ebf-1 (Vallespinos, Fernandez et al. 2011) and amplification of calcium signalling (Habib, Park et al. 2007). In the B cell lymphoma

murine cell line WEHI 231, BCR-mediated apoptosis is linked with a reduction of c-Myc expression resulting from a drop in NF-κB/Rel (Wu, Arsura et al. 1996). c-Myc has also been shown to play an important role in antibody secretion as c-Myc deficient B cells hyper-secrete IgM and cannot undergo CSR due to AID not being activated (Fernandez, Ortiz et al. 2013).

Initially, c-Myc was considered to not to have a role in GC B cell proliferation (Klein, Tu et al. 2003) as GC B cells, compared to cells in the surrounding compartments, express very little c-Myc. Moreover, the master regulator of GC B cell phenotype, Bcl-6, interacts with Miz-1, a transcription factor that, like c-Myc, represses CDK inhibitors (Phan, Saito et al. 2005). Therefore, GC B cells express high amounts of a transcription factor, Miz-1, that can act as an alternative to c-Myc. Bcl-6 can also repress the transcription of c-Myc and of cyclin D2, a c-Myc target (Shaffer, Yu et al. 2000). Furthermore, GC B cells express mainly cyclin D3, which controls G1/S-phase transition and is not controlled by c-Myc (Perez-Roger, Kim et al. 1999).

By using a c-Myc conditional KO, Calado and co-workers demonstrated that c-Myc is expressed in both mature and immature GCs and that c-Myc is indeed essential for the formation and maintenance of GCs (Calado, Sasaki et al. 2012). During the early stages of GC formation, GC B cells express both cyclin D2 and cyclin D3, which contribute to the hyper-proliferative characteristics of GC B cells. In mature GCs, c-Myc expressing cells were localised mostly in the LZ and these cells have the characteristics of activated cells (Calado, Sasaki et al. 2012). The authors suggested that GC B cells have a "cyclic dependence" on c-Myc for their proliferation, characterised by a very transient expression of c-Myc that is able to trigger competence for a GC B cell to enter a phase of proliferative expansion (Calado, Sasaki et al. 2012).

Using c-Myc GFP reporter mice, Dominguez-Sola and colleagues observed a transient expression of c-Myc in B cells that were engaging with T cells in the early phases of GC commitment (Dominguez-Sola, Victora et al. 2012). The authors further found that c-Myc expression in the GCs was restricted to a few cells in the LZ (around 10%) and that this expression may specify re-entry of cells into the DZ B cell pool. The few cells that express c-Myc may be the reason why other works have reported that GC B cells do not express c-Myc. (Dominguez-Sola, Victora et al. 2012). Dominguez-Sola and co-workers hypothesised that repression of c-Myc expression in the DZ is important to limit the rounds of cell division each cell undergoes before each round of affinity-based selection to one division. This is important to allow the normal progression of somatic hyper-mutation (Dominguez-Sola, Victora et al. 2012).

3.1.3 Objectives of this chapter

The work presented in this chapter has investigated the response of ACKR4-deficient mice to T-dependent and T-independent antigens (NP-CGG, SRBC and NP-Ficoll) at various times after immunisation. The role of ACKR4 has been studied extensively in T cells and various cancer models. Despite specific expression of ACKR4 at the late stages of B cell differentiation, the role of ACKR4 has never been studied before in regard to the B cell response.

The work has aimed to test whether ACKR4 deficiency in the B cells or in the surrounding environment has a role in the GC response, detailed as follows:

1. Where are ACKR4 and related molecules expressed in the murine spleen and lymph nodes, in terms of both at the mRNA and protein?

2. Does ACKR4 deficiency have an effect on the germinal centre response? Specifically, on:
    a. GC B cell numbers and LZ/DZ differentiation
    b. GC output: plasma cells and memory B cells
    c. Expression of key signalling molecules
    d. Affinity maturation and antibody production
    e. Secondary response

3.2 Results

3.2.1 Ackr4 expression at mRNA level

In order to investigate the stages of mature B cell differentiation at which the atypical chemokine receptor 4, Ackr4 (previously known Ccrl1) is expressed, a search was performed using the Immunological Genome project (Immgen) dataset. Immgen is an online data base containing gene expression data from a large variety of cells types of the murine immune system (Heng and Painter 2008). A first overview of Immgen data for Ackr4 expression revealed that it is expressed in one population of B cells and two populations of stromal cells (green squares Fig. 3.1 upper). The stromal cells that express Ackr4 are lymphatic endothelial cells (LECs) from lymph nodes and cortical and medullary epithelial cells from the thymus. Within the forty key haematopoietic cell populations for which mRNA expression profiles are deposited in the Immgen database, Ackr4 mRNA was found to be specifically upregulated just in splenic GC B cells (Fig. 3.1 lower). For the purposes of this project, expression of Ackr4 in the B cell population is of particular interest as the role of Ackr4 in the lymphatic endothelial cells of the lymph node subcapsular sinus has been previously studied (Ulvmar, Werth et al. 2014).

Ackr4 shares the ligands CCL19 and CCL21 with Ccr7. Hence, expression of Ccr7 was also checked as to the database (Fig. 3.2). Contrary to Ackr4, Ccr7 expression was observed to be more abundant among the different haematological populations (green and red squares Fig. 3.2 upper), especially among the different T cell and DC subpopulations. Interestingly, Ccr7 mRNA level is greatly downregulated in GC B cells (Fig. 3.2 lower).

Victora and co-workers (Victora, Dominguez-Sola et al. 2012) have performed a gene array analysis of murine and human LZ and DZ GC B cells. These data are available

online at the GEO (Gene Expression Omnibus) database, with accession numbers GSE38696 for *Mus musculus* and GSE38697 for *Homo sapiens*. Comparison of murine Ackr4 and Ccr7 levels for the above two cell types revealed an inverse expression pattern, with Ackr4 strongly up-regulated in the DZ and Ccr7 up-regulated in the LZ (Fig. 3.3). This pilot data encouraged further study of Ackr4 expression during the course of an immune response. Total RNA was isolated at different time points from splenic tissue sections of WT mice immunised with SRBC. Ackr4 expression was analysed by qPCR. Fig. 3.4a shows that Ackr4 expression increases at a constant rate from day 2 to day 3 post-immunisation (Fig. 3.4a). Ackr4 expression plateaus at its highest level around a week post primary immunisation. This indicates that Ackr4 may indeed be expressed specifically in structures that appear later in the immunological response, for example, the germinal centre. To confirm these results further, different populations of B cells were sorted from the draining and distant lymph nodes of WT mice that have received Cγ1-Cre x QM ROSAeYFP B cells and 8 days post-immunisation in the hind feet with NP-CGG (Fig. 3.4b). The qPCR analysis of the different FACS-sorted populations confirmed that Ackr4 was up-regulated up to a thousand times in GC B cells compared to naïve B cells, while memory B cells (MBCs), both from draining and distant LN, had intermediate levels of expression, 5-10 times higher than naïve B cells. In plasma cells, Ackr4 expression was found to be low (Fig. 3.4c, left). Ccr7 expression was studied in the same sorted populations and revealed a constant level of Ccr7 mRNA expression among all B cell populations studied except for plasma cells, where expression was low (Fig. 3.4c, right).

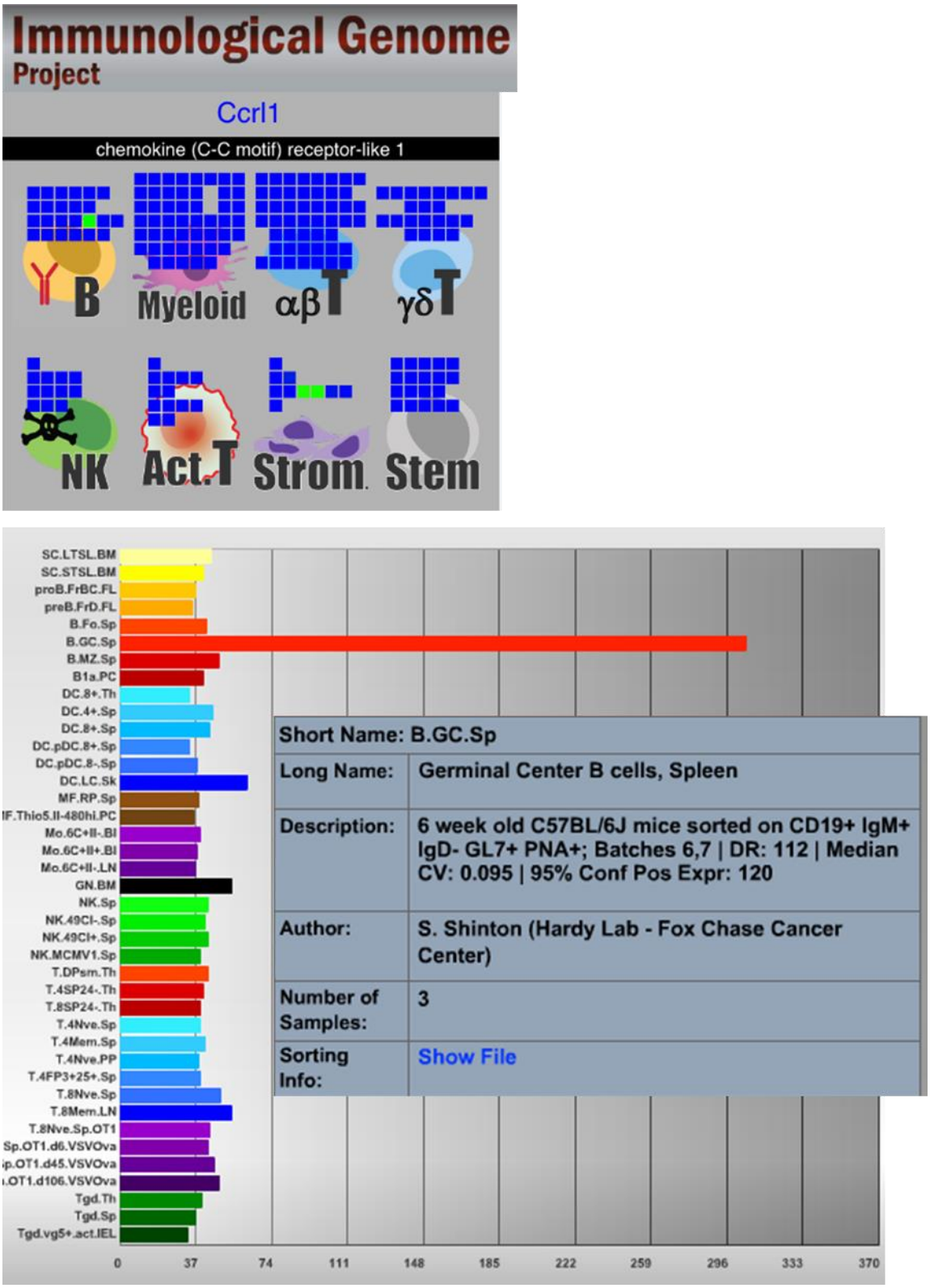

Figure 3.1: Ackr4 is expressed by germinal centre B cells. Ackr4 (Ccrl1) gene expression in the haematopoietic populations as revealed from the Immgen database.

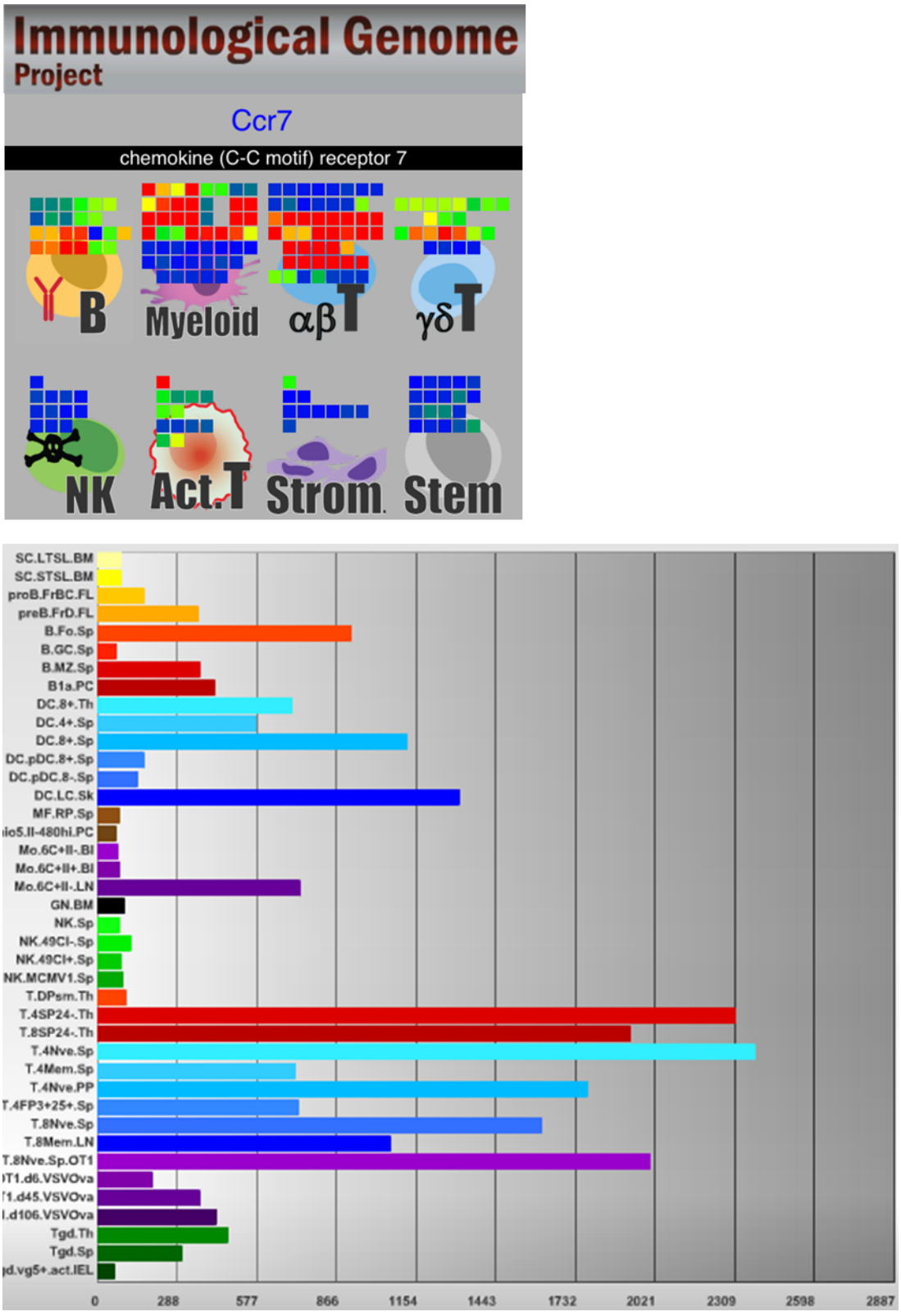

Figure 3.2: Ccr7 is broadly expressed by cells of the haematopoietic system. Ccr7 gene expression in the haematopoietic populations as revealed from the Immgen database.

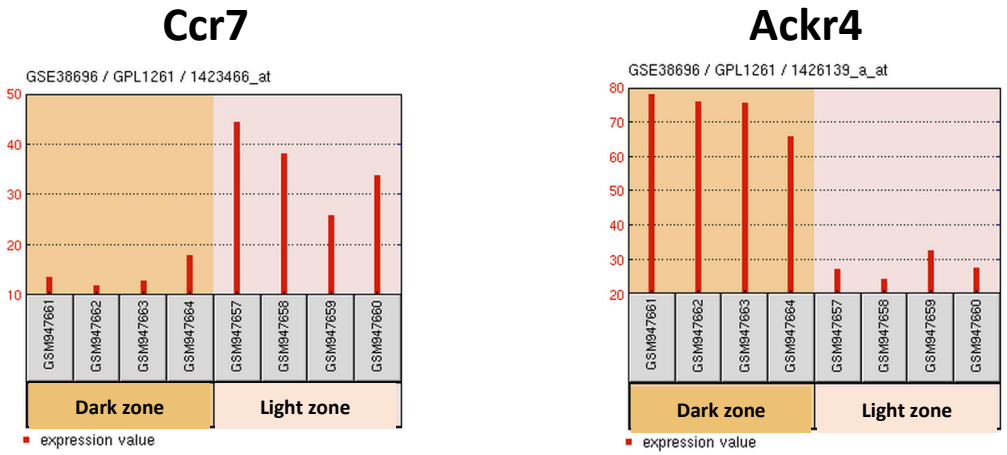

Figure 3.3: Ackr4 and Ccr7 expression GC B cell subsets. Ccr7 (left) and Ackr4 (right) expression as measured by gene array in germinal centre B cell subsets (GSE38696, Victora et al. Blood 2012).

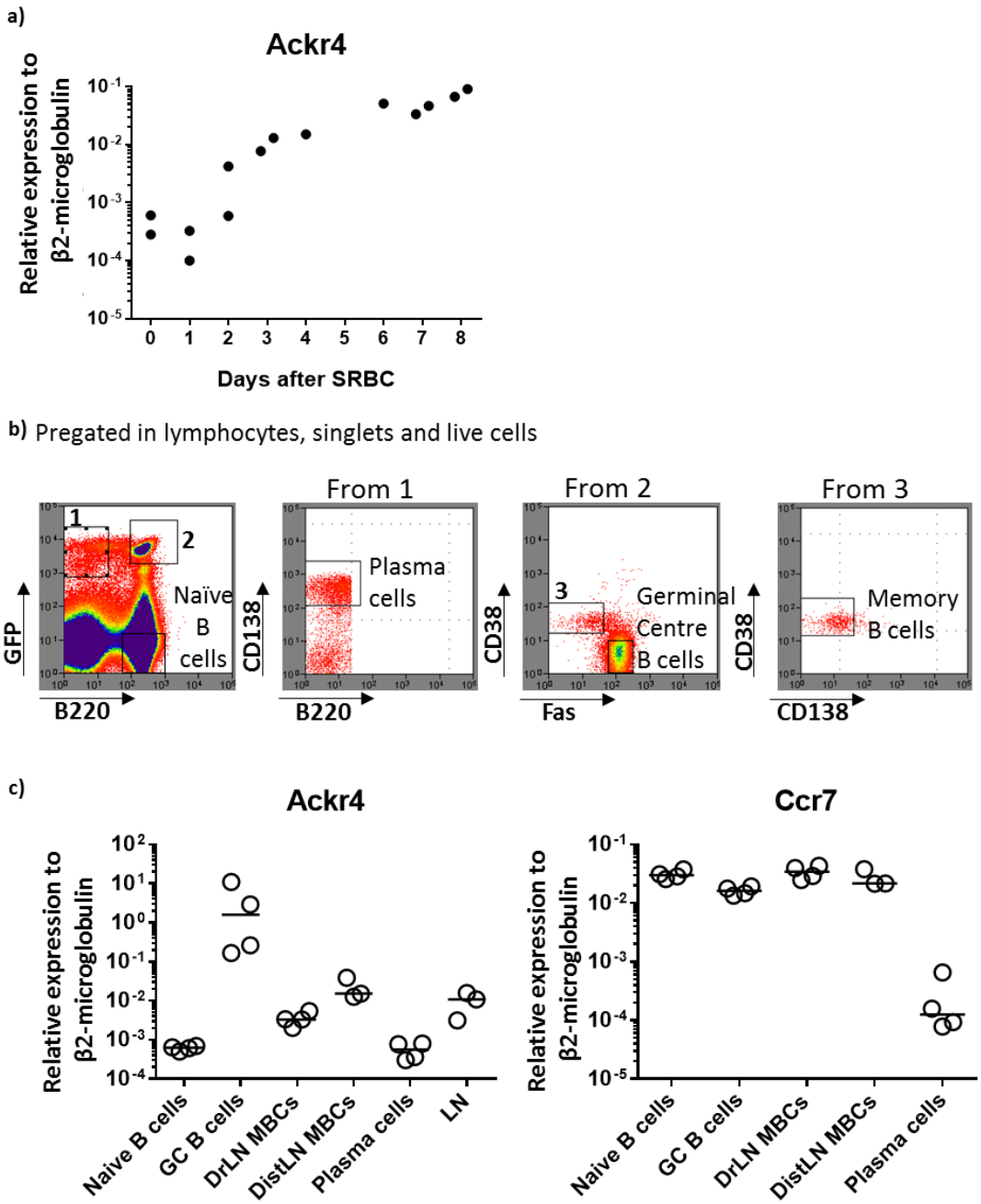

Figure 3.4: Ackr4 is expressed by GC B cells (2). a) Ackr4 expression was measured by qPCR from splenic sections during a time course response of WT mice immunised with SRBC. b) Representative sorting strategy for different B cell subsets sorted from lymph nodes of WT mice transferred with Cγ1-Cre x QM ROSAeYFP B cells 8 days post-immunisation with NP-CGG. c) Ackr4 (left) and Ccr7 (right) expression measured by qPCR in B cell subsets sorted in b).
Each symbol represents one mouse. Horizontal line represents the median.
Key: DrLN: draining lymph node; DistLN: distant lymph node; GC: germinal centre, MBCs: memory B cells, SRBC: sheep red blood cells.

3.2.2 ACKR4 expression at protein level

To determine the tissue distribution of ACKR4 expression at the protein level, immunofluorescence histology of splenic and popliteal lymph node sections was performed. For this purpose, mice were immunised with SRBC i.v. or with NP-CGG in the hind feet and the response analysed 8 days later. Immunofluorescence staining of spleen sections showed than ACKR4 is expressed on PNA^+ B cells and levels expressed by DZ and LZ GC B cells were indistinguishable (Fig. 3.5a, 3.5b). In the spleen of $ACKR4^{+/GFP}$ mice, where GFP replaces one copy of the Ackr4 gene (See Materials and Methods 2.1.3), GFP expression is also observable in the GCs (Fig. 3.5d, 3.5e). Antibody staining and $ACKR4^{+/GFP}$ mice both revealed that ACKR4 is expressed by a thin layer of cells surrounding the marginal zone in the red pulp. Negative staining controls without primary antibody (Fig. 3.5c) or on $ACKR4^{-/-}$ tissue (Fig. 3.5f, 3.5g) demonstrated the specificity of ACKR4 staining in the GC. However, a weak staining could be observed in the follicle area that may be due to un-specificity of the secondary antibody. In lymph nodes, ACKR4 expression corresponded with that seen in the spleen, with ACKR4 being homogenously expressed throughout the GC (Fig. 3.5h, 3.5i). Additionally, as described by Ulvmar et al. (Ulvmar, Werth et al. 2014), ACKR4 was observed to be expressed by the lymphatic endothelial cells in the subcapsular sinus of the lymph node independently of immunisation (Fig. 3.5h). This area of ACKR4 expression may functionally correspond to the stroma staining found around white pulp in the spleen. The function of stromal ACKR4 in spleen has not been studied in detail (personal communication Antal Rot, University of York)

The distribution of the chemokines that bind ACKR4 and CCR7 was studied by immunofluorescence histology. CCL19 and CCL21 are equipotent ligands of ACKR4. While CCL19 is soluble, CCL21 binds to the matrix and has stronger pro-migratory

properties than CCL19 (Ulvmar, Werth et al. 2014). Because CCL19 is soluble, it is almost undetectable in mouse tissues and its distribution is impossible to assess, but it can be speculated that, as CCL19 is produced at the same locations than CCL21, ACKR4 is able to form similar gradients of both of its ligands (Ulvmar, Werth et al. 2014).

CCL21 expression was investigated by antibody staining. In the spleen, CCL21 was observed to be expressed in the T zone areas and diffuses to the exterior of the white pulp. CCL21 was also highly expressed in HEVs, as previously described (Carlsen, Haraldsen et al. 2005) (Fig. 3.6a). There were no obvious differences in the distribution and expression levels of CCL21 between spleens from ACKR4$^{+/-}$ and ACKR4$^{-/-}$ mice (Fig 3.6b). CCL21 expression was also analysed in draining LNs post-immunisation with NP-CGG. In ACKR4$^{+/+}$ pLNs (Fig. 3.7a), CCL21 was mainly present in the SCS and in the T zone. A gradient of CCL21 from the T zone to the SCS was observed. This gradient is caused by the scavenging of CCL19/21 by the ACKR4 expressed in the lymphatic endothelial stroma in the SCS (Ulvmar, Werth et al. 2014). In ACKR4$^{-/-}$ pLN (Fig. 3.7b), CCL21 was also observed to be present in the SCS and in the T zone, but there is no gradient between the T zone and the SCS. The positive staining for CCL21 in the SCS can be explained by passive adhesion of CCL21 to ACKR4 and not by the production of CCL21 by lymphatic endothelial cells (personal communication Antal Rot, University of York). The presence of GCs was not seen to influence CCL21 distribution, neither in ACKR4$^{+/+}$ nor in ACKR4$^{-/-}$ pLNs.

As CCL19 is impossible to detect by antibody staining, CCL19-eYFP mice which express Cre after the Ccl19 promoter were examined as in these mice there is specific expression of eYFP in CCL19^{+} cells. Five days post SRBC immunisation (Fig. 3.8a),

the eYFP signal was mainly observed in the T zone and the outer follicle. Follicles were seen to be negative for CCL19. In GCs, low level of CCL19 production was observed which is comparable to the levels observed in the T zone. In non-immunised conditions (Fig. 3.8b), CCL19 was also observed to be produced in the T zone and in the outer follicles.

CCR7 expression was studied at the protein level in different B cell subsets by flow cytometry. CD4 T cells are positive for CCR7 expression (Debes, Hopken et al. 2002) and these cells were used to gate a positive cell population. Eight days post NP-CGG immunisation, CCR7 was seen to be expressed in MBCs, both from the draining and distant lymph nodes and PCs, while GC B cells and naïve B cells had very low levels of CCR7 expression (Fig. 3.9a and 3.9b). Protein expression levels in the different B cell subsets did not correlate with the results obtained by qPCR (Fig. 3.4c), where mRNA expression was constant in all B cell subsets and lower in PCs. This difference may reflect post-translational modifications playing an important role in regulating protein surface levels.

Outcomes from the above studies have revealed the expression of chemokine receptors ACKR4 and CCR7, and of their shared ligands CCL19 and CCL21, in the spleen and lymph nodes. While CCR7 is broadly expressed by T lymphocytes, B lymphocytes do not express it at high levels. ACKR4 is only expressed in GC B cells and in a layer of LECs in the SCS or stroma surrounding MZ. This differential expression may indicate that CCR7-dependent responses are regulated by fluctuating levels of ACKR4 expression in the SLOs, which creates gradients of their ligands from the T zone, where CCL19 and CCL21 are produced, towards the outer zone of the follicles.

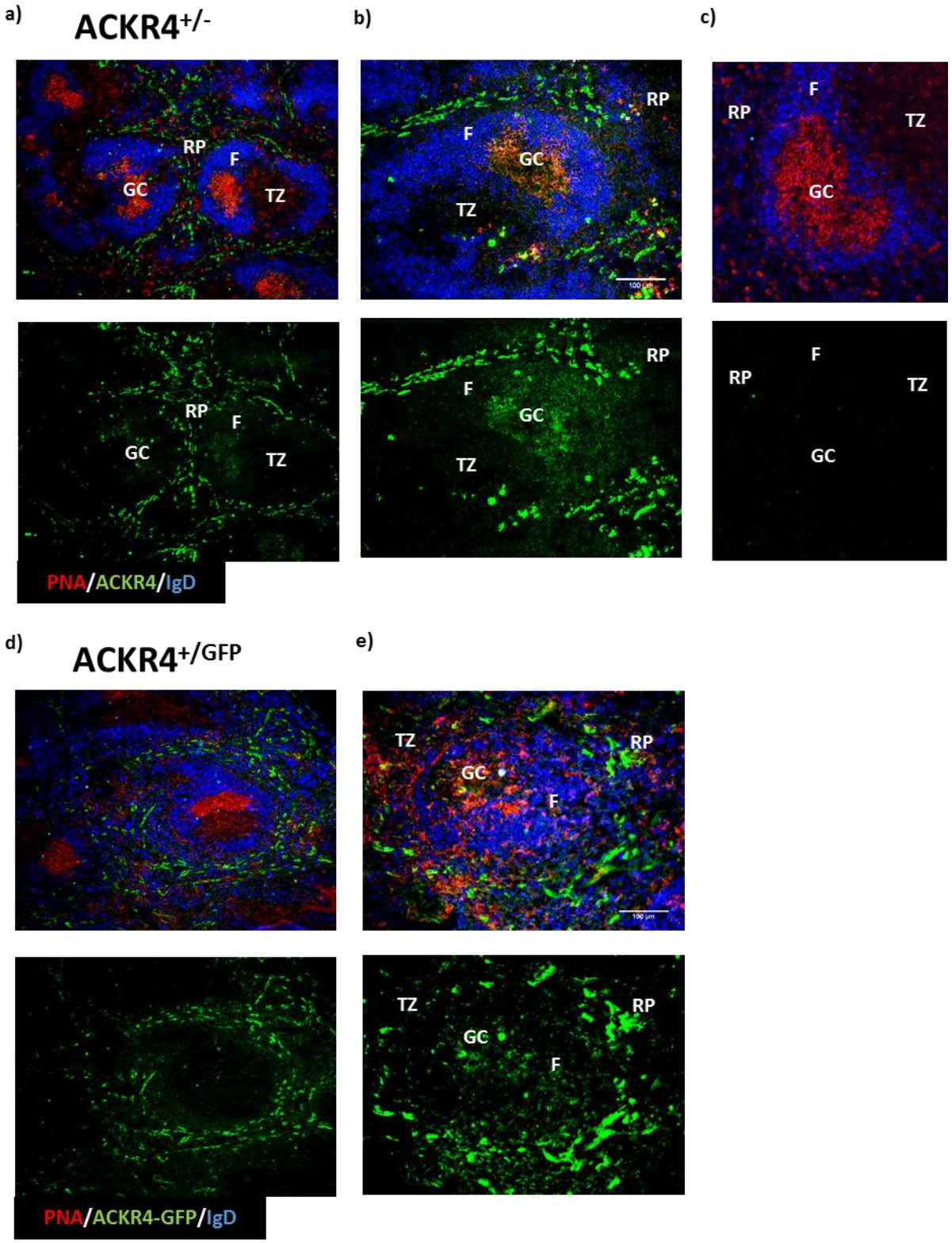

Figure 3.5 (1): ACKR4 is expressed by GC B cells. a-e) Representative splenic immunofluorescence images of ACKR4 (green), PNA (red), IgD (blue). a-b) ACKR4$^{+/-}$ spleen 8 days post-immunisation with SRBC i.v. c) Negative control for secondary antibody in ACKR4$^{+/-}$ spleen 8 days post-immunisation with SRBC i.v. d-e) ACKR4-GFP (green), PNA (red), IgD (blue) from ACKR4$^{+/GFP}$ spleen 8 days post-immunisation with SRBC i.v.
Key: F: B follicle; TZ: T zone; RP: red pulp; GC: germinal centre; PNA: peanut agglutinin; SCS: subcapsular sinus; PC: plasma cells. Scale bar: 100 µm.

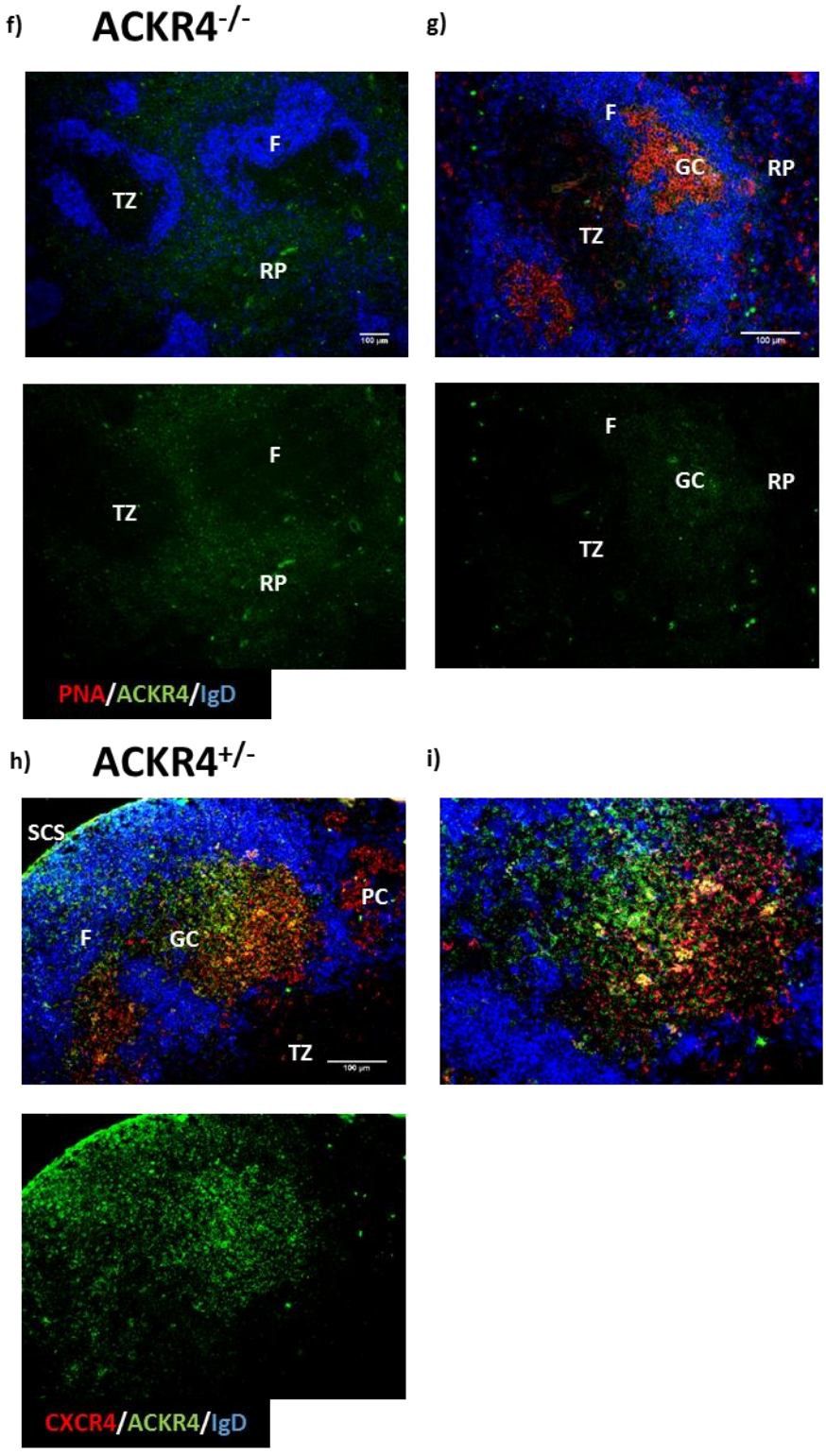

Figure 3.5 (2): ACKR4 is expressed by GC B cells. f-g) Representative immunofluorescence images of ACKR4$^{-/-}$ spleen 8 days post-immunisation with SRBC i.v. h-i) Representative immunofluorescence images of CXCR4 (red), ACKR4 (green), IgD (blue) of WT popliteal lymph node 8 days post-immunisation with NP-CGG s.c. in the hind feet.
Key: F: B follicle; TZ: T zone; RP: red pulp; GC: germinal centre; PNA: peanut agglutinin; SCS: subcapsular sinus; PC: plasma cells. Scale bar: 100 µm.

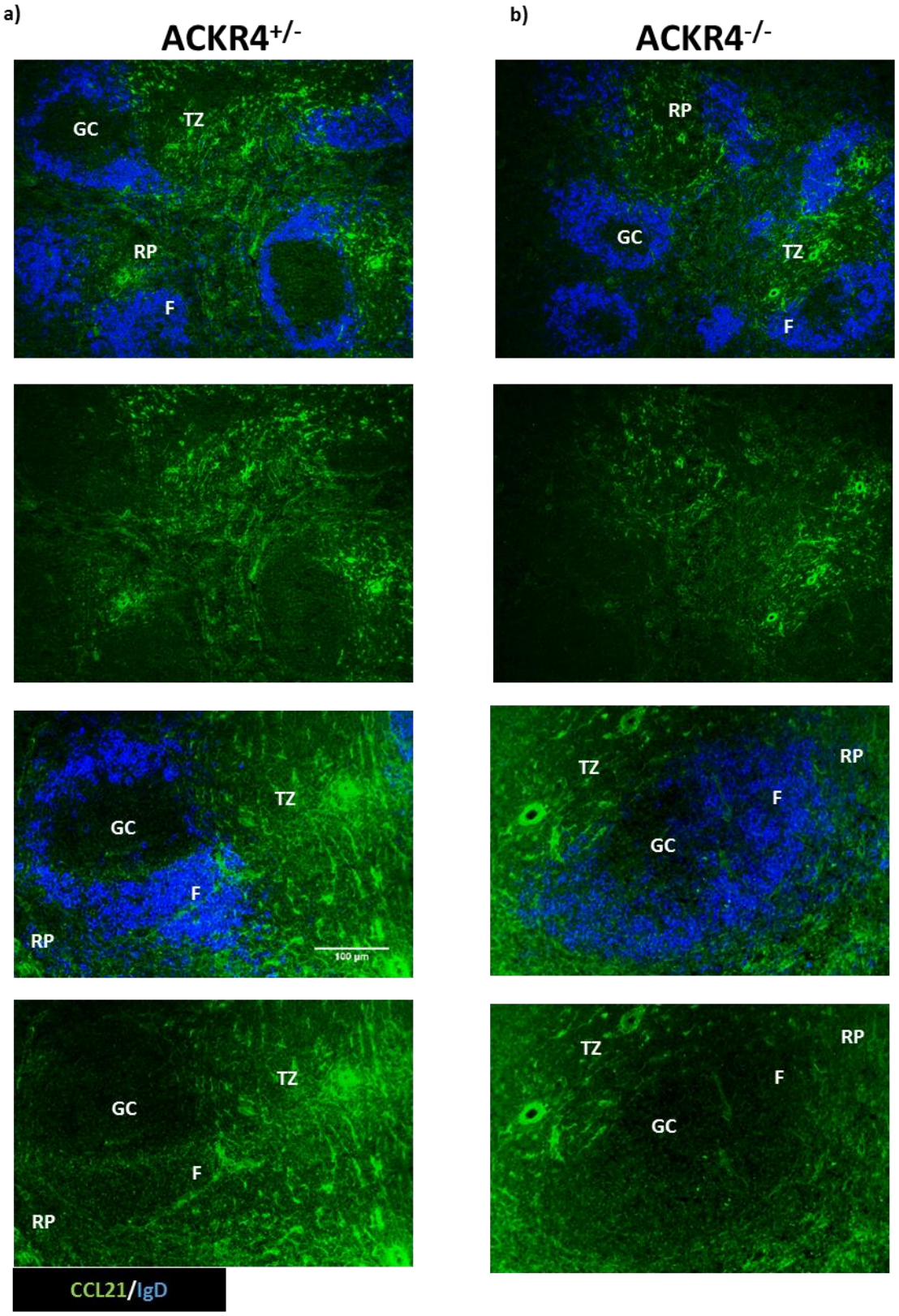

Figure 3.6: CCL21 expression in the spleen. a-b) Representative splenic immunofluorescence images for CCL21 (green), IgD (blue). a) WT spleen 8 days post-immunisation with NP-CGG i.p. b) ACKR4$^{-/-}$ spleen 8 days post-immunisation with NP-CGG i.p. Upper: lower magnification images. Lower: higher magnification images.
Key: F: B follicle; TZ: T zone; RP: red pulp; GC: germinal centre. Scale bar: 100 µm.

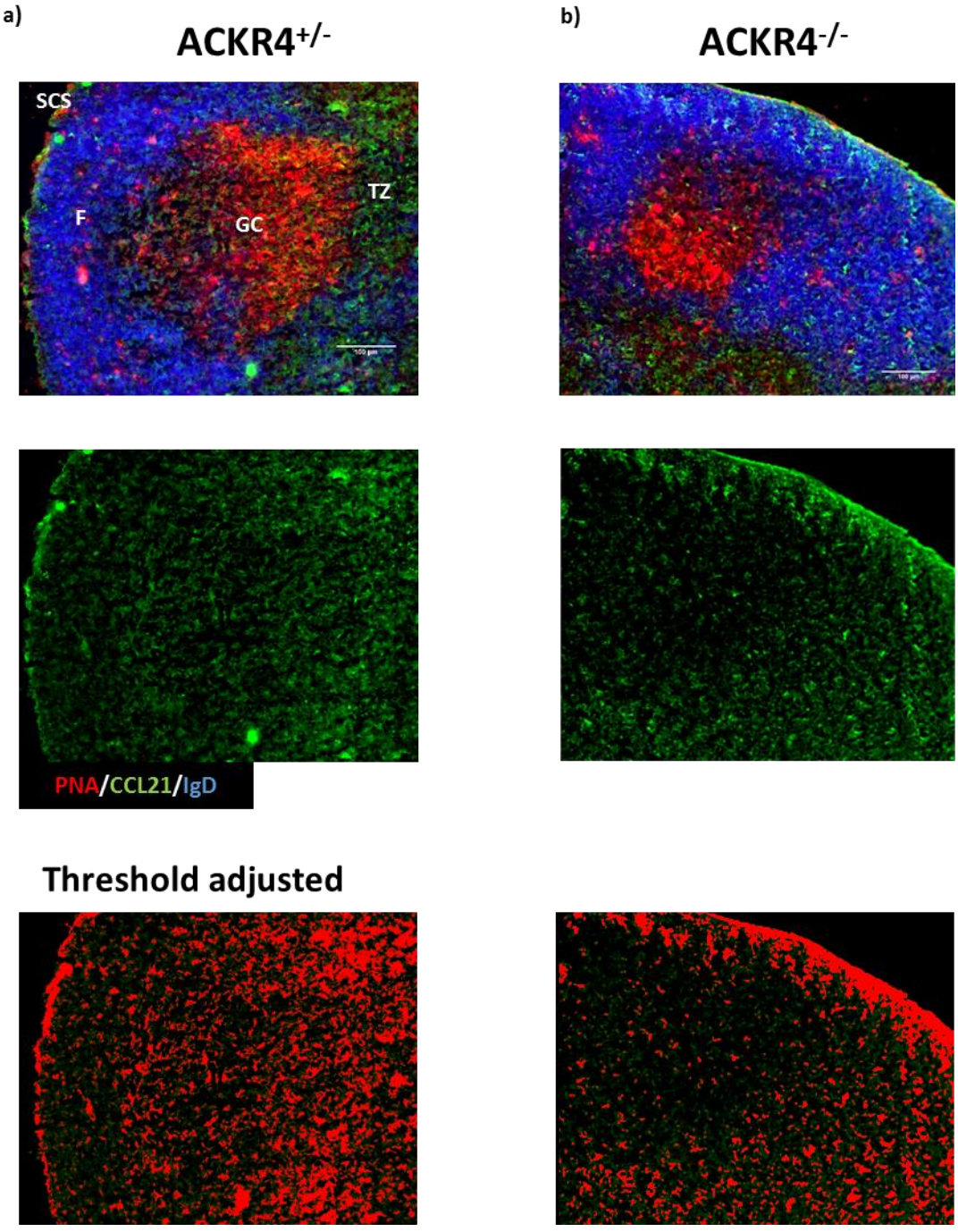

Figure 3.7: CCL21 expression in the draining lymph nodes. a-b) Representative immunofluorescence images of popliteal LNs for CCL21 (green), PNA (red), IgD (blue). a) WT pLN 8 days post-immunisation with NP-CGG s.c. in the hind feet. b) ACKR4$^{-/-}$ LN 8 days post-immunisation with NP-CGG s.c. in the hind feet. Images were thresholded using the "Moments" Thresholding method.
Key: F: B follicle; TZ: T zone; GC: germinal centre; PNA: peanut agglutinin; SCS: subcapsular sinus. Scale bar: 100 µm.

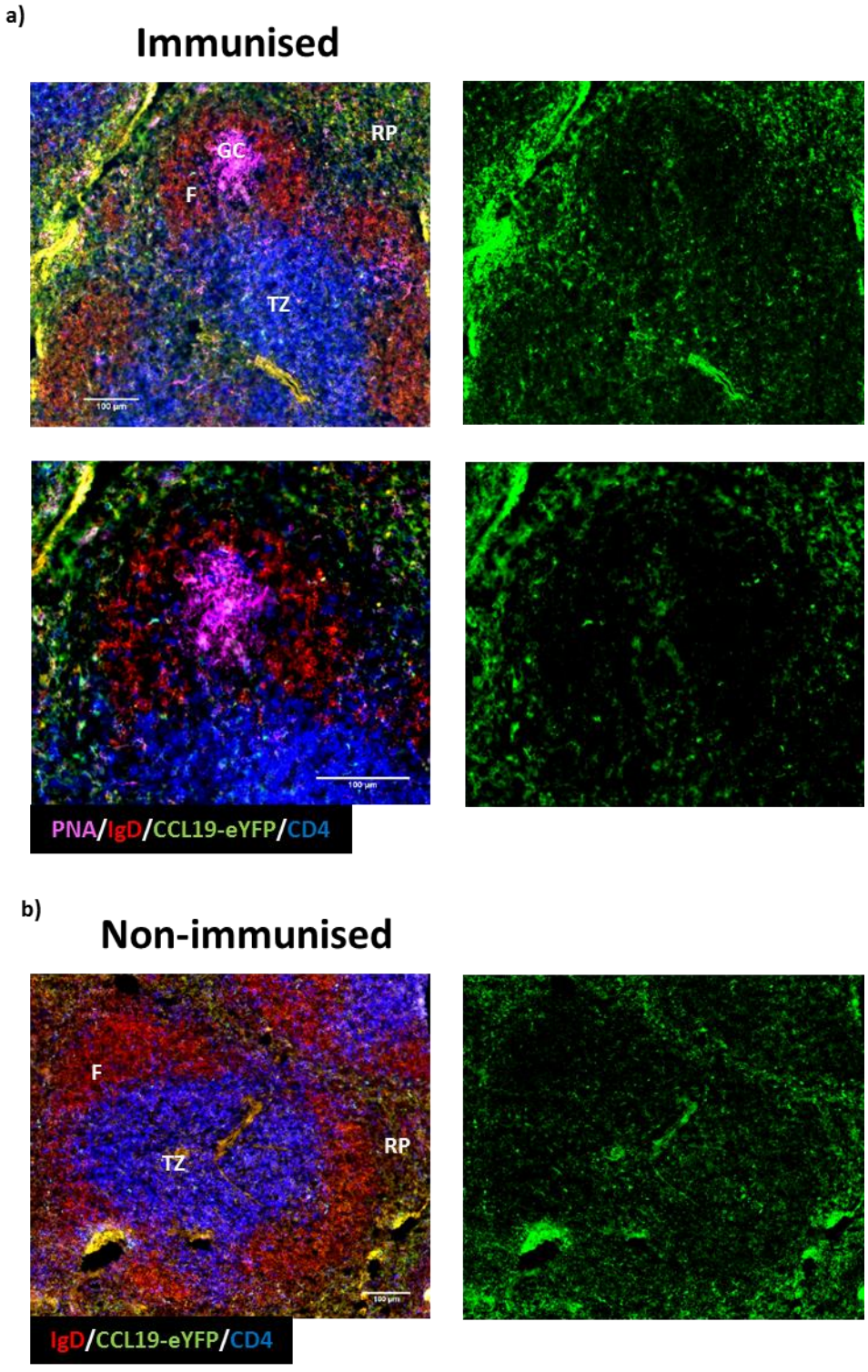

Figure 3.8: CCL19-eYFP expression in the spleen. a-b) Representative splenic immunofluorescence images for CCL19-eYFP (green), PNA (magenta), IgD (red) and CD4 (blue). a) CCL19-eYFP mice, 5 days post-immunisation with SRBC i.v. b) CCL19-eYFP mice, non-immunised.
Key: F: B follicle; TZ: T zone; RP: red pulp; GC: germinal centre; PNA: peanut agglutinin; SCS: subcapsular sinus.
Scale bar: 100 µm.

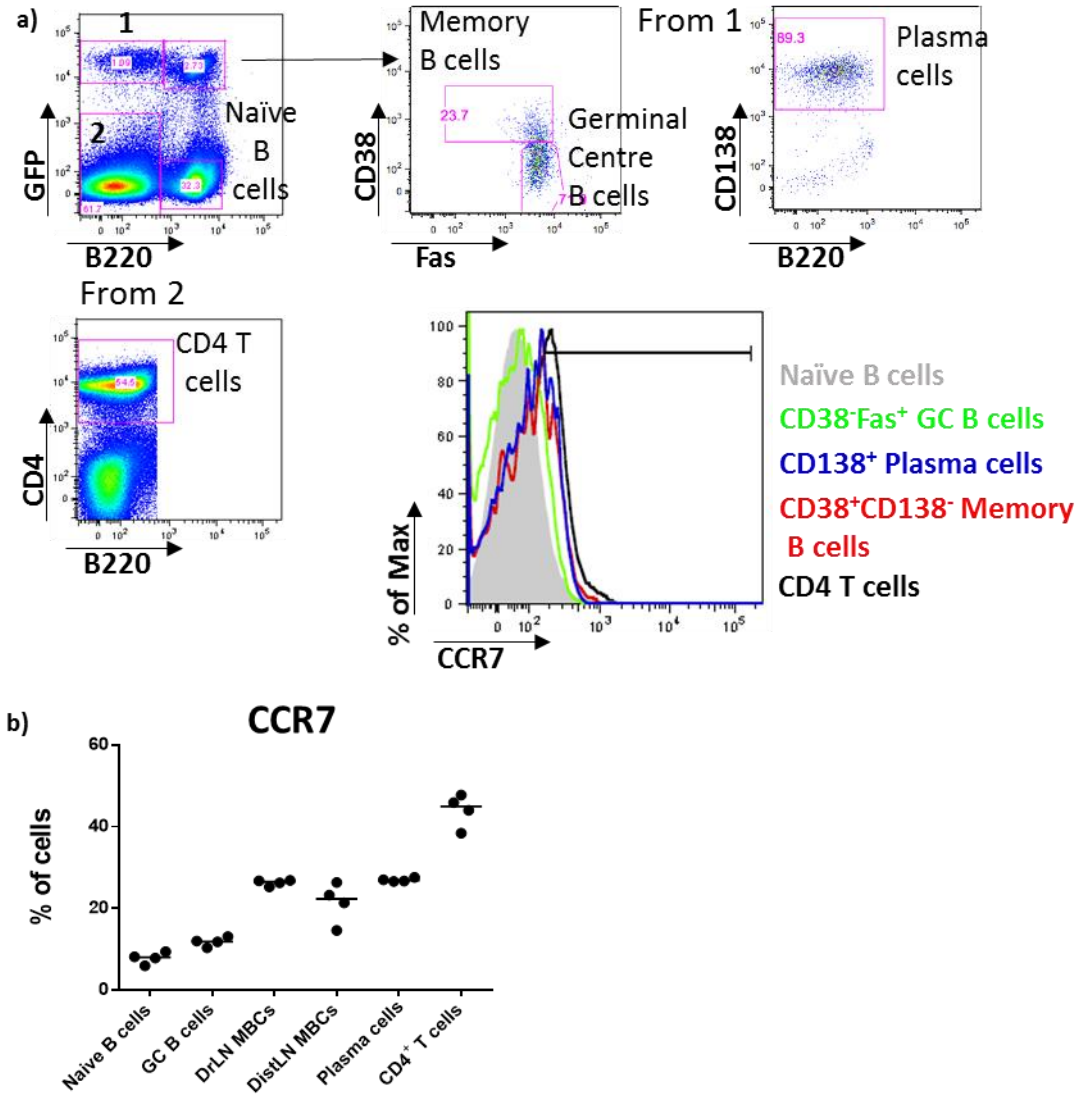

Figure 3.9: CCR7 expression in lymph nodes of immunised mice. a) Different B cell subsets were gated by flow cytometry from lymph nodes of WT mice transferred with Cγ1-Cre x QM ROSAeYFP B cells 8 days post-immunisation with NP-CGG and CCR7 surface expression analysed. b) Quantification of the % of $CCR7^+$ cells in each B cell subset.
Each symbol represents one mouse. Horizontal line represents the median.
Key: F: B follicle; TZ: T zone; RP: red pulp; GC: germinal centre; PNA: peanut agglutinin; SCS: subcapsular sinus.

3.2.3 Unimmunised ACKR4$^{-/-}$ mice present normal T and B cell populations

To test whether ACKR4 affects the differentiation and/or survival of T and B cells during steady state, different splenic T and B cell populations of unimmunised ACKR4$^{+/-}$ and ACKR4$^{-/-}$ mice were analysed by flow cytometry. The gating strategy is shown in Fig. 3.10a for T cells and Fig. 3.10b for B cells. T cells were gated as CD3^{+} lymphocytes and further subdivided into CD4^{+} and CD8^{+}. Each of these populations was further subdivided according to the expression of CD44 and CD62L into memory, activated and naïve T cells. Total numbers (CD3^{+}CD4^{+}CD8^{-} or CD3^{+}CD4^{-}CD8^{+}), activated T cells (CD3^{+}CD62L^{+}CD44^{+}), naïve T cells (CD3^{+}CD62L^{+}CD44^{-}) and memory T cells (CD3^{+}CD62L^{-}CD44^{+}) were analysed for both CD4^{+} (Fig. 3.11a) and CD8^{+} populations (Fig. 3.11b). ACKR4$^{-/-}$ mice had normal splenic T cell populations when compared to ACKR4$^{+/-}$ mice. B cells were gated on the basis of their expression of B220 and CD19 and were further subdivided into marginal zone, follicular (B2) and B1 B cells according to the expression of CD21/35 and CD23. B1 B cells were further subdivided into B1a and B1b B cells according to their expression of CD5. As to unimmunised ACKR4$^{-/-}$ mice significant differences were not detected as to any of the populations analysed, which included: total B cells (CD19^{+}B220^{+}), B1 B cells (CD21/35^{-}CD23^{-}), B1a B cells (CD21/35^{-}CD23^{-}CD5^{+}), B1b B cells (CD21/35^{-}CD23^{-}CD5^{-}), follicular B cells (CD23^{+}) and marginal zone B cells (CD21/35^{+}CD23^{-}) (Fig. 3.12a). In addition, histological analysis of spleen sections was performed following immunohistochemistry staining to examine the distribution of cell populations. In resting conditions, ACKR4$^{+/-}$ and ACKR4$^{-/-}$ sections were comparable as to the distribution and volumes of cells observed in the B cell follicles (IgD^{+} areas, brown) and T cell zones (CD3^{+} areas, blue) (Fig. 3.12b). These findings confirm that ACKR4 deficiency does not have a major effect on non-activated B and T cells.

In summary, ACKR4$^{-/-}$ mice have similar numbers of B cells and T cells in resting conditions as compared to ACKR4$^{+/-}$ mice. It might, therefore, be assumed that any effect of ACKR4 deficiency post-immunisation is due to an effect on B cell activation and differentiation and not related to an intrinsic developmental defect.

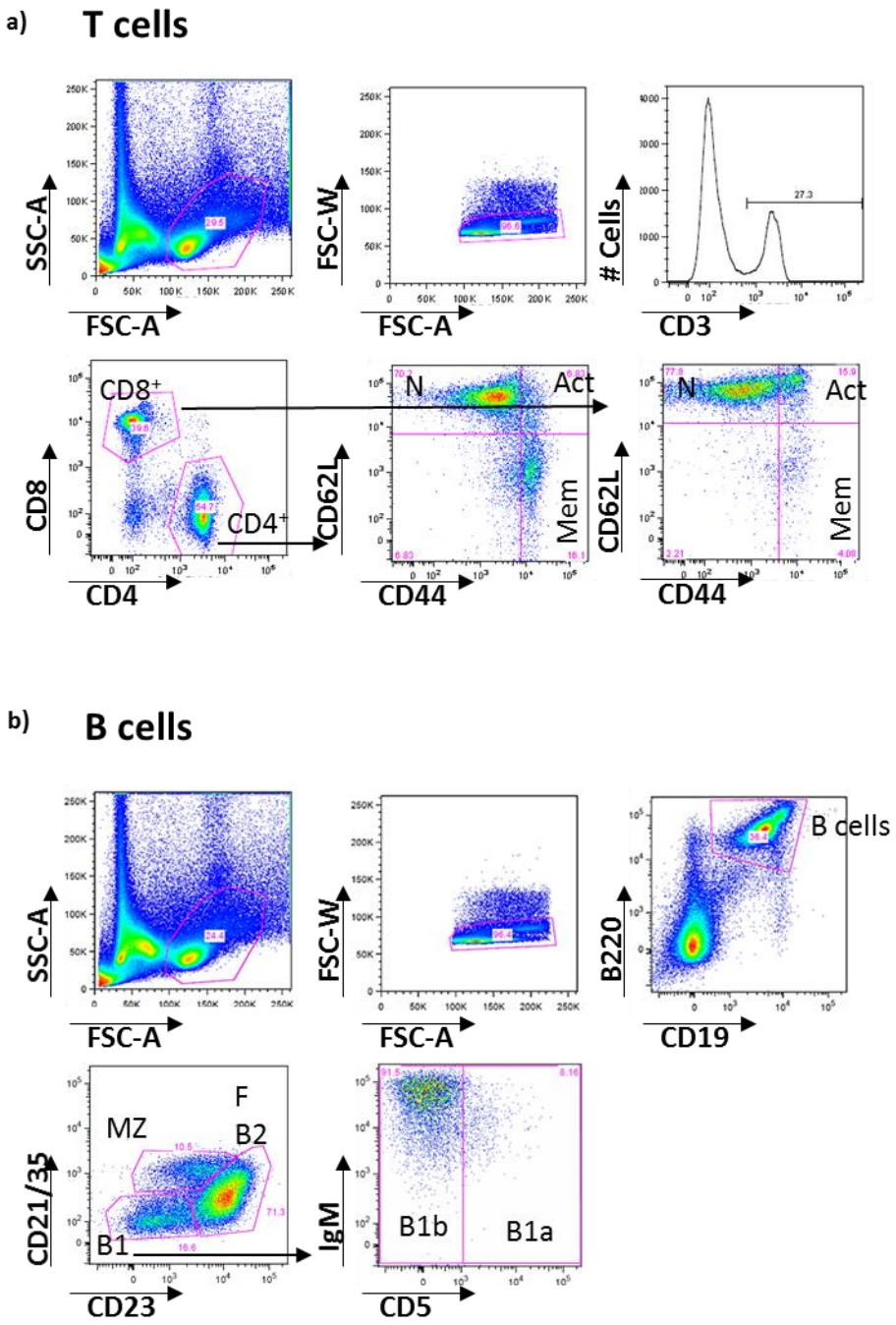

Figure 3.10: Representative gating strategy for splenic T and B cell populations in non-immunised mice. a) Flow cytometry gating strategy for splenic T cells from non-immunised mice. b) Flow cytometry gating strategy for splenic B cells from non-immunised mice.
Key: N: Naïve; Mem: Memory; Act: Activated; F: B follicle; MZ: marginal zone.

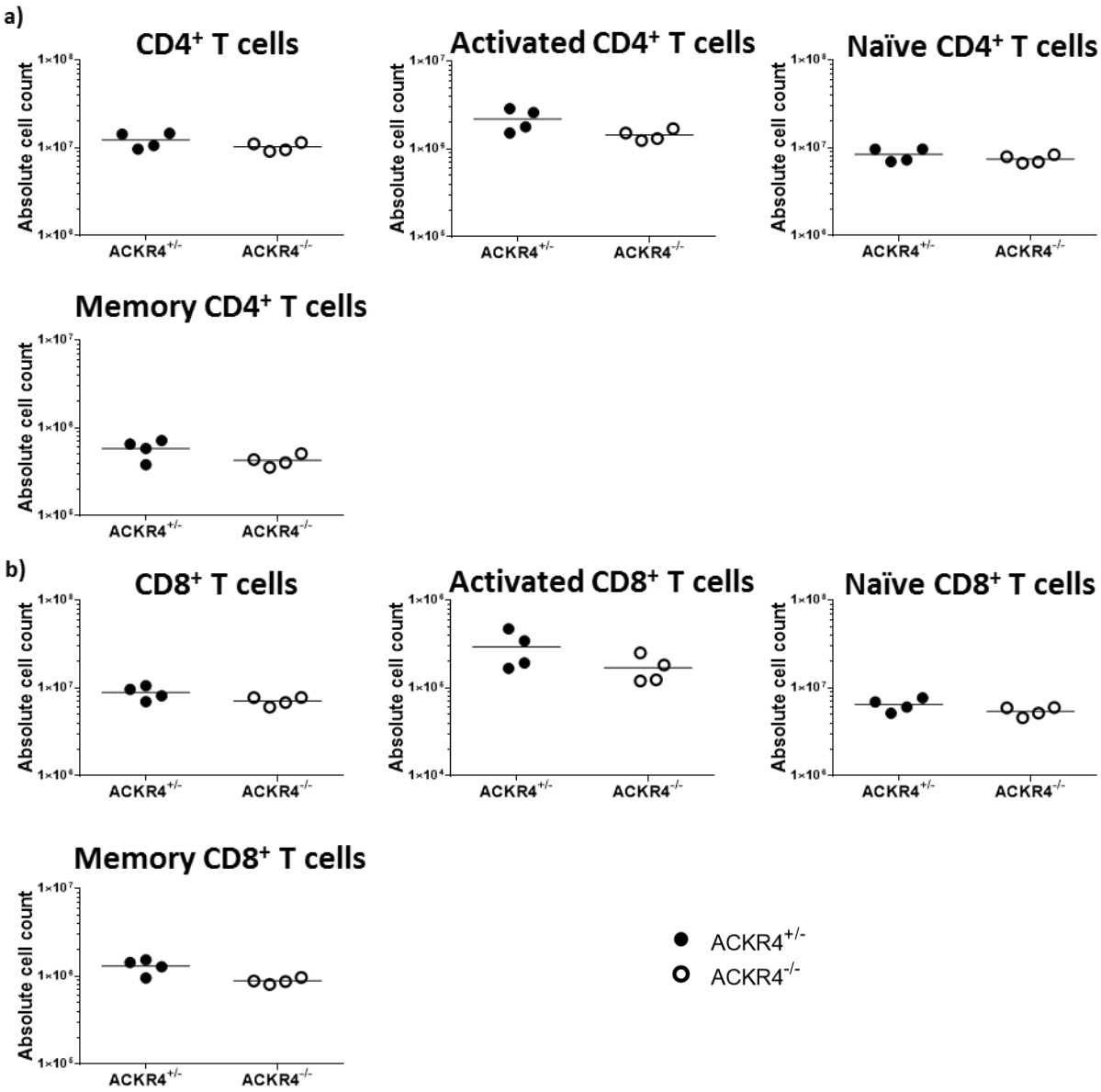

Figure 3.11: Splenic T and B cell populations in non-immunised ACKR4$^{-/-}$ mice are similar to ACKR4$^{+/-}$ (1). a-b) Absolute splenic cell numbers in the different T cell populations depicted in Fig. 3.10a. a) CD4^{+} T cells. b) CD8^{+} T cells.
1 independent experiment with 4 mice per group. Each symbol represents one mouse. Horizontal line represents the median.

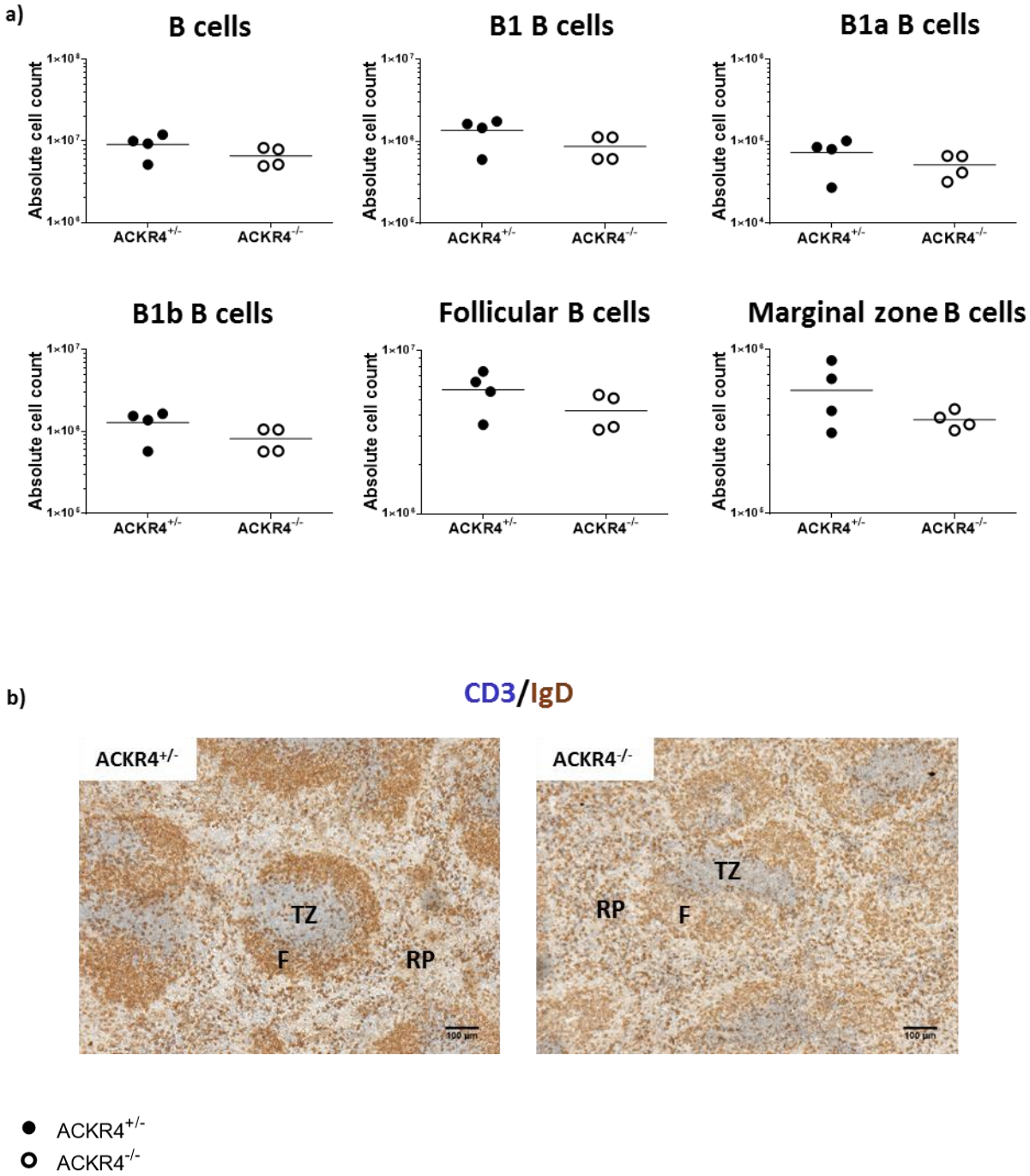

Figure 3.12: Splenic T and B cell populations in non-immunised ACKR4$^{-/-}$mice are similar to ACKR4$^{+/-}$ (2). a) Absolute splenic cell numbers in the different B cell populations depicted in Fig. 3.10b. b) Representative immunohistochemistry staining for CD3 (blue) and IgD (brown) of non-immunised spleens from ACKR4$^{+/-}$ (left) and ACKR4$^{-/-}$ (right) mice.
1 independent experiment with 4 mice per group. Each symbol represents one mouse. Horizontal line represents the median.
Key: F: B follicle; TZ: T zone; RP: red pulp. Scale bar: 100 µm.

3.2.4 ACKR4$^{-/-}$ B cells migrate normally to T-B borders 4 hours post-immunisation

Activated B cells encounter antigen in the splenic marginal zone and they then migrate in a CCR7-dependent manner to the T cell zone- B cell follicle border within 4-48h (Introduction 1.8). To test whether ACKR4 expression has an effect on this initial migration, QM ACKR4$^{+/+}$ and ACKR4$^{-/-}$ mice were immunised with the TI-II antigen NP-Ficoll and the response was analysed by immunohistological staining 4h after immunisation (Fig. 3.13). QM B cells are hemizygous for a rearranged V(D)J segment at the Ig heavy chain locus, the other allele being non-functional. They also have a non-functional kappa light chain allele. The heavy chain, when paired with any lambda light chain, is specific for NP (Cascalho, Ma et al. 1996). Splenic sections from unimmunised QM ACKR4$^{+/-}$ and ACKR4$^{-/-}$ mice did not show any differences in the distribution of NP^{+} B cells, which were located mainly around the follicular areas (Fig. 3.13a). NP-Ficoll immunisation of QM mice causes strong mobilisation of activated B cells to the T-B border (Marshall, Zhang et al. 2011). NP^{+} B cells (blue) were observed at both the marginal zones and the T cell- B follicle borders 4 h post-immunisation (Fig. 3.13b). No differences were observed when the area of NP^{+} cells at the T zone –B follicle interphase was quantified in ACKR4$^{+/-}$ and ACKR4$^{-/-}$ mice (Fig. 3.13c). Therefore, ACKR4 deficiency does not have an effect during the early B cell activation nor influences the migration of activated B cells to the T-B zone border in regard to the immediate time post-immunisation.

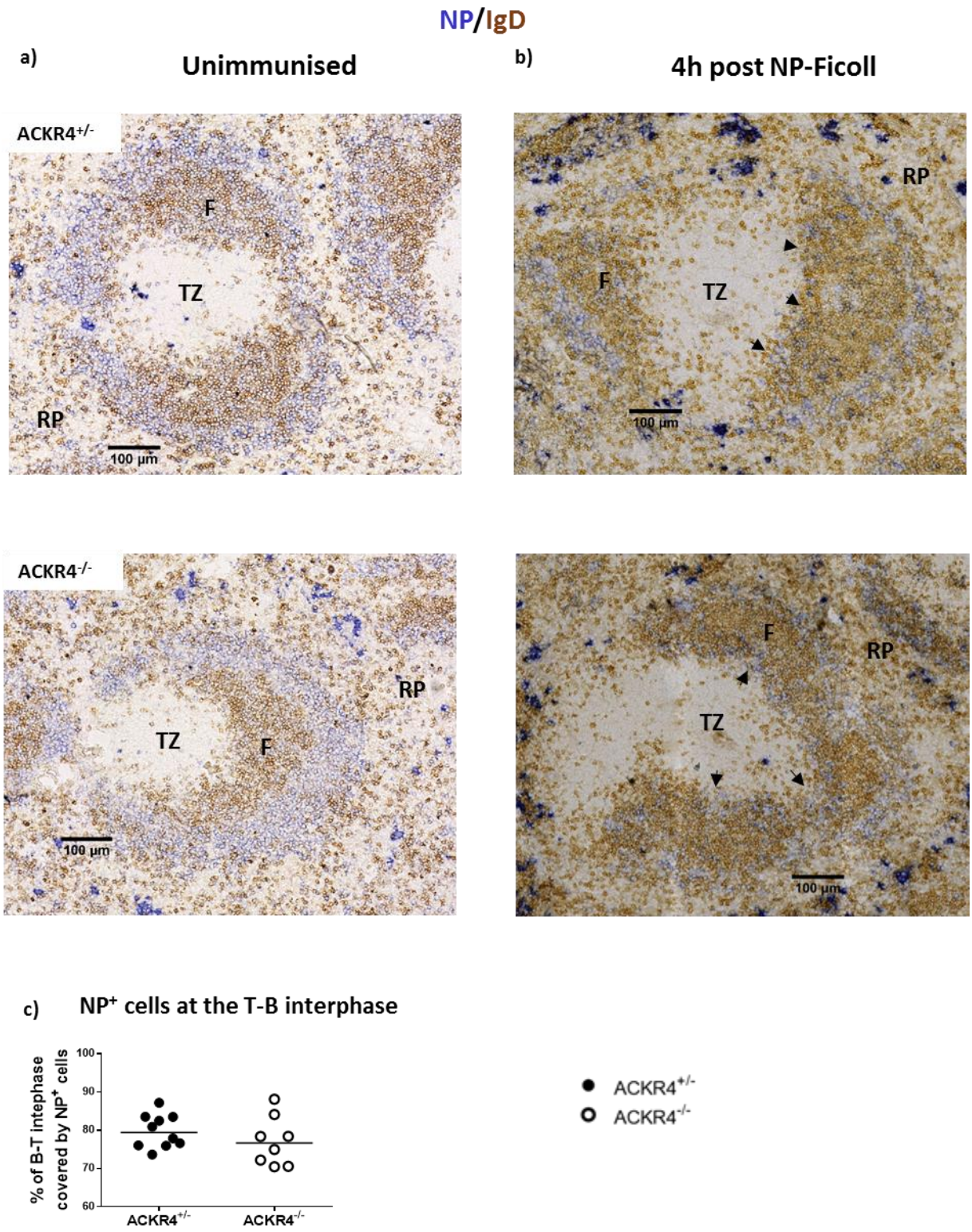

Figure 3.13: Initial antigen-induced migration of B cells to the T-B zone border occurs normally in the absence of ACKR4. a) Representative examples of immunohistochemistry images for NP (blue) and IgD (brown) of non-immunised QM ACKR4$^{+/-}$ (upper) and QM ACKR4$^{-/-}$ (lower) spleens. b) Representative immunohistochemistry images for NP (blue) and IgD (brown) of ACKR4$^{+/-}$ (upper) and ACKR4$^{-/-}$ (lower) spleens 4 h post-immunisation with NP-Ficoll. c) Quantification of % of NP^{+} cells at the T zone –B follicle interphase.
Each symbol represent the median of 4-5 different areas in one individual mouse.
Arrow heads indicate NP^{+} B cells that have migrated to the T-B interphase.
Key: F: B follicle; TZ: T zone; RP: red pulp. Scale bar: 100 µm.

3.2.5 ACKR4$^{-/-}$ GC counts are normal but GCs show abnormal histology 8 days post-immunisation

As outlined above, non-immunised ACKR4$^{-/-}$ mice do not have detectable alterations in their T cell or B cell populations and the initial migration of activated ACKR4$^{-/-}$ B cells to the T-B border after immunisation with TI-II antigen is normal. To test whether the germinal centre stages of B cell differentiation are normal in ACKR4$^{-/-}$ mice, primary immunisation of ACKR4$^{+/-}$ and ACKR4$^{-/-}$ mice with the TD antigen NP-CGG i.p. was performed. The response was analysed by flow cytometry. The gating strategy is shown in Fig. 3.14a. Eight days post primary immunisation, the numbers of plasma cells (NP^+CD138^+) and germinal centre B cells ($B220^+$ $NP^+CD38^-Fas^+$) numbers and LZ/DZ distribution in the GC were observed to be similar when ACKR4$^{-/-}$ mice were compared to ACKR4$^{+/-}$ (Fig. 3.14b).

Interestingly, while cell numbers were normal, immunohistological staining of spleen sections revealed that the shape of GCs in ACKR4$^{-/-}$ mice was different (Fig. 3.15a). In WT mice (ACKR4$^{+/-}$), GCs are compact assemblies of IgD^- B cells in the centre of the B cell follicle with a well-defined border (Fig. 3.15a left). However, GCs from ACKR4$^{-/-}$ splenic sections presented irregular borders and the perimeter was not well defined. Naïve B cells were observed to intermingle with GC B cells at the GC border and infiltrate the GC area more (Fig. 3.14a right). These differences were quantified in GCs from splenic sections. GCs from ACKR4$^{-/-}$ mice contained a larger proportion of IgD^+ cells than GCs of ACKR4$^{+/-}$, both 8 days post primary immunisation (Fig. 3.15b) and 14 days post primary immunisation (Fig. 3.15c).

While ACKR4$^{-/-}$ mice have normal numbers of GC B cells and plasma cells after primary immunisation, ACKR4$^{-/-}$ GCs have fuzzy borders with IgD^+ cells intermingling

with the GC B cells. This dysregulated shape of the GCs may have an important bearing as to the GC response, such as altered GC output or altered affinity maturation.

3.2.6 IgD^+ B cells infiltrate the GC area when the environment is $ACKR4^{-/-}$

To examine the cause of the abnormal GC shape in $ACKR4^{-/-}$ mice (3.2.5), $ACKR4^{+/+}$ or $ACKR4^{-/-}$ NP^+-specific QM B cells were transferred into $ACKR4^{+/-}$ and $ACKR4^{-/-}$ host mice. This experiment allows dissection of the effect of absence of ACKR4 expression by the B cells, that take part in the response (transferred B cells) and absence in regard to the stromal environment (stroma plus B cells that do not take part in the response, e.g. naïve B cells NP^-).

Adoptive transfer of QM B cells into host mice and immunisation with NP-Ficoll results in strong plasma cell differentiation and the development of T independent GCs by day 4 of the response (Marshall, Zhang et al. 2011). This set up was chosen as it is ideal to study GC formation in the spleen without carrier priming. The response was analysed by immunohistological staining 4 days post-immunisation, before GCs start to abort (de Vinuesa, Cook et al. 2000) (Fig. 3.16).

In order to identify GCs, splenic sections were stained for PNA (GC B cells) and IgD (naïve B cells). Transferred cells were distinguished by their expression of eYFP. Analysis of these tissue sections confirmed the results obtained by flow cytometry as there was no difference in the spleen area covered by GCs, measured as PNA^+ area (in μm^2), in any of the conditions (Fig. 3.16b and 3.16e).

Also, transfer of $ACKR4^{+/+}$ or $ACKR4^{-/-}$ QM B cells into a wt environment (Fig. 3.16a-c) did not result in a change to the area of GC infiltrated by naïve B cells, calculated as

PNA^+ area divided by the IgD^- area (Fig. 3.16c). However, when $ACKR4^{+/+}$ B cells were transferred into an $ACKR4^{-/-}$ environment (Fig. 3.16d-f), despite there not being a difference in the size of GCs, the fraction of GC area that had been infiltrated by naïve B cells was significantly increased when compared to the control conditions (Fig. 3.16f). These findings have demonstrated that the differences observed after TD primary response in $ACKR4^{+/-}$ and $ACKR4^{-/-}$ mice are caused by ACKR4 expression in the host and emphasise the importance of the expression of ACKR4 in the splenic stroma to the maintenance of GC shape. There are potential implications to the GC response as to affinity maturation and entry and exit of cells.

Chimeric spleens were also analysed by flow cytometry (Fig. 3.17). $ACKR4^{+/+}$ (QM into) or $ACKR4^{-/-}$ (QM ACKR4-ko into) NP-specific B cells were transferred into $ACKR4^{+/+}$ (wt) or $ACKR4^{-/-}$ (ko) hosts, mice were immunised with NP-Ficoll one day after and the response was analysed 4 days post-immunisation. The above experiments confirmed that the absence of ACKR4 from B cells or from the environment does not lead to changes to the numbers or percentages of lymphocytes of NP-specific GC B cells per spleen (Fig. 3.17a). Furthermore, changes in GC DZ or GC LZ B cell numbers and proportions were not observed (Fig. 3.17b and 3.17c). The DZ/LZ ratio was also analysed and no differences were observed (Fig. 3.17d). ACKR4 deficiency also had no effect on NP-specific plasma cell numbers per spleen or percentages (Fig. 3.18a). Analysis of $CD73^+$ and $CD80^+$ MBCs (Fig. 3.18b and 3.18c) showed a slight increase of $CD73^+$ and $CD80^+$ MBCs, which reached significance when absolute numbers of $CD80^+$ MBCs were examined for mice in which ACKR4 is absent from the environment.

In summary, the GC fuzziness observed by immunohistology in ACKR4-deficient environments appears to have no major consequences as to the differentiation of B cell subsets 4 days post NP-Ficoll immunisation.

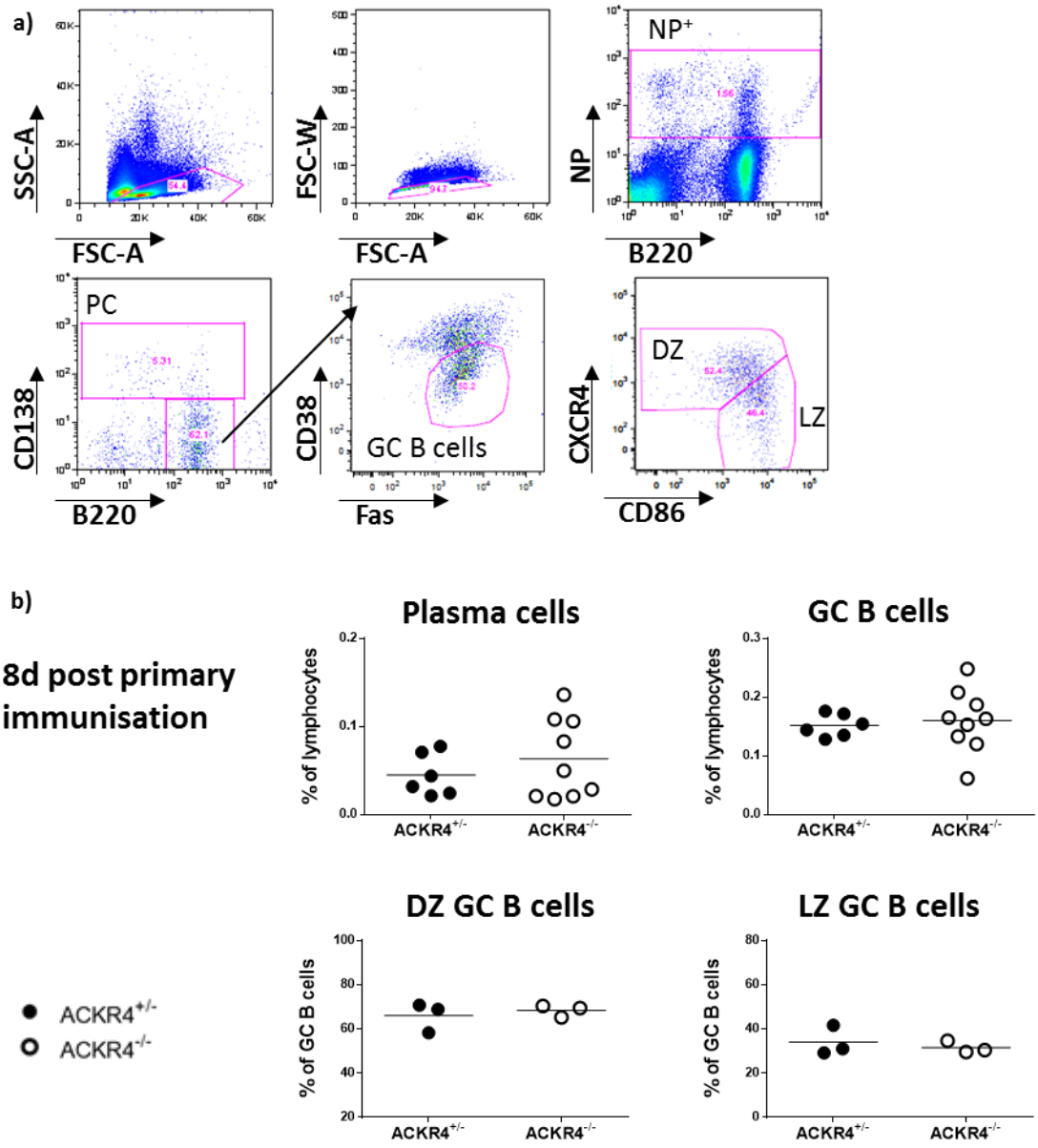

Figure 3.14: GCs B cells from ACKR4$^{-/-}$ mice 8 days post NP-CGG are normal. a) Flow cytometry gating strategy for splenic NP-specific B cells from ACKR4$^{+/-}$ and ACKR4$^{-/-}$ immunised mice. b) % of lymphocytes of GC B cells and plasma cells (upper) and % of GC B cells of dark zone and light zone (lower) on day 8 post-immunisation with NP-CGG.
In section b upper, data were combined from 2 independent experiments with 3-6 mice per group. In section b lower, data is representative from 1 out of 2 independent experiments. Each symbol represents one mouse. Horizontal line represents the median.
Key: PC: plasma cell; GC: germinal centre; LZ: light zone; DZ: dark zone

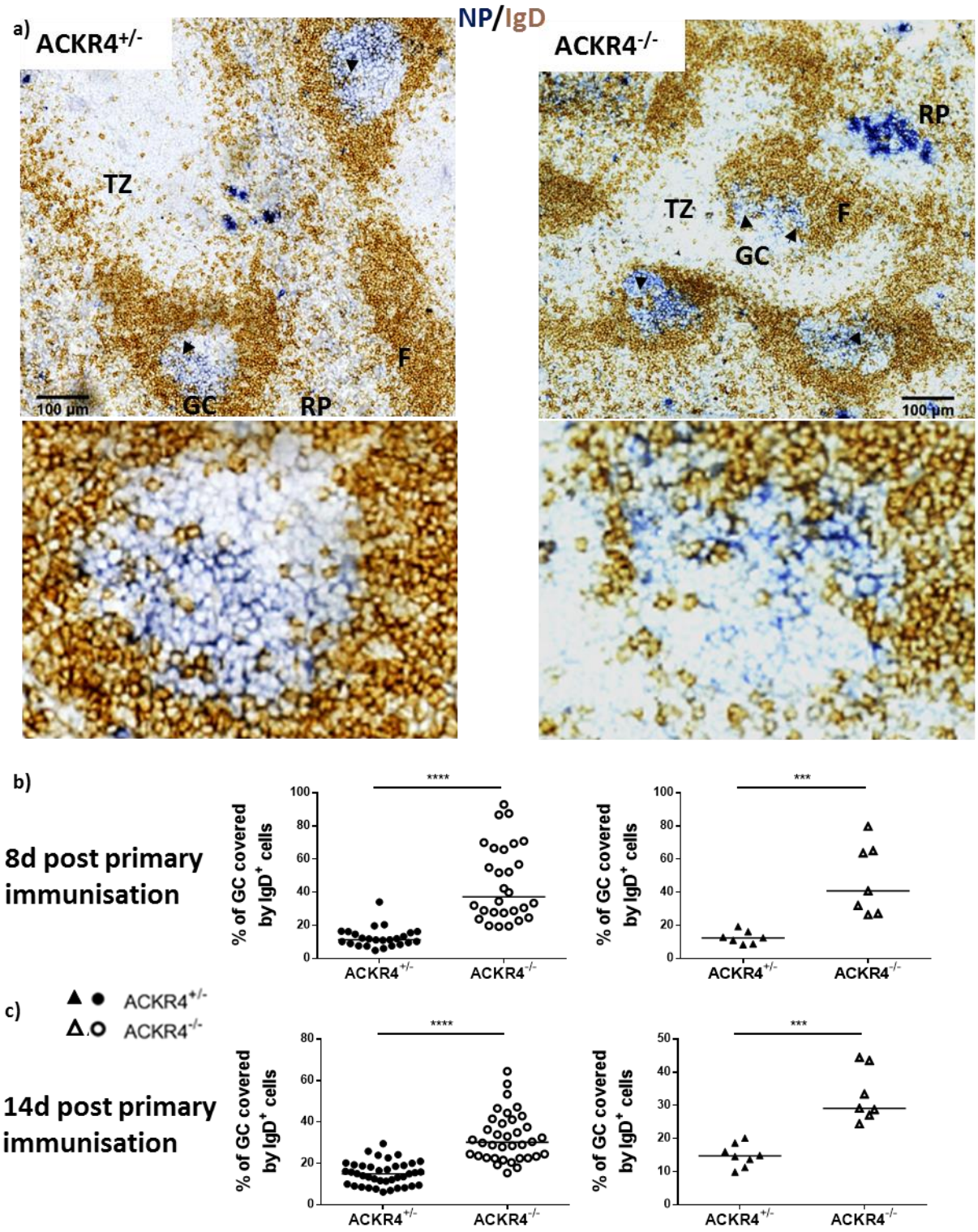

Figure 3.15: GCs from ACKR4$^{-/-}$ mice 8 days post NP-CGG show abnormal histology. a) Representative immunohistochemistry staining images for NP (blue) and IgD (brown) of splenic sections from ACKR4$^{+/-}$ (left) and ACKR4$^{-/-}$ (right) 8 days post-immunisation with NP-CGG. b) Quantification of the % of GC covered by IgD^{+} cells 8 days post-immunisation with NP-CGG. c) 14 days post-immunisation.

GCs were counted from 2 independent experiments with 3-4 mice per group. Individual circles represent GCs. Individual triangles represent the median of 4-5 different GCs in one individual mouse. Horizontal line represents the median. Arrow heads indicate IgD^{+} cells that have infiltrated the GC area.

Key: F: B follicle; TZ: T zone; RP: red pulp; GC: germinal centre

Scale bar: 100 µm.

Non-parametric Mann-Whitney test ***p<0.001; ****p<0.0001

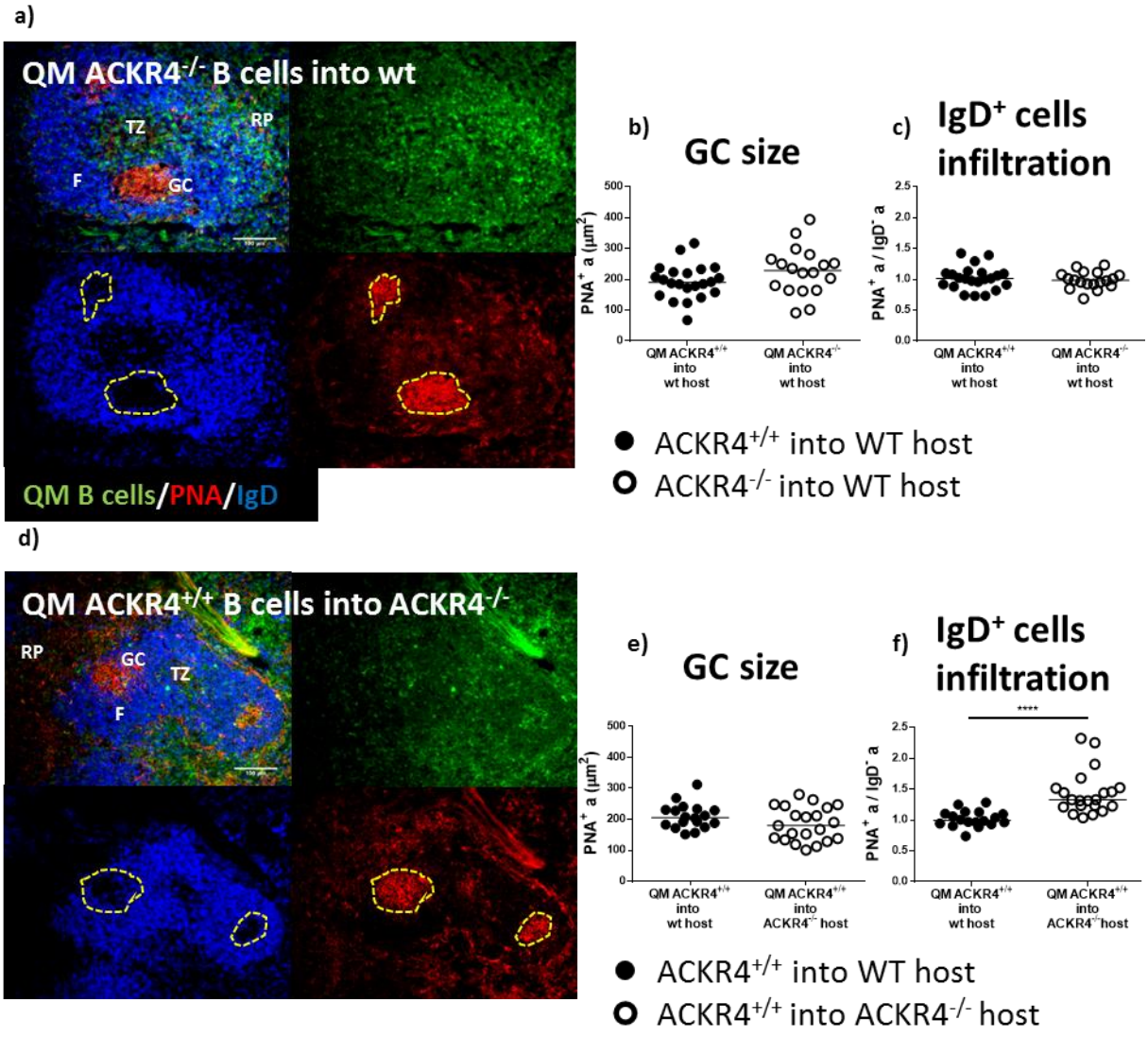

Figure 3.16: IgD^{+} cells infiltrate GC area when the environment is ACKR4$^{-/-}$. a-c) WT and ACKR4$^{-/-}$ QM B cells were transferred into WT mice, immunised with NP-Ficoll i.p. and the response studied 4 days later. a) Representative example of immunofluorescence staining for eYFP (transferred QM B cells), PNA (red) and IgD (blue). b) GC area. c) Fraction of GC infiltrated by naïve B cells. d-f) WT QM B cells were transferred into WT and ACKR4$^{-/-}$ mice, immunised with NP-Ficoll i.p. and the response studied 4 days later. d) Representative example of immunofluorescence staining for eYFP (transferred QM B cells), PNA and IgD (blue). e) GC area. f) Fraction of GC infiltrated by naïve B cells.

Each symbol represents one GC. 18-23 GCs in total were counted from 4 mice. Horizontal line represents the median.

Key: TZ: T zone; F: B follicle; GC: germinal centre; RP: red pulp. Scale bar: 100 µm.

Non-parametric Mann-Whitney test ****p<0.0001

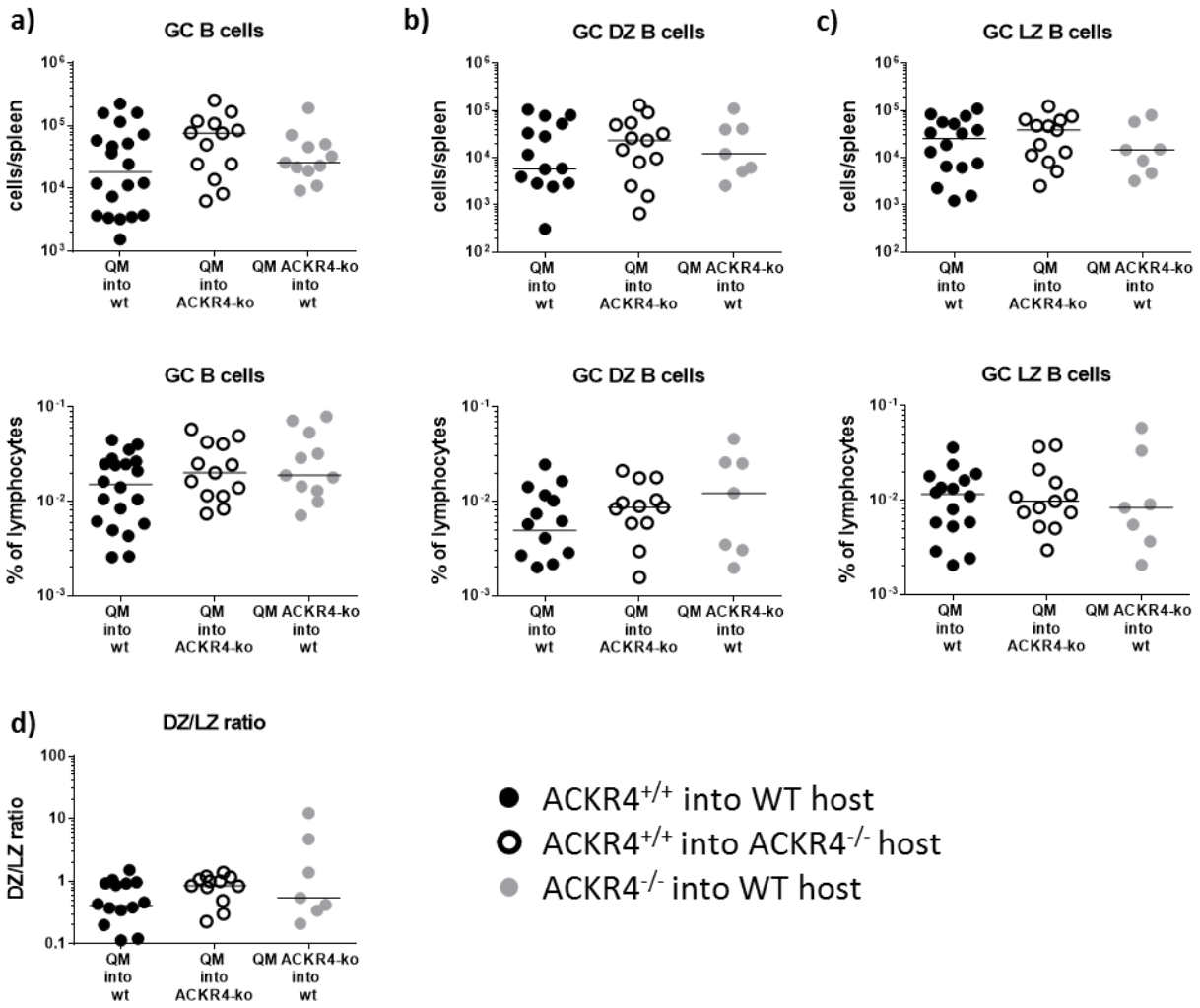

Figure 3.17: No major differences in the cell numbers in spleen when QM B cells (ACKR4$^{+/+}$ or ACKR4$^{-/-}$) are transferred into ACKR4$^{+/+}$ or ACKR4$^{-/-}$ environments 4 days post-immunisation with NP-Ficoll. a-d) WT or ACKR4$^{-/-}$ QM B cells were transferred into WT or ACKR4$^{-/-}$ recipients and cell populations were analysed by flow cytometry 4 days post immunisation with NP-Ficoll. Absolute cell populations (upper) and % of lymphocytes (lower) of a) GC B cells ($B220^{+}NP^{+}CD38^{-}Fas^{+}$). b) Dark zone GC B cells ($B220^{+}NP^{+}CD38^{-}Fas^{+}CXCR4^{+}CD86^{-}$). c) Light zone GC B cells ($B220^{+}NP^{+}CD38^{-}Fas^{+}CXCR4^{-}CD86^{+}$). d) DZ/LZ ratio.
ACKR4$^{+/+}$ into WT host vs ACKR4$^{+/+}$ into ACKR4$^{-/-}$ host comparisons were performed in 2 independent experiments with 4-5 mice per group. ACKR4$^{+/+}$ into WT host vs ACKR4$^{-/-}$ into WT host comparisons were performed in 2 independent experiments with 3-4 mice per group. Comparison of the 3 groups was performed in 1 independent experiment with 4-5 mice per group. Each symbol represents one mouse. Horizontal line represents the median.
Key: GC: germinal centre; LZ: light zone; DZ: dark zone.
Non-parametric Mann-Whitney test **p<0.01

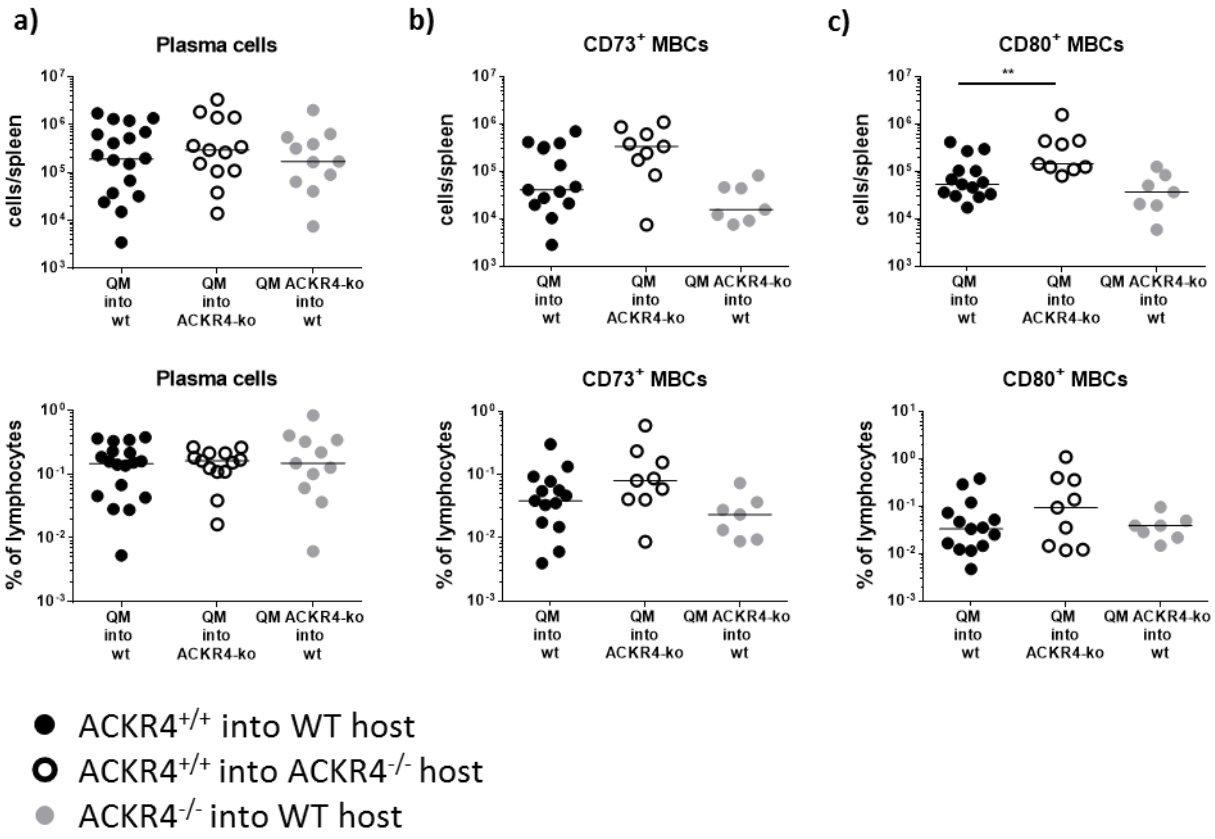

Figure 3.18: No major differences in the cell numbers in spleen when QM B cells (ACKR4$^{+/+}$ or ACKR4$^{-/-}$) are transferred into ACKR4$^{+/+}$ or ACKR4$^{-/-}$ environments 4 days post-immunisation with NP-Ficoll (2). a-c) WT or ACKR4$^{-/-}$ QM B cells were transferred into WT or ACKR4$^{-/-}$ recipients and cell populations were analysed by flow cytometry 4 days post immunisation with NP-Ficoll. Absolute cell populations (upper) and % of lymphocytes (lower) of a) Plasma cells (B220^{+}NP^{+}CD138^{+}). e) CD73^{+} MBCs (B220^{+}NP^{+}CD38^{+}GL7^{-}CD138^{-}CD73^{+}). f) CD80^{+} MBCs (B220^{+}NP^{+}CD38^{+}GL7^{-} CD138^{-}CD80^{+}).
ACKR4$^{+/+}$ into WT host vs ACKR4$^{+/+}$ into ACKR4$^{-/-}$ host comparisons were performed in 2 independent experiments with 4-5 mice per group. ACKR4$^{+/+}$ into WT host vs ACKR4$^{-/-}$ into WT host comparisons were performed in 2 independent experiments with 3-4 mice per group. Comparison of the 3 groups was performed in 1 independent experiment with 4-5 mice per group. Each symbol represents one mouse. Horizontal line represents the median.
Key: MBC: memory B cell.
Non-parametric Mann-Whitney test **p<0.01

3.2.7 At later stages of the GC response, DZ/LZ ratio is altered in ACKR4$^{-/-}$ mice

To test whether the changes to the shape of GCs in ACKR4$^{-/-}$ mice have a functional consequence during later stages of the GC response, ACKR4$^{+/-}$ and ACKR4$^{-/-}$ mice were immunised with NP-CGG and the splenic response studied 14 days post-immunisation (Fig. 3.19). As seen on day 8 post NP-CGG immunisation, GC B cell numbers per spleen or percentages were unaltered (Fig. 3.19a). Plasma cells as well as memory B cell numbers and percentages were also similar in both ACKR4$^{-/-}$ and ACKR4$^{+/-}$ mice (Fig. 3.19b, 3.19c). Intriguingly, ACKR4$^{-/-}$ mice had reduced percentage of DZ GC B cells and a higher percentage of LZ GC B cells (Fig. 3.19d), resulting in a reduced DZ/LZ ratio in ACKR4$^{-/-}$ mice (Fig. 3.19e).

This altered ratio could have profound effects in the later stages of the GC response. Therefore, experiments were undertaken to verify that this effect was also observable under other immunogenic conditions. ACKR4$^{+/-}$ and ACKR4$^{-/-}$ mice were immunised with SRBC and the response was analysed 8, 14 and 21 days post-immunisation by flow cytometry. The gating strategy is shown in Fig. 3.20. After SRBC immunisation, antigen-specific B cells were indistinguishable and they were gated in relation to their expression of B220. Subsequently, B cells were gated for PCs, GCs and for GC subpopulations LZ B cells and DZ B cells. As expected from the results obtained after NP-CGG primary immunisation, 8 days post-immunisation, a difference was not observed as to GC B cells or in DZ/LZ distribution for ACKR4$^{-/-}$ mice versus ACKR4$^{+/-}$ mice (Fig. 3.21a). At later time points, 14 days (Fig. 3.21b) and 21 days (Fig. 3.21c) post-immunisation, GC B cell percentages were unaltered but the LZ/DZ ratio was skewed towards LZ in ACKR4$^{-/-}$ spleens. These results confirm that the effect observed after NP-CGG immunisation occurs also in regard to immunisation with SRBC.

The skewed distribution of LZ/DZ ratio was confirmed by histological analysis. Splenic sections from ACKR4$^{+/-}$ and ACKR4$^{-/-}$ mice taken at day 8, 14 and 21, were stained with PNA (to denote GCs), CXCR4 (to denote DZ) and IgD (to denote follicles) (Fig. 3.22). As observed 8 days post primary immunisation, the perimeters in ACKR4$^{-/-}$ GCs were also altered and less defined 14 days after SRBC immunisation (Fig. 3.22a). GC and DZ areas were measured on splenic sections using digital image analysis. The fraction of GC occupied by DZ (Fig. 3.22b) and the GC area (Fig. 3.22c) were analysed. Consistent with flow cytometry results, 8 days post-immunisation, there was no differences in the GC area or in DZ area when ACKR4$^{-/-}$ mice were compared with ACKR4$^{+/-}$ mice (Fig. 3.22b upper, 3.22c upper). Furthermore, 14 days (Fig. 3.22b middle, 3.22c middle) and 21 days post-immunisation (Fig. 3.22b lower, 3.22c lower), while GC area was unchanged, DZ fraction was reduced.

The findings described above have revealed that ACKR4$^{-/-}$ mice have an altered distribution of GC B cell subpopulations, with bigger LZ and smaller DZ, while GC B cell numbers are normal. This skewed ratio may have functional consequences such as altered affinity maturation.

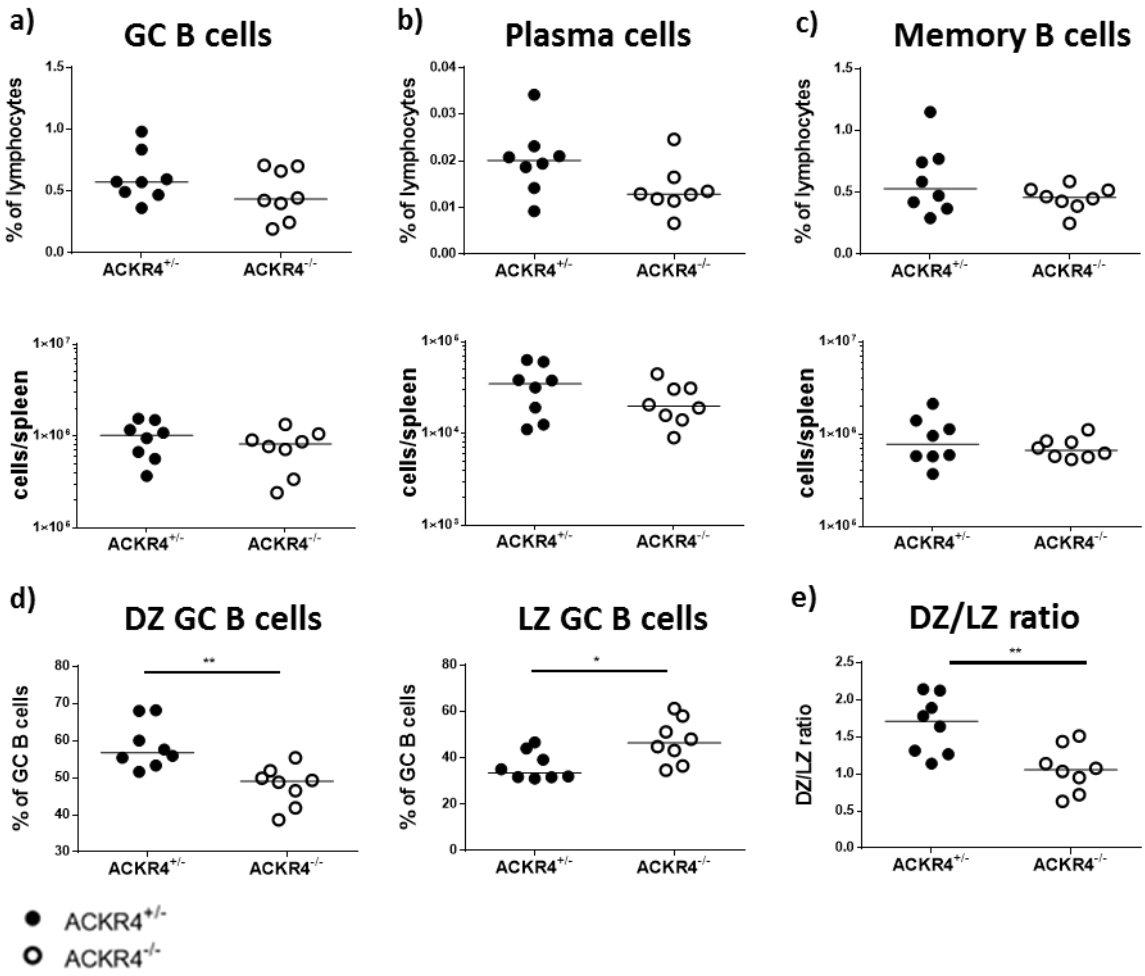

Figure 3.19: DZ/LZ ratio is altered in ACKR4$^{-/-}$ mice 14 days after NP-CGG. a-d) ACKR4$^{+/-}$ and ACKR4$^{-/-}$ mice were immunised with NP-CGG and B cell populations analysed on day 14 by flow cytometry. Absolute cell counts (upper) and % of lymphocytes (lower) were determined. a) GC B cells (B220^{+}NP^{+}CD38^{-}Fas^{+}). b) Plasma cells (B220^{+}NP^{+}CD138^{+}). c) MBCs (B220^{+}NP^{+}CD38^{+}CD138^{-}). d) % of GC B cells of dark zone (B220^{+}NP^{+}CD38^{-}Fas^{+}CXCR4^{+}CD86^{-}) and light zone (B220^{+}NP^{+}CD38^{-}Fas^{+}CXCR4^{-}CD86^{+}) GC B cells. e) DZ/LZ ratio.
2 independent experiments with 4 mice per group. Each symbol represents one mouse. Horizontal line represents the median.
Key: GC: germinal centre; LZ: light zone; DZ: dark zone.
Non-parametric Mann-Whitney test *p<0.05; **p<0.01

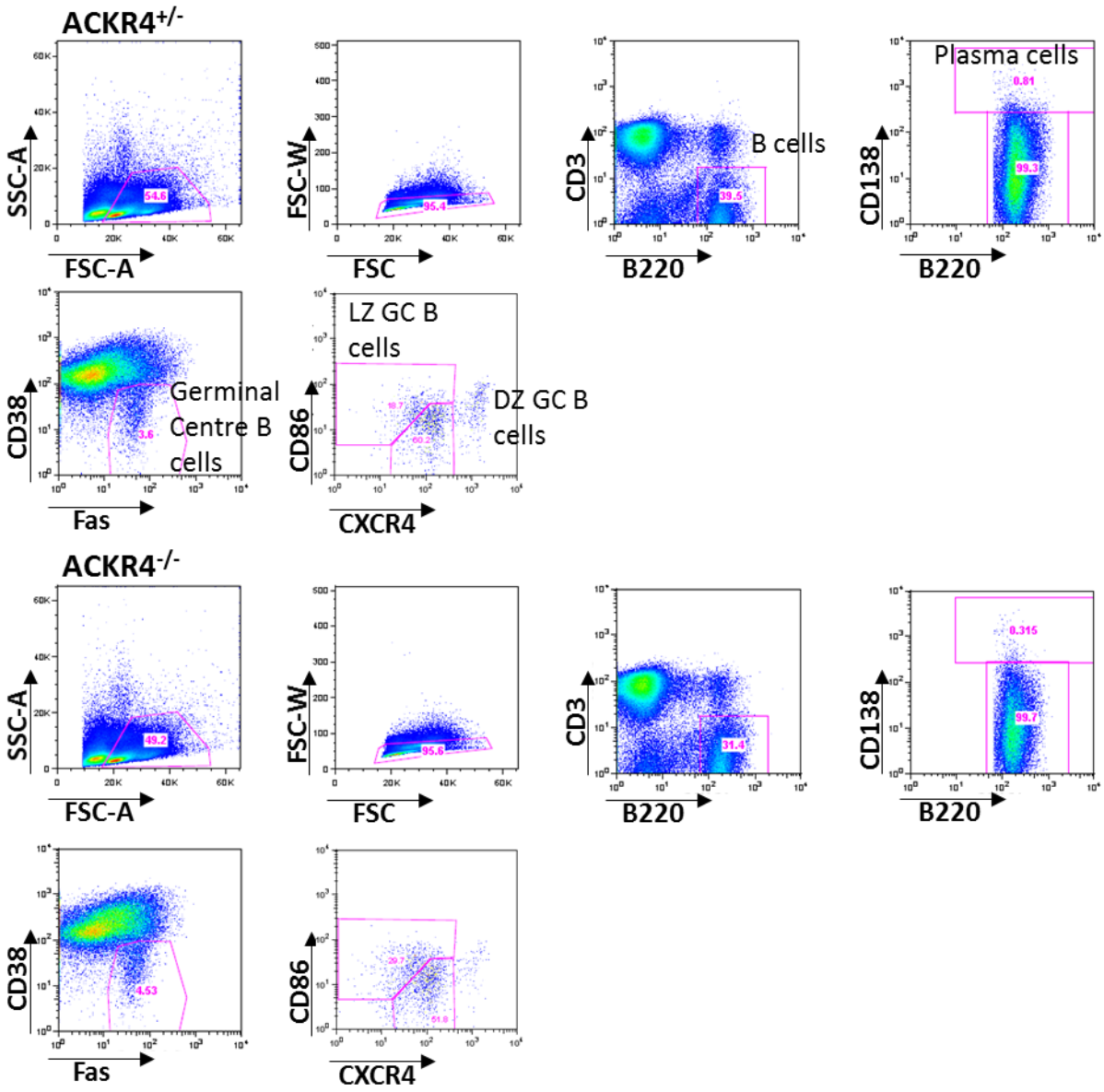

Figure 3.20: Gating strategy for the splenic response of ACKR4$^{+/+}$ and ACKR4$^{-/-}$ mice to SRBC. Flow cytometry gating strategy for different B cell populations from ACKR4$^{+/-}$ and ACKR4$^{-/-}$ mice immunised with SRBC. The response was studied 8, 14 and 21 days post immunisation.
Key: GC: germinal centre; LZ: light zone; DZ: dark zone.

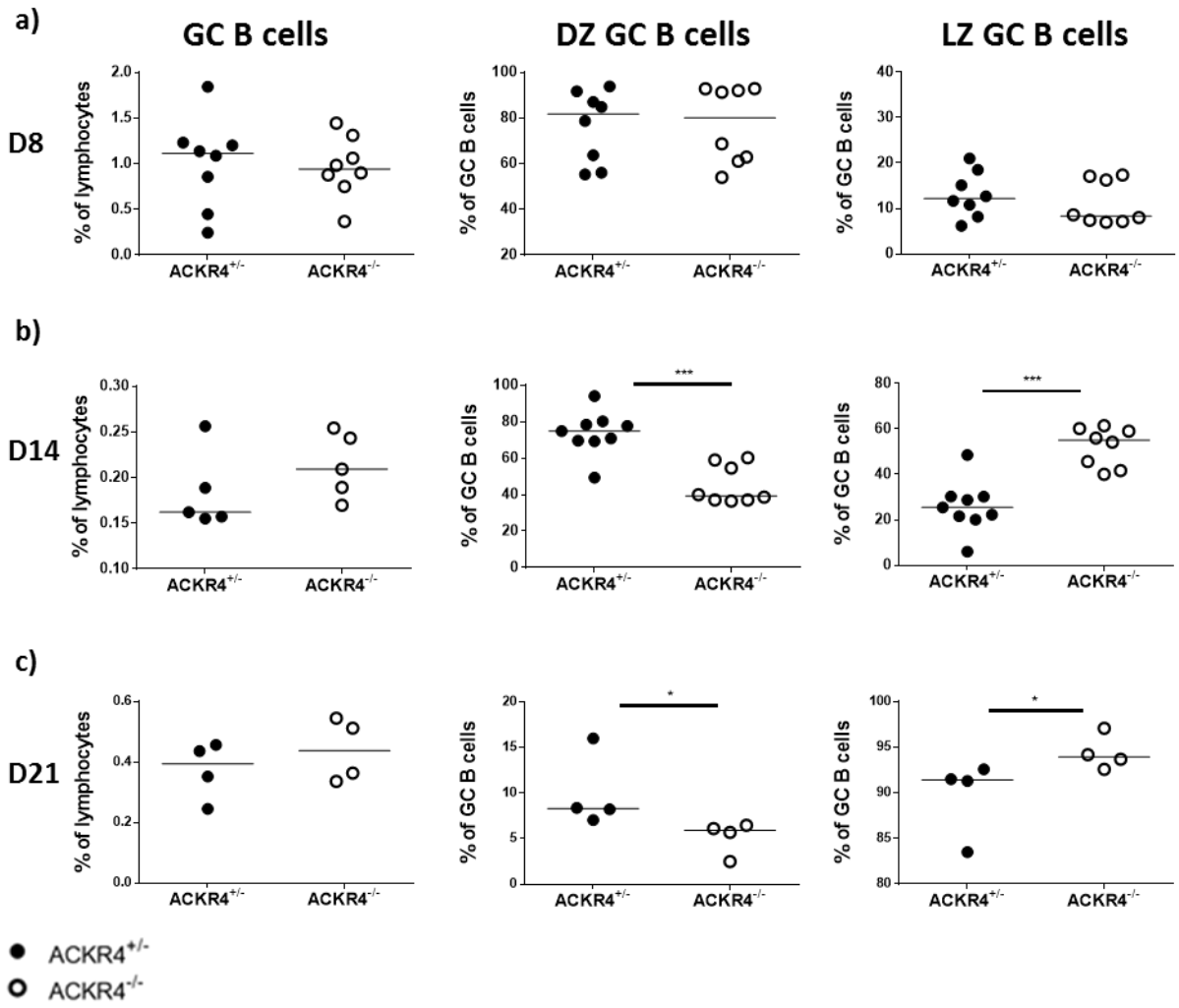

Figure 3.21: DZ/LZ ratio is altered in ACKR4$^{-/-}$ mice 14 days after SRBC (1). a-c) ACKR4$^{+/-}$ and ACKR4$^{-/-}$ mice were immunised with SRBC and GC B cells (B220^{+}CD38^{-}Fas^{+}), dark zone (B220^{+}CD38^{-}Fas^{+}CXCR4^{+} CD86^{-}) and light zone (B220^{+}CD38^{-}Fas^{+}CXCR4^{-}CD86^{+}) GC B cells were analysed on a) day 8, b) day 14 and c) day 21 post-immunisation.
For gating strategy see Figure 3.20.
In section a, data were combined from 2 independent experiments with 4 mice per group. In section b, data were combined from 2 independent experiments with 4-5 mice per group, except for GC B cells were plot is representative of 2 independent experiments. In section c, plots are representative of 2 independent experiments with 4 mice per group. Each symbol represents one mouse. Horizontal line represents the median.
Key: GC: germinal centre; LZ: light zone; DZ: dark zone; D: day.
Non-parametric Mann-Whitney test *p<0.05; ***p<0.001

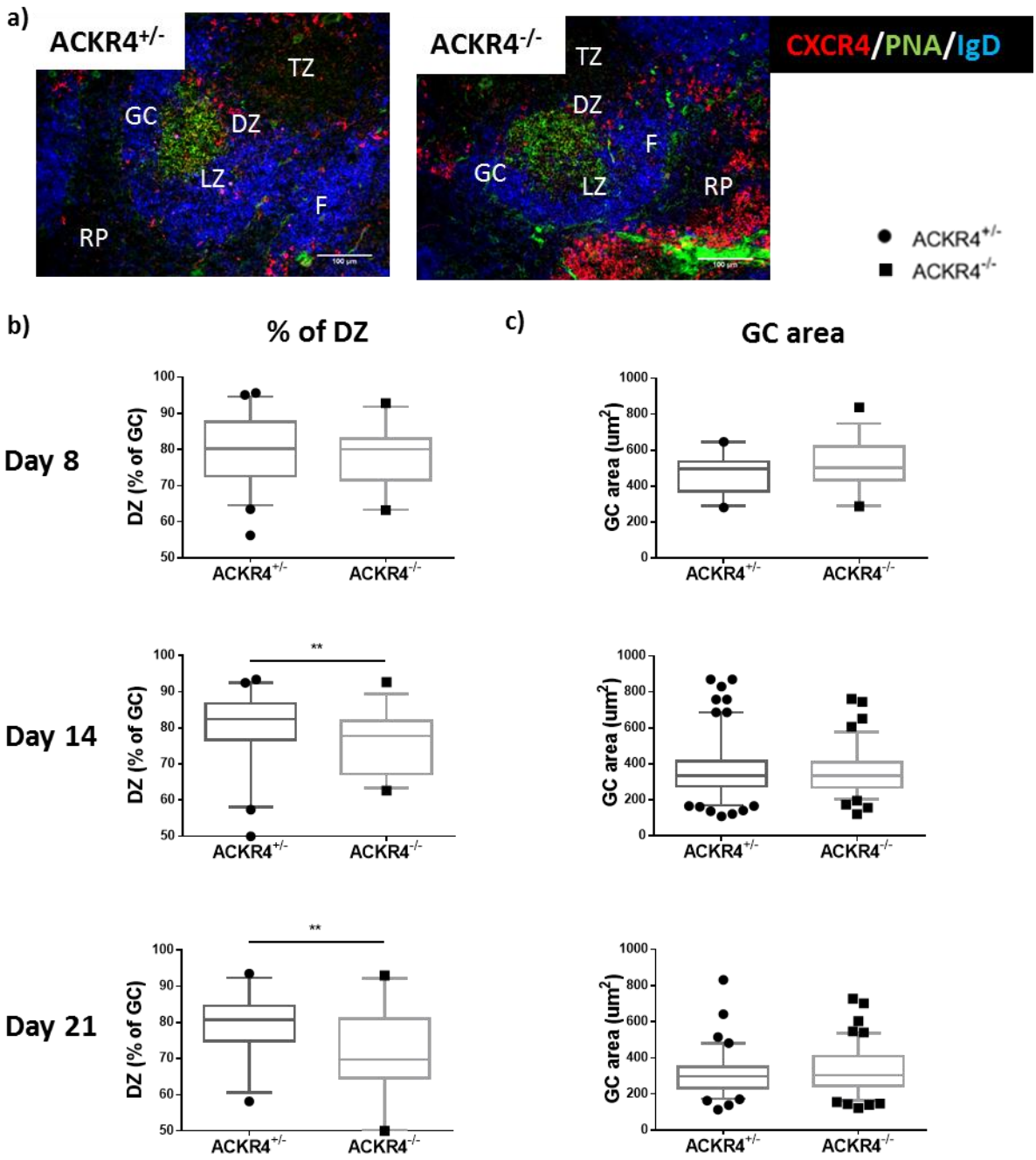

Figure 3.22: DZ/LZ ratio is altered in ACKR4$^{-/-}$ mice 14 days after SRBC (2). a-c) ACKR4$^{+/-}$ and ACKR4$^{-/-}$ mice were immunised with SRBC and spleens were stained by immunofluorescence. a) Representative example of immunofluorescence staining from 14 days post-immunisation. b) Percentage of DZ per GC from days 8, 14 and 21 post-immunisation. c) GC area, in µm^2, as measured in immunofluorescence staining sections from 8, 14 and 21 days post-immunisation.
GCs from whole splenic sections from 2 independent experiments with 4-5 mice per group. Each symbol represents one GC. Horizontal line represents the median.
Key: TZ: T zone; F: B follicle; GC: germinal centre; RP: red pulp; DZ: dark zone; LZ: light zone.
Scale bar: 100 µm.
Box and whiskers plot with 5-95 percentile. Non-parametric Mann-Whitney test **p<0.01

3.2.8 GC B cell proliferation is not altered in ACKR4$^{-/-}$ mice

One reason for enlarged LZ and smaller DZ areas in ACKR4$^{-/-}$ mice versus ACKR4$^{+/-}$ mice could be a reduced cell proliferation. To test this, proliferation rates were examined by using EdU (5-ethynyl-2'-deoxyuridine) incorporation. EdU is a thymidine analogue that is incorporated in the DNA during the S phase of cell cycle and can be detected by histology or flow cytometry. ACKR4$^{+/-}$ and ACKR4$^{-/-}$ mice were immunised with NP-CGG and injected with EdU 1 h prior to sacrifice at days 8, 14 and 21 days post-immunisation. The response was studied by flow cytometry and the gating strategy is shown in Fig. 3.23a. The EdU^{+} gate was set up according to naïve B cells, which should be mainly negative for EdU. GC B cell, LZ GC B cell and DZ GC B cell EdU incorporation was measured at the different time points and a difference was not observed between ACKR4$^{-/-}$ mice versus ACKR4$^{+/-}$ (Fig. 3.23b). Fourteen days post-immunisation, there was a tendency towards higher cell proliferation in ACKR4$^{-/-}$ GCs. This difference was reproducible in independent experiments, but statistically not significant (Fig. 3.23b middle). Furthermore, this tendency had disappeared by day 21 (Fig. 3.23b lower). MFI values for EdU were also studied at the different time points and a difference was not observed (data not shown).

A difference in cell proliferation, as measured by EdU incorporation does not appear to underlie for the skewed LZ/DZ distribution in ACKR4$^{-/-}$ GCs.

3.2.9 The number of plasma cells at the GC-T zone interphase is not altered in ACKR4$^{-/-}$ mice

According to the analysis undertaken of GEO data for gene expression by DZ/LZ GC B cell subsets (Victora, Dominguez-Sola et al. 2012) (Fig. 3.3), ACKR4 is specifically upregulated in DZ GC B cells. Plasmablasts are exiting the GC from the GC-dark zone interface (Meyer-Hermann, Mohr et al. 2012) (Yang Zhang, unpublished). To test whether ACKR4 expression in the dark zone is influencing the exit of plasmablasts through the GC-T zone interphase towards T zone (Fig. 3.24), spleen sections from ACKR4$^{+/-}$ and ACKR4$^{-/-}$ mice immunised with SRBC and 8, 14 and 21 days post-immunisation were stained for CXCR4 (to denote plasmablasts), PNA (to denote GCs) and IgD (to denote follicles) (Fig. 3.24a). CXCR4^{+} plasmablasts leaving the GC through the DZ were counted in GCs when the GC-T zone interphase was visible. To ensure that the sections through GCs were oriented such that they represented the entire GC, GCs were chosen that showed a clear differentiation between LZ and DZ based on CXCR4 expression. An example of the GCs counted is shown in Fig 3.24a. For ACKR4$^{-/-}$ mice versus ACKR4$^{+/-}$ mice, differences were not observed when CXCR4^{+} plasmablasts numbers were expressed in relation to the length of the GC-T zone interphase, neither 8 days after SRBC (Fig. 3.24b upper) nor 14 days (Fig. 3.24b lower). Therefore, it can be concluded that ACKR4 specific expression in the DZ is not influencing the movement of plasmablasts out of the GC through the DZ and GC-T zone interphase.

3.2.10 The number of CD3^{+} cells in GCs is not altered in ACKR4$^{-/-}$ mice

To test the possibility of enlargement of the LZ because of the presence of a higher number of T follicular helper (Tfh) cells, CD3^{+} cells inside GCs were counted in

histological splenic sections from ACKR4$^{+/-}$ and ACKR4$^{-/-}$ mice immunised with SRBC 8, 14 and 21 days post-immunisation (Fig. 3.24c). Tfh cells express Bcl6 and CXCR5 and are important for the maintenance of GCs as they provide signals for the selection of high-affinity GC B cells and that regulate GC B cell differentiation into PCs or MBCs (Crotty 2011). Though CD3 will also label non-Tfh GC T cells, it does provide a good approximation for Tfh cells, as only 10-12% of GC T cells are Tfr cells (Sage, Tan et al. 2015). Fourteen days post-immunisation, ACKR4$^{-/-}$ GCs had lower number of Tfh cells (Fig. 3.24c middle). However, this difference was minimal and was not reproducible either 8 (Fig. 3.24c upper) or 21 days post-immunisation (Fig. 3.24c lower). Moreover, this change cannot account for the skewed LZ/DZ ratio, as less T cells in the LZ would mean smaller LZ areas. It has been shown that the altered LZ/DZ distribution in ACKR4$^{-/-}$ mice at later stages of the GC response is not caused by differences in proliferation, nor by increased PC exit in the GC-T zone interphase, nor by increased numbers of T cells in the LZ. Further events that can cause an alteration to the LZ/DZ distribution are differences in the expression of key molecules that are involved in inter-zonal migration within GCs.

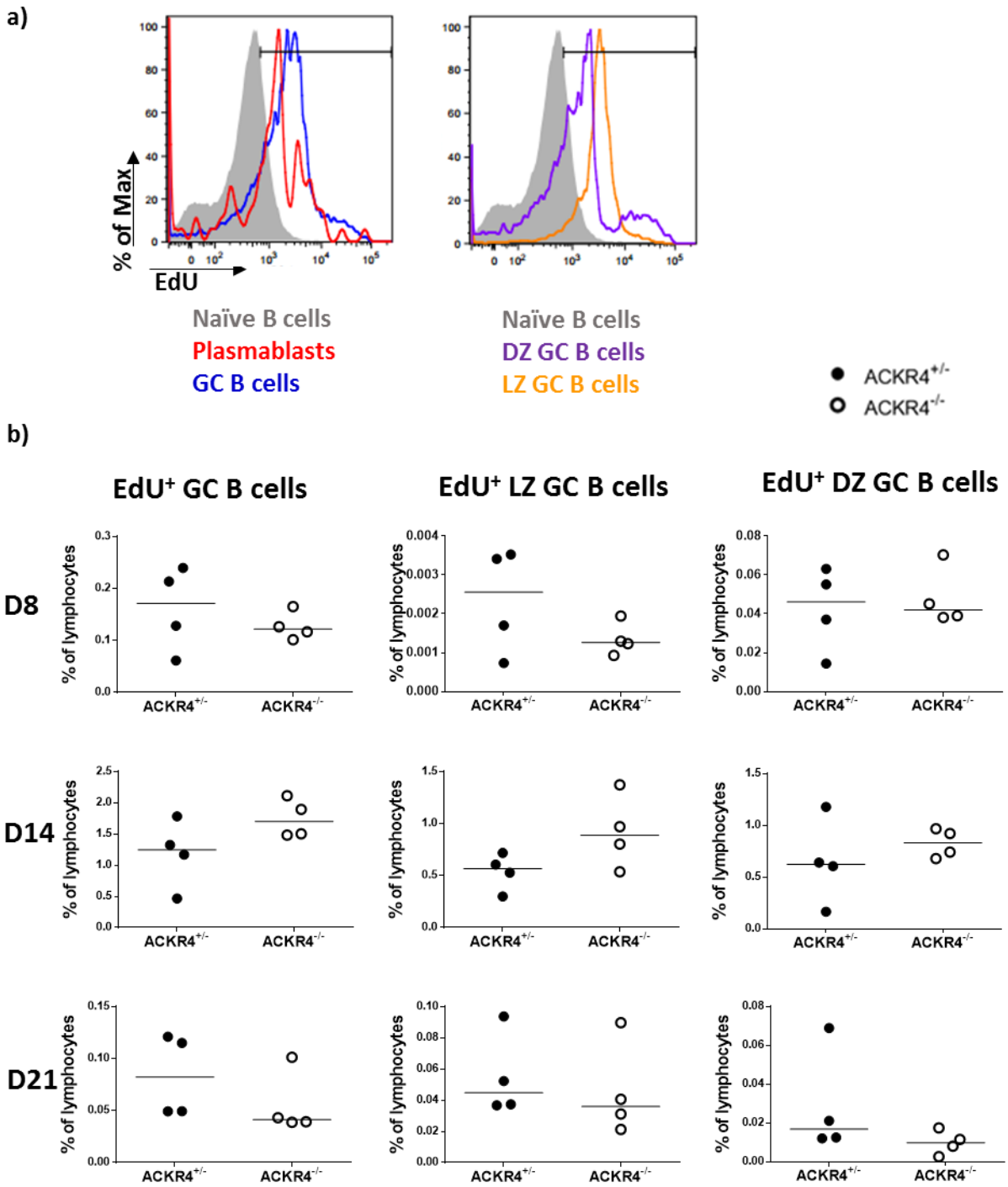

Figure 3.23: Proliferation is not altered in GCs from ACKR4$^{-/-}$ mice. a-b) ACKR4$^{+/-}$ and ACKR4$^{-/-}$ mice were immunised with NP-CGG and EdU incorporation was assessed by flow cytometry. a) Flow cytometry gating strategy for EdU^{+} B cell populations. b) EdU^{+} GC B cells at day 8 (upper), 14 (middle) and 21 (lower) post-immunisation. EdU was injected 1 h prior to death.
Plots are representative of 2 independent experiments with 4-5 mice per group. Each symbol represents one mouse. Horizontal line represents the median.
Key: EdU: 5-ethynyl-2'-deoxyuridine; GC: germinal centre; LZ: light zone; DZ: dark zone; D: day.

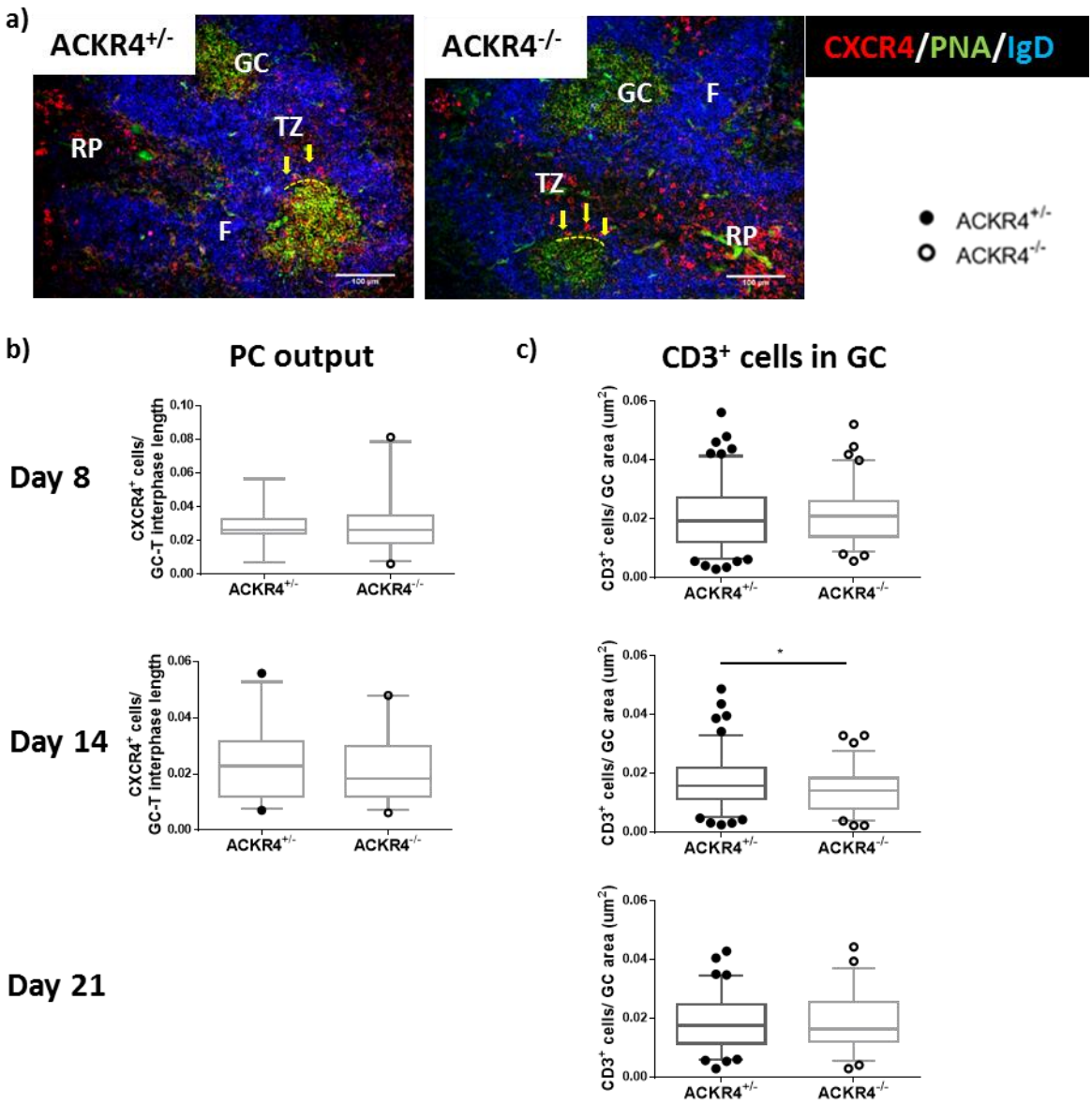

Figure 3.24: Output of PCs (CXCR4^{high}) at GC-TZ interphase and CD3$^+$ cell numbers per GC are normal in ACKR4$^{-/-}$ mice. a-c) ACKR4$^{+/-}$ and ACKR4$^{-/-}$ mice were immunised with SRBC and spleens were stained by immunofluorescence. a) Representative example of immunofluorescence staining for CXCR4 (red), PNA (green) and IgD (blue) 8 days post-immunisation. b) Counts for CXCR4$^+$ plasmablasts per GC-T zone interphase length in 8 days (left) and 14 days (right) post-immunisation. c) Counts for CD3$^+$ cells per GC area, in µm^2, 8 (left), 14 (middle) and 21 (right) days post-immunisation.
GCs from whole splenic sections from 2 independent experiments with 4-5 mice with per group. Each symbol represents one GC. Horizontal line represents the median.
Key: TZ: T zone; F: B follicle; GC: germinal centre; RP: red pulp. PC: plasma cell. Scale bar: 100 µm.
Box and whiskers plot with 5-95 percentile. Non-parametric Mann-Whitney test *p<0.05

3.2.11 GCs from ACKR4$^{-/-}$ mice express more c-Myc and p-Akt at later stages of GC response

A recent publication has linked the expression of ACKR4 with reduced expression of the transcription factor c-Myc in hepatocellular carcinoma (Shi, Yang et al. 2015). Importantly, c-Myc is a major regulator of B cell differentiation and proliferation in the GC (Dominguez-Sola, Victora et al. 2012). In the absence of ACKR4, more ligand binds to CCR7 and in consequence, there is higher activation of the downstream signalling components. Signalling downstream of CCR7 towards c-Myc includes phosphorylation of the Akt-GSK3β pathway (Shi, Yang et al. 2015). To test the effect of ACKR4 deficiency on c-Myc expression, splenic sections from ACKR4$^{+/-}$ and ACKR4$^{-/-}$ mice 8, 14 and 21 days post SRBC immunisation were stained for c-Myc, PNA (to denote GCs) and IgD (to denote follicles) (Fig. 3.25a). c-Myc^{+} cells were counted manually using the same contrast and brightness settings for all images. The numbers of c-Myc^{+} nuclei were analysed in relation to PNA^{+} area. As previously described, GCs expressed lower levels of c-Myc compared to their adjacent cells. Eight days post-immunisation with SRBC, ACKR4$^{+/-}$ mice had more c-Myc^{+} cells per PNA^{+} area than ACKR4$^{-/-}$ (Fig. 3.25b left). Fourteen days post-immunisation, this ratio was inverted and ACKR4$^{-/-}$ mice had more c-Myc^{+} cells per PNA^{+} area than ACKR4$^{+/-}$ mice (Fig. 3.25b middle). 21 days post-immunisation, ACKR4$^{-/-}$ GCs continue to have more c-Myc^{+} cells per PNA^{+} area than ACKR4$^{+/-}$ GCs (Fig. 3.25b right, 3.25c). It is important to note that at day 14 and 21, the differences are statistically more significant (lower p value) and the medians are respectively 1.2 and 1.7 times increased in ACKR4$^{-/-}$ GCs. An increase of 1.2-1.7 times in c-Myc^{+} cells may not appear at first sight to be an elevated number, but may constitute a substantial difference as to cells that recirculate from LZ to DZ and post-GC effects. More B cells that are expressing c-Myc

in the LZ of ACKR4$^{-/-}$ GCs may imply the accumulation of GC B cells in the LZ, as they require downregulation of c-Myc in order to migrate back to the DZ, leading to dysregulated LZ/DZ distribution.

To investigate whether the increase in c-Myc^{+} cells was caused by signalling through the Akt-GSK3β pathway, the phosphorylation status of p-Akt (Ser473) was examined in GC B cells by flow cytometry (Fig. 3.26). ACKR4$^{+/-}$ and ACKR4$^{-/-}$ mice were immunised with NP-CGG and the response analysed 8 and 14 days later. p-Akt levels were higher than naïve B cells (filled grey, Fig. 3.26a) in all of the B cell populations studied, including GC B cells (blue, Fig. 3.26a), memory B cells (green, Fig. 3.26a). Plasma cells expressed the highest levels of p-Akt (red, Fig. 3.26a). In the GC subpopulations, LZ GC B cells (orange, Fig. 3.26a) expressed higher levels than DZ GC B cells (purple, Fig. 3.26a). The gate indicates numbers of p-Akt^{+} cells. When ACKR4$^{-/-}$ mice were compared with ACKR4$^{+/-}$ mice there were no differences in number of p-Akt^{+} cells at any of the time points studied (data not shown).

Eight days post-immunisation, p-Akt MFI levels were observed to be comparable in ACKR4$^{+/-}$ and ACKR4$^{-/-}$ mice in regard to GC B cells, LZ GC B cells and DZ GC B cells (Fig. 3.26b, 3.26c). Fourteen days post-immunisation, p-Akt levels, measured as MFI, were elevated in ACKR4$^{-/-}$ GCs (Fig. 3.27a left, 3.27b left). Dissection of p-Akt levels as to DZ and LZ, revealed that the differences were due to increased phosphorylation levels in LZ GC B cells (Fig. 3.27a right, 3.27b right) and not related to differences in DZ GC B cells (Fig. 3.27a middle, 3.27b middle). Plasma cell p-Akt phosphorylation levels were the same as to both genotypes (Fig. 3.27b lower) and. Therefore, the effect is GC-specific.

To further confirm that the effect observed is generated due to activation of the pathway CCL19/21-CCR7-p-Akt-c-Myc in absence of the scavenging receptor ACKR4, splenocytes from QM, QM CCR7$^{-/-}$ and QM ACKR4$^{-/-}$ mice were stimulated for 30 min *in vitro* with NP-Ficoll and CCL19. Akt phosphorylation levels were measured by flow cytometry and represented as to their MFI (Fig. 3.28). When splenocytes were stimulated only with NP-Ficoll, no differences could be observed among the three genotypes analysed. However, after stimulation of splenocytes with NP-Ficoll and CCL19, p-Akt levels were significantly elevated in ACKR4$^{-/-}$ splenocytes compared to CCR7$^{-/-}$, whose levels remained lower than WT splenocytes.

The above results have confirmed that when ACKR4 is absent, there is more ligand binding to CCR7 and, therefore, more signalling *via* the Akt-c-Myc pathway, resulting in more Akt phosphorylation and c-Myc expression.

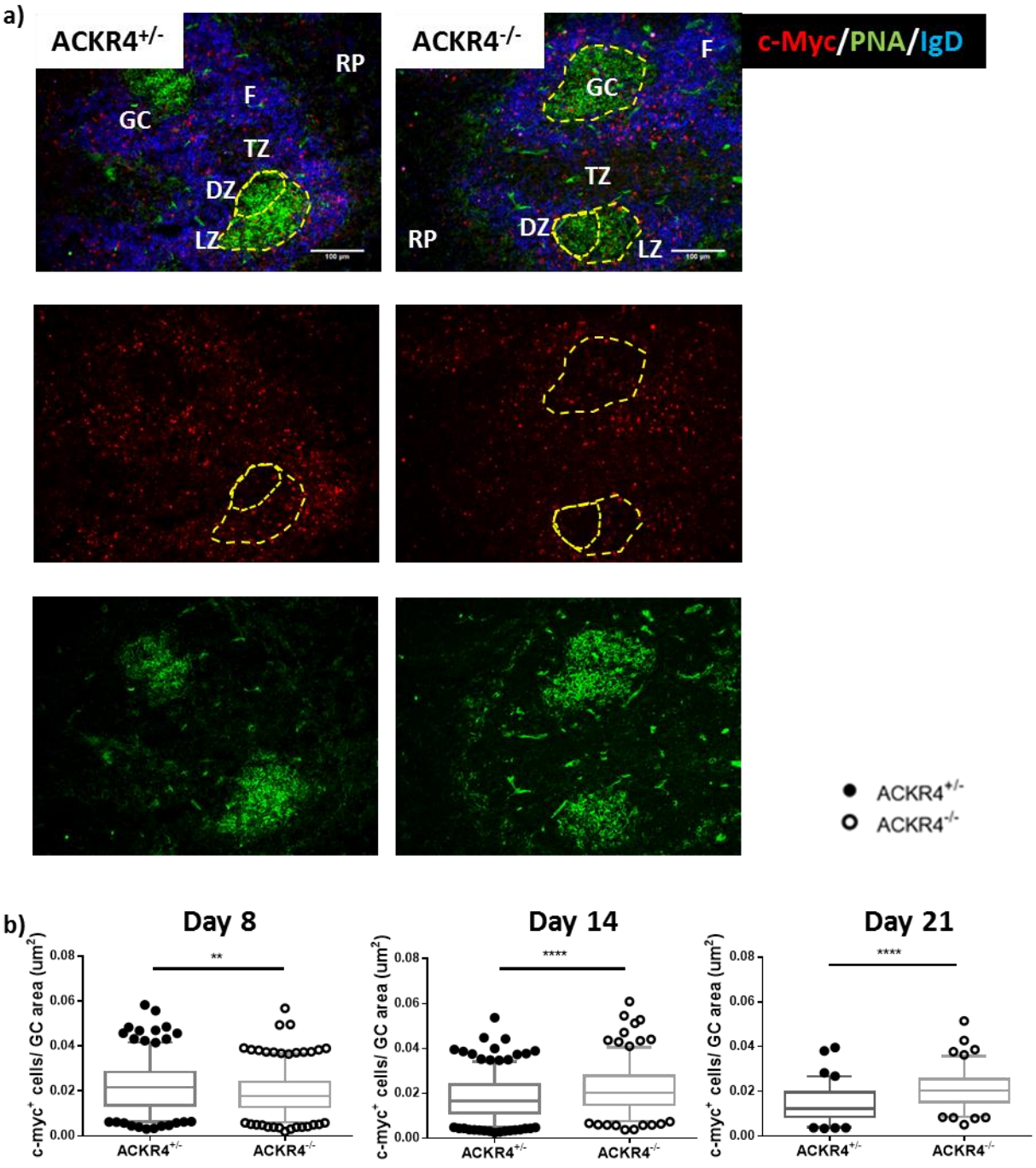

Figure 3.25 (1): GCs from ACKR4$^{-/-}$ mice have more c-Myc^{+} cells 14 and 21 days after SRBC. a-c) ACKR4$^{+/-}$ and ACKR4$^{-/-}$ mice were immunised with SRBC and spleens were stained by immunofluorescence. a) Representative example of immunofluorescence staining for c-Myc (red), PNA (green) and IgD (blue) 8 days post-immunisation. b) Counts for c-Myc+ cells per GC area, in µm^2, 8 (left), 14 (middle) and 21 (right) days post-immunisation. c) Representative example of immunofluorescence staining for c-Myc (red), PNA (green) and IgD (blue) 21 days post-immunisation (see next page).
GCs from whole splenic sections from 2 independent experiments with 4-5 mice per group. Each symbol represents one GC. Horizontal line represents the median.
Key: TZ: T zone; F: B follicle; GC: germinal centre; DZ: dark zone; LZ: light zone; RP: red pulp.
Scale bar: 100 µm.
Box and whiskers plot with 5-95 percentile. Non-parametric Mann-Whitney test **p<0.01; ****p<0.0001

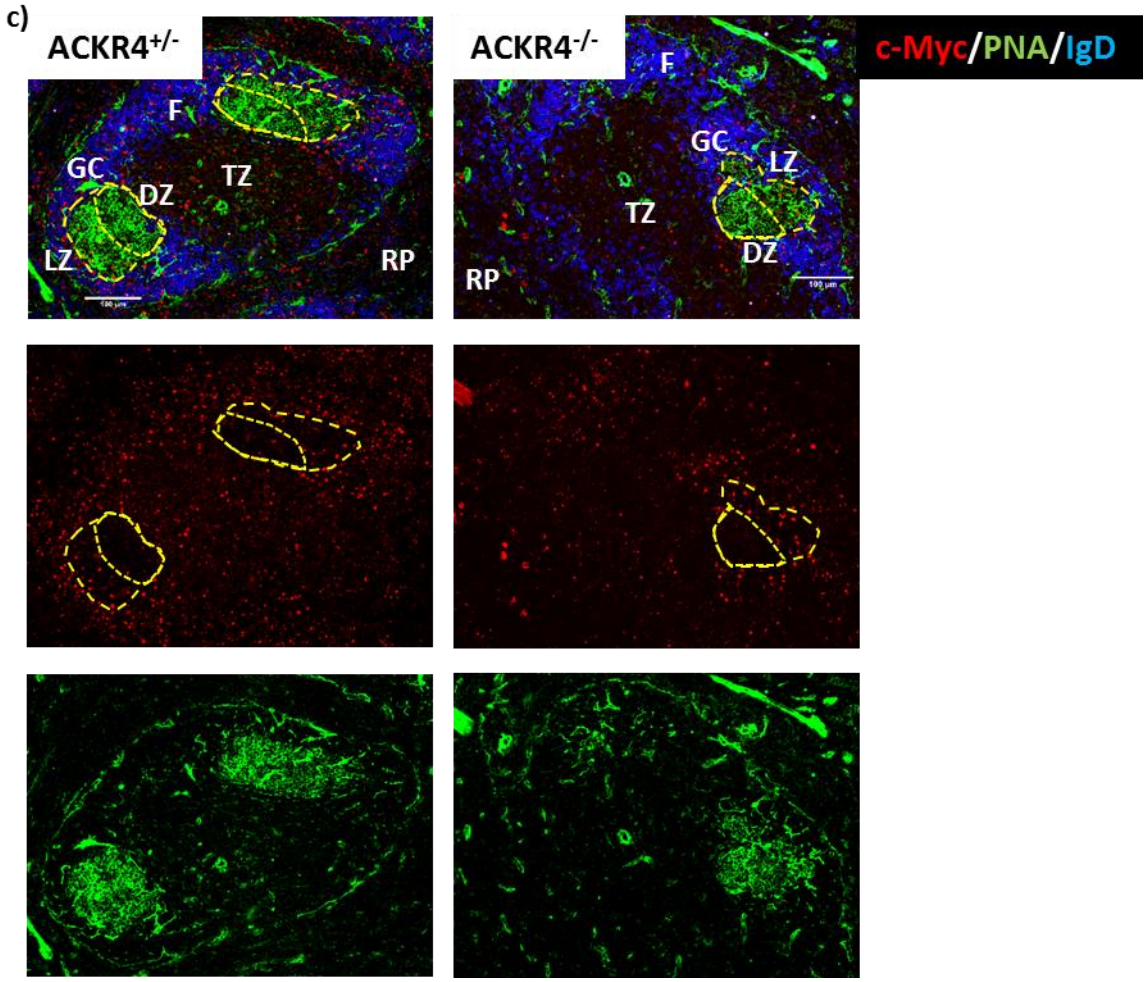

Figure 3.25 (2): GCs from ACKR4$^{-/-}$ mice have more c-Myc^{+} cells 14 and 21 days after SRBC. c) Representative example of immunofluorescence staining for c-Myc (red), PNA (green) and IgD (blue) 21 days post-immunisation.
GCs from whole splenic sections from 2 independent experiments with 4-5 mice per group. Each symbol represents one GC. Horizontal line represents the median.
Key: TZ: T zone; F: B follicle; GC: germinal centre; DZ: dark zone; LZ: light zone; RP: red pulp.
Scale bar: 100 µm.
Box and whiskers plot with 5-95 percentile. Non-parametric Mann-Whitney test **p<0.01; ****p<0.0001

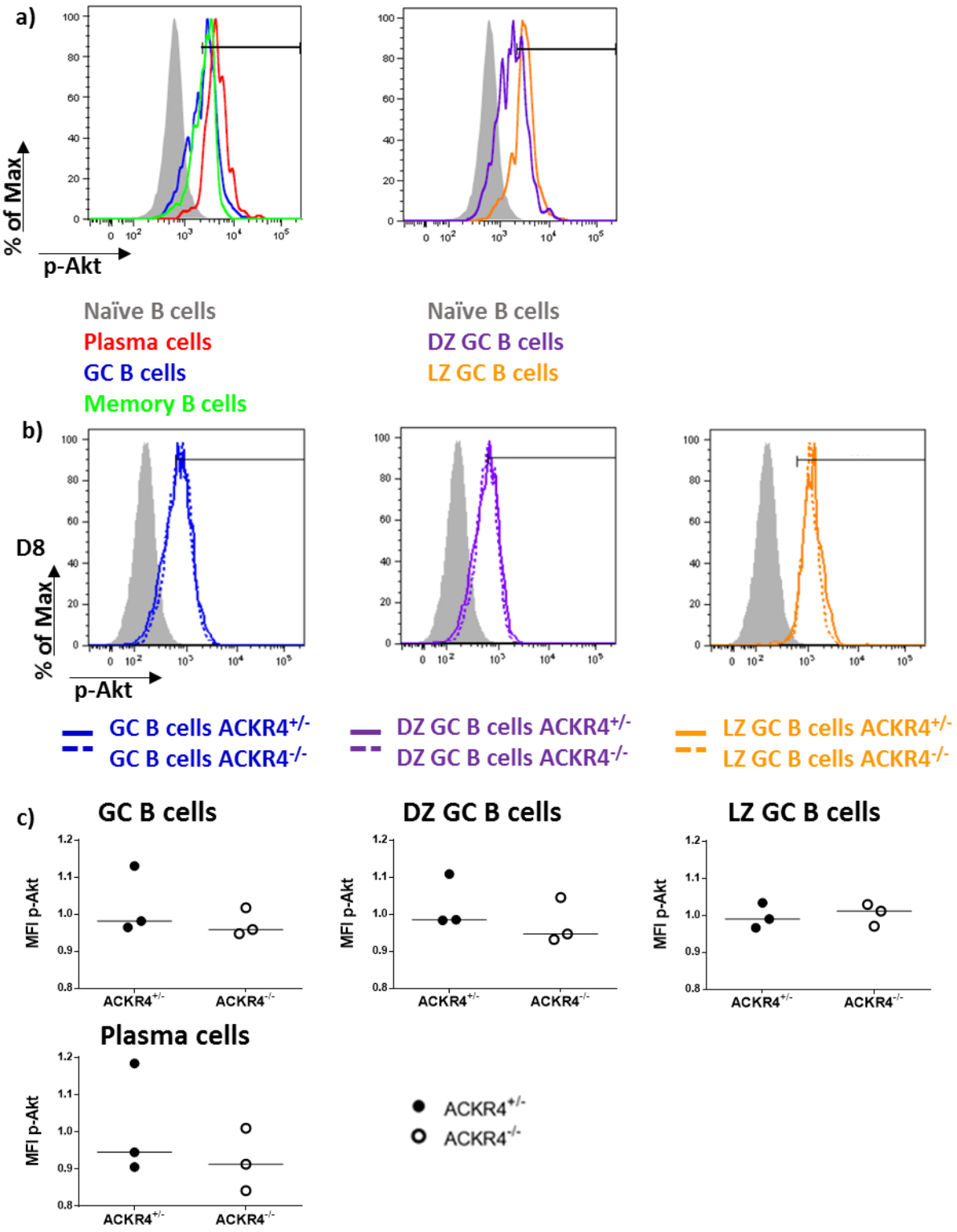

Figure 3.26: GCs from ACKR4$^{-/-}$ mice express same levels of p-Akt 8 days post NP-CGG. a) Flow cytometry gating strategy for p-Akt^{+} (Ser473) in different B cell populations. b) Flow cytometry gating strategy for GC B cells comparing ACKR4$^{+/-}$ and ACKR4$^{-/-}$ mice at day 8 post-immunisation with NP-CGG. c) MFI flow cytometry data for p-Akt^{+} GC B cells, DZ GC B cells, LZ GC B cells and plasma cells at day 8 post-immunisation.
Data were normalised for each experiment. Plots are representative of 2 independent experiments with 3-4 mice per group. Each symbol represents one mouse. Horizontal line represents the median.
Key: GC: germinal centre; DZ: dark zone; LZ: light zone; MFI: mean fluorescent intensity.

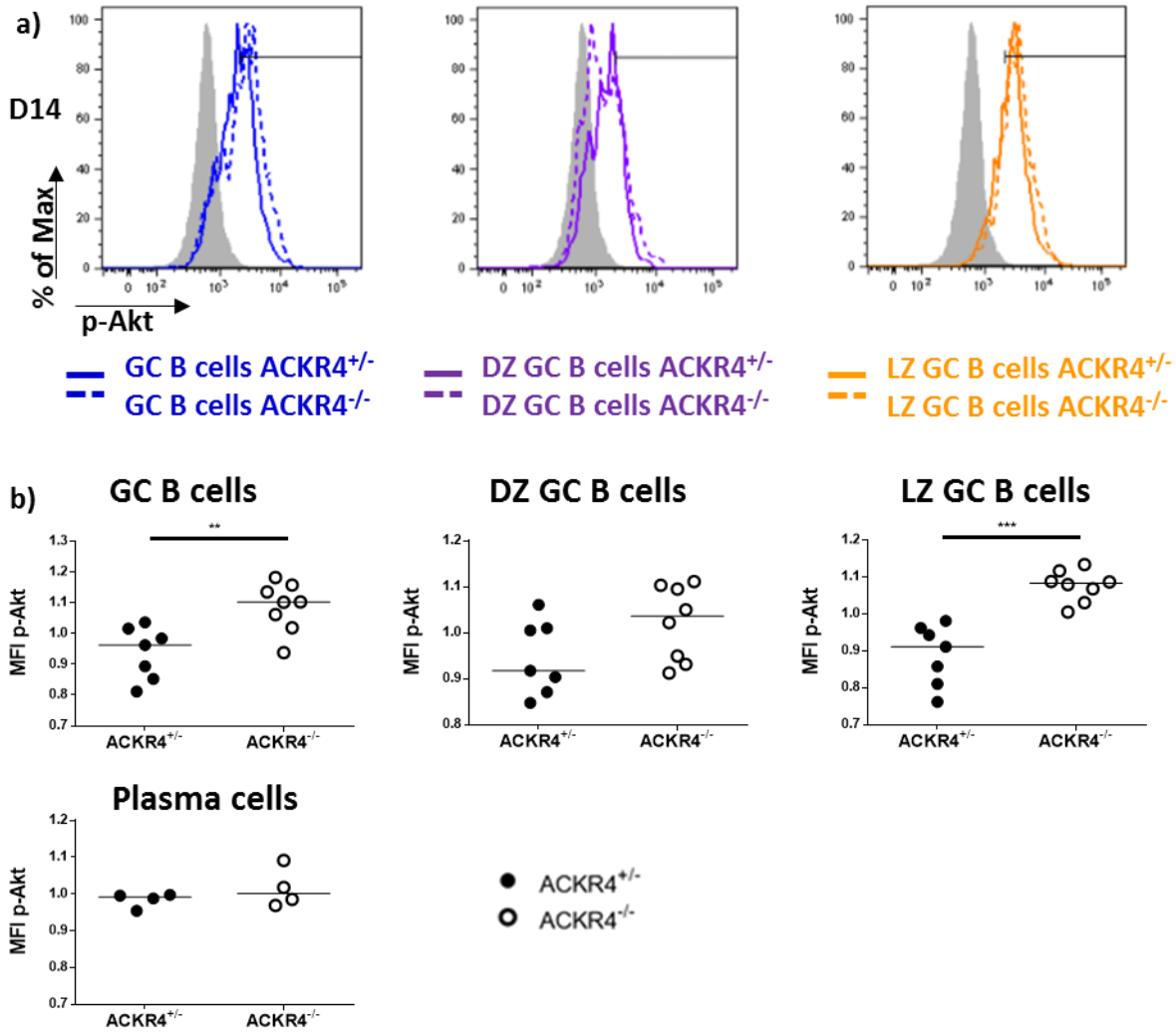

Figure 3.27: GCs from ACKR4$^{-/-}$ mice express higher levels of p-Akt at day 14 after NP-CGG. a) Flow cytometry gating strategy for GC B cells comparing ACKR4$^{+/-}$ and ACKR4$^{-/-}$ mice at day 14 post-immunisation with NP-CGG. c) MFI flow cytometry data for p-Akt^{+} GC B cells, DZ GC B cells, LZ GC B cells and plasma cells 14 days post-immunisation.
Data were normalised for each experiment. Data were combined from 2 independent experiments with 4 mice per group, except for Plasma cells, where plot is representative of 2 independent experiments. Each symbol represents one mouse. Horizontal line represents the median.
Key: GC: germinal centre; DZ: dark zone; LZ: light zone; MFI: mean fluorescent intensity.
Non-parametric Mann-Whitney test **p<0.01; ***p<0.001

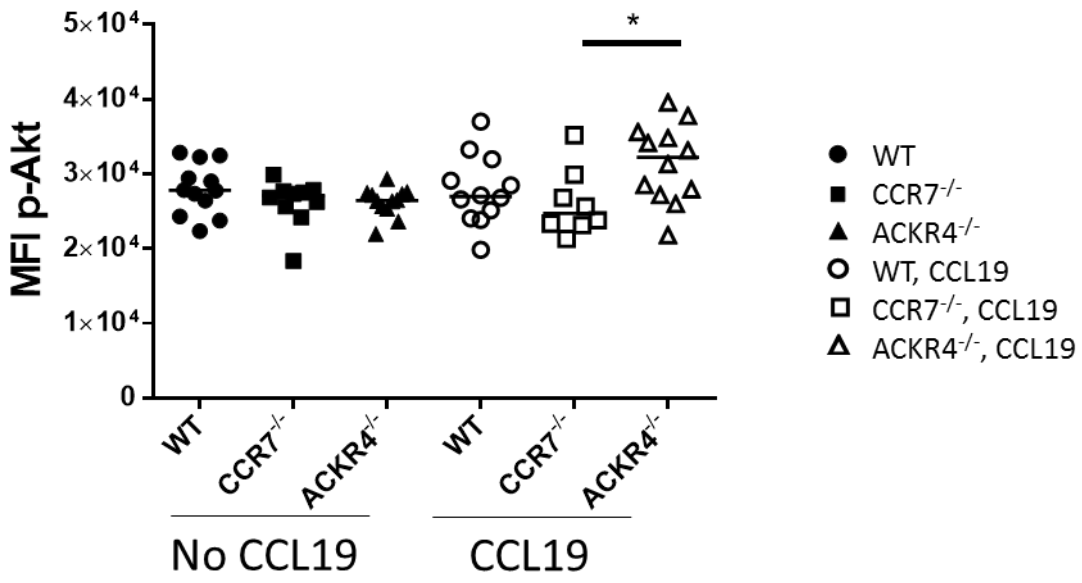

Figure 3.28: *In vitro* stimulation of ACKR4$^{-/-}$ splenocytes with CCL19 causes elevated Akt phosphorylation. p-Akt (Ser473) levels were measured by flow cytometry in splenocytes from QM, QM CCR7$^{-/-}$ and QM ACKR4$^{-/-}$ mice stimulated *in vitro* with NP-Ficoll +/- CCL19.
1 independent experiment. Each symbol represents one mouse. Horizontal line represents the median.
Key: WT: wild type; MFI: mean fluorescent intensity
Non-parametric Mann-Whitney test *$p<0.05$

3.2.12 Secondary response to NP-CGG is normal in ACKR4$^{-/-}$ mice

To investigate if enlarged LZ areas and reduced DZ areas had any relevance in the secondary response to NP-CGG, ACKR4$^{+/-}$ and ACKR4$^{-/-}$ mice were primed with CGG and boosted 5 weeks later with NP-CGG. Five days after boosting, spleens were analysed by flow cytometry. There was no difference when differentiation into NP-specific plasma cells, GC B cells and memory B cells was studied (Fig. 3.29). Moreover, LZ/DZ distribution was normal in ACKR4$^{-/-}$ mice compared to ACKR4$^{+/-}$ mice (Fig. 3.29). These results indicate that ACKR4$^{-/-}$ mice are able mount an effective secondary response. The skewed LZ/DZ distribution does not seem to have an effect in the generation of competent memory B cells, as these are able to mount secondary responses to the same extent as ACKR4$^{+/-}$ mice.

3.2.13 There are no major changes in antibody titres and antibody affinity in ACKR4$^{-/-}$ mice

One consequence of enlarged LZ areas and reduced DZ areas could be an alteration to affinity maturation and antibody titres of the GC-derived plasma cells. In order to explore this possibility antibody titres and affinity to NP were measured by ELISA. ACKR4$^{+/-}$ and ACKR4$^{-/-}$ mice were immunised with NP-CGG and the serum was collected at different time points post immunisation. NP-CGG immunisation causes the induction of Cγ1 switch transcript production from the third day after immunisation and also IL-4 and IFN-γ production (Toellner, Luther et al. 1998). Eight days post-immunisation, differences were not observed as to any of the antibody isotypes analysed in the case of ACKR4$^{-/-}$ mice (Fig. 3.30a). Fourteen days post-immunisation, an increase was observed in the relative antibody titres to NP_{15}-IgG that was not seen in

regard to in IgG1 titres (Fig. 3.30b). However, 21 days post-immunisation, there was no difference in relative antibody titres (Fig. 3.30c). When relative affinity of IgG1 was examined (Fig. 3.30d), there was a reduction in affinity 14 days post-immunisation in ACKR4$^{-/-}$ mice (Fig. 3.30d middle) that was not noticeable 21 days post-immunisation (Fig. 3.30d right).

Antibody affinities were also measured during the secondary response. Mice were primed with CGG, boosted 5 weeks later with NP-CGG and the response analysed 5 days later. Again, there were no significant differences between ACKR4$^{+/-}$ and ACKR4$^{-/-}$ mice (Fig. 3.30e).

These results have shown that the skewed LZ/DZ distribution in ACKR4$^{-/-}$ mice that seems to be a result of increased p-Akt-c-Myc expression does not have a major effect on the relative antibody titres and antibody affinities to NP.

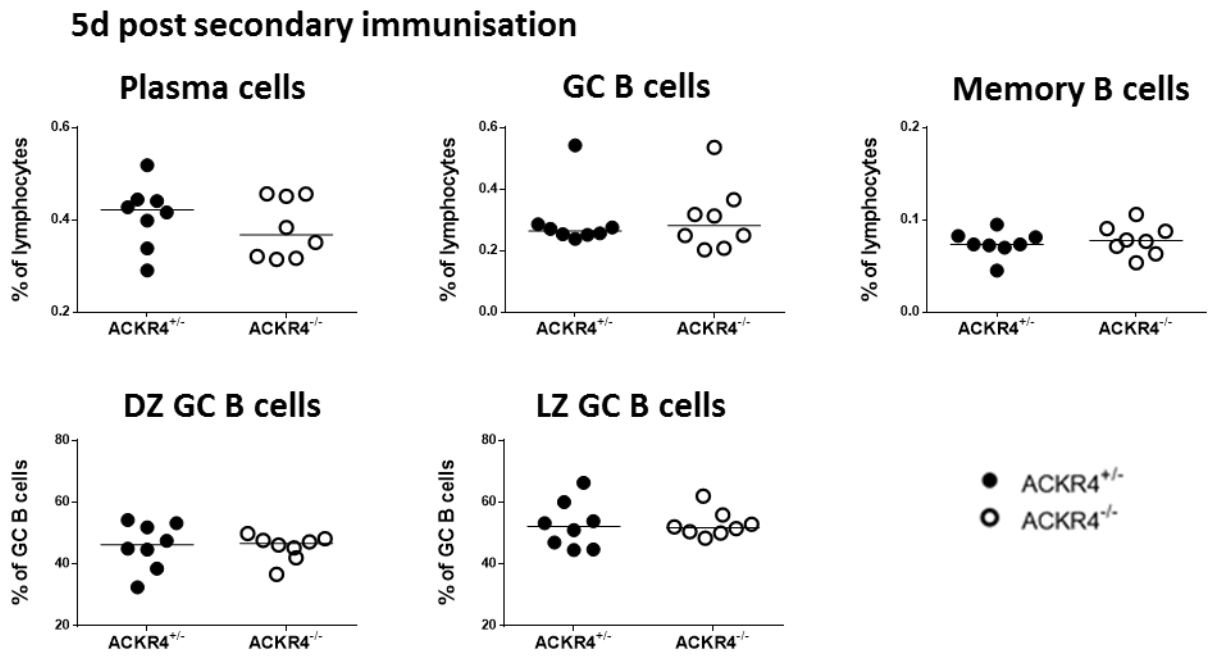

Figure 3.29: Secondary response to NP-CGG is normal in ACKR4$^{-/-}$ mice. ACKR4$^{+/-}$ and ACKR4$^{-/-}$ mice were primed with CGG, boosted 5 weeks later NP-CGG and the response studied 5 days after boosting. % of lymphocytes of plasma cells, GC B cells and memory B cells (upper). % of GC B cells of dark zone and light zone GC B cells (lower).
Data were combined from 2 independent experiments with 4 mice per group. Each symbol represents one mouse. Horizontal line represents the median.
Key: GC: germinal centre; DZ: dark zone; LZ: light zone.

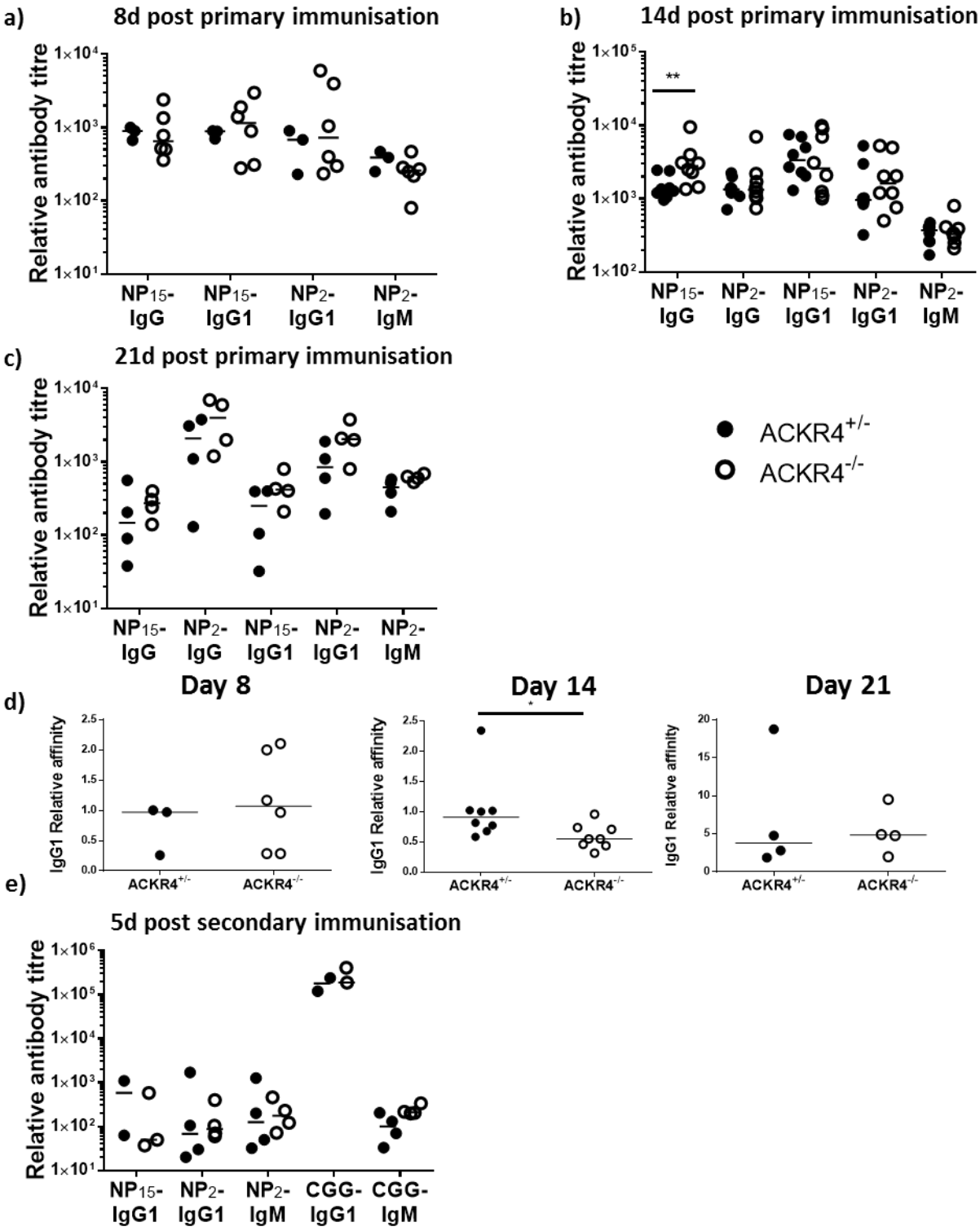

Figure 3.30: No major changes in antibody titres and antibody affinity in ACKR4$^{-/-}$ mice after NP-CGG. a-c) Relative antibody titres from ACKR4$^{+/-}$ and ACKR4$^{-/-}$ mice immunised with NP-CGG a) 8 days b) 14 days c) 21 days post-immunisation. d) IgG1 relative antibody affinity from ACKR4$^{+/-}$ and ACKR4$^{-/-}$ mice immunised with NP-CGG 8 days (left), 14 days (middle) 21 days (right) post-immunisation. e) Relative antibody titres from ACKR4$^{+/-}$ and ACKR4$^{-/-}$ mice when they were primed with CGG and boosted 5 weeks later with NP-CGG and the response studied 5 days after boosting.
Plots from days 8 and 21 post primary and day 5 post secondary immunisation are representative of 2 independent experiments with 3-6 mice. Data from day 14 post primary immunisation were combined from 2 independent experiments with 4 mice per group. Each symbol represents one mouse. Horizontal line represents the median.
Non-parametric Mann-Whitney test *p<0.05; **p<0.01

3.3 Discussion

3.3.1 ACKR4 expression in B cells

The findings from experiments described in this chapter revealed that ACKR4 is expressed both at the mRNA and protein level in germinal centre B cells from spleen and lymph nodes. This was predicted from the analysis of the data deposited in Immgen (Heng and Painter 2008) and by a large scale gene expression analysis of GC B cell subpopulations (Victora, Dominguez-Sola et al. 2012). Moreover, findings have confirmed the expression of ACKR4 in a layer of lymphatic endothelial cells of the lymph node subcapsular sinus (Ulvmar, Werth et al. 2014) and around the splenic marginal zone (Antal Rot, University of York, unpublished). Experiments have further shown that ACKR4 is also expressed at intermediate levels in memory B cells, from their generation in draining LN to their arrival in distant LN, while ACKR4 is downregulated to levels similar to levels found in naïve B cells in plasma cells.

Contrary to CCR7, ACKR4 expression levels vary through the different stages of antigen-induced B cell differentiation. For this reason, the work focused on ACKR4 expression. ACKR4 is able to modulate CCR7 responsiveness by scavenging CCR7 ligands CCL19 and CCL21 (Comerford, Milasta et al. 2006). Interestingly, ACKR4 and CCR7 are differentially expressed between the GC subpopulations of centrocytes in the LZ and centroblasts in the DZ. ACKR4 is expressed at higher levels in the DZ while CCR7 is expressed stronger in the LZ (Victora, Dominguez-Sola et al. 2012). This dichotomy in expression levels opens up the possibility of a role of their shared ligands, CCL19 and CCL21 (Comerford, Harata-Lee et al. 2013) in regulating migration and differentiation of B cells during the germinal centre response.

ACKR4 deficiency in non-immunised mice does not lead to a change in the composition of B cell or T cell subpopulations or their anatomical locations regarding their recirculation through spleen and lymph nodes. An absence of effects on B cell development was expected, as ACKR4 is not expressed during the early stages of B cell development or by the stroma that interacts with developing B cells (Immgen). Due to the absence of effects on mature B cell differentiation stages, it is safe to assume that any difference observed during antigen-induced immune responses are due to the effects of ACKR4 deficiency during the response itself. Therefore, antigen-induced responses were studied directly in ACKR4 deficient mice. This is different from CCR7-deficient mice, which have profound alterations as to migration of naïve lymphocytes into secondary lymphoid organs and also altered lymph node microarchitecture (Forster, Schubel et al. 1999).

3.3.2 IgD^+ cell infiltration in the GC area

For studies of antigen-induced response, all of the mice used were males and $ACKR4^{+/-}$ mice were used as control mice. In a previous publication that has examined the role of ACKR4 in T cell lymphopoiesis in adult mice comparable results were obtained for $ACKR4^{+/+}$ and $ACKR4^{+/-}$ littermates and there were slight differences between males and females (Lucas, White et al. 2015). Moreover, preliminary results in antigen-induced responses showed similar results to those published (S. Cook, personal communication).

When $ACKR4^{+/-}$ and $ACKR4^{-/-}$ mice are subjected to NP-CGG immunisation and at the peak of the GC response, day 8 post-immunisation (Toellner, Gulbranson-Judge et al. 1996), differences in the numbers of GC B cells or plasma cells were not observed.

Strikingly, ACKR4$^{-/-}$ GCs have an abnormal shape, with poorly delimited borders and fuzzy perimeters.

To investigate the reason for the fuzzy shape, particularly if it was caused by ACKR4 expression on the B cells or by cells in the environment, QM B cells, ACKR4$^{+/+}$ or ACKR4$^{-/-}$, were transferred to wt or ko hosts. Under such conditions, it was observed that the fuzziness was not caused by GC B cells spreading out (same PNA^{+} area) but by the infiltration of IgD^{+} cells (naïve B cells) into the GC area. This effect is dependent on the expression of ACKR4 in the environment and not on the expression of ACKR4 by the transferred B cells.

Despite the above severe effect, when the chimeras were analysed at early stages of the GC response by flow cytometry there were no effects other than a small increase in memory B cell numbers. Classically, memory B cells were thought to be produced only *via* the germinal centre pathway (McHeyzer-Williams and McHeyzer-Williams 2005). However, in past years it has been demonstrated that memory B cells can also be produced *via* a GC-independent pathway (Dogan, Bertocci et al. 2009) (Pape, Taylor et al. 2011) (Taylor, Pape et al. 2012). CD73^{+} MBCs are generated independently of GCs and express IgM^{+} (Taylor, Pape et al. 2012). CD80^{+} has been described as a differentiation marker that identifies memory B cells differentiating from the GC pathway, normally express switched Ig memory B cells and have a higher somatic mutation rate. CD80^{+} and PD-L2^{high} and/or CD35^{low} MBCs are considered more memory-like cells as they also have higher mutation rates and are generally switched (Tomayko, Steinel et al. 2010) (Anderson, Tomayko et al. 2007). The increase in CD80^{+} memory B cells observed in ACKR4$^{-/-}$ B cells suggests that B cell selection is de-regulated during GC differentiation.

In regard to the fuzziness of the GC perimeters in absence of ACKR4, the following hypothesis was tested. ACKR4 expression in the surroundings of the GC, by either LECs in the subcapsular sinus or stroma cells in the red pulp of the spleen or even by naïve B cells, might fix naïve B cells in the follicles and prevents them for accessing to the GC area. This would help to create two distinct microenvironments within the B cell areas: the follicle and the GC. In the absence of ACKR4 these microenvironments are intermingled, as follicular B cells are no longer anchored to follicular areas and are able to access the GC areas, where CCL19/CCL21 are available at the same concentration than in the follicle. Accordingly, the borders become diffuse.

The functional consequences of the infiltration of naïve B cells 8 days post-immunisation are not so clear. Increased numbers of naïve B cells in the GC area may restrict the accessibility of GC B cells to other cells such as FDCs and Tfh cells, with which they need to interact. This restricted access may have functional consequences as to the recirculation capacity of cells and the output of cells from GCs.

3.3.3 Skewed LZ/DZ distribution

As to the GC itself, an altered LZ/DZ distribution was observed from 14 days post-immunisation, though GC size was unchanged. This skewed distribution was persistent at least until day 21 post-immunisation and was detected both by flow cytometry and histology and also post-immunisation with different TD antigens, NP-CGG and SRBC. During the first 8 days B cells are activated by T cells present in the T zone- B follicle border. They then, migrate back into follicles where they expand (MacLennan, Liu et al. 1988, Toellner 2014). The fact that no changes were observed 8 days post-immunisation means that ACKR4 is not relevant during the expansion phase of the GC. This was

expected as mature GC B cells are the only B cell subset that expresses ACKR4. However, the increase in LZ GC B cells and the increase in c-Myc-expressing GC B cells 14 days post-immunisation may indicate that the later stages of B cell differentiation, recirculation and migration in the GC, induction of c-Myc and/or proliferation of B cells become regulated by ACKR4 and/or CCR7.

Analysis of GEO data from an earlier publication on genes that are differentially expressed between the light and dark zones (Victora, Dominguez-Sola et al. 2012) showed that ACKR4 is differentially expressed in the DZ of the GC. The transition from centroblast to centrocyte appears to be governed by a timed program that works independently of signals emanating in the DZ (Bannard, Horton et al. 2013). According to this model, the decrease in CXCR4 surface expression, of pro-proliferative genes and of SHM-related genes associated with the transition from DZ to LZ differentiation stage is not a consequence of the phenotype transition but the cause of it. On the other hand, re-entry into centroblast status from LZ requires B cells to examine the new mutated BCRs. B cells do not compete for adhesion to FDC-bounded antigen but high-affinity B cells may be able to capture more antigen from FDCs and also able to remove antigen from the surface of low-affinity B cells (Allen, Okada et al. 2007, Zhang, Meyer-Hermann et al. 2013). Long contacts with T cells should be established but these contacts are infrequent, so it is possible that T cell help restricts selection of clones with high-affinity BCRs (Allen, Okada et al. 2007).

The differential expression of ACKR4 between the LZ and the DZ would make it a candidate gene as to involvement in GC recirculation and fits with the results obtained that the inability to express ACKR4 prevents cells from cycling back to the DZ leading to the accumulation of cells in the LZ at later stages of the GC response. In this case, as

seen, the size of the GC B cell population is unaltered. There are other reasons why ACKR4 deficiency could be causing an increase in LZ B cells which include differences in proliferation, increased numbers of T cells in the LZ and/or increased output of plasma cells from the DZ. ACKR4$^{-/-}$ mice have normal levels of cell proliferation, as measured by EdU incorporation. Moreover, smaller DZ areas are not caused by an increased plasmablast exit towards the T cell area. Additionally, enlarged LZ are not caused by an increased accumulation of Tfh cells.

c-Myc is a master regulator of proliferation and differentiation and its role in GC biology has been very controversial as c-Myc was previously proposed not to have a role in GC biology (Klein, Tu et al. 2003). In a recent publication, c-Myc expression was shown to be triggered by the CCR7-CCL19/CCL21 axis in hepatocellular carcinoma (Shi, Yang et al. 2015). c-Myc expression is reduced when ACKR4 is expressed, as ACKR4 competes with CCR7 and represses CCR7-dependent chemotaxis (Shi, Yang et al. 2015). Accordingly, results presented in this chapter on c-Myc expression have revealed an increase in c-Myc protein expression by day 14 post-immunisation that persisted at least until day 21 which were not present at day 8. GEO data analysis from a previous study (Dominguez-Sola, Victora et al. 2012) (Fig. 3.31) that investigated differential gene expression between c-Myc^{+} and c-Myc^{-} populations from the GC showed that ACKR4 expression negatively correlates with c-Myc expression.

To test whether the increased c-Myc expression is caused by increased signalling through CCR7 *via* the Akt/GSKβ pathway when ACKR4 is absent, p-Akt status was analysed. In parallel to c-Myc expression, Akt phosphorylation (Ser473) was increased in LZ GC B cells 14 days post NP-CGG but not 8 days post-immunisation, where p-Akt

levels were similar between ACKR4$^{+/-}$ and ACKR4$^{-/-}$ GC B cells. To further substantiate that this effect is due to more CCL19/21 binding to CCR7 when ACKR4 is not scavenging these chemokines, WT, ACKR4$^{-/-}$ and CCR7$^{-/-}$ splenocytes were stimulated *in vitro* and p-Akt levels measured. In CCR7$^{-/-}$ splenocytes p-Akt levels remained constant after CCL19 stimulation, whereas ACKR4$^{-/-}$ splenocytes expressed higher p-Akt levels and WT splenocytes expressed intermediate levels.

Akt has not been linked to c-Myc previously in the physiological GC response. However, synergy between Akt and c-Myc has been previously described in the case of Burkitt's lymphoma, which is a GC-derived malignancy (Spender and Inman 2014). Moreover, in GC-derived diffuse large B cell lymphoma (DLBCL), inhibition of signalling PI3K/Akt axis induces down-regulation of the transcription of Myc and rescues the tumorigenic phenotype in DLBCL cell lines (Pfeifer, Grau et al. 2013).

Overall, the findings described support a role for ACKR4 in recirculation of cells within the GC and in the distribution of B cell subpopulations within the GC. ACKR4 is linked to the CCR7-p-Akt-c-Myc axis in the GC response, although the relevance of ACKR4 to the whole GC response is still not clear as the effects observed are very subtle. A small but significant decrease in the affinity of NP-specific antibodies was observed 14 days post-immunisation but this effect was not seen by day 21. Affinity maturation to NP is robustly increased by a few dominant mutations (Jacob, Przylepa et al. 1993) and it is possible that using the NP-system, subtle differences in affinity maturation have gone unnoticed. ACKR4$^{-/-}$ GC B cells have restricted access to the DZ and this may have influenced their chances of undergoing effective somatic hypermutation. It is possible that studies of responses to complex antigens may reveal these subtle differences, as affinity maturation to complex antigens requires sequential accumulation

of many mutations during GC reaction and multiple entries to the DZ (Kuraoka, Schmidt et al. 2016) and this possibility needs to be investigated. It has been shown here that ACKR4-deficiency increases c-Myc expression in the GC. Most DLBCL tumours do not have Myc translocations but they continuously express c-Myc, although dysregulation of c-Myc is not sufficient to cause lymphoma, as the constitutive activation of c-Myc does not cause tumours (Shaffer, Young et al. 2012). It is possible that ACKR4$^{-/-}$ mice are more susceptible to the development of GC-derived lymphomas such as DLBCL, though other hits, such as p53 dysregulation, are highly likely to be required. This possible susceptibility needs to be investigated.

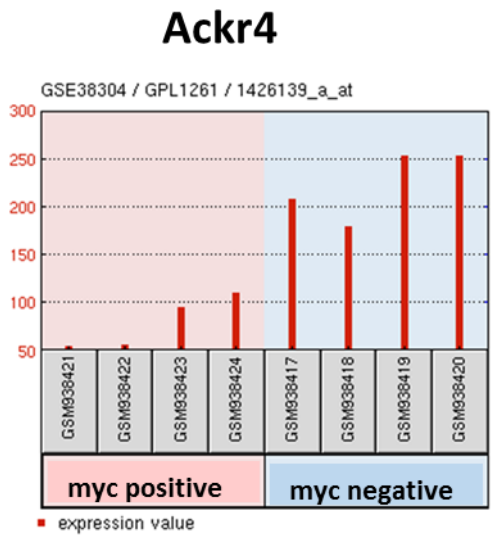

Figure 3.31: Ackr4 expression in GC Myc positive and negative cells. Ackr4 expression measured by gene array (GSE38304, Dominguez-Sola et al. Nature Immunol 2012).

Chapter 4. The CCL19/CCL21 axis regulates memory B cell migration

4.1 Introduction and objectives

4.1.1 Memory B cell generation

Memory B cells are mostly generated in response to T-cell dependent antigens. Two stages of MBC generation have been described accordingly to their T cell requirements. After antigenic challenge, a first wave of T cell-independent MBCs occurs followed by a T cell-dependent wave (Okumura, Metzler et al. 1976). More recently, it has been shown that some IgM^+ MBCs can be generated in response to TI antigens (Good-Jacobson and Tarlinton 2012), but these cells are not the focus of this section. TD-generated MBCs can be the result of the GC reaction or can develop independently of the GC reaction. Both classes of MBCs can persist in a quiescent state over a long period and are equally capable of producing greater amounts of recall antibody responses than naïve B cells (Takemori, Kaji et al. 2014). GC-independent and –dependent MBCs express MBC markers CD80, PDL1, PDL2, CD35, MHC class II and CD40 at comparable level (Anderson, Tomayko et al. 2007) (Takemori, Kaji et al. 2014). In the spleen, MBCs are equally distributed among the follicles and the marginal zones (Anderson, Tomayko et al. 2007). Moreover, IgM^+ MBCs and switched MBCs localise in distinct areas of the spleen. Switched MBCs localise preferentially close to contracted GCs in the spleen (Aiba, Kometani et al. 2010).

4.1.1a GC-independent MBCs

MBCs generated independently of GCs are detected as early as 3 days post-immunisation and do not carry somatic mutations (Takemori, Kaji et al. 2014). They originate from a precursor which is GL7 and CD38 positive (Taylor, Pape et al. 2012). CD40, which is provided by T cells, can by itself cause MBC differentiation. In culture, CD40 signals from T cells induce the differentiation of human GC B cells towards a MBC phenotype (Casamayor-Palleja, Feuillard et al. 1996). In mice, MBC development is impaired by blockade of the interaction between CD40 and CD40L (Siepmann, Skok et al. 2001).

At the initial T-B cell interaction, in the border between the T zone and the follicle there are two possibilities: if the duration of the contact between a T cell and a B cell is long, meaning that B cell has high antigen affinity, B cells will then enter the GC pathway. If the duration is relatively short, B cells are more prone to enter the GC-independent memory pool (Kurosaki, Kometani et al. 2015). Moreover, if ICOS is blocked in the early stages of the immune response, there is no reduction in the total numbers of MBCs, although there are fewer mutated MBCs (Inamine, Takahashi et al. 2005), further demonstrating that MBCs can be generated independently of GCs. MBCs can express IgM or other antibody isotypes (IgG, IgE). However, IgM MBCs do not contribute much to the secondary response (Pape, Taylor et al. 2011). IgE MBCs are generated mainly in response to membrane IgD cross-linking and their generation requires a limited duration of cognate T cell interaction (Le Gros, Schultze et al. 1996).

The generation of MBCs by the GC-independent pathway is dedicated to preserving germ line antibody specificities and prepares the body to elicit rapid responses to variants of the invading antigen (Kaji, Ishige et al. 2012). GC-independently generated

MBCs provide protection against pathogens with antigens and epitopes that are related to the initial invading pathogen.

4.1.1b GC-dependent MBCs

GC-derived MBCs are thought to be dedicated to generate high affinity somatic antibody mutants (Kaji, Ishige et al. 2012). Mutated MBCs are not generated in the absence of Tfh cells, which has been demonstrated in Bcl-6 deficient mice (Kaji, Ishige et al. 2012). CD80 expression identifies the MBCs mutated compartment. CD80 deletion in B cells has shown that CD80 has a role in Tfh maturation and the maintenance of late GC responses and differentiation of MBCs and long-lived plasma cells (Good-Jacobson, Song et al. 2012).

There are two hypotheses regarding the generation of GC-dependent MBCs. The first postulates a master regulator of transcription that guides GC B cells towards the memory pool compartment, as Blimp-1 does for plasma cells (Shaffer, Lin et al. 2002). However, this transcription factor is still to be identified. The second hypothesis is that MBCs differentiate from GC stochastically if they receive survival signals (Kurosaki, Kometani et al. 2015). In support of the last hypothesis is that it has been shown that overexpression of the pro-survival factor Bcl2 or downregulation of pro-apoptotic signals such as Bim, leads to an increase in the memory compartment (Fischer, Bouillet et al. 2007). Quantitative modelling of terminal differentiation of GC B cells has showed that abrogation of IRF4-mediated Blimp-1 activation leads to a steady state resembling MBC phenotype (Martinez, Corradin et al. 2012). In keeping with this model is that IRF4 is not required for MBC generation, though it may have a role in long-term survival (Klein, Casola et al. 2006).

High affinity GC B cells are selected for differentiation into plasma cells. Low-affinity B cells survive in the GC without undergoing plasma cell differentiation, so the mechanism that regulates plasma cell differentiation is independent of the regulation of GC B cell survival (Phan, Paus et al. 2006). Lymphoid tissues have a limited capacity to sustain plasma cells (Sze, Toellner et al. 2000) and it is uncertain whether they also have a limited capacity to sustain MBCs. Nonetheless, and contrary to what it has been described for plasma cells, low affinity LZ GC B cells are actively selected into the MBC pool (Shinnakasu, Inoue et al. 2016). These low affinity B cells specifically express Bach2, a transcriptional repressor that is expressed when B cells receive weak T cell help (Shinnakasu, Inoue et al. 2016). Recently it has been shown that as the GC matures it undergoes a switch in its output (Weisel, Zuccarino-Catania et al. 2016). BrdU pulse labelling was used to show that non-switched MBCs are produced first in the response, followed by switched MBCs and followed by switched long lived PCs.

The persistence of MBCs, contrary to their generation, has been shown to require little, if any, T cell help (Vieira and Rajewsky 1990). IgM^+ MBCs have been shown to live longer than switched MBCs (Pape, Taylor et al. 2011). However, there is controversy on this matter. Schittek and Rajewsky have shown that switched MBCs survive in the order of 0.01% cells of the spleen for at least 200 days (Schittek and Rajewsky 1990). Other studies that have analysed the half-life of IgM^+ and IgG^+ MBCs, utilising a non-toxic pulse chase labelling approach, have shown that IgM^+ and IgG^+ MBCs survived in a similar manner and with a half-life even greater than the 2 years life span of the mouse (Jones, Wilmore et al. 2015). Further studies are needed to clarify this matter.

Upon re-challenge, MBCs have the capacity to respond quickly and to mount effective antibody responses in a shorter time than naïve B cells (Kurosaki, Kometani et al.

2015). According to several reports, switched MBCs are responsible of the potent antibody response, by differentiating rapidly to plasmablasts. IgM^+ MBCs only contribute to the secondary reaction after the disappearance of switched MBCs and enter the GC reaction (Pape, Taylor et al. 2011). Class-switched MBCs diversify their BCRs in the secondary GC reaction (McHeyzer-Williams, Milpied et al. 2015). There is disagreement about whether IgM^+ MBCs undergo CSR after re-stimulation. When the antigen is PE, IgM^+ MBCs do not undergo CSR (Pape, Taylor et al. 2011), but SRBC-specific IgM^+ MBCs do undergo CSR and produce IgG^+ secreting plasma cells (Dogan, Bertocci et al. 2009). Gitlin and colleagues (Gitlin, von Boehmer et al. 2016) designed a very clever way to dissect the role of AID for SHM and CSR in immune responses. Switching to IgG1 favoured B cell differentiation towards the PC compartment, whereas SHM reduced the longevity of MBCs. This correlates with IgM^+ MBCs having longer life spams (Pape, Taylor et al. 2011) as typically only a small proportion of IgM^+ MBCs will have accumulated mutations, while IgG^+ MBCs, as they have been produced in the GC, will have expressed AID and, therefore, accumulated mutations.

There are conflicting reports regarding a major role for switched-MBCs upon re-challenge. In a murine model for ehrlichiosis, which is caused by a bacterial infection transmitted by ticks, IgM^+ MBCs are generated in high numbers and are essential to the mouse mounting a secondary response (Yates, Racine et al. 2013). Moreover, *Plasmodium*-specific MBCs survive in three different subpopulations: mutated IgM^+, mutated IgG^+ and un-mutated IgD^+, but upon re-challenge, IgM^+ MBCs dominated the response and gave rise to plasmablasts faster than IgG^+ MBCs (Krishnamurty, Thouvenel et al. 2016). When MBCs are generated in response to viral particles, both IgM^+ and IgG^+ MBCs are induced and both populations respond rapidly to secondary immunisation producing high amounts of high affinity antibodies (Zabel, Mohanan et

al. 2014). These controversial results demonstrate the importance of the antigen, pathogen and vector that is transmitting the pathogen and it is becoming more and more apparent that different pathogens cause different types of memory responses.

4.1.2 Human MBCs

In humans, the signals and pathways that lead to the generation of MBCs are even less clear. Presently, six MBCs subsets have been defined based on their antigen-experienced phenotype and the differential expression of CD27 and IgH isotypes (Berkowska, Driessen et al. 2011). Human MBCs can also originate from three different pathways, primary GC reactions ($CD27^-IgG^+$ and $CD27^+IgM^+$), secondary GC reactions ($CD27^+IgA^+$ and $CD27^+IgG^+$) or GC-independent B cell activation ($CD27^-IgA^+$) (Berkowska, Driessen et al. 2011). The genes that are expressed by human IgM^+ MBCs and IgG^+ MBCs are similar, but these two populations of cells have different functional capacities (Seifert, Przekopowitz et al. 2015).

4.1.3 Memory B cell migration

The exit of PCs and MBCs from the GC is not very well understood. PCs that leave the GC up-regulate CXCR4 and are attracted towards CXCL12 to a greater extent than their precursors in the GC. CXCL12 is expressed in the splenic red pulp, lymphatic medullary cords and bone marrow. PCs leaving the GC also downregulate CXCR5 and CCR7 (Hargreaves, Hyman et al. 2001). CXCR4-deficient PCs accumulate in the blood, emphasising the importance of CXCL12-directed migration to entrance of PCs to the bone marrow (Hargreaves, Hyman et al. 2001). Emigration of PC from secondary

lymphoid organs also requires signalling through S1P1. S1P1 ligand, S1P, is plentiful in the blood as it is produced by red blood cells (Roth, Oehme et al. 2014).

It has been clear for a long time that there is a population of B cells, defined as memory B cells, that has migratory properties and that is functionally different from GC B cells, as they are long-lived and able to enter the recirculating pool (Kraal, Weissman et al. 1988). *In vitro* GC B cells do not chemotax to chemokines, such as CXCL13, CXCL12 or CCL19, and *in vivo* the GC B cells are confined to the GC area and do not express adhesion factors such as L-Selectin and CLA, whereas MBCs do. This shift in the migratory phenotype takes place in the GC under the control of cytokines such as IL-2, IL-4 and IL-10 (Roy, Kim et al. 2002). Specifically, IL-4 is able to modulate and abbrogate responses to CXCL12 and CXCL13. Once human GC B cells mature to MBCs and plasmablasts, they downregulate CXCR5 surface expression and upregulate ACKR3 (CXCR7) expression, an atypical chemokine receptor that binds CXCL12 and CXCL11. This is a transient expression and regulates exit from the GC to the follicle, as ACKR3-expression ensures that cells are not retained by CXCL12 in the GC, thus limiting CXCR4-associated migratory capacity (Humpert, Pinto et al. 2014).

Memory T cell generation and migration is much better understood (Mueller, Gebhardt et al. 2013). Memory T cells are sub-divided into Central Memory (Tcm), Effector Memory (Tem) and tissue-resident memory (Trm) (Sallusto, Langenkamp et al. 2000). Although Tcm express CCR7, it is known that their migration back to lymph nodes is CCR7-independent (Vander Lugt, Tubo et al. 2013). CD4 memory T cells have been shown to localise to the bone marrow at the end of an immune response, and they position themselves close to IL-7 producing stromal cells (Tokoyoda, Hauser et al. 2010).

4.1.4 Objectives of this chapter

The experiments described in this chapter have investigated the role of ACKR4 in the generation and migration of MBCs. As described in Chapter 3, ACKR4 is specifically expressed on GC B cells and on lymphatic endothelial cells of the subcapsular sinus (SCS). This restricted pattern of expression suggests a role for ACKR4 in regulating the migration of GC B cells as to output. It has been shown before that ACKR4 expression in the SCS causes a CCL19/21 gradient from the T zone to the capsule that influences the migration of DCs inwards (Ulvmar, Werth et al. 2014). As MBCs exit the GC from the LZ and migrate towards the SCS (Y. Zhang, unpublished), the CCL19/21 gradient may also be influencing MBC migration towards the capsule and their appearance in distant lymphoid organs, as MBCs express CCR7 and ACKR4. The areas investigated are as follows:

1. MBC generation in ACKR4$^{-/-}$ mice during TD response to NP-CGG.
2. MBC migration rate to distant sites and MBC localisation within distant LN in ACKR4$^{-/-}$ mice.
3. The importance of ACKR4 expression by MBCs and stromal cells.
4. The relation to CCR7$^{-/-}$ MBCs. MBC generation and migration in CCR7$^{-/-}$ B cells
5. Is this process CCL19/21 dependent?

4.2 Results

4.2.1 Memory B cells from Cγ1-Cre mTmG ACKR4$^{-/-}$ appear in higher numbers in the distant LN from 8 days after NP-CGG

Chapter 3 has documented that ACKR4 is expressed by GC B cells (Fig. 3.4, 3.5) and has a minor role in intra-GC migration at the mature stage of the GC response (Fig. 3.19). ACKR4 does not seem to have a role in GC output generation in the spleen (Fig. 3.14, 3.19). In order to investigate whether this is true also in the case of LN and if ACKR4 has a role in the migration of MBCs from the draining LN to other non-reactive sites, Cγ1-Cre x mTmG mice that were backcrossed into the ACKR4$^{-/-}$ strain were used for experiments.

mTmG is a double-fluorescent reporter system whereby all of the body cells initially express the membrane-bound tandem-dimer Tomato (TdTomato) protein (mT) under the control of CMV β-actin enhancer promoter. After Cre expression, TdTomato is deleted and this leads to the expression of membrane-bound GFP protein (mG) (Muzumdar, Tasic et al. 2007). Cγ1-Cre mice (See 2.1.5) express Cre recombinase after transcription of the Iγ1-Cg1 constant region gene germline transcript, expressed during the initiation of IgG1 class-switch recombination (Casola, Cattoretti et al. 2006). Cg1 germline transcripts are expressed after cognate Th2-B cell interaction, for example: during initial the T-B interaction after T cell priming has taken place (Toellner, Luther et al. 1998), or during Tfh cell- B cell interaction in the GC (Liu, Malisan et al. 1996). Limitations of the Cγ1-Cre mice include: (i) 2% of the IgM^{+} B cells pre-immunisation shows Cre-mediated recombination, (ii) Cre-mediated recombination labels 85-95% of the GC B cell population and 70-80% of the memory B cell population, (iii) Cre-mediated recombination involves most IgG1-, but also a fraction of IgG3-, IgG2a-,

IgG2b- and IgA-expressing GC and post-GC B cells (Casola, Cattoretti et al. 2006). These limitations imply that some of the antigen-specific B cells that are involved in the immune response are not detected.

F1 crosses of these two strains (Cγ1-Cre x mTmG) produce mice where B cells that have interacted with T cells and expressed the Cγ1 gene will be GFP^+. This includes most GC B cells and their descendants, plasma cells and T-dependent MBCs. Therefore, MBCs derived from GC, but also from the initial T-B interactions (GC-independent MBCs) will be detectable by flow cytometry. Because the fluorescent reporters are membrane anchored, they are also suitable for immunofluorescence histology.

In Cγ1-Cre eYFP mice, post NP-CGG immunisation subcutaneously in the hind feet, $eYFP^+$ GC B cells peaked at day 7 post-immunisation in the drLN, as analysed by flow cytometry (Y. Zhang, unpublished, Fig. 4.1a). $eYFP^+$ MBCs in the drLN peaked slightly later, between day 7 and day 10, and numbers were maintained until day 14. By day 21, MBCs were imperceptible. In the distLN, MBCs peaked parallelly to the drLN (Y. Zhang, unpublished, Fig. 4.1b and 4.1c). These preliminary results indicated the best time points to study T-dependent MBC generation.

The primary response to NP-CGG in alum with b.p. in Cγ1-Cre mTmG $ACKR4^{+/+}$ and Cγ1-Cre mTmG $ACKR4^{-/-}$ mice was analysed 5, 8 and 14 days post subcutaneous immunisation in the hind feet. The popliteal lymph node drains immunisation in the foot (Harrell, Iritani et al. 2008). The primary response and GC development are restricted to the popliteal LN (from now on, draining LN or drLN). From there, MBCs will migrate to other sites, while PCs will home to the bone marrow (Tellier and Kallies 2014). Different B cell subpopulations in the drLN of Cγ1-Cre mTmG $ACKR4^{+/+}$ and Cγ1-Cre mTmG $ACKR4^{-/-}$ mice were analysed by flow cytometry. The gating strategy is shown

in Fig. 4.2. Cγ1-expressing B cells were gated according to the expression of GFP and further subdivided in plasma cells ($CD138^+$) and germinal centre B cells ($CD138^-$ $B220^+CD38^-Fas^+$). GC B cells were further subdivided into DZ and LZ on the basis of their expression of CXCR4 and CD86. MBCs were gated from the GFP^+ population as $CD38^+CD138^-$, in keeping with naïve B cell expression of these markers (gate 2, Fig. 4.2), but as these are GFP^+ this indicates that they have seen the antigen and interacted with T cells. MBCs were further subdivided in $CD73^+$, $CD80^+$ and $PDL2^+$ MBCs. These subpopulations of MBCs have been previously described (Anderson, Tomayko et al. 2007).

Five days post-immunisation, Cγ1-Cre mTmG $ACKR4^{-/-}$ mice had numbers of GFP^+ cells, plasma cells, GC B cells and a distribution of GC in LZ and DZ comparable to Cγ1-Cre mTmG $ACKR4^{+/+}$ mice (Fig. 4.3). MBCs were not analysed in the drLN at this time point due to their low numbers (Fig. 4.1) and that they might be recently activated B cells. At the peak of the GC response to NP-CGG, which was 8 days post-immunisation, Cγ1-Cre mTmG $ACKR4^{-/-}$ mice presented comparable numbers than Cγ1-Cre mTmG $ACKR4^{+/+}$ mice of all the B cell subpopulations analysed, which included GFP^+ cells, plasma cells, GC B cells, LZ and DZ GC B cells, MBCs, $CD73^+$, $CD80^+$ and $PDL2^+$ MBCs (Fig. 4.4). The response of Cγ1-Cre mTmG $ACKR4^{+/+}$ and Cγ1-Cre mTmG $ACKR4^{-/-}$ mice to NP-CGG immunisation was also studied in the drLN 14 days post-immunisation. GFP^+ cell, plasma cell and GC B cell populations were similar in Cγ1-Cre mTmG $ACKR4^{+/+}$ and Cγ1-Cre mTmG $ACKR4^{-/-}$ mice (Fig. 4.5). As previously observed for the splenic response to NP-CGG (Fig. 3.19), GCs from $ACKR4^{-/-}$ mice presented a skewed LZ/DZ distribution, with elevated LZ GC B cell numbers and reduced DZ GC B cell numbers (Fig. 4.5). MBCs and the different MBCs subpopulations analysed were comparable for both mice (Fig. 4.5).

Analysis of the distant lymph nodes (axillary and brachial, distLN) from Cγ1-Cre mTmG ACKR4$^{+/+}$ and Cγ1-Cre mTmG ACKR4$^{-/-}$ mice showed an increased appearance of GFP^{+} cells in the ACKR4$^{-/-}$ distLNs (Fig. 4.6a). The expression of mGFP showed that these cells had seen antigen and undergone T-dependent activation. The expression of CD38 confirmed that these cells were not GC B cells, and the absence of CD138 expression indicated that they were not PCs. Before immunisation, there were barely any GFP^{+} cells in the distLN, indicating that the cells that appeared afterwards had been generated specifically in the immune response provoked by the immunisation (Day 0, Fig. 4.6a and 4.6b). At early stages of the immune response, there were no difference in the numbers of GFP^{+}MBCs in the distLN from Cγ1-Cre mTmG ACKR4$^{+/+}$ and Cγ1-Cre mTmG ACKR4$^{-/-}$ mice (Day 5, Fig. 4.6b). Strikingly, from day 8 post-immunisation onwards, in ACKR4$^{-/-}$ distLN there were significantly more GFP^{+}MBCs (Day 8, Day 14, Fig. 4.6b).

Several reasons might account for the increased appearance of MBCs in distant lymphoid sites. For example: increased differentiation of B cells into MBCs in the drLN will lead to elevated MBC migration out of the drLN and, therefore, increased appearance in distant sites; preference of MBCs to leave the drLN in ACKR4$^{-/-}$ mice; or preference of MBCs to enter distLN in ACKR4$^{-/-}$ mice can also lead to an increased appearance of MBCs in distLN; increased retention of MBCs in distLN from ACKR4$^{-/-}$ mice can also lead to elevated numbers of MBCs in distLN. The results showed in Fig. 4.4 and 4.5 indicated that ACKR4$^{-/-}$ mice did not seem to have an increased level of generation of MBCs.

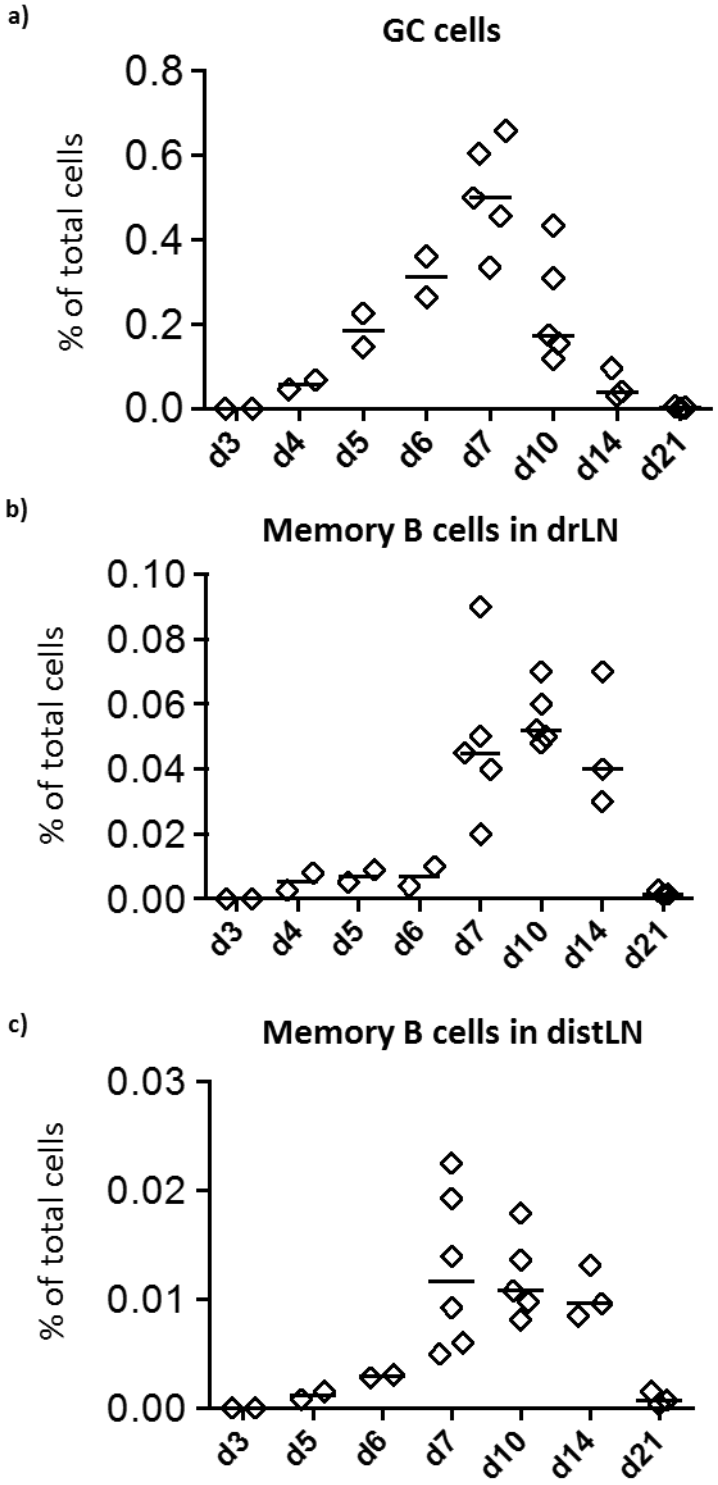

Figure 4.1: MBCs numbers reach the maximum in draining lymph node and distant lymph node in parallel to GC B cells. Cγ1-Cre eYFP mice were immunised with NP-CGG s.c. in the rear feet and the response studied at different time points post-immunisation in the drLN and distLN by flow cytometry. a) GC B cells, as to the % of total number of cells in the drLN. b) MBCs, as to the % of total number of cells in the drLN. c) MBCs, as to the % of total number of cells in the distLN.

1 independent experiment. Each symbol represents one mouse. Horizontal line represents the median.

Key: GC: germinal centre; MBCs: memory B cells; drLN: draining lymph node; distLN: distant lymph node; d: day; s.c: subcutaneously.

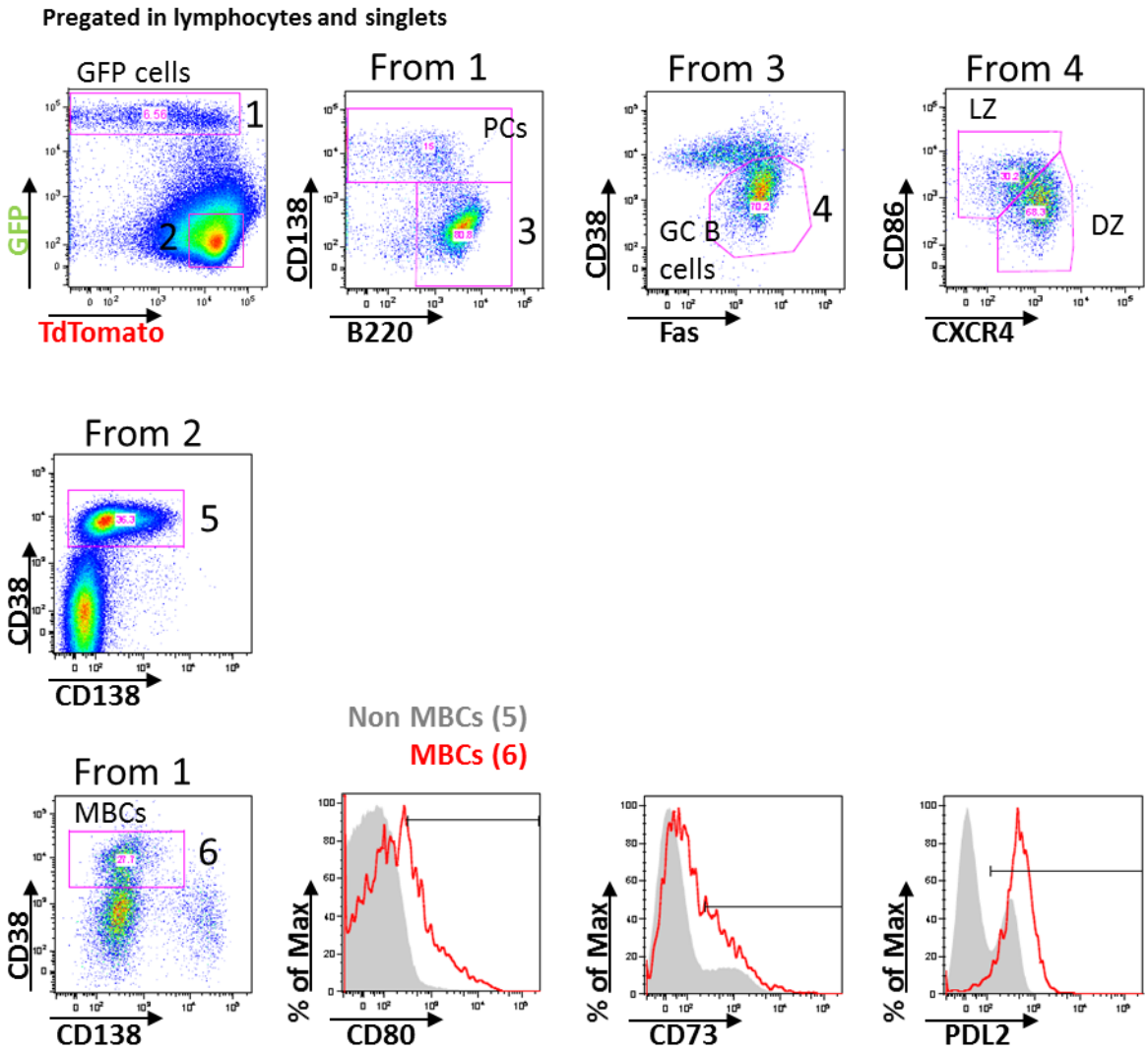

Figure 4.2: Representative gating strategy for antigen-specific B cell populations in the draining lymph node of Cγ1-Cre mTmG mice 8 days post-immunisation with NP-CGG. Cγ1-Cre mTmG ACKR4$^{+/+}$ and Cγ1-Cre mTmG ACKR4$^{-/-}$ mice were immunised with NP-CGG s.c. in the rear feet and the response was studied at different times post-immunisation. The figure shows the flow cytometry gating strategy for different B cell subsets from drLN 8 days post-immunisation. Key: GFP: green fluorescent protein; GC: germinal centre; DZ: dark zone; LZ: light zone; MBCs: memory B cells; s.c: subcutaneously.

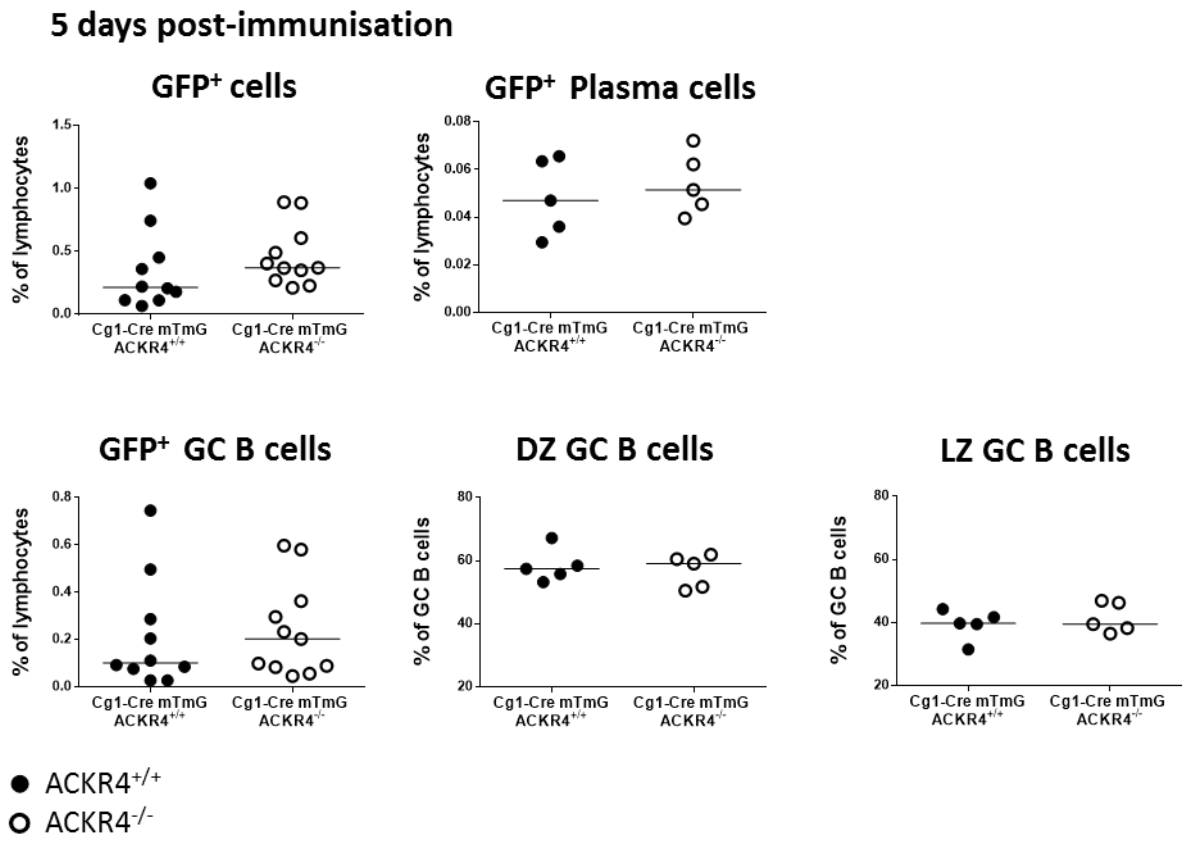

Figure 4.3: Cγ1-Cre mTmG ACKR4$^{-/-}$ mice have a normal response in the draining lymph node to NP-CGG, 5 days post-immunisation. Cγ1-Cre mTmG ACKR4$^{+/+}$ and Cγ1-Cre mTmG ACKR4$^{-/-}$ mice were immunised with NP-CGG s.c. in the rear feet and the was response studied 5 days post-immunisation. Quantification, as to the % of lymphocytes, of GFP^{+} cells, plasma cells (GFP^{+} CD138^{+}), GC B cells (GFP^{+}CD38^{-}Fas^{+}). Quantification as to the % of GC B cells, of DZ GC B cells (GFP^{+}CD38^{-}Fas^{+}CXCR4^{+}CD86^{-}) and LZ GC B cells (GFP^{+}CD38^{-}Fas^{+}CXCR4^{+}CD86^{-}) from pLN (draining LN) 5 days post-immunisation.
Data were combined from 2 independent experiments with 5 mice per group, except for DZ and LZ GC B cells, where plots are representative of 2 independent experiments. Each symbol represents one mouse. Horizontal line represents the median.
Key: GFP: green fluorescent protein; GC: germinal centre; DZ: dark zone; LZ: light zone; s.c: subcutaneously; drLN: draining lymph node.

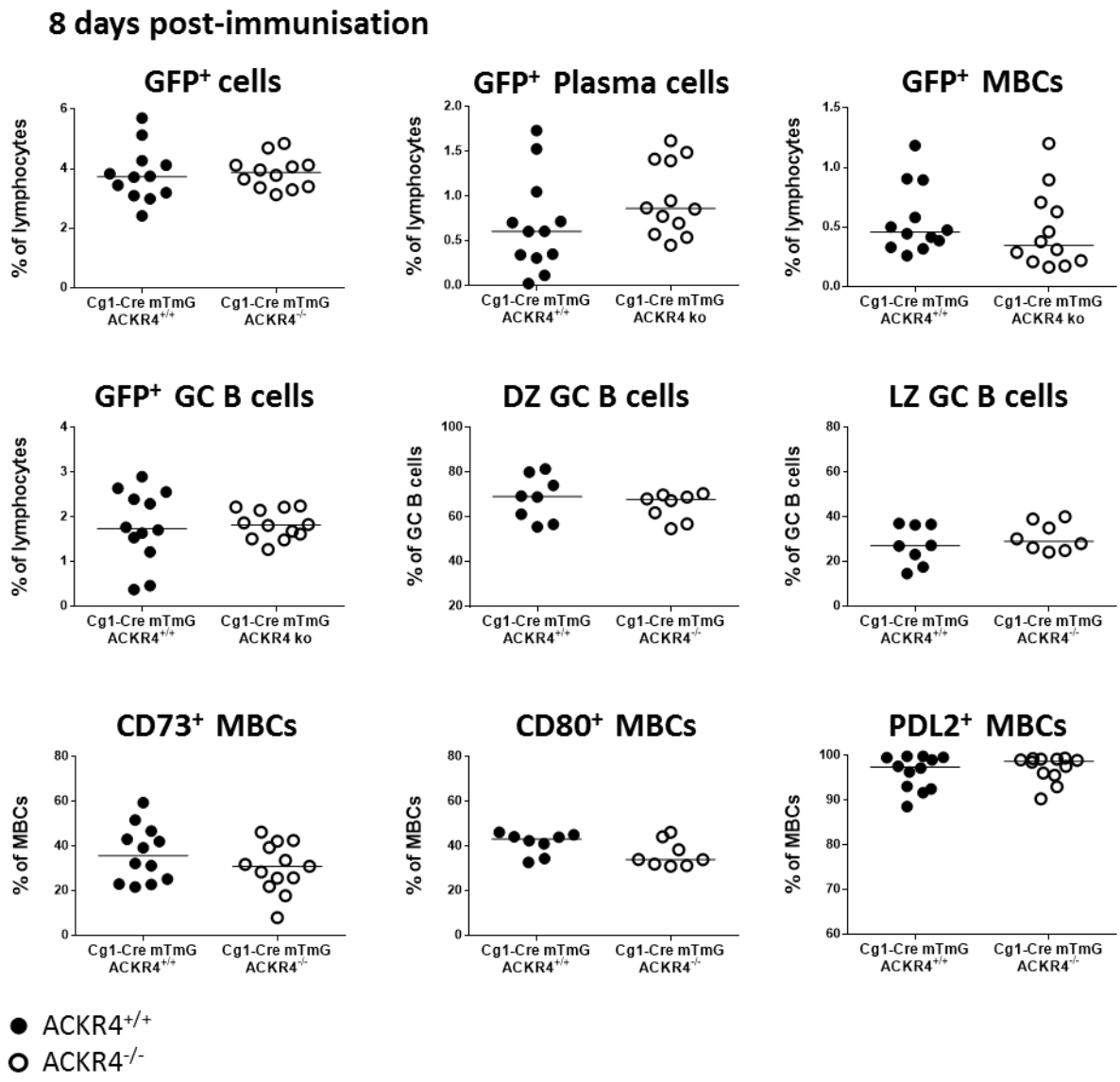

Figure 4.4: Cγ1-Cre mTmG ACKR4$^{-/-}$ mice have a normal response in the draining lymph node to NP-CGG, 8 days post-immunisation. Cγ1-Cre mTmG ACKR4$^{+/+}$ and Cγ1-Cre mTmG ACKR4$^{-/-}$ mice were immunised with NP-CGG s.c. in the rear feet and the response was studied 8 days post-immunisation. Quantification, as to the % of lymphocytes, of GFP^{+} cells, plasma cells (GFP^{+} CD138^{+}), memory B cells (GFP^{+}CD38^{+}CD138^{-}), GC B cells (GFP^{+}CD38^{-}Fas^{+}). Quantification, as to the % of GC B cells, of DZ GC B cells (GFP^{+}CD38^{-}Fas^{+}CXCR4^{+}CD86^{-}) and LZ GC B cells (GFP^{+}CD38^{-}Fas^{+}CXCR4^{+}CD86^{-}). Quantification, as to the % of MBCs, of CD73^{+}, CD80^{+} and PDL2^{+} MBCs from pLN (draining LN) 8 days post-immunisation.
Data were combined from 3 independent experiments with 4 mice per group, except for DZ, LZ GC B cells and CD80^{+} MBCs, where data were combined from 2 independent experiments. Each symbol represents one mouse. Horizontal line represents the median.
Key: GFP: green fluorescent protein; GC: germinal centre; DZ: dark zone; LZ: light zone; MBCs: memory B cells; s.c: subcutaneously.

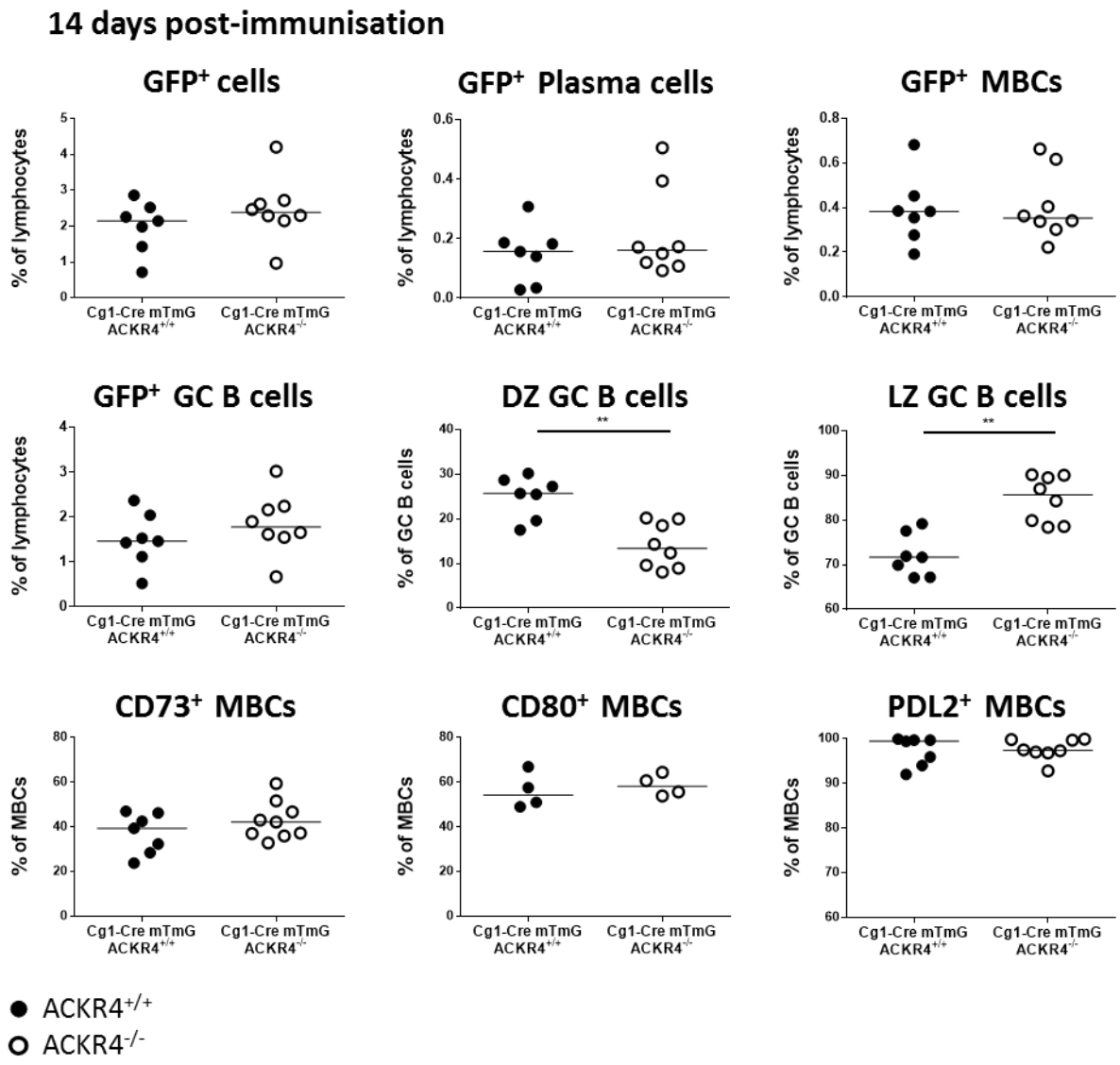

Figure 4.5: Cγ1-Cre mTmG ACKR4$^{-/-}$ mice have a normal response in the draining lymph node to NP-CGG, 14 days post-immunisation. Cγ1-Cre mTmG ACKR4$^{+/+}$ and Cγ1-Cre mTmG ACKR4$^{-/-}$ mice were immunised with NP-CGG s.c. in the rear feet and the response studied 14 days post-immunisation. a) Quantification, as to the % of lymphocytes, of GFP^{+} cells, plasma cells (GFP^{+}CD138^{+}), memory B cells (GFP^{+}CD38^{+}CD138^{-}), GC B cells (GFP^{+}CD38^{-}Fas^{+}). Quantification, as to the % of GC B cells, of DZ GC B cells (GFP^{+}CD38^{-}Fas^{+}CXCR4^{+}CD86^{-}) and LZ GC B cells (GFP^{+}CD38^{-} Fas^{+}CXCR4^{+}CD86^{-}). Quantification, as to the % of MBCs, of CD73^{+}, CD80^{+} and PDL2^{+} MBCs from pLN (draining LN) 14 days post-immunisation.
Data were combined from 2 independent experiments with 3-4 mice per group, except for CD80^{+} MBCs, where data were representative from 2 independent experiments. Each symbol represents one mouse. Horizontal line represents the median.
Key: GFP: green fluorescent protein; GC: germinal centre; DZ: dark zone; LZ: light zone; MBC: memory B cell; s.c: subcutaneously; drLN: draining lymph node.

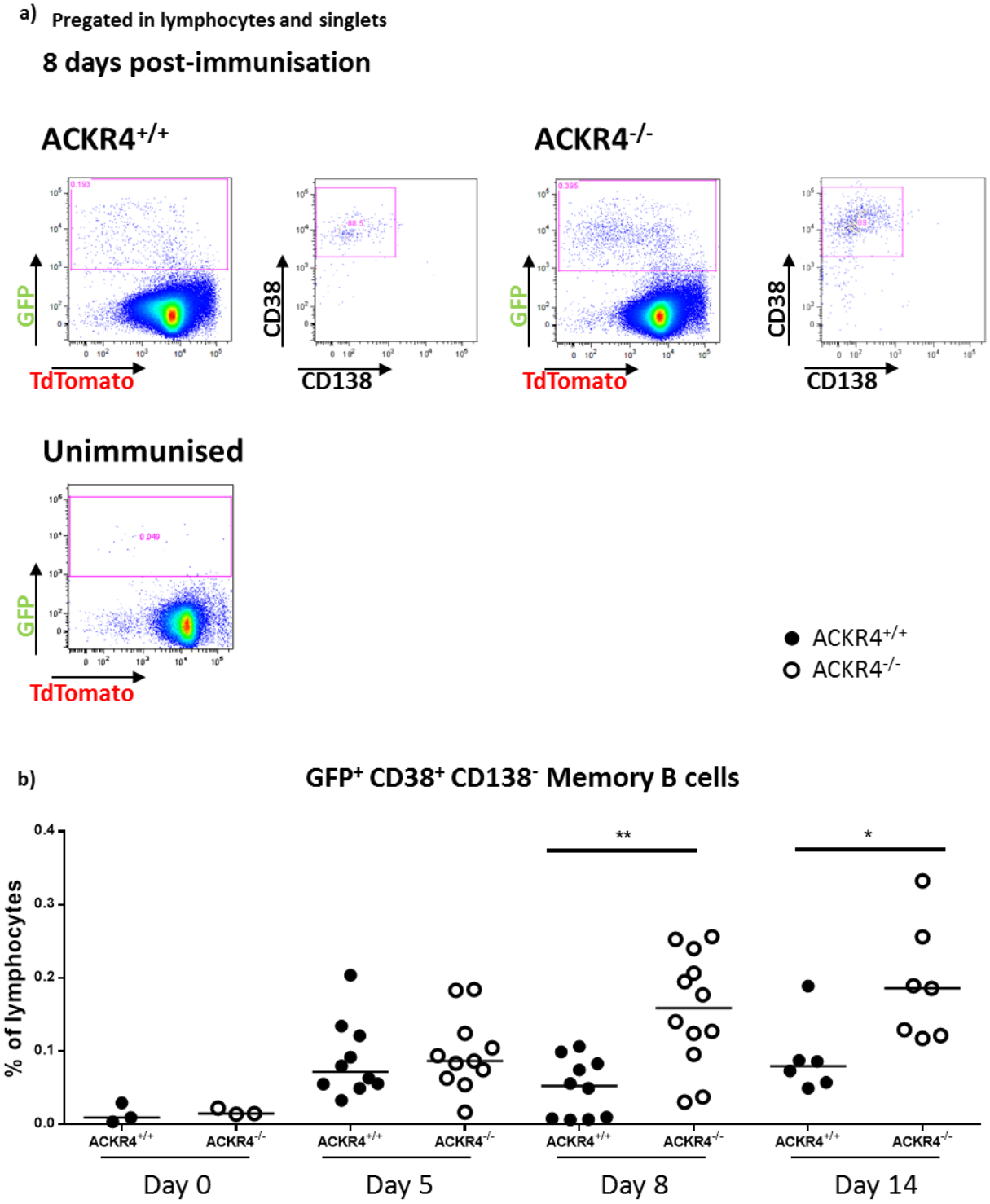

Figure 4.6: GFP$^+$ memory B cells from Cγ1-Cre mTmG ACKR4$^{-/-}$ appear in higher numbers in the distant LN from 8 days after NP-CGG. Cγ1-Cre mTmG ACKR4$^{+/+}$ and Cγ1-Cre mTmG ACKR4$^{-/-}$ mice were immunised with NP-CGG s.c. in the rear feet and the response was studied at different times post-immunisation. a) Flow cytometry gating strategy for memory B cells from axillary lymph nodes (distant LN) 8 days post-immunisation. b) Quantification, as to the % of lymphocytes, of memory B cells (GFP$^+$CD38$^+$CD138$^-$) from axillary lymph nodes (distant LN) 0, 5, 8 and 14 days post-immunisation.
Data were combined from 2 (day 5 and day 14) or 3 (day 8) independent experiments with 3-5 mice per group. Each symbol represents one mouse. Horizontal line represents the median.
Key: GFP: green fluorescent protein; s.c: subcutaneously; LN: lymph node.

Non-parametric Mann-Whitney test *p<0.05; **p<0.01

4.2.2 Memory B cells from Cγ1-Cre mTmG ACKR4$^{-/-}$ mice exit the drLN in increased numbers than in Cγ1-Cre mTmG ACKR4$^{+/+}$ mice

To explore the possibilities listed above regarding the elevated number of MBCs in the distant lymph nodes of ACKR4$^{-/-}$ mice, the GFP^{+}MBCs that appeared in the distLN were further subdivided into GFP^{+}TdTomato^{+} and GFP^{+}TdTomato^{-} MBCs (Fig. 4.7 upper). GFP^{+}TdTomato^{+} MBCs were viewed as recent arrivals from the drLN, because they still expressed TdTomato, while the GFP^{+}TdTomato^{-} MBCs were viewed as cells that had been activated longer ago and, therefore, they may had left the GC response and the drLN longer ago. Re-analysis of the data from Fig. 4.6 as to this further subdivision revealed that 8 days post-immunisation, the major differences resided with the GFP^{+}TdTomato^{+} MBCs (Fig. 4.8a), while 14 days post-immunisation, the differences were not statistically significant (Fig. 4.8b). These results are compatible with the hypothesis that MBCs in ACKR4$^{-/-}$ mice leave the drLN or enter the distLN in higher numbers. These new entrants in distant lymph nodes were detected throughout the response.

To further test the hypothesis that MBCs in ACKR4$^{-/-}$ mice leave the drLN or enter the distLN better, Cγ1-Cre mTmG ACKR4$^{+/+}$ and Cγ1-Cre mTmG ACKR4$^{-/-}$ mice immunised with NP-CGG were injected with EdU 8 days post-immunisation. Twelve hours later the tissues were taken. MBCs that have proliferated in the drLN in the last 12 h and arrived in the distLN will be EdU^{+}, while the MBCs that were in the distLN for longer than 12 h will be EdU^{-} (Fig. 4.7 lower). For both ACKR4$^{+/+}$ and ACKR4$^{-/-}$ mice there were more EdU^{+} MBCs in the GFP^{+}TdTomato^{+} subpopulation (Fig. 4.9a). This was true for all the mice analysed (Fig. 4.9b), independent of their genotype, confirming that double positive MBCs may be recent emigrants, as there is a larger proportion of cells that have proliferated within the last 12 h. MBCs from ACKR4$^{-/-}$

mice had a trend to higher percentages of EdU^+ cells, confirming that in $ACKR4^{-/-}$ mice emigration from the draining LN is increased. Pulsing with EdU with one i.p. injection and measurement of the response 12 h later may present some inconveniences for the detection of MBCs. It may prevent the detection of some GC B cells that were initially labelled but have proliferated and differentiated into MBCs between the injection and detection time, and therefore, diluted the EdU that was previously incorporated.

MBC accumulation in certain areas of the distant LNs would indicate a defect in MBC recirculation throughout the body and, therefore, increased retention of MBCs in $ACKR4^{-/-}$ mice. An equal distribution of MBCs would be further evidence to support the viewpoint that ACKR4 does not play a role in MBC retention in distLN and instead plays a role in entry. To investigate if MBCs distributed in the same way in $ACKR4^{+/+}$ and $ACKR4^{-/-}$ distLN, axillary LNs from Cγ1-Cre mTmG $ACKR4^{+/+}$ and Cγ1-Cre mTmG $ACKR4^{-/-}$ mice 8 days post-immunisation with NP-CGG in the rear feet were collected, sectioned and stained by immunofluorescence. A representative example of an axillary LN can be seen in Fig. 4.10. Because there is no antigen-dependent activation, axillary LNs do not have GCs or PCs. GFP^+MBCs can be seen in three different areas: most of the MBCs are in the follicles (IgD^+ areas) or in the vessels ($Lyve\text{-}1^+$ areas), but some cells can also be seen in the T cell zone ($IgD^-Lyve\text{-}1^-$ areas) and they are probably transiting from the vessels to the follicles, as MBCs continuously recirculate between blood and tissue, entering secondary lymphoid organs through HEV in a CD62L-dependent manner (Rasmussen, Lodahl et al. 2004).

MBCs were quantified in the three different areas mentioned previously and the data obtained are presented graphically (Fig. 4.11). As expected from the flow cytometry results, $ACKR4^{-/-}$ mice had significantly more MBCs per total LN area (Fig. 4.11a, left)

and also in the different areas analysed: vessels (Fig. 4.11a, middle), follicles (Fig. 4.11a, right) and T cell zones (Fig. 4.11a, lower). Nevertheless, when the percentage of MBCs was represented in relation to the zone in which they were located (Fig. 4.11b), no difference could be observed, indicating that even if ACKR4$^{-/-}$ distLN do have more MBCs, these distribute in the same way in the different areas. Around 50% of MBCs were seen to be spread randomly throughout the follicular B cell areas, 45% were in lymphatic vessels and only about 5-10% was seen to be disseminated in the T cell areas. Before immunisation (day 0), GFP^{+}MBCs were not detectable by immunofluorescence histology (Fig. 4.12).

In summary, distLN from ACKR4$^{-/-}$ mice contain more MBCs from day 8 post-immunisation. The data are compatible with the notion that these differences are caused by increased migration from the draining LN towards the distLN. Additionally, in ACKR4$^{-/-}$ distLN, MBCs distribute similarly to MBCs in ACKR4$^{+/+}$ distLN. This is in line with the hypothesis that ACKR4 does not have an effect on entrance of MBCs into the distLN, nor on their retention in this site. In conclusion, MBCs appear in higher number in distLN of ACKR4$^{-/-}$ mice due to an increased exit from the draining LN.

4.2.3 In the draining LN, memory B cells from Cγ1-Cre mTmG ACKR4$^{-/-}$ mice appear in higher numbers in the subcapsular sinus

How MBCs leave the GC in the drLN and migrate to other LNs is still not very well understood. It is possible that MBCs leave the GC from the LZ towards the outside of the follicle and the SCS (Y. Zhang unpublished), where they would join a net of lymphatic vessels that connects with the medullary sinus and the efferent lymphatics that would drive them out of the drLN (Girard, Moussion et al. 2012). In a mouse model

where B cells in cell cycle (Cdt-1$^+$) were labelled in red and plasma cells in green (Blimp-1$^+$), Cdt-1$^+$ MBCs were observed by intravital microscopy to migrate to the SCS of the drLN, from day 6 post-immunisation (Y. Zhang unpublished, Fig. 4.13). Further evidence showing that MBCs appear in the SCS of Cγ1-Cre mTmG mice is the visualisation of their movement by light-sheet microscopy (Fig. 4.14a). The movement of MBCs was observed *ex vivo* in an explanted popliteal lymph node from a Cγ1-Cre mTmG mice 8 days post-immunisation with NP-CGG s.c. in the hind feet. In focus appears the capsule and SCS of the lymph node (TdTomato$^+$) and some GFP$^+$ individual cells, which are MBCs. Out of focus, which means the cells are deeper in the tissue, there are two GCs (GFP$^+$) and clusters of sessile PCs (GFP$^+$). GFP$^+$ MBCs were observed to sit and crawl under the capsule of the drLN (Fig. 4.14b).

Further analysis of immunised drLN from Cγ1-Cre mTmG ACKR4$^{+/+}$ and Cγ1-Cre mTmG ACKR4$^{-/-}$ mice by immunofluorescence histology showed that GFP$^+$ MBCs spread throughout the follicles around GCs and also some of them located in the SCS (Fig. 4.15). These MBCs are in the Lyve-1$^+$ area (Fig. 4.15a), which corresponds with the floor lymphatic endothelial cells (fLECs) of the SCS. Some of these GFP$^+$ MBCs were still Ki67$^+$ (Fig. 4.15b). Plasma cells are also GFP$^+$ and there is a possibility that these GFP$^+$ cells in the SCS may be PCs. However, PCs leave the GC through the DZ towards the T zone and they are unlikely to have migrated towards the SCS (Y. Zhang, unpublished). GFP$^+$ cells in the SCS were counted and represented as the number of cells in relation to the length of the SCS analysed (Fig. 4.16a). Only intact SCS was analysed, meaning that the floor and the ceiling LECs are present, as determined by Lyve-1 and TdTomato expression. Coinciding with the increased appearance of MBCs in distant LN (Fig. 4.6), 8 days post-immunisation there was an increase in GFP$^+$ MBCs in the SCS of ACKR4$^{-/-}$ drLN compared to drLN from ACKR4$^{+/+}$ mice (Fig. 4.16b),

while total MBC numbers in drLN of ACKR4$^{+/+}$ and ACKR4$^{-/-}$ mice were similar (Fig. 4.4). Although GFP^{+} MBCs were observable in the SCS from day 5 post-immunisation, there were not obvious differences in the numbers of GFP^{+} MBCs in the SCS of drLN neither 5 days nor 14 days post-immunisation (Fig. 4.16b).

The experiments presented in this section comparing ACKR4$^{+/+}$ and ACKR4$^{-/-}$ mice 8 days post-immunisation have revealed that MBCs appear in higher numbers in the SCS of drLNs in ACKR4$^{-/-}$ mice. This may explain why MBCs appear in higher numbers in distLN (4.2.1).

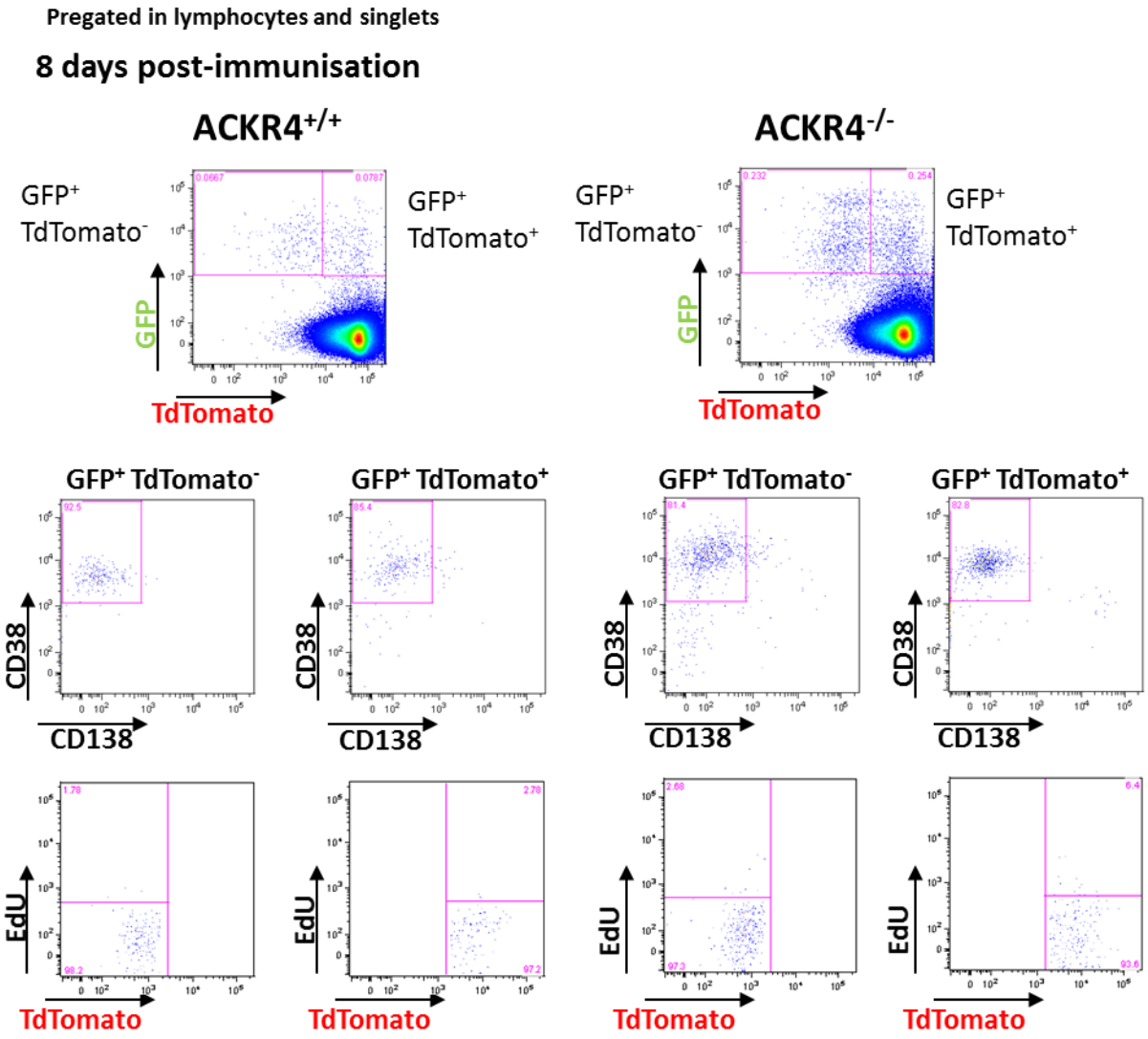

Figure 4.7: Representative gating strategy for GFP$^+$ memory B cells from the distant lymph nodes of Cγ1-Cre mTmG ACKR4$^{+/+}$ and Cγ1-Cre mTmG ACKR4$^{-/-}$ mice according to TdTomato level and EdU incorporation 8 days after NP-CGG. The figure shows the flow cytometry gating strategy for memory B cells from axillary lymph nodes (distant LN) from Cγ1-Cre mTmG ACKR4$^{+/+}$ and Cγ1-Cre mTmG ACKR4$^{-/-}$ mice 8 days post-immunisation with NP-CGG s.c. in the rear feet. EdU was injected i.p. 12 h prior to sacrifice.

Key: GFP: green fluorescent protein; s.c: subcutaneously; LN: lymph node; EdU: 5-ethynyl-2′-deoxyuridine; i.p: intraperitoneally

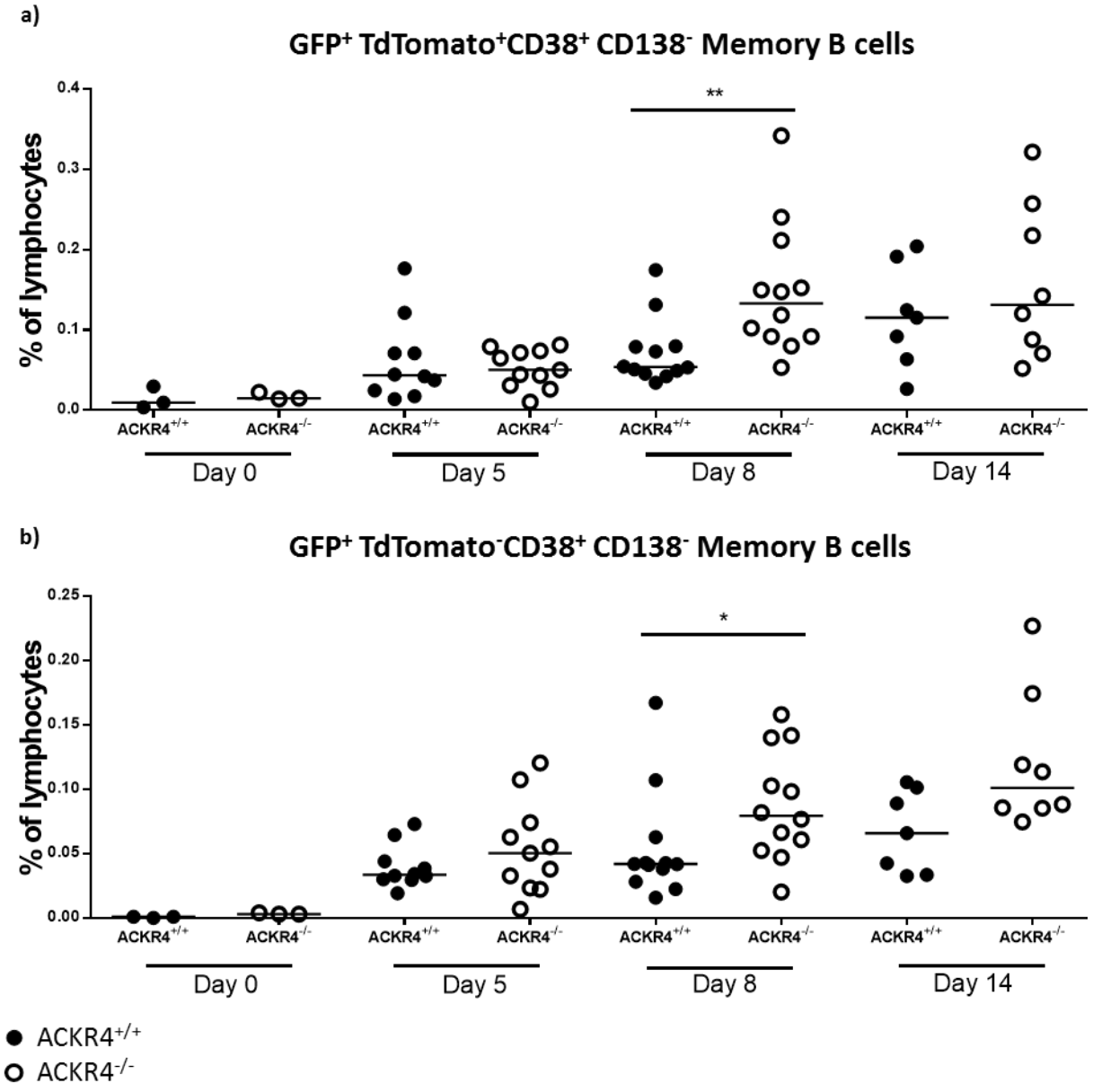

Figure 4.8: GFP^{+}TdTomato^{+} memory B cells are the fraction that causes higher appearance of memory B cells in Cγ1-Cre mTmG ACKR4$^{-/-}$ mice 8 days after NP-CGG. Cγ1-Cre mTmG ACKR4$^{+/+}$ and Cγ1-Cre mTmG ACKR4$^{-/-}$ mice were immunised with NP-CGG s.c. in the rear feet and the response studied at different times post-immunisation. a) Quantification, as to the % of lymphocytes, of memory B cells (GFP^{+}TdTomato^{+}CD38^{+}CD138^{-}) from axillary lymph nodes (distant LN) 0, 5, 8 and 14 days post-immunisation. b) Quantification, as to the % of lymphocytes, of memory B cells (GFP^{+}TdTomato^{-}CD38^{+}CD138^{-}) from axillary lymph nodes (distant LN) 0, 5, 8 and 14 days post-immunisation. For gating see Figure 4.7.
Data were combined from 2 (day 5 and day 14) or 3 (day 8) independent experiments with 3-5 mice per group..Each symbol represents one mouse. Horizontal line represents the median.
Key: GFP: green fluorescent protein; s.c: subcutaneously; LN: lymph node.
Non-parametric Mann-Whitney test *p<0.05; **p<0.01

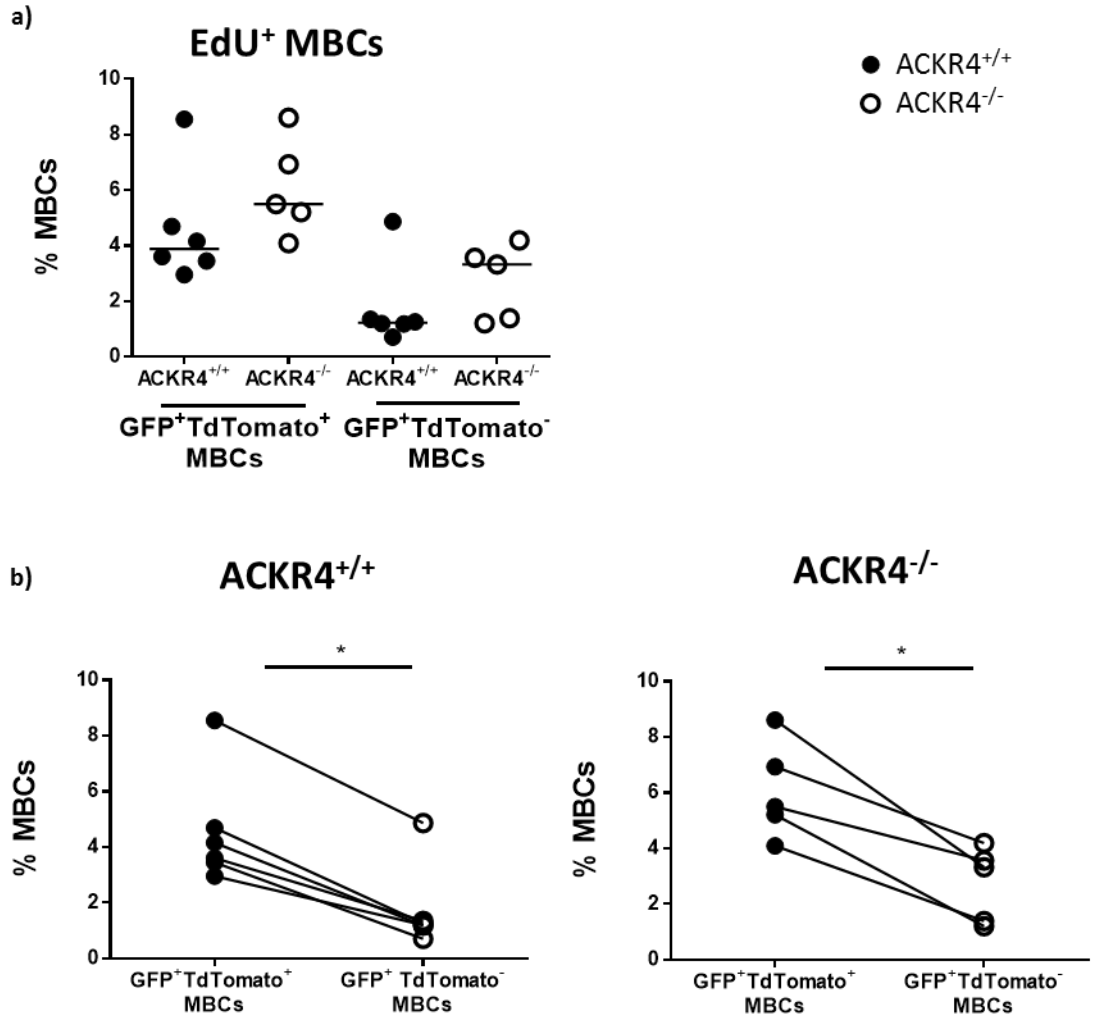

Figure 4.9: Memory B cells from Cγ1-Cre mTmG ACKR4$^{-/-}$ appear in higher numbers in distant LN from 8 days after NP-CGG due to increased exit from drLN. Cγ1-Cre mT ACKR4$^{+/+}$ and Cγ1-Cre mTmG ACKR4$^{-/-}$ mice were immunised with NP-CGG s.c. in the rear feet the response studied 8 days post-immunisation. EdU was injected i.p. 12h prior to sacrifice Quantification, as to the % of MBCs, of EdU^{+} memory B cells (GFP^{+}CD38^{+}CD138^{-}) cells f axillary lymph nodes (distant LN). b) Linked data from individual mice of GFP^{+}Tomato^{+} GFP^{+}Tomato^{-} MBCs. See gating in Figure 4.7.

1 independent experiment with 5 mice per group. Each symbol represents one mouse. Horizontal represents the median.

Key: GFP: green fluorescent protein; MBC: memory B cell; s.c: subcutaneously; LN: lymph nc EdU: 5-ethynyl-2′-deoxyuridine; i.p: intraperitoneally.

Same host compared using Wilcoxon matched-pairs signed rank test *p<0.05

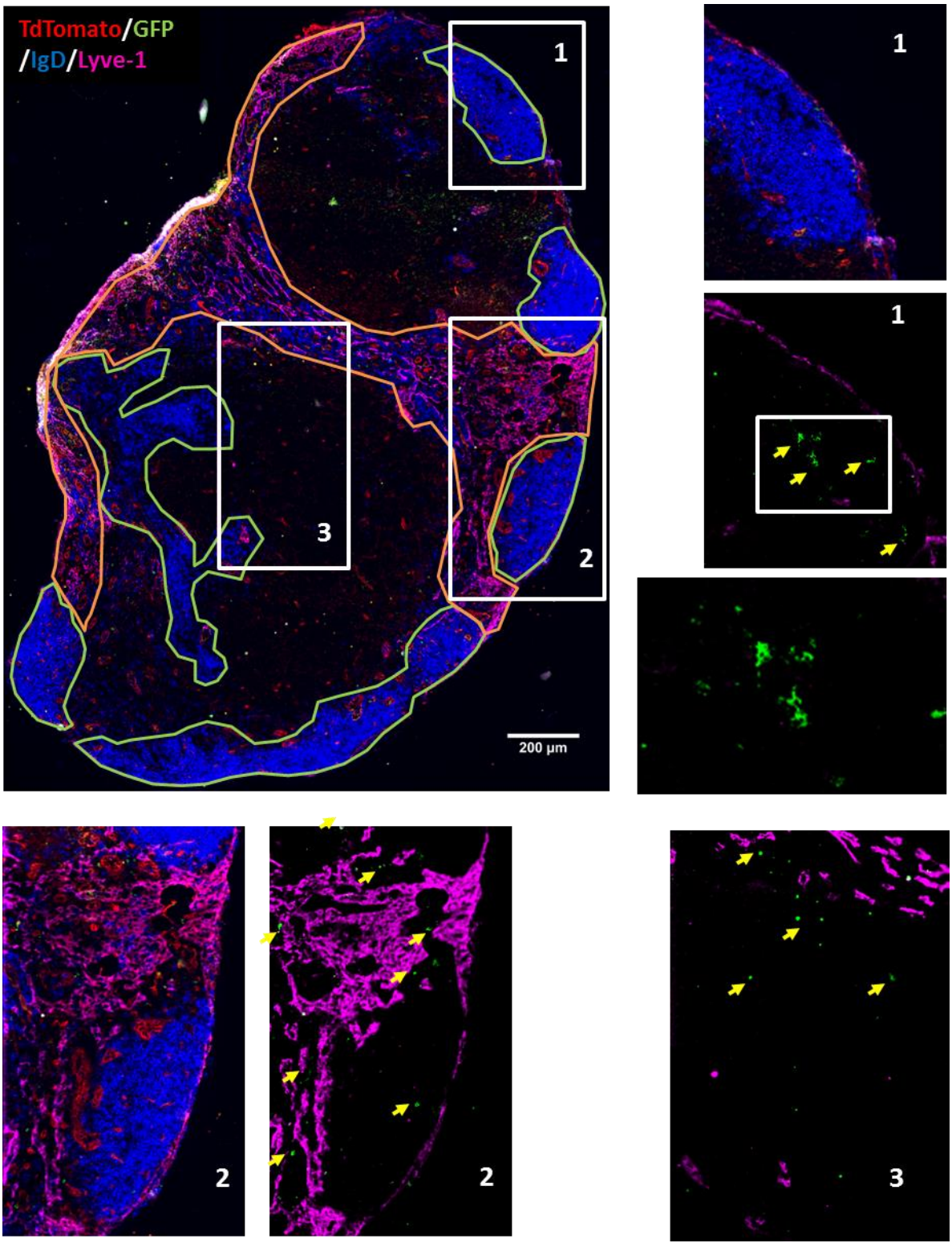

Figure 4.10: Memory B cells from Cγ1-Cre mTmG ACKR4$^{-/-}$ in distant lymph nodes mainly localise in IgD^{+} and Lyve-1^{+} areas. Representative example of immunofluorescence staining image for Tomato (red), Lyve-1 (pink), GFP (green) and IgD (blue) from axillary LN (distant LN) from Cγ1-Cre mTmG ACKR4$^{-/-}$ mouse 8 days post-immunisation with NP-CGG s.c. in the rear feet. Green marked areas denote IgD^{+} areas, orange marked areas denote Lyve-1^{+} areas, interarea space corresponds to CD3^{+} areas. Yellow arrows indicate GFP^{+} MBCs.
Scale bar: 200 µm
Key: GFP: green fluorescent protein; s.c: subcutaneously; LN: lymph node.

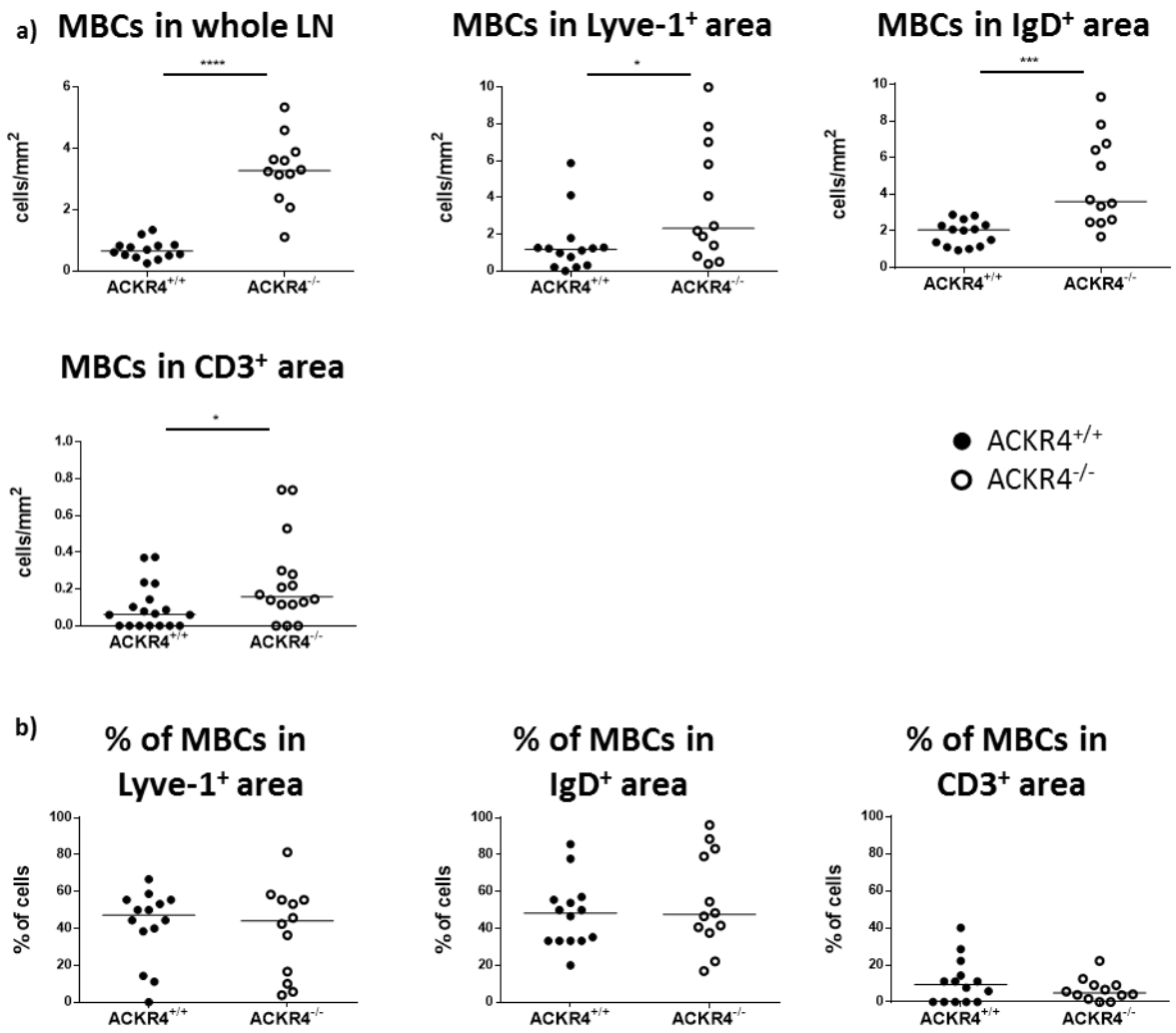

Figure 4.11: Memory B cells in Cγ1-Cre mTmG ACKR4$^{-/-}$ distant lymph nodes distribute as in Cγ1-Cre mTmG ACKR4$^{+/+}$ mice. Cγ1-Cre mTmG ACKR4$^{+/+}$ and Cγ1-Cre mTmG ACKR4$^{-/-}$ mice were immunised with NP-CGG s.c. in the rear feet and the response studied 8 days post-immunisation. a) Quantification of immunofluorescence staining images, in cells/mm^2, of GFP$^+$ MBCs that have migrated to distant LN. Upper left, total MBC numbers in whole LN. Upper middle, MBC numbers in Lyve-1$^+$ areas. Upper right, MBC numbers in IgD$^+$ areas. Lower left, MBC numbers in CD3$^+$ areas. b) Quantification of immunofluorescence staining images, in % of cells, of GFP+ MBCs. Left, % of MBCs in Lyve-1$^+$ areas. Middle, % of MBCs in IgD$^+$ areas. Right, % of MBCs in CD3$^+$ areas. See Figure 4.10 for explanation of different areas.
Data were combined from 2 independent experiments with 4-5 mice per group. Each symbol represents one lymph node. Horizontal line represents the median.
Key: GFP: green fluorescent protein; s.c: subcutaneously; LN: lymph node; MBCs: memory B cell.
Non-parametric Mann-Whitney test *p<0.05; ***p<0.001; ****p<0.0001

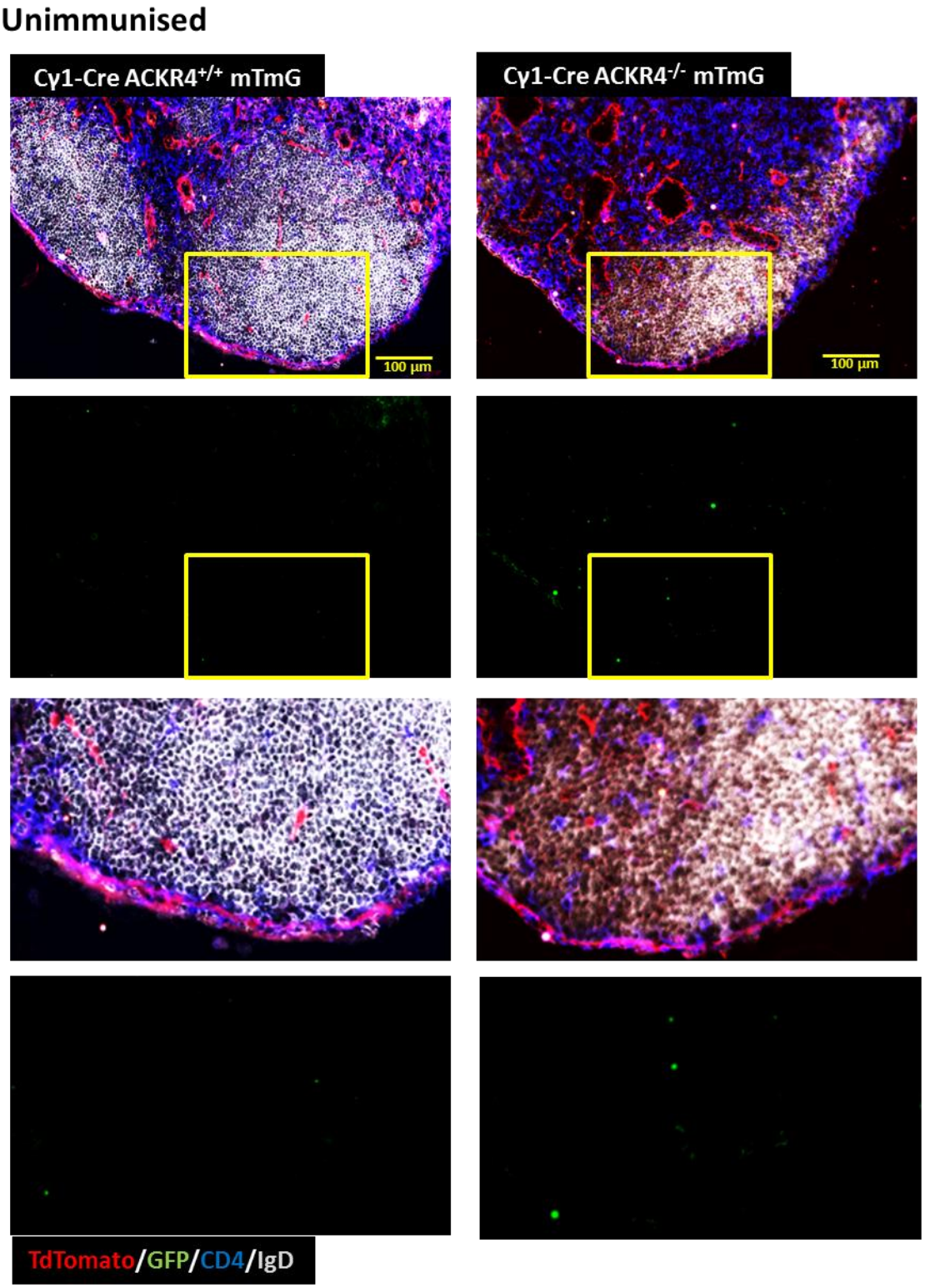

Figure 4.12: GFP^{+} memory B cells are absent in Cγ1-Cre mTmG ACKR4$^{+/+}$ and Cγ1-Cre mTmG ACKR4$^{-/-}$ mice before immunisation. Representative examples of immunofluorescence staining images and higher magnification for Tomato (red), GFP (green), CD4 (blue) and IgD (white) from axillary lymph nodes (distant LN) from non-immunised Cγ1-Cre mTmG ACKR4+/+ and Cγ1-Cre mTmG ACKR4-/- mice.
Scale bar: 100 µm
Key: GFP: green fluorescent protein; LN: lymph node.

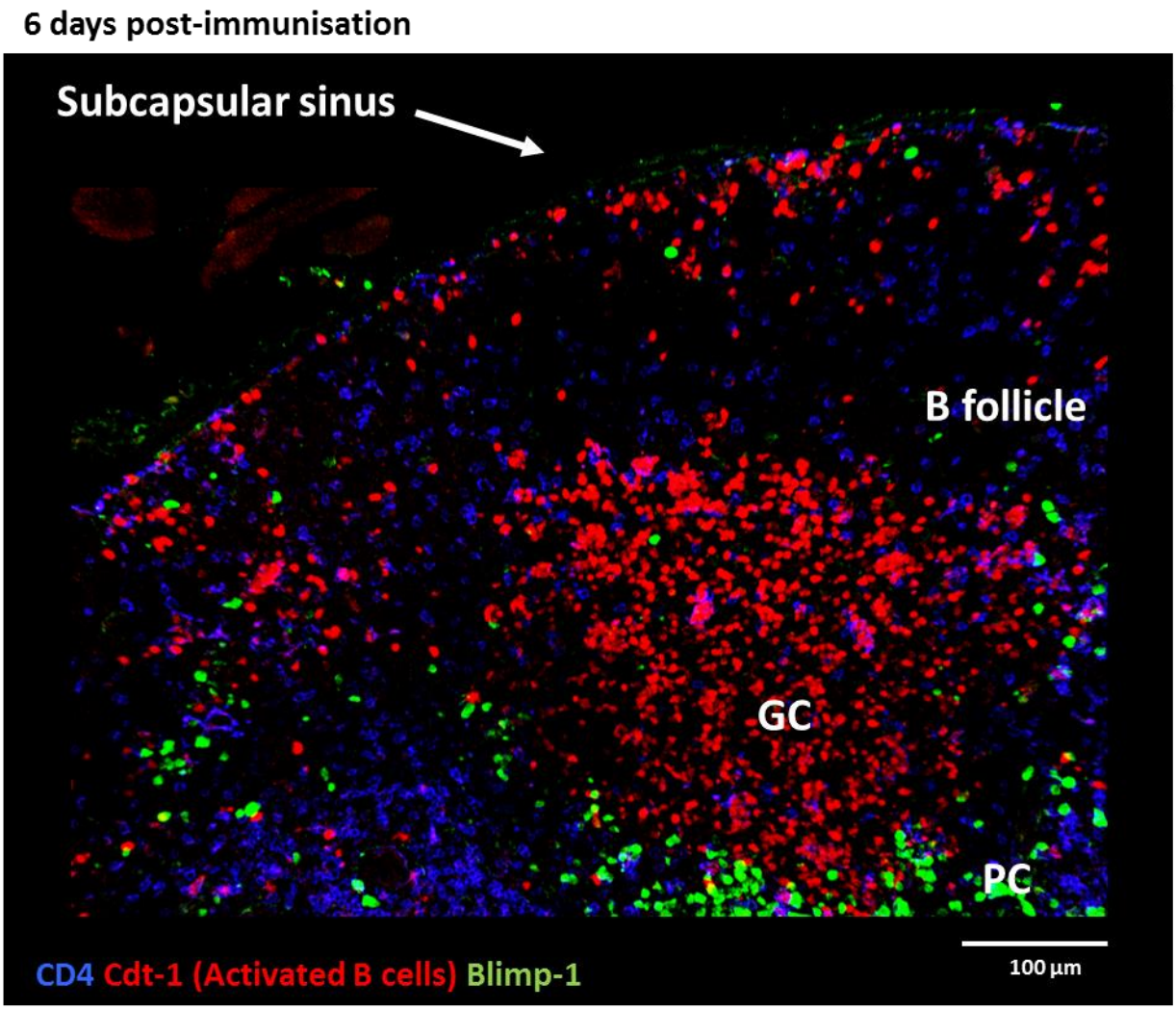

Figure 4.13: Memory B cells leave the GC from the LZ and migrate towards the subcapsular sinus. Representative example of immunofluorescence staining images for Cdt-1 (red), Blimp-1 (green) and CD4 (blue) from popliteal lymph node (draining LN) 6 days post-immunisation with NP-CGG s.c. in the rear feet from Fucci x Blimp-1-GFP mice.
Key: GC: germinal centre; LZ: light zone; LN: lymph node; s.c: subcutaneously.

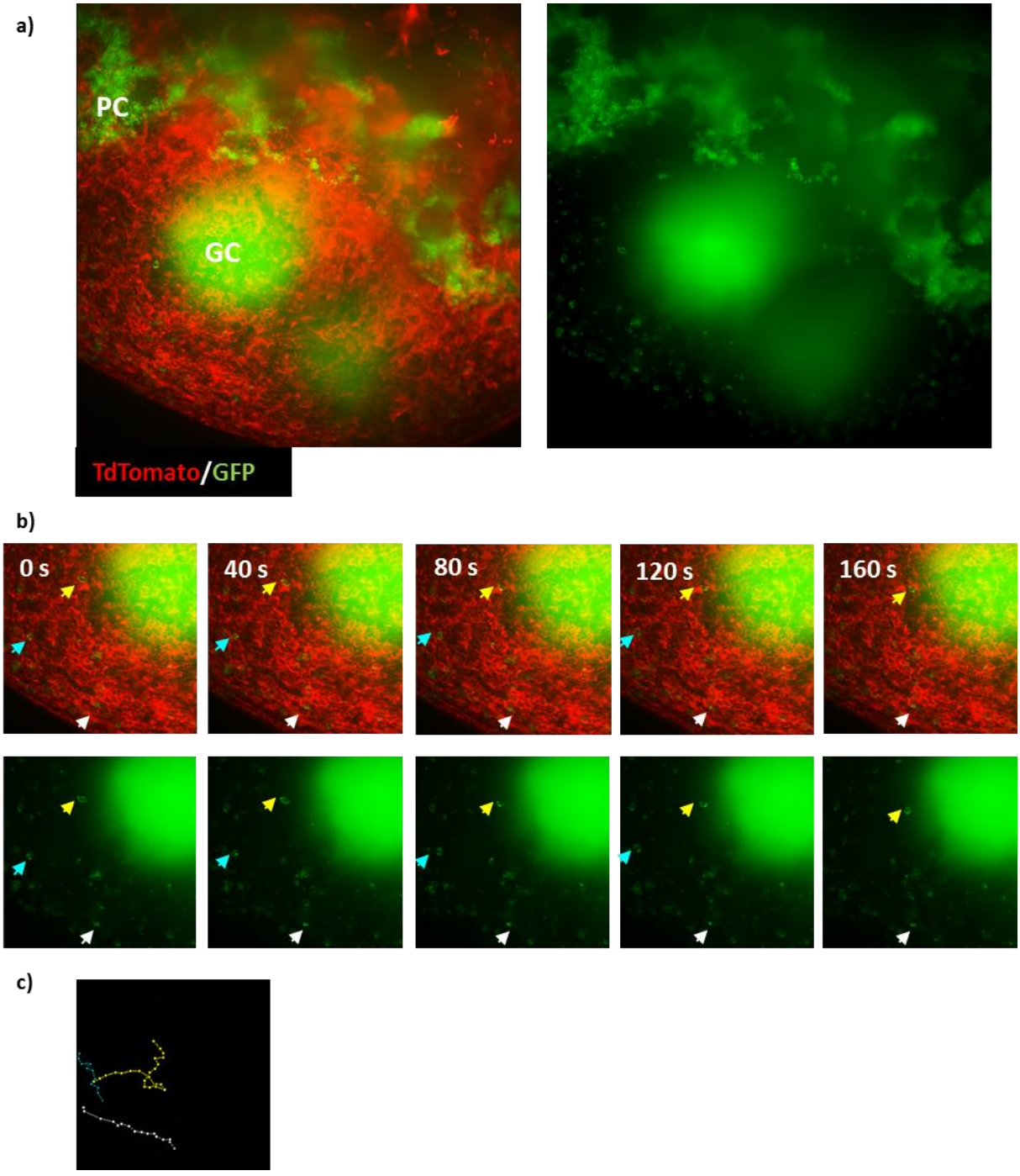

Figure 4.14: GFP$^+$ memory B cells appear and move in the SCS of drLN. Cγ1-Cre mTmG ACKR4$^{+/+}$ mice were immunised with NP-CGG s.c. in the rear feet and the response was analysed 8 days post-immunisation. Explanted drLN were observed under light sheet microscope *ex vivo*. A total of 60 footages in 40 min were captured. TdTomato (red), GFP (green). a) Representative maximum intensity projection of one independent footage. b) Sequential footage. Arrow heads indicate the different positions of three GFP$^+$ MBCs in their movement under the capsule. c) Tracking of the migration in the SCS of three different GFP$^+$ MBCs for the complete lenght of the observation.
Key: GFP: green fluorescent protein; GC: germinal centre; PC: plasma cells; MBC: memory B cell; drLN: draining lymph node; s.c: subcutaneously.

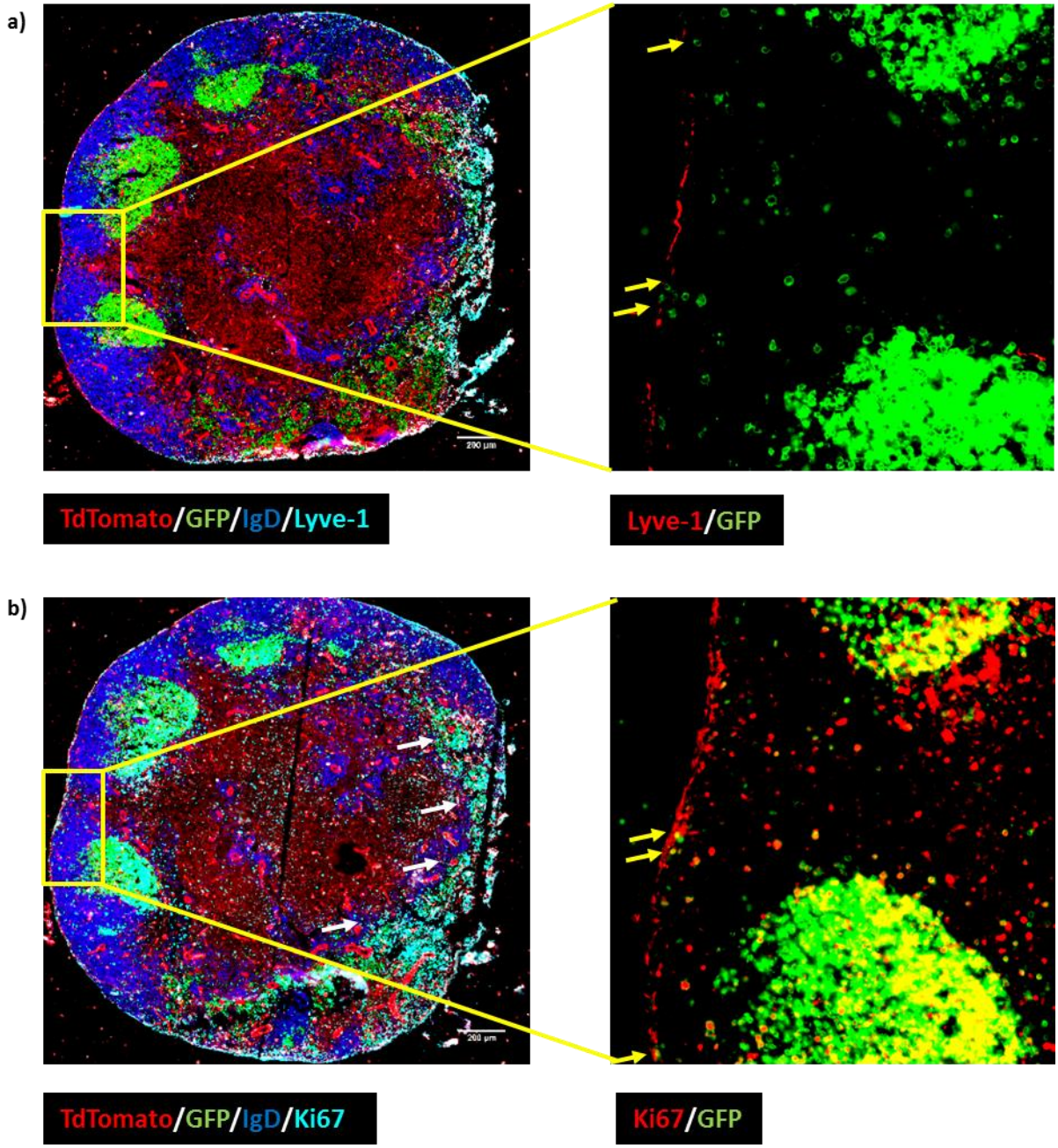

Figure 4.15: Trafficking of memory B cells in the subcapsular sinus of draining lymph node from Cγ1-Cre mTmG mice 8 days after NP-CGG. Representative examples of immunofluorescence staining images from popliteal lymph nodes (draining LN) from Cγ1-Cre mTmG ACKR4$^{-/-}$ mice 8 days post-immunisation with NP-CGG s.c. in the rear feet. Yellow arrows denote GFP^{+} MBCs in the SCS. White arrows denote GFP^{+} PCs. a) TdTomato (red), GFP (green), IgD (blue) and Lyve-1 (cyan) and higher magnification Lyve-1 (red), GFP (green). b) TdTomato (red), GFP (green), IgD (blue) and Ki67 (cyan) and higher magnification Ki67 (red) and GFP (green).
Key: GFP: green fluorescent protein; PC: plasma cells; MBC: memory B cell; SCS: subcapsular sinus; s.c: subcutaneously.
Scale bar: 200 μm

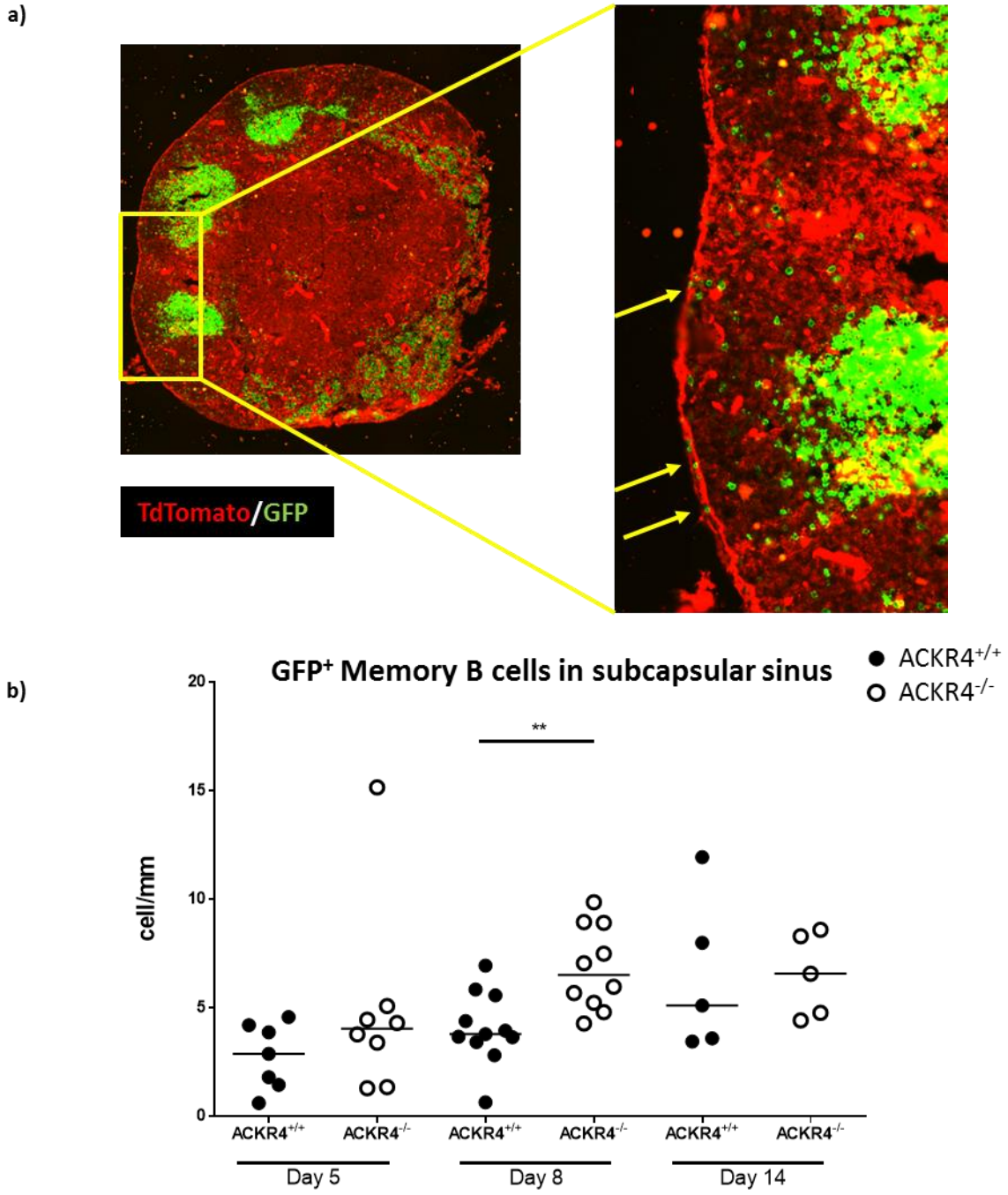

Figure 4.16: In the draining LN, memory B cells from Cγ1-Cre mTmG ACKR4$^{-/-}$ appear in higher numbers in the subcapsular sinus from 8 days after NP-CGG. Cγ1-Cre mTmG ACKR4$^{+/+}$ and Cγ1-Cre mTmG ACKR4$^{-/-}$ mice were immunised with NP-CGG s.c. in the rear feet and the response studied at different time points post-immunisation. a) Representative example of immunofluorescence staining images for TdTomato (red) and GFP (green) from popliteal lymph node (draining LN) from Cγ1-Cre mTmG ACKR4$^{-/-}$ mice 8 days post-immunisation. Yellow arrows denote GFP^{+} MBCs. b) Quantification, as to cells per mm of subcapsular sinus, of GFP^{+} MBCs that have migrated to the subcapsular sinus 5, 8 and 14 days post-immunisation.
Data were combined from 2 (day 5 and day 14) or 3 (day 8) independent experiments with 3-5 mice per group. Each symbol represents one mouse. Horizontal line represents the median.
Key: GFP: green fluorescent protein; s.c: subcutaneously; LN: lymph node; MBCs: memory B cell.
Non-parametric Mann-Whitney test **p<0.01

4.2.4 ACKR4$^{-/-}$ hosts had reduced numbers of MBCs in the drLN independently of the MBC genotype

So far it has been shown that in ACKR4$^{-/-}$ mice, MBCs appear in higher numbers in distLN from 8 days post-immunisation due to increased exit through the SCS in the drLN. There are two possible explanations. The effect might have been caused by a B cell intrinsic deficiency of ACKR4. Alternatively, loss of ACKR4 expression by cells in the surrounding environment (host), for example by naïve follicular B cells, stroma or SCS endothelium, might be important.

In order to examine the role of ACKR4 expression in the MBCs or in the host for the migration of MBCs towards distant sites, chimeric mice were produced by transferring NP-specific B cells from QM ACKR4$^{+/+}$ and QM ACKR4$^{-/-}$ mice into ACKR4$^{+/+}$ and ACKR4$^{-/-}$ recipients (Fig. 4.17a). Due to the general expression of the 2 different fluorescent proteins (TdTomato and eYFP) in mice, ACKR4$^{+/+}$ and ACKR4$^{-/-}$ NP-specific B cells could be co-transferred into the same host and their response to NP-CGG be studied in direct competition. Mice were given primary immunisation with NP-CGG into the rear feet subcutaneously and lymph nodes were taken for analysis 8 days post-immunisation. When LNs from mice that were not immunised were analysed barely any transferred cell survived for 8 days (Fig. 4.17b). Therefore, it is safe to assume that the fluorescent cells detected in the distLN 8 days post-immunisation are MBCs and not naïve B cells.

Flow cytometry was used to detect different immunisation-induced B cell subpopulations in the drLN. A representative example of the gating strategy for GC B cells and PCs from drLN 8 days post-immunisation is shown in Fig. 4.18. There were no major differences in the propensity of ACKR4$^{+/+}$ or ACKR4$^{-/-}$ antigen-specific B

cells in a ACKR4$^{+/+}$ or ACKR4$^{-/-}$ environment to differentiate into GC B cells (B220^{+}CD138^{-}CD38^{-}Fas^{+}), with on average 80% of the transferred cells differentiating into GC B cells by day 8 (Fig. 4.19a, left). There was also not a major difference in the percentages of GC B cells of lymphocytes (Fig. 4.19a, right), with 0.5% of the total lymphocyte cell population becoming GC B cells from each of the genotypes transferred. The representation of the data by linking the response by ACKR4$^{+/+}$ and ACKR4$^{-/-}$ B cells in the same hosts (Fig. 4.19b) allows the study of B cell intrinsic effects. Absence of ACKR4 in B cells led to slightly higher numbers of GC B cells compared to ACKR4$^{+/+}$ B cells when placed in the same ACKR4$^{-/-}$ environment (Fig. 4.19b right). So, it can be presumed that ACKR4$^{-/-}$ B cells differentiate slightly better into GC B cells only when they are placed into an ACKR4-deficient environment.

Next, LZ/DZ distribution was investigated. As seen in the later stages of the splenic GC response (Fig. 3.19), the LZ/DZ distribution is skewed towards LZ. (Fig. 4.20). This effect is dependent on the expression of ACKR4 in B cells and independent of ACKR4-expression in the environment (Fig. 4.20a). These differences are clearer when data from the same mice are linked (Fig. 4.20b). ACKR4$^{+/+}$ B cells enter preferably the DZ compartment while ACKR4$^{-/-}$ B cells go into the LZ GC B cell subpopulation. This result was to be expected as ACKR4 is differentially expressed in DZ GC B cells. It is interesting that the skewed distribution is observable earlier in pLN than in the case of the splenic response. This may indicate that the time course in spleen and in LN is slightly different, that the changes are more pronounced in the LN response, or that the route of administration of the antigen marks the time point at which some differences are visible.

Plasma cells ($CD138^+$) were also analysed in the drLN. Neither in percentage of transferred cells (Fig. 4.21a, left) nor in the percentage of lymphocytes (Fig. 4.21a, right) was any difference observed. Moreover, when the data from the same hosts was linked, there was not a difference (Fig. 4.21b). Therefore, it can be concluded that ACKR4 expression, neither on B cells nor on the environment, has an appreciable role in PC generation 8 days after NP-CGG immunisation.

Analysis of MBCs numbers in the drLN (the gating strategy is shown in Fig. 4.22) showed that, both the percentage of MBCs developing within transferred B cells (Fig. 4.23a, left) and the percentage of MBCs within all lymphocytes, which corresponds to the absolute number of MBCs (Fig. 4.23a, right) were lower when the host was $ACKR4^{-/-}$. ACKR4 deficiency in B cells did not have an effect (Fig. 4.23b). This finding reveals that when ACKR4 is expressed in the lymph node environment, B cells differentiate into MBCs better. In order to study subpopulations of MBCs, CD73, CD80 and PDL2 were stained on drLN MBCs. CD80 and/or PDL2-high expression identify the more memory-like population that accumulates a higher number of mutations. MBCs that express CD73 are the more naïve-like, have a lower rate of mutation and are infrequently isotype switched (Tomayko, Steinel et al. 2010, Zuccarino-Catania, Sadanand et al. 2014). There was no difference in the percentage of MBCs that expressed CD73 (Fig. 4.24a, b upper). Surprisingly, in the GC-dependent $CD80^+$ subpopulation, there was a major reduction in the percentage of $CD80^+$ MBCs, if B cells were deficient for ACKR4 (Fig. 4.24a, b middle). In the $PDL2^+$ subpopulation there was a minor difference when $ACKR4^{-/-}$ B cells were placed in a WT environment (Fig. 4.24a, b lower).

In summary, when the drLNs of chimeric mice were analysed, the major differences were found in the MBC compartment. There are less MBCs when the host is ACKR4$^{-/-}$. There was a reduction of GC-derived CD80^{+} MBCs if B cells do not express ACKR4.

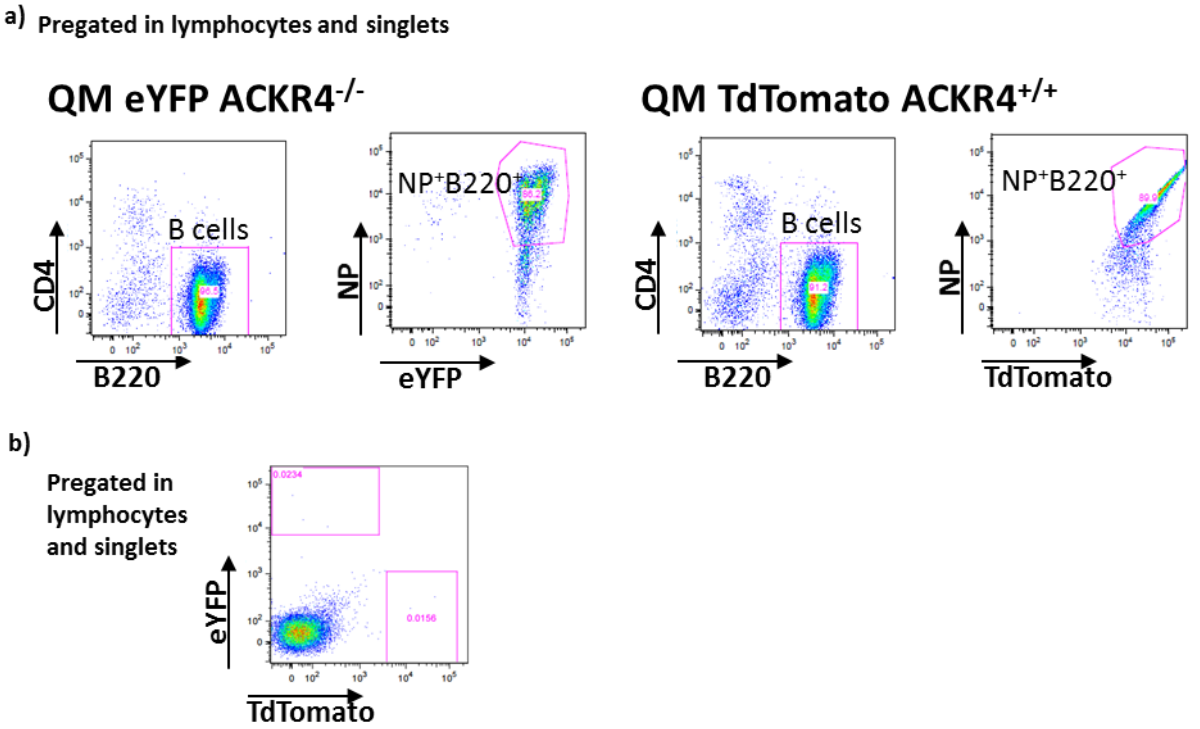

Figure 4.17: Transfer of QM ACKR4$^{+/+}$ and QM ACKR4$^{-/-}$ NP^{+}B220^{+} cells into WT or ACKR4$^{-/-}$ hosts. a) Representative diagram for the flow cytometry gating of NP^{+}B220^{+} cells from QM ACKR4$^{+/+}$ and QM ACKR4$^{-/-}$ mice. 1x10^{5} NP^{+}B220^{+} cells from each genotype were co-transferred into the same hosts i.v. and immunised 24 h later with 20 µg NP-CGG alum precipitated with 1x10^{5} *Bordetella pertussis* s.c. in the rear feet. b) Representative example of a non-immunised host 8 days post-transfer with 1x10^{5} NP^{+}B220^{+} cells from each genotype.
Key: i.v: intravenously; s.c: subcutaneously; eYFP: enhanced yellow fluorescent protein.

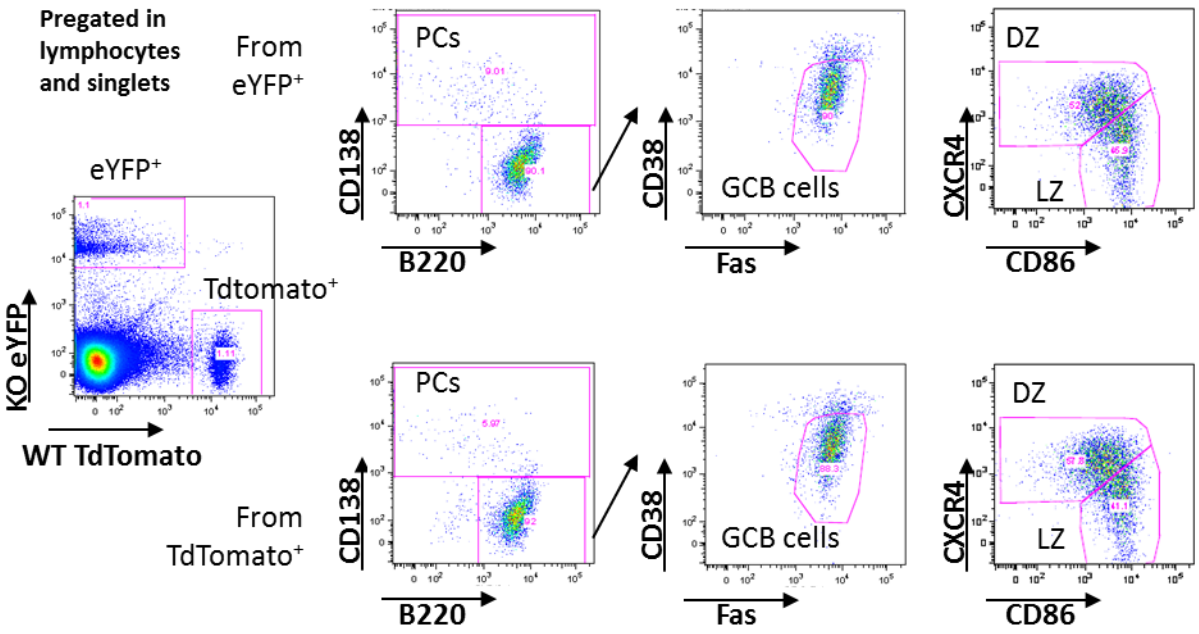

Figure 4.18: Gating strategy for GC B cells and plasma cells after transfer of QM ACKR4$^{+/+}$ and QM ACKR4$^{-/-}$ NP^{+}B220^{+} cells into WT or ACKR4$^{-/-}$ hosts. 1x10^{5} NP^{+}B220^{+} cells from QM ACKR4$^{+/+}$ and same number from QM ACKR4$^{-/-}$ were co-transferred to WT or ACKR4$^{-/-}$ hosts i.v. and immunised 24 h later with NP-CGG s.c. in the rear feet. The response was studied 8 days post-immunisation. Representative diagram for flow cytometry gating of plasma cells, GC B cells, DZ GC B cells and LZ GC B cells.
Key: KO: knock-out; WT: wild type; PCs: plasma cells; GC: germinal centre; DZ: dark zone; LZ: light zone; i.v: intravenously; s.c: subcutaneously; eYFP: enhanced yellow fluorescent protein.

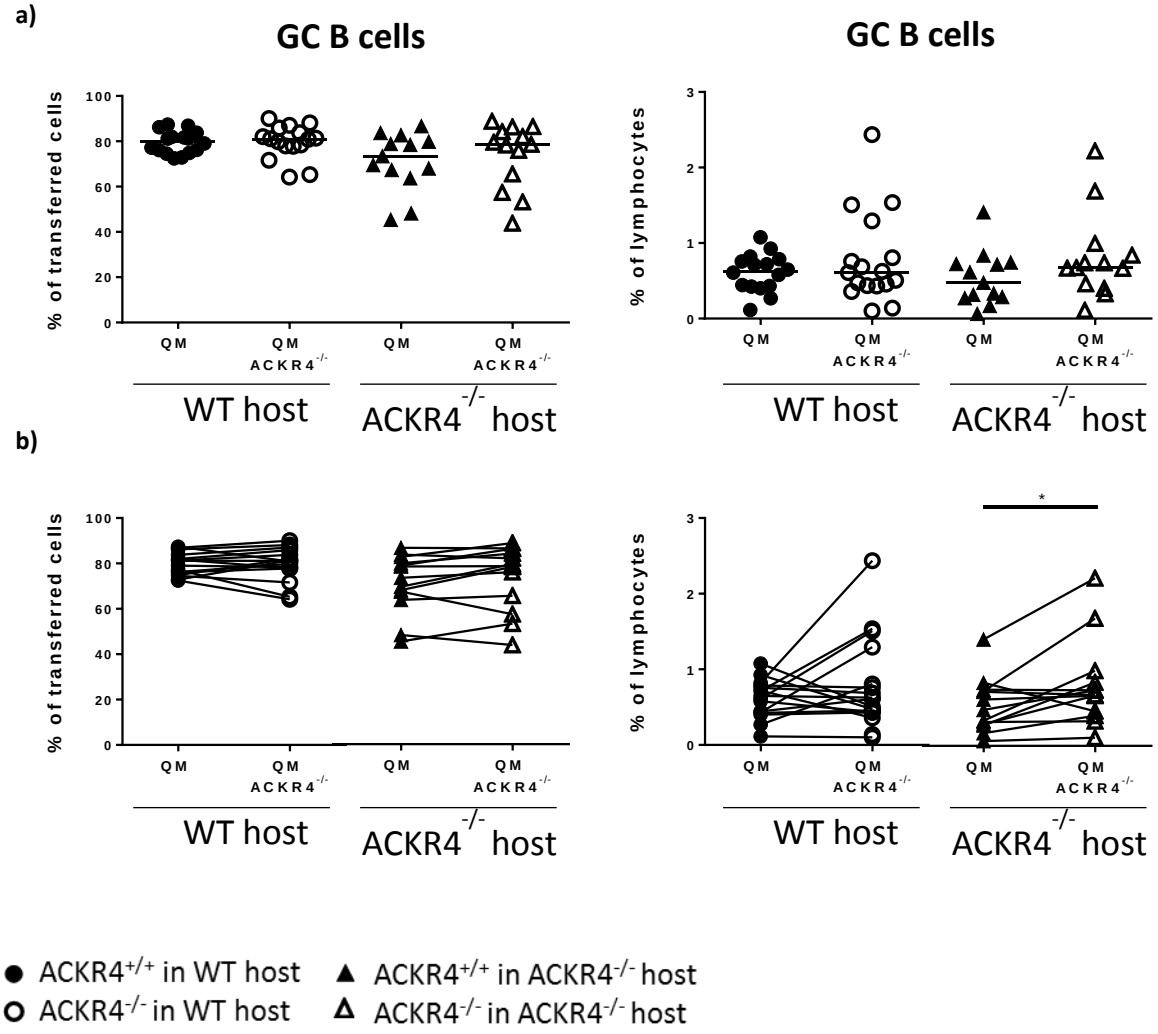

Figure 4.19: **In the draining LN, QM ACKR4$^{+/+}$ and QM ACKR4$^{-/-}$ NP^{+}B220^{+} differentiate better into GCs when the host does not express ACKR4**. WT or ACKR4$^{-/-}$ hosts were co-transferred with 1x10^{5} NP^{+}B220^{+} cells from QM ACKR4$^{+/+}$ and same number from QM ACKR4$^{-/-}$ i.v. and immunised 24 h later with NP-CGG s.c. in the rear feet. The response was studied 8 days post-immunisation in the drLN. a) Flow cytometry data, as to the % of transferred cells (left) or % of lymphocytes (right), of GC B cells from b) Linked flow cytometry data from the same hosts for GC B cells.
Data were combined from 3 independent experiments with 5-6 mice per group. Each pair of symbols represents one mouse. Horizontal line represents the median.
Key: WT: wild type; i.v: intravenously; s.c: subcutaneously; drLN: draining lymph node; GC: germinal centre.
Same host compared using Wilcoxon matched-pairs signed rank test *p<0.05

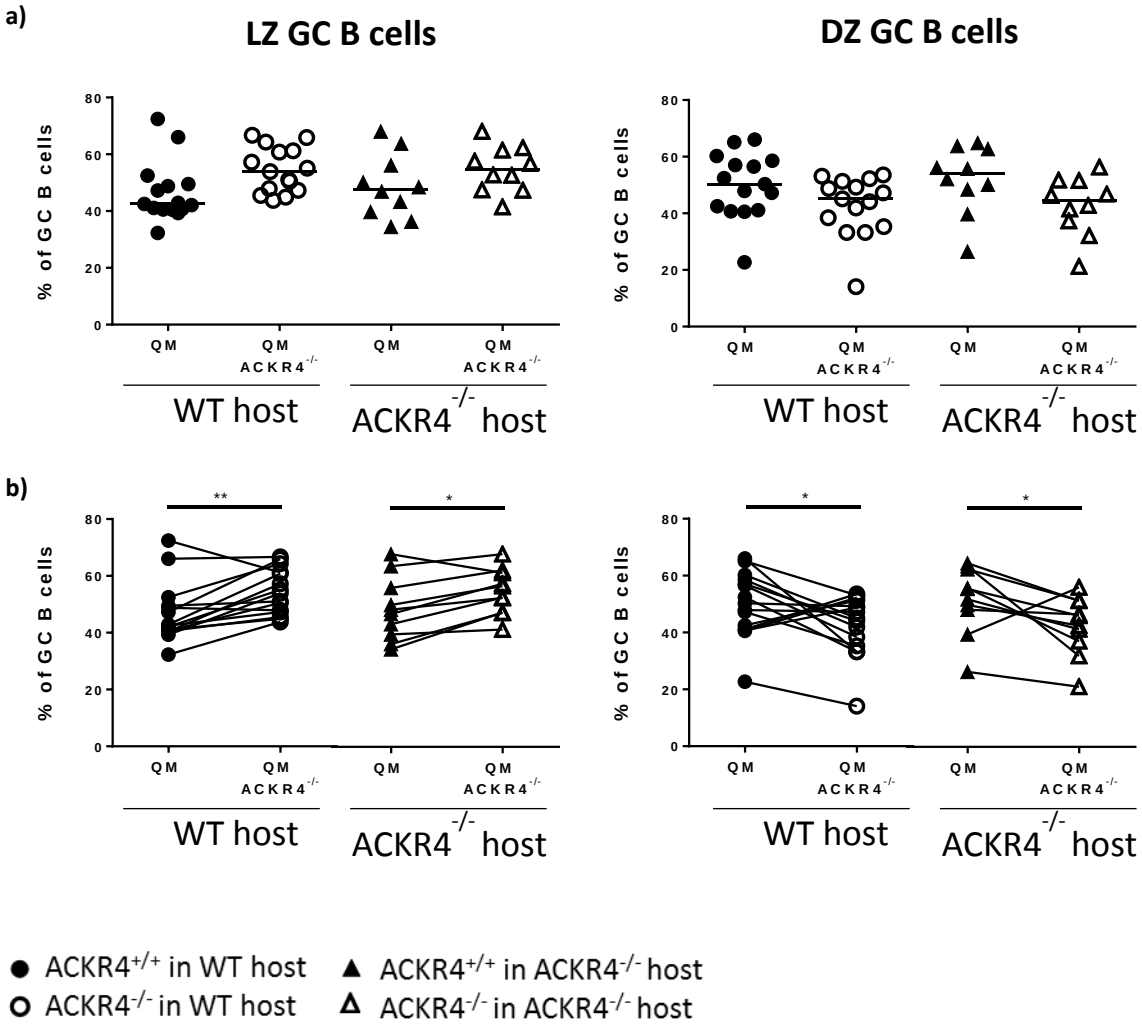

Figure 4.20: In the draining LN, QM ACKR4$^{-/-}$ form smaller DZ and bigger LZ, independently of the host. WT or ACKR4$^{-/-}$ hosts were co-transferred with 1x10^5 NP$^+$B220$^+$ cells from QM ACKR4$^{+/+}$ and same number from QM ACKR4$^{-/-}$ i.v. and immunised 24 h later with NP-CGG s.c. in the rear feet. The response was studied 8 days post-immunisation in the drLN. a) Flow cytometry data, as to the % of GC B cells, of LZ GC B cells (left) and DZ GC B cells (right). b) Linked flow cytometry data from the same hosts for LZ GC B cells (left) and DZ GC B cells (right).
Data were combined from 3 independent experiments with 5-6 mice per group. Each pair of symbols represents one mouse. Horizontal line represents the median.
Key: WT: wild type; i.v: intravenously; s.c: subcutaneously; drLN: draining lymph node; GC: germinal centre; LZ: light zone; DZ: dark zone.
Same host compared using Wilcoxon matched-pairs signed rank test *p<0.05; **p<0.01

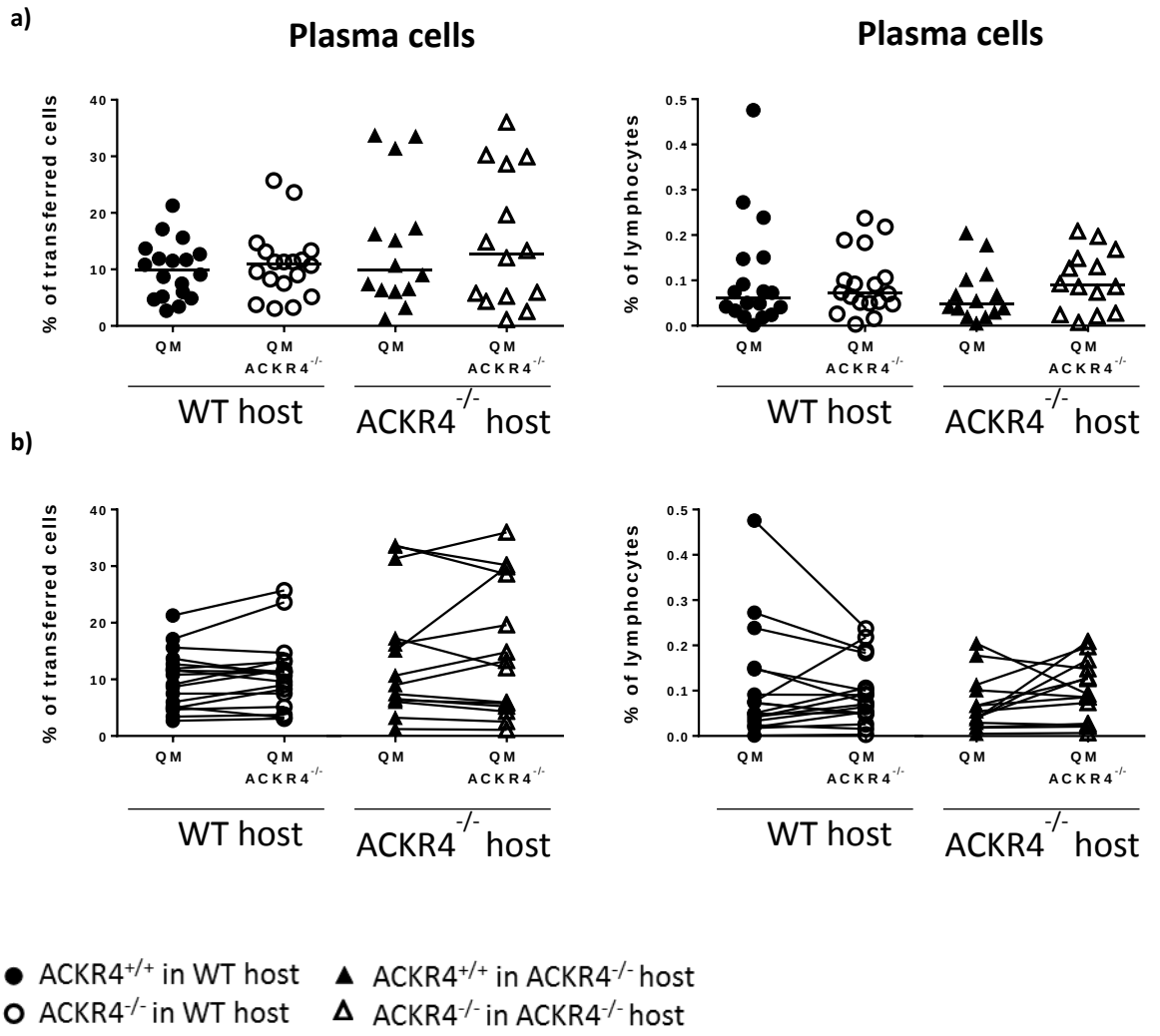

Figure 4.21: In the draining LN, QM ACKR4$^{+/+}$ and QM ACKR4$^{-/-}$ NP^{+}B220^{+} differentiate equally into plasma cells, independently of the host. WT or ACKR4$^{-/-}$ hosts were co-transferred with 1x10^{5} NP^{+}B220^{+} cells from QM ACKR4$^{+/+}$ and same number from QM ACKR4$^{-/-}$ i.v. and immunised 24 h later with NP-CGG s.c. in the rear feet. The response was studied 8 days post-immunisation in the drLN. a) Flow cytometry data, as to the % of transferred cells (left) or % of lymphocytes (right), of plasma cells. b) Linked flow cytometry data from the same hosts for plasma cells.
Data were combined from 3 independent experiments with 5-6 mice per group. Each pair of symbols represents one mouse. Horizontal line represents the median.
Key: WT: wild type; i.v: intravenously; s.c: subcutaneously; drLN: draining lymph node; GC: germinal centre.

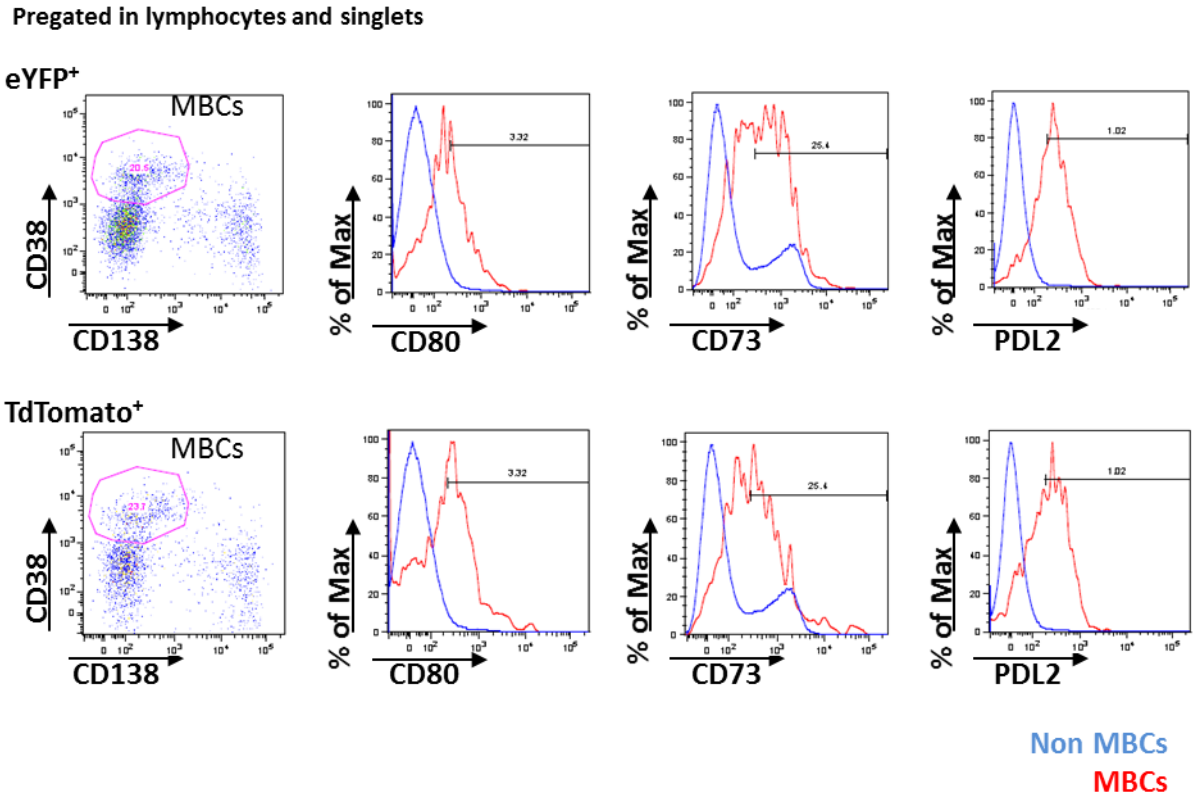

Figure 4.22: Gating strategy for memory B cells after transfer of QM ACKR4$^{+/+}$ and QM ACKR4$^{-/-}$ NP^{+}B220^{+} cells into WT or ACKR4$^{-/-}$ hosts. 1x10^{5} NP^{+}B220^{+} cells from QM ACKR4$^{+/+}$ and same number from QM ACKR4$^{-/-}$ were co-transferred to WT or ACKR4$^{-/-}$ hosts i.v. and immunised 24 h later with NP-CGG s.c. in the rear feet. The response was studied 8 days post-immunisation in the drLN. The figure shows representative diagrams for flow cytometry gating of memory B cells, CD73^{+} MBCs, CD80^{+} MBCs and PDL2^{+} MBCs.
Key: eYFP: enhanced yellow fluorescent protein; i.v: intravenously; s.c: subcutaneously; drLN: draining lymph node; MBC: memory B cell.

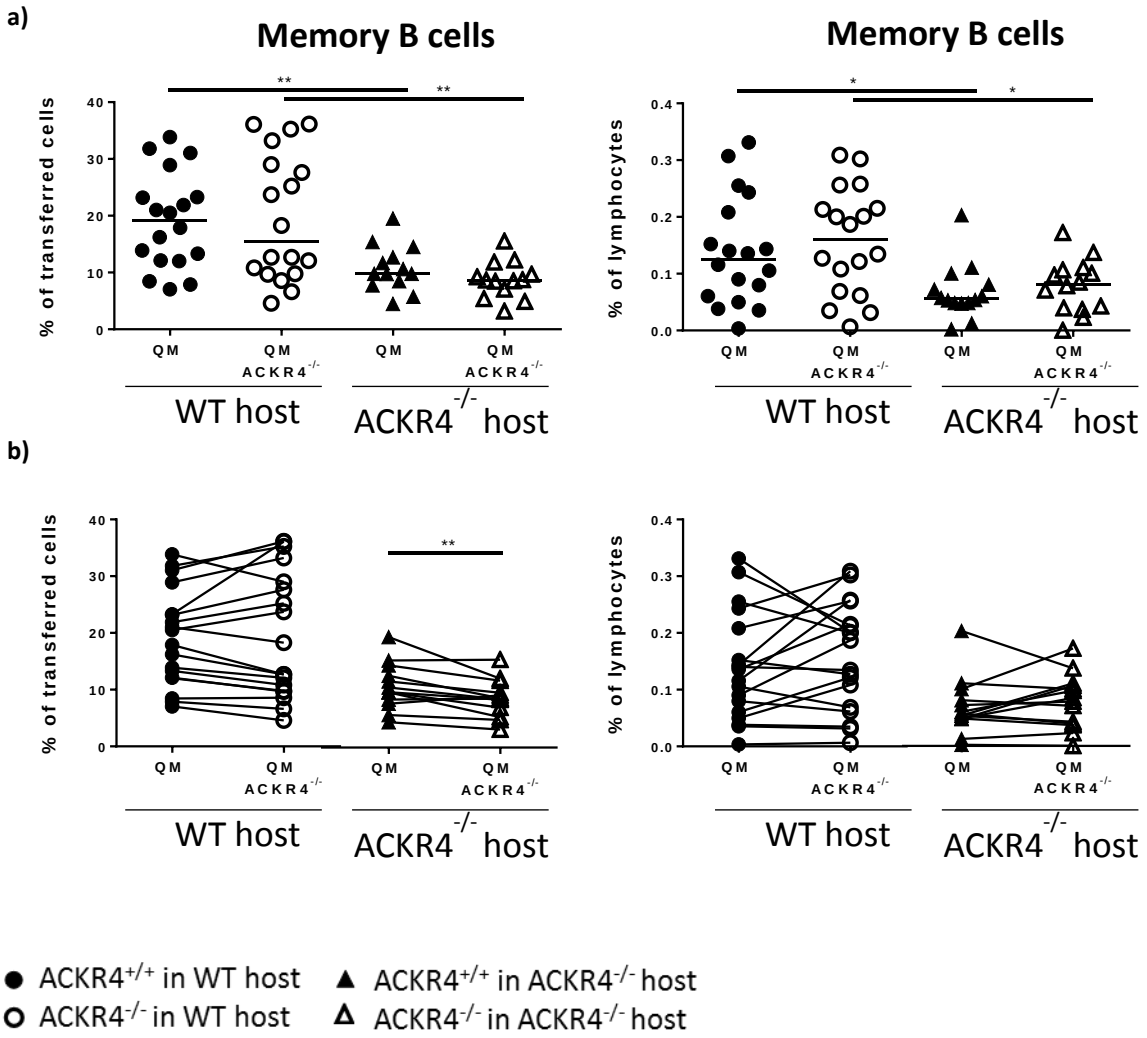

Figure 4.23: In the draining lymph node, there are more memory B cells when the host expresses ACKR4. WT or ACKR4$^{-/-}$ hosts were co-transferred with 1x10^5 NP$^+$B220$^+$ cells from QM ACKR4$^{+/+}$ and same number from QM ACKR4$^{-/-}$ i.v. and immunised 24 h later with NP-CGG s.c. in the rear feet. The response was studied 8 days post-immunisation in the drLN. a) Flow cytometry data, as to the % of transferred cells (left) or % of lymphocytes (right), of memory B cells. b) Linked flow cytometry data from the same hosts for MBCs.
Data were combined from 3 independent experiments with 5-6 mice per group. Each pair of symbols represents one mouse. Horizontal line represents the median.
Key: WT: wild type; i.v: intravenously; s.c: subcutaneously; drLN: draining lymph node; MBC: memory B cells.
Different hosts compared using Mann-Whitney test *p<0.05; **p<0.01
Same host compared using Wilcoxon matched-pairs signed rank test **p<0.01

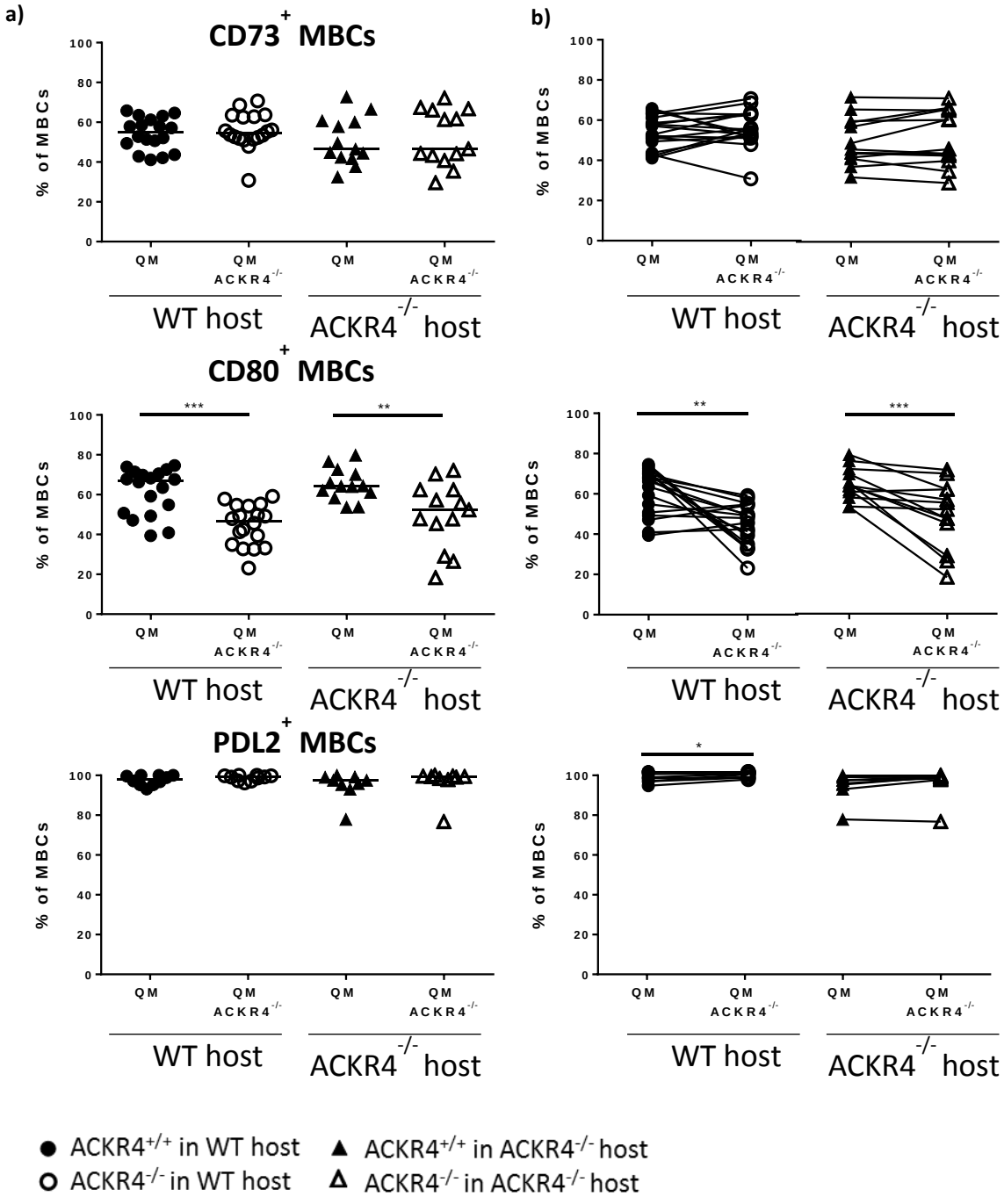

Figure 4.24: In the draining lymph node, CD80$^+$ memory B cells are reduced in ACKR4$^{-/-}$ memory B cells, independently of the host. WT or ACKR4$^{-/-}$ hosts were co-transferred with 1x10^5 NP$^+$B220$^+$ cells from QM ACKR4$^{+/+}$ and same number from QM ACKR4$^{-/-}$ i.v. and immunised 24 h later with NP-CGG s.c. in the rear feet. The response was studied 8 days post-immunisation in the drLN. a) Flow cytometry data, in % of MBCs, of CD73$^+$ MBCs (upper), CD80$^+$ MBCs (middle) and PDL2$^+$ MBCs (lower). b) Linked flow cytometry data from the same hosts for CD73$^+$ MBCs (upper), CD80$^+$ MBCs (middle) and PDL2$^+$ MBCs (lower).

Data were combined from 3 independent experiments with 5-6 mice per group. Each pair of symbols represents one mouse. Horizontal line represents the median.

Key: WT: wild type; i.v: intravenously; s.c: subcutaneously; drLN: draining lymph node; MBC: memory B cells.

Same host compared using Wilcoxon matched-pairs signed rank test *p<0.05; **p<0.01; ***p<0.001

4.2.5 ACKR4$^{-/-}$ MBCs migrate in higher proportion to distant LN

The above experiments have shown that MBCs appear in higher numbers in distLN in mice completely deficient for ACKR4 compared to WT animals (4.2.1). In order to test whether MBC migration depends on ACKR4 expression on B cells or in the environment, MBC migration was studied in chimeric mice, in which ACKR4 was absent either in antigen-specific B cells or in the host environment. Analysis of the distLN from the chimeric mice (described in 4.2.4) by flow cytometry was undertaken 8 days post primary immunisation in the hind feet. Eight days post-immunisation is the time when the number of MBCs reach the maximum in the distLN (Fig. 4.1). It is also the time when there is the biggest difference between WT and complete ACKR4-deficient animals (Fig. 4.6). The analysis showed that, in the distLNs, the frequency of eYFP^{+} and TdTomato^{+} cells was about 50 times lower than in the drLN. A vast percentage of these cells were MBCs (CD38^{+}CD138^{-}) (Fig. 4.25a). It has been previously discussed that CD38^{+} cells that express either eYFP or TdTomato cannot be naïve B cells as these do not survive for 8 days without encountering antigen (Fig. 4.17b).

Contrary to what was seen in the drLN, more MBCs appeared in the distLN when the B cells were ACKR4$^{-/-}$. This was independent of whether ACKR4 was expressed in the environment or not (Fig. 4.25b). This result indicates that the appearance of elevated number of MBCs in the distant LN of Cγ1-Cre mTmG mice completely deficient in ACKR4 was due to the absence of ACKR4 on the B cells. To test whether the result is an artefact caused by an inhibitory effect due to the expression of TdTomato or eYFP in the different MBC populations, the experiment was repeated with the fluorescent proteins interchanged as to the ACKR4$^{+/+}$ and ACKR4$^{-/-}$ populations. The experiment showed that, independent of the fluorescent protein expressed, ACKR4$^{-/-}$ MBCs appear

in higher number than ACKR4$^{+/+}$ MBCs in distLN (Fig. 4.25c). Different MBC subpopulations in the distLN were analysed on the basis of their expression of CD73, CD80 and PDL2 (Fig. 4.26). This analysis showed no significant differences in the frequencies of the different MBC subpopulations arriving in distLN. However, a reduced number of samples made it difficult to draw any conclusion. There is a tendency to a lower frequency of PDL2^{+} MBCs in the distLN when B cells are ACKR4$^{-/-}$. It is relevant to note that while in the drLN almost 100% of MBCs expressed PDL2, only 50-80% expressed PDL2 in the distLN. The frequency of CD80^{+} MBCs had increased as to comparing MBCs in the drLN and in the distLN. It is unknown whether these MBCs shift PDL2 and CD80 expression during their migration or whether only MBCs that express a lower level of PDL2 and/or high level of CD80 are able to migrate to distLN. The frequency of CD73^{+} MBCs did not seem to be altered when MBCs in the drLN and distLNs were compared. These differences in the frequencies of MBCs appearing in distLN can be explained by the selective migration of specific subsets of MBCs or further differentiation during their migration to distLN. It is unlikely that these eYFP^{+} or TdTomato^{+} cells were naïve B cells for the reasons mentioned above (Fig. 4.17b) and these cells are not GC B cells or PCs, as activation of axillary LNs was not observed post-immunisation in the hind feet (Fig. 4.10).

4.2.6 Memory B cells leave from draining LN in higher proportion when the host is ACKR4$^{-/-}$

It has been shown that MBCs appear in the blood within one week post-immunisation (Blink, Light et al. 2005). Presumably, MBCs leave the drLN *via* the SCS that communicates through the trabecular sinus with the efferent lymphatics (von Andrian

and Mempel 2003) from where they transit into the blood circulation. From the blood stream they may enter other LNs *via* HEVs (Rasmussen, Lodahl et al. 2004). Memory T cells have been shown to migrate with the same pattern than naïve T cells. Memory T cells enter the LNs *via* HEVs and migrate into the T cell area of LN with similar kinetics than naïve T cells. They also enter non-lymphoid organs (Westermann, Ehlers et al. 2001).

Peripheral blood mononuclear cells (PBMC) from chimeric mice (described in 4.2.4) were analysed by flow cytometry. Only very small numbers of $eYFP^+$ and $TdTomato^+$ cells could be detected in blood (Fig. 4.27a). However 100% of these cells found were MBCs ($CD38^+CD138^-$), as naïve B cells do not survive for 8 days without antigen encounter. In stark contrast to what was observed in drLN, there were significantly more MBCs in the blood of $ACKR4^{-/-}$ hosts compared to $ACKR4^{+/+}$ hosts and this was not dependent on ACKR4 expression on the antigen-specific B cells (Fig. 4.27b).

$ACKR4^{-/-}$ hosts had reduced numbers of MBCs in the drLN, independently of the genotype of the B cells, compared to $ACKR4^{+/+}$ hosts. However, in the blood of $ACKR4^{-/-}$ hosts there were more MBCs, independently of the genotype of the B cells. This increased number of MBCs in the blood of $ACKR4^{-/-}$ hosts indicates that the reduced number of MBCs in the drLN of $ACKR4^{-/-}$ hosts was not due to deficient generation but due to increased exit of MBCs from the drLN, as these MBCs seem to be appearing in the blood. This result also agrees with increased migration of MBCs to the SCS of $ACKR4^{-/-}$ mice (4.2.3).

MBCs in $ACKR4^{-/-}$ environment leave the drLN in higher number, as indicated by their reduced number in the drLN and their increased number in blood. However, $ACKR4^{-/-}$ MBCs enter better into distLN independently of the genotype of the host.

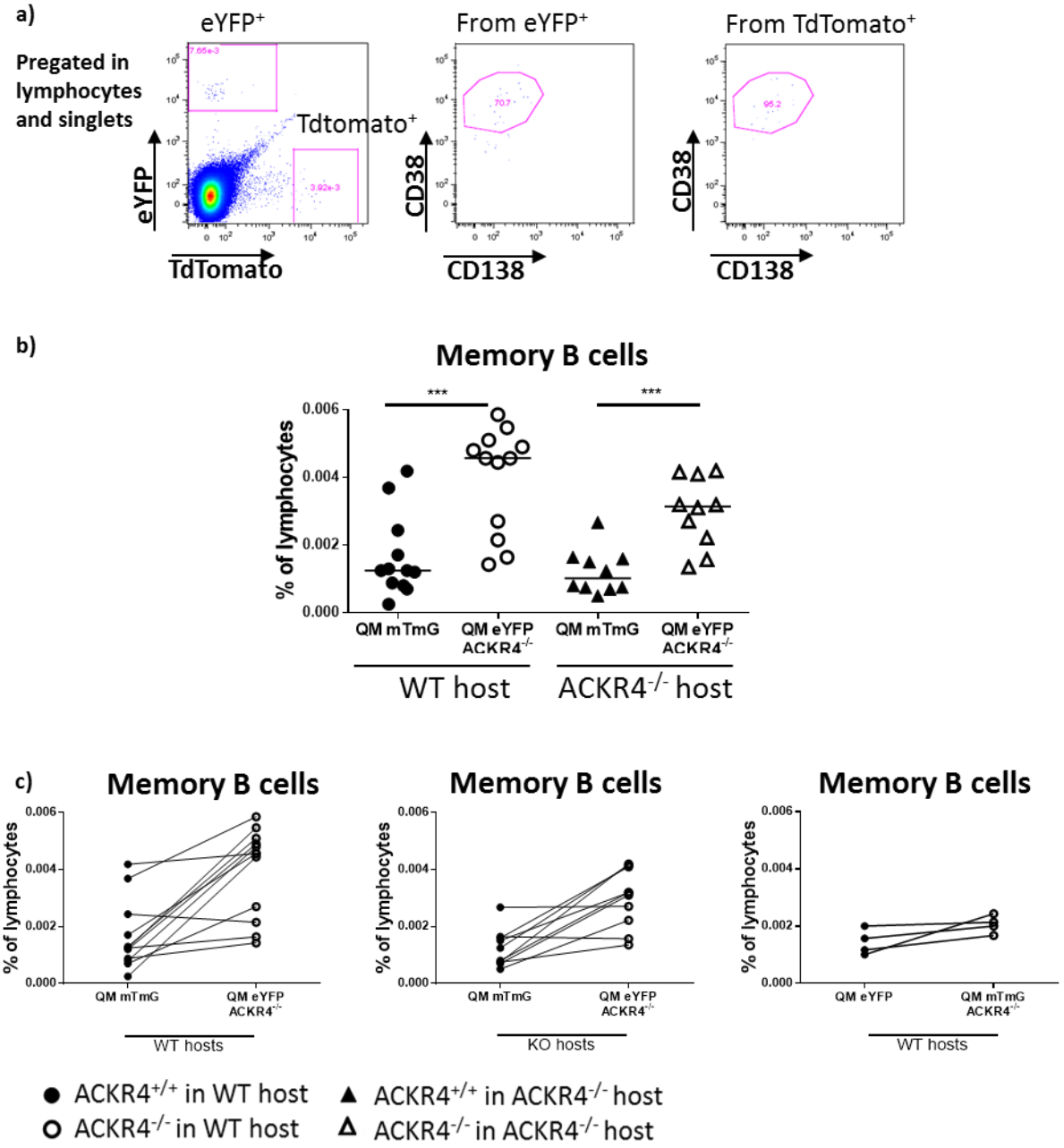

Figure 4.25: ACKR4$^{-/-}$ memory B cells migrate in higher proportion to distant lymph nodes. WT or ACKR4$^{-/-}$ hosts were co-transferred with 1x10^5 NP$^+$B220$^+$ cells from QM ACKR4$^{+/+}$ and same number from QM ACKR4$^{-/-}$ i.v. and immunised 24 h later with NP-CGG s.c. in the rear feet. The response was studied 8 days post-immunisation in distLN. a) Representative diagram for flow cytometry gating for memory B cells from distant LN (axillary LN). b) Flow cytometry data, as to the % of lymphocytes, of MBCs from distant LN. c) Flow cytometry data, as to the % of lymphocytes, linking data points from the same mice. Also, fluorescent proteins were interchanged in order to eliminate the possibility of an effect caused by them.
Data were combined from 3 independent experiments with 5-6 mice per group. Each pair of symbols represents one mouse. Horizontal line represents the median.
Key: WT: wild type; i.v: intravenously; s.c: subcutaneously; distLN: distant lymph node; MBC: memory B cell.
Same host compared using Wilcoxon matched-pairs signed rank test ***p<0.001

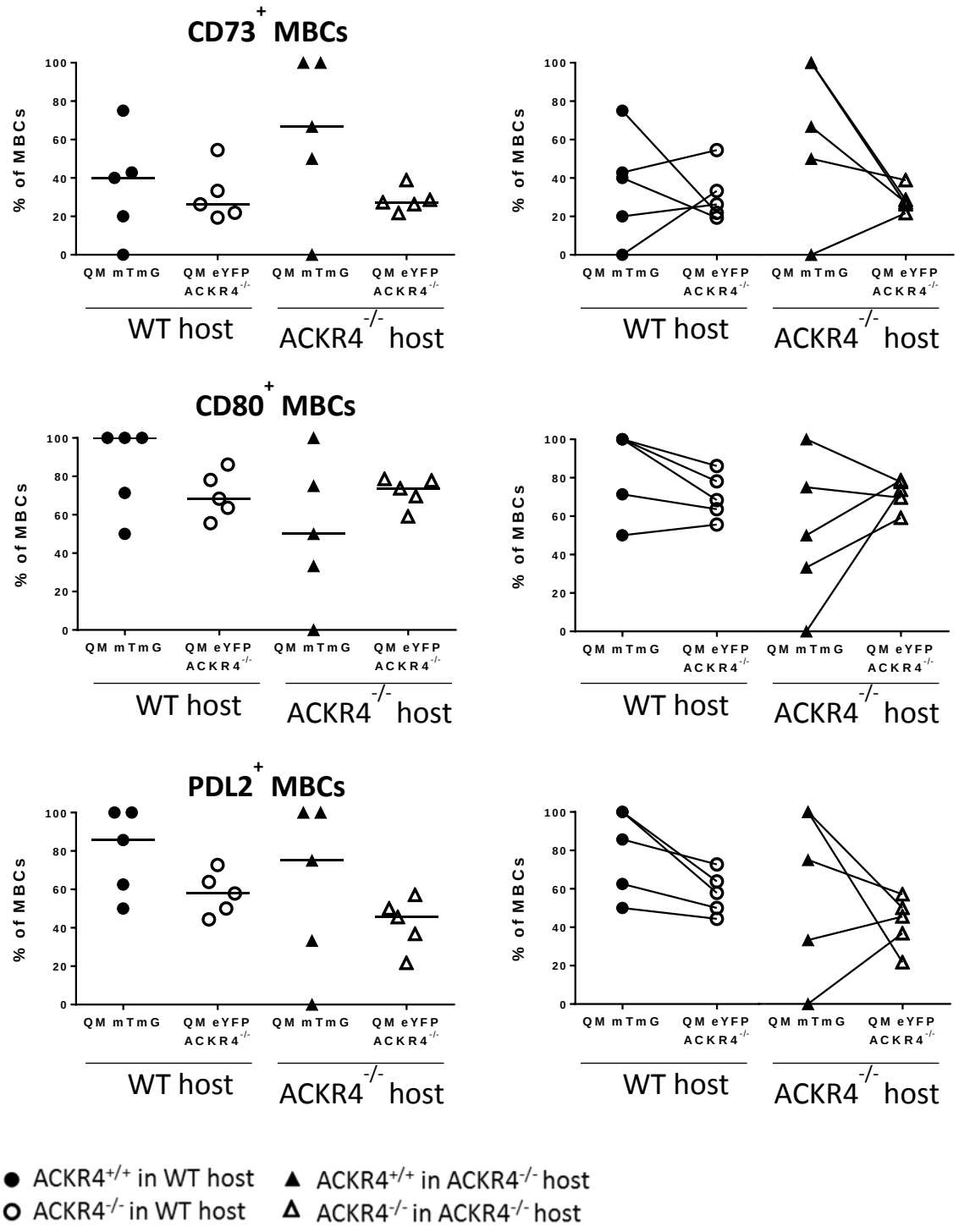

Figure 4.26: ACKR4$^{-/-}$ MBC subpopulations migrate in similar proportions to distant LN. WT or ACKR4$^{-/-}$ hosts were co-transferred with 1x10^5 NP$^+$B220$^+$ cells from QM ACKR4$^{+/+}$ and same number from QM ACKR4$^{-/-}$ i.v. and immunised 24 h later with NP-CGG s.c. in the rear feet. The response was studied 8 days post-immunisation in distLN. Flow cytometry data, as to the % of MBCs, of CD73$^+$ MBCs (upper), CD80$^+$ MBCs (middle) and PDL2$^+$ MBCs (lower).
Plots are representative from 3 independent experiments with 5-6 mice per group. Each pair of symbols represents one mouse. Horizontal line represents the median.
Key: WT: wild type; i.v: intravenously; s.c: subcutaneously; distLN: distant lymph node; MBC: memory B cell.
Same host compared using Wilcoxon matched-pairs signed rank test ***p<0.001

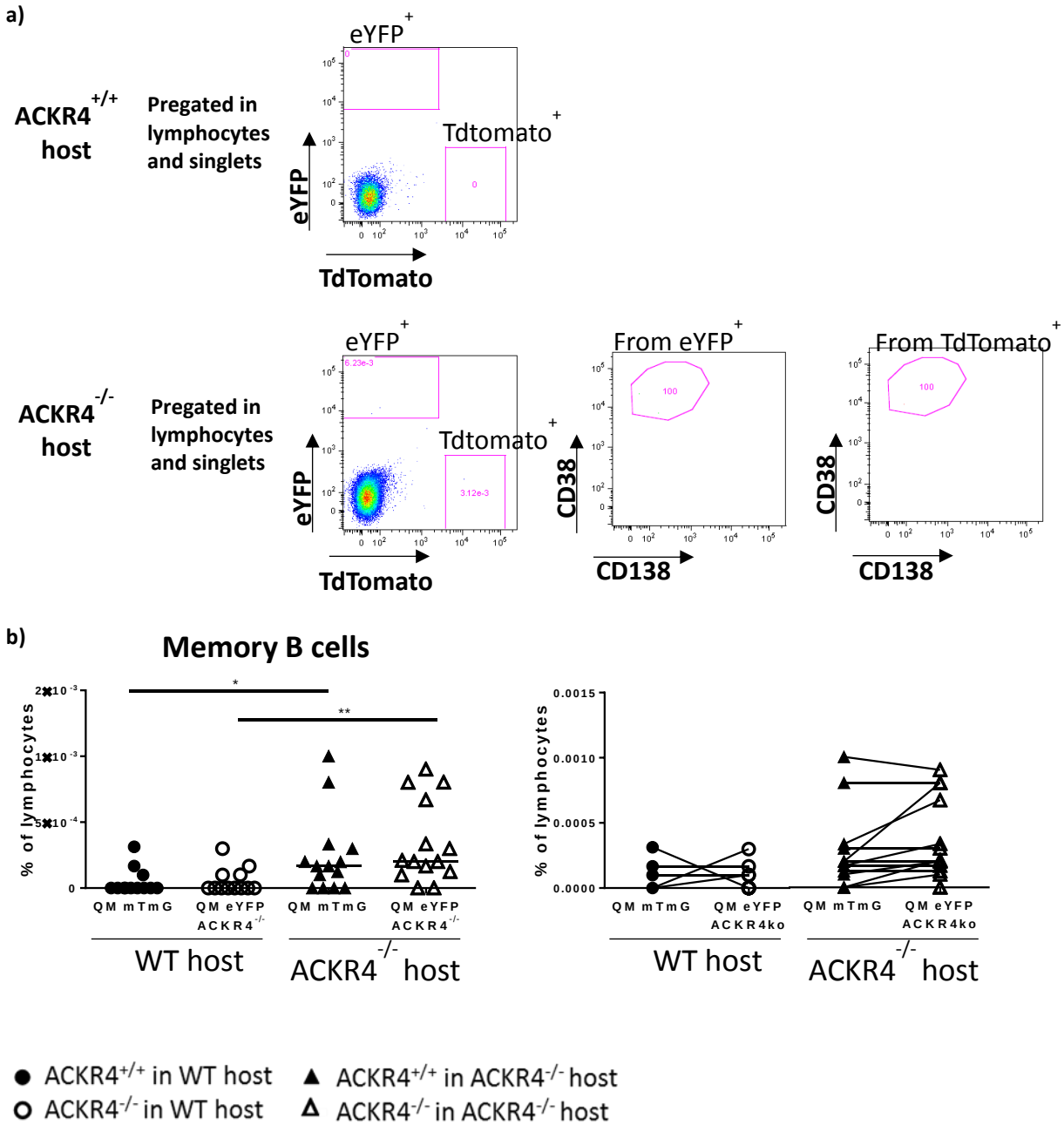

Figure 4.27: Memory B cells leave from draining lymph node in higher proportion when the host is ACKR4$^{-/-}$. WT or ACKR4$^{-/-}$ hosts were co-transferred with 1x10^{5} NP^{+}B220^{+} cells from QM ACKR4$^{+/+}$ and same number from QM ACKR4$^{-/-}$ i.v. and immunised 24 h later with NP-CGG s.c. in the rear feet. The response was studied 8 days post-immunisation. a) Representative diagram for flow cytometry gating for memory B cells from blood. b) Flow cytometry data, in % of lymphocytes, for MBCs from blood.
Data were combined from 3 independent experiments with 5-6 mice per group. Each pair of symbols represents one mouse. Horizontal line represents the median.
Key: WT: wild type; i.v: intravenously; s.c: subcutaneously; MBC: memory B cell.
Same host compared using Wilcoxon matched-pairs signed rank test *p<0.05; **p<0.01

4.2.7 $CCR7^{-/-}$ B cells are selected negatively when they compete with $CCR7^{+/+}$ B cells in WT hosts

ACKR4 and CCR7 share the ligands CCL19/CCL21. In order to test whether the increased migration from drLN of $ACKR4^{-/-}$ hosts is a process that is dependent on CCL19/CCL21, the generation and migration of $CCR7^{-/-}$ MBCs was studied.

The primary response to NP-CGG in the lymph nodes draining the rear feet of chimeric mice with NP-specific B cells from QM $CCR7^{+/+}$ and QM $CCR7^{-/-}$ mice into WT hosts was studied 8 days post-immunisation. In this series of experiments, B cells could not be transferred to $CCR7^{-/-}$ hosts, as they develop defective secondary lymphoid tissues. $CCR7^{-/-}$ mice have enlarged spleen with increased number of lymphocytes, accumulation of T cells within the red pulp and reduced lymphocyte counts in mesenteric LNs (Ohl, Henning et al. 2003). When drLN were analysed, all of the populations studied (GC B cells, PCs and MBCs) appeared in lower numbers when the transferred antigen-specific B cells were CCR7-deficient (Fig. 4.28a). Despite the lower numbers of $CCR7^{-/-}$ cells differentiating, analysis of the frequencies of different B cell subpopulations within the $CCR7^{+/+}$ or $CCR7^{-/-}$ population showed that the extent to which $CCR7^{-/-}$ B cells differentiated into the different B cell populations was the same for PCs and MBCs (Fig. 4.28b). However, $CCR7^{-/-}$ B cells differentiated into GC B cells with a lower frequency compared to $CCR7^{+/+}$ B cells. The generally lower numbers of $CCR7^{-/-}$ B cells that appeared on day 8 is most likely due to the importance of CCR7 during the initial B cell activation, when antigen-activated B cells migrate in a CCR7-dependent manner to the border between the follicle and the T zone to interact and obtain further activation signals from CD4 antigen-specific T cells (Reif, Ekland et al. 2002) (Okada, Miller et al. 2005). The reduced numbers of $CCR7^{-/-}$ antigen-specific B cells in the drLN could also be explained by a defect in the entrance of $CCR7^{-/-}$ naïve

B cell into the LN through the HEVs. It has been previously shown that $CCR7^{-/-}$ B cells bound preferentially to larger HEVs than WT B cells and localised in follicles located closer to the LN medullary region, perhaps because they had used CXCR4 for entrance (Park, Hwang et al. 2012). After adhesion, WT and $CCR7^{-/-}$ naïve B cells behaved similarly and presented same transendothelial migration times (Park, Hwang et al. 2012). It would be interesting to further investigate if same numbers of WT and $CCR7^{-/-}$ B cells are present in the LN before immunisation. The similar propensities of the different subpopulations to differentiate into PC and MBCs indicate that, if a $CCR7^{-/-}$ B cell manages to enter the LN, get activated and enter the GC B cell compartment, CCR7 has no significant role in the downstream differentiation processes to PC or MBC. Moreover, analysis of GC subpopulations showed that $CCR7^{-/-}$ GC B cells entered the LZ in a lower frequency than $CCR7^{+/+}$ GC B cells (Fig. 4.29a). The LZ/DZ ratio was shifted towards the LZ for $CCR7^{+/+}$ GC B cells while $CCR7^{-/-}$ GC B cells had a ratio shifted towards the DZ. When the different MBC subpopulations in the drLN were analysed, there was a significant reduction in $PDL2^{+}$ MBCs while no significant difference could be observed in the $CD73^{+}$ MBC subpopulation. There was a slight but not significant reduction in the $CD80^{+}$ MBC subpopulation (Fig. 4.29c).

In summary, despite CCR7 being important for initial activation, as demonstrated by a generally lower number of $CCR7^{-/-}$ antigen-specific B cells and lower frequency of $CCR7^{-/-}$ GC B cells, it does not play a role in the subsequent differentiation into PCs or MBCs. These results are in concordance with those observed in ACKR4-deficient animals, as ACKR4 expression on B cells did not play a major role in antigen-induced B cell differentiation. $CCR7^{-/-}$ GC B cells enter preferentially the DZ GC B cell compartment and this is expected as CCR7 is preferentially expressed in LZ GC B cells

(Fig. 3.3) and confirms the role of chemokines CCL19/21 in intra-germinal centre distribution and recirculation.

4.2.8 $CCR7^{-/-}$ MBCs appear in higher proportion in distant lymphoid sites

To test the migratory capacity of $CCR7^{-/-}$ MBCs, appearance of MBCs was analysed in distant LNs of chimeric mice (described in 4.2.7). In the distLN, $CCR7^{-/-}$ MBCs appeared in higher proportion than WT MBCs (Fig. 4.30b). Due to the very low numbers of MBCs detectable, this difference was not noticeable in the blood (Fig. 4.30a). $CCR7^{-/-}$ MBCs appeared in higher numbers in the bone marrow (Fig. 4.30c) and in the spleen (Fig. 4.30d) 8 days post-immunisation. It is important to note here that the number of $CCR7^{-/-}$ MBCs is lower in the drLN compared to $CCR7^{+/+}$ MBCs (Fig. 4.28), where these cells are being generated, so an increased appearance of $CCR7^{-/-}$ MBCs in distLNs, spleen and bone marrow, implies a major advantage of $CCR7^{-/-}$ MBCs during their migration to other sites. It is likely that CCR7 is involved in the exit of MBCs from the drLN, as it is unlikely that the entrance to such different microenvironments as bone marrow, spleen and LN is controlled by a single receptor. In the bone marrow B cells are localised to an extravascular location, recirculate freely and cluster around vascular sinusoids (Pillai and Cariappa 2009). Entry into LN is mediated by L-selectin binding to ligands on HEV and triggering a chemokine-mediated integrin activation and adhesion (Butcher, Williams et al. 1999). Entry into the white pulp of the spleen has some redundancies with LNs in terms of integrin involvement, but lymphocytes entry the spleen through follicular arterioles that terminate in the marginal zone (van Ewijk and Nieuwenhuis 1985).

ACKR4-deficiency in the environment of antigen-specific B cells (destroying the CCL19/21 gradient from the T zone to the SCS in the LN) and CCR7-deficiency in the antigen-specific B cells themselves (making them irresponsive to CCL19/21) causes the same effect on the emigration of MBCs from the drLN. Both increase the emigration of MBCs and, therefore, favour MBC appearance in other lymphoid tissues. We hypothesise that migration of MBCs from the GC in the B cell follicle centre to the SCS is inhibited by CCL19/21 gradient, with the highest concentrations of CCL19/21 close to the T zone in the centre of the LN and the lowest in the SCS. When this gradient is disrupted or MBCs are $CCR7^{-/-}$, MBCs are able to overcome the CCL19/21 attracting effect, migrating to the SCS better and appearing in distant sites in higher number.

Moreover, ACKR4 has an added effect during entrance of MBCs into distant LN. $ACKR4^{-/-}$ MBCs enter in higher frequency to distLN, independently of the presence or absence of ACKR4 in the host environment. It is hypothesised that $ACKR4^{-/-}$ MBCs are able to bind CCL21-expressing HEV (Carlsen, Haraldsen et al. 2005) better and therefore they enter distLN in a higher number. Increased binding to CCL21-HEV and, therefore, increased signalling through CCR7, correlates with the effect previously described in 3.2.11, where $ACKR4^{-/-}$ B cells showed increased signalling through CCR7, including phosphorylation of Akt. However, ACKR4 does not play a role in the localisation of MBCs throughout the distLN, as $ACKR4^{-/-}$ MBCs distribute as $ACKR4^{+/+}$ in the different zones of the distLN (Fig. 4.10, 4.11).

4.2.9 CCL19/21 do not have a major effect on MBC proliferation

In order to confirm that the differences observed in the model of double transfer of QM $CCR7^{+/+}$ and QM $CCR7^{-/-}$ antigen-specific B cells were due to actual differences in

migration and not due to differences in proliferation, QM ACKR4$^{+/+}$ CCR7$^{+/+}$, QM CCR7$^{-/-}$ ACKR4$^{+/+}$ or QM CCR7$^{+/+}$ ACKR4$^{-/-}$ NP-binding B cells were separately transferred to WT hosts. The primary response in drLN to NP-CGG injected into the hind feet was studied 8 days later. One hour prior to sacrifice, mice were injected with EdU in order to study cell proliferation by flow cytometry.

Transferred cells in drLN were gated according to the expression of TdTomato fluorescent protein and GC B cells, plasma cells and MBCs as previously shown (Fig. 4.18). GC B cells (Fig. 4.31a) and PCs (Fig. 4.31b) from CCR7$^{-/-}$ and ACKR4$^{-/-}$ showed a reduced proliferation compared to WT B cells. This reduced proliferation correlated with reduced CCR7$^{-/-}$ GC B cell numbers and PCs (Fig. 4.28). MBCs (Fig. 4.31c) did not show any detectable differences in proliferation. Although MBCs by definition are quiescent cells (McHeyzer-Williams, Okitsu et al. 2012), they need T cell help and recognition of the antigen to enter cell division and differentiate into effector cells (Tangye, Avery et al. 2003), a substantial percentage of the cells here (30%) are still in cell cycle, which may reflect their very recent differentiation from GC B cells. This is confirmed by their expression of Ki67 (Fig. 4.15b). The absence of differences in MBC proliferation between WT, CCR7$^{-/-}$ and ACKR4$^{-/-}$ MBCs in the drLN makes it unlikely that the increased number seen in distLN is due to anything else than an effect on the migration of MBCs.

4.2.10 In the draining LN, CCR7$^{-/-}$ MBCs migrate in larger number than CCR7$^{+/+}$ MBCs to the subcapsular sinus

The data shown above are compatible with the hypothesis that CCR7$^{-/-}$ MBCs overcome the retention by CCL19/21 more easily and migrate better to the SCS. In order to

examine the exit of MBCs from the LN into the SCS, numbers of MBCs present in the SCS of the drLN of chimeric mice (described in 4.2.9) were quantified by microscopy (Fig. 4.32a).

Transferred antigen-specific B cells can be identified in histology by the expression of TdTomato. GCs are formed mainly by antigen-specific transferred cells. Lyve-1 staining allows the recognition of LECs in the SCS. IgD and CD4 allow the delimitation of follicles and T zone, respectively. MBCs were observed sitting in the Lyve-1^{+} SCS, as seen previously (Fig. 4.16). Differences between the number of $CCR7^{-/-}$ MBCs and WT MBCs that have migrated to the SCS were not statistically significant (Fig. 4.32b). However, this result suggests that $CCR7^{-/-}$ MBCs have done better in migrating towards the SCS than WT MBCs given the reduced number of $CCR7^{-/-}$ MBCs in the drLN compared to WT MBC numbers (Fig. 4.28). Surprisingly, $ACKR4^{-/-}$ MBCs migrated in an even higher number to the SCS than $CCR7^{-/-}$ MBCs. This finding indicates that the absence of ACKR4 in the MBCs prevents the retention of cells by CCL19/21 gradients. A similar effect from B cell intrinsic deficiency and from ACKR4 deficiency in the environment on B cell migration appears counterintuitive. A likely explanation is that ACKR4 expression on individual B cells creates a microenvironment surrounding the cell that enables B cells to sense and be retained by CCL19/21 gradients. A similar mechanism of action has been demonstrated for ACKR3 (CXCR7) (Dona, Barry et al. 2013, Venkiteswaran, Lewellis et al. 2013). During zebrafish embryogenesis, the primordium epithelial cells have to migrate collectively along the body of the fish until they reach the tip end. ACKR3 expression on the rear primordium reduces the concentration of CXCL12 through protein scavenging, generating a gradient of CXCL12 that is able to self-direct tissue migration (Dona, Barry et al. 2013, Venkiteswaran, Lewellis et al. 2013).

4.2.11 Five weeks post primary immunisation CCR7$^{-/-}$ and ACKR4$^{-/-}$ MBCs are present in same numbers than WT MBCs in distant LN

In order to test the consequences of the increased migration of CCR7$^{-/-}$ MBCs towards other lymphoid sites to the long-term survival of the MBCs and their response to secondary challenges, chimeric mice (described in 4.2.9) were analysed 5 weeks post-primary immunisation and 5 days post-secondary immunisation.

In order to establish that the results from the double transfer of WT and ACKR4$^{-/-}$ NP-specific B cells (4.2.4) or WT and CCR7$^{-/-}$ NP-specific B cells (4.2.7) into WT hosts were reproducible by separated transfers, the response was also analysed 8 days post-immunisation. Transferred cells were gated in base of their expression of the fluorescent protein TdTomato (Fig. 4.33). As expected, in the drLN, CCR7$^{-/-}$ MBCs were less abundant while numbers of WT and ACKR4$^{-/-}$ MBCs were comparable (Fig. 4.33a). Due to low sample number, the differences in the distLN between the numbers of CCR7$^{-/-}$ and ACKR4$^{-/-}$ MBCs compared to WT MBCs were not statistically significant (Fig. 4.33a). However, these results correlated to those observed previously during the double transfer experiments. The number of CCR7$^{-/-}$ and ACKR4$^{-/-}$ MBCs that had migrated into the distLN was comparable, and correlated with the affinity of both receptors for the ligands (Forster, Davalos-Misslitz et al. 2008). Interestingly, in the distLN and 5 weeks post primary immunisation, WT MBC numbers were comparable to CCR7$^{-/-}$ and ACKR4$^{-/-}$ MBC numbers (Fig. 4.33c). This may indicate that distLNs have a limited capacity to sustain MBC survival long-term and accumulation of WT MBCs reaches their maximum capacity. It may also mean that CCR7$^{-/-}$ and ACKR4$^{-/-}$ MBCs have some intrinsic defects that reduce their survival rate.

Five weeks after primary immunisation mice were boosted with soluble antigen in the contralateral feet in order to stimulate the pLN in the opposite side from the primary immunisation. In the contralateral LN, the only cells that will be able to respond to the soluble antigen will be the MBCs that have migrated there from the primary response. Naïve transferred cells did not survive in the host for 5 weeks without antigen encounter. The secondary response was analysed 5 days post-boosting. The gating strategy is shown in Fig. 4.34a. There was no significant difference in the numbers of GC B cells (Fig. 4.34b left) or plasma cells (Fig. 4.34b right) that had differentiated after boosting from each genotype. There was a tendency to higher numbers of $CCR7^{-/-}$ MBCs (Fig. 4.34b lower). These results indicate that $CCR7^{-/-}$ and $ACKR4^{-/-}$ MBCs do not have any defect or advantage to mount effective secondary responses, compared to WT MBCs.

In summary, $CCR7^{-/-}$ and $ACKR4^{-/-}$ MBCs survive to the same extent than WT MBCs and absence of CCR7 or ACKR4 expression in MBCs does not have a negative nor positive effect on the secondary response to NP-CGG.

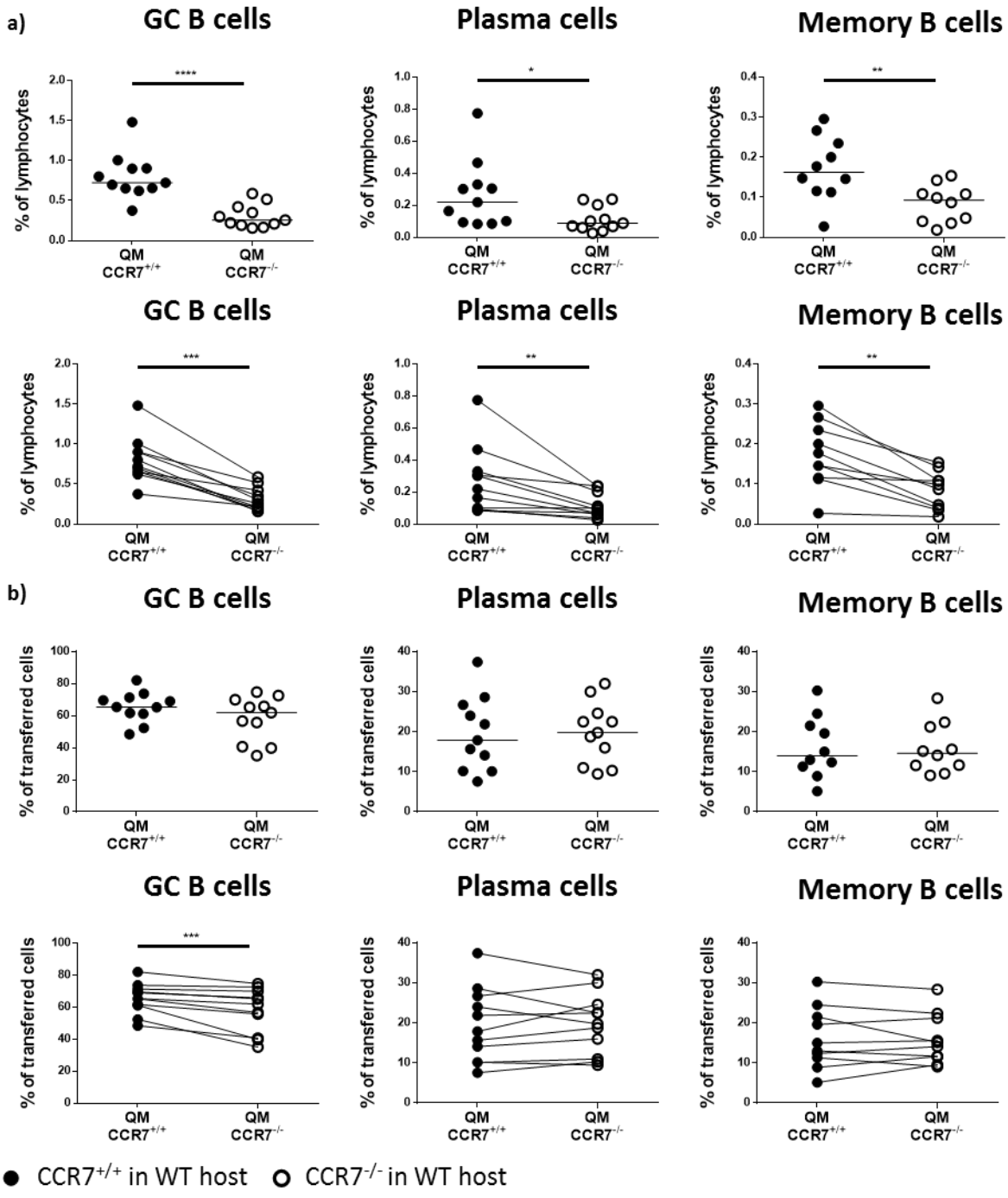

Figure 4.28: CCR7$^{-/-}$ B cells are negatively selected when they compete with CCR7$^{+/+}$ B cells in WT hosts. WT hosts were co-transferred with 1x10^5 NP$^+$B220$^+$ cells from QM CCR7$^{+/+}$ and same number from QM CCR7$^{-/-}$ i.v. and immunised 24 h later with NP-CGG s.c. in the rear feet. The response was studied 8 days post-immunisation in the drLN. a) Flow cytometry data, as to the % of lymphocytes (upper) and % of lymphocytes (lower) with linked data from same host of GC B cells (left), plasma cells (middle) and MBCs (right). b) Flow cytometry data, as to the % of transferred cells (upper) and % of transferred cells (lower) with linked data from same host of GC B cells (left), plasma cells (middle) and MBCs (right).

Data were combined from 2 independent experiments with 5-6 mice per group. Each pair of symbols represents one mouse. Horizontal line represents the median.

Key: i.v: intravenously; s.c: subcutaneously; drLN: draining lymph node; GC: germinal centre; MBC: memory B cell.

Unlinked data compared using Mann-Whitney test *p<0.05; **p<0.01; ****p<0.0001

Linked data compared using Wilcoxon matched-pairs signed rank test **p<0.01; ***p<0.001

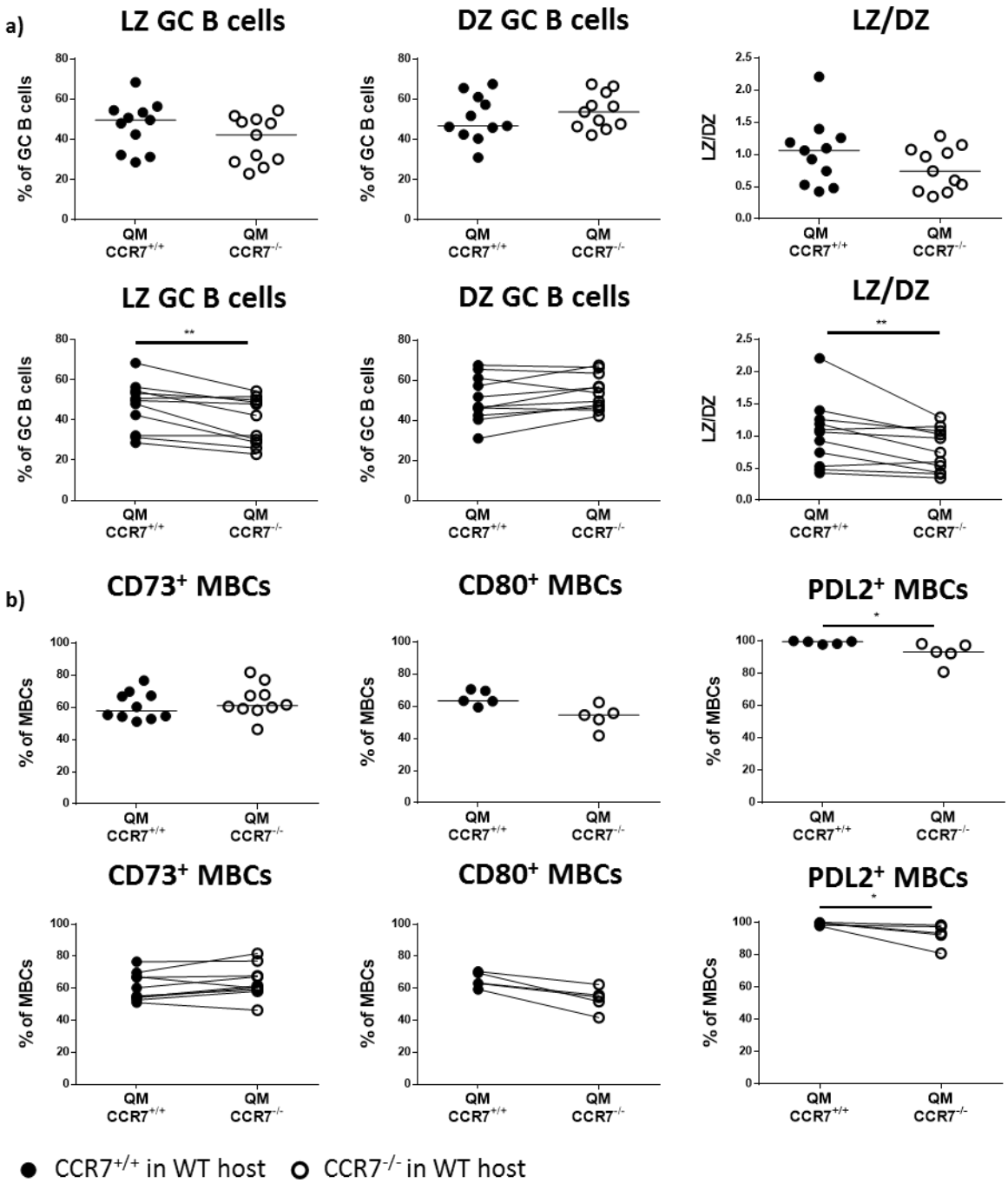

Figure 4.29: CCR7$^{-/-}$ B cells enter preferentially the DZ when they compete with CCR7$^{+/+}$ B cells in WT hosts. WT hosts were co-transferred with 1x10^5 NP$^+$B220$^+$ cells from QM CCR7$^{+/+}$ and same number from QM CCR7$^{-/-}$ i.v. and immunised 24 h later with NP-CGG s.c. in the rear feet. The response was studied 8 days post-immunisation in the drLN. a) Flow cytometry data, as to the % of GC B cells (upper) and % of GC B cells with linked data from the same host (lower) of LZ GC B cells (left), DZ GC B cells (middle) and LZ/DZ ratio (right). b) Flow cytometry data, as to the % of MBCs (upper) and % of MBCs with linked data from the same host (lower) of CD73$^+$ MBCs, CD80$^+$ MBCs and PDL2$^+$ MBCs.

Data were combined from 2 independent experiments with 5-6 mice per group. Each pair of symbols represents one mouse. Horizontal line represents the median.

Key: i.v: intravenously; s.c: subcutaneously; drLN: draining lymph node; GC: germinal centre; LZ: light zone; DZ: dark zone; MBC: memory B cell.

Unlinked data compared using Mann-Whitney test *p<0.05

Linked data compared using Wilcoxon matched-pairs signed rank test *p<0.05; **p<0.01

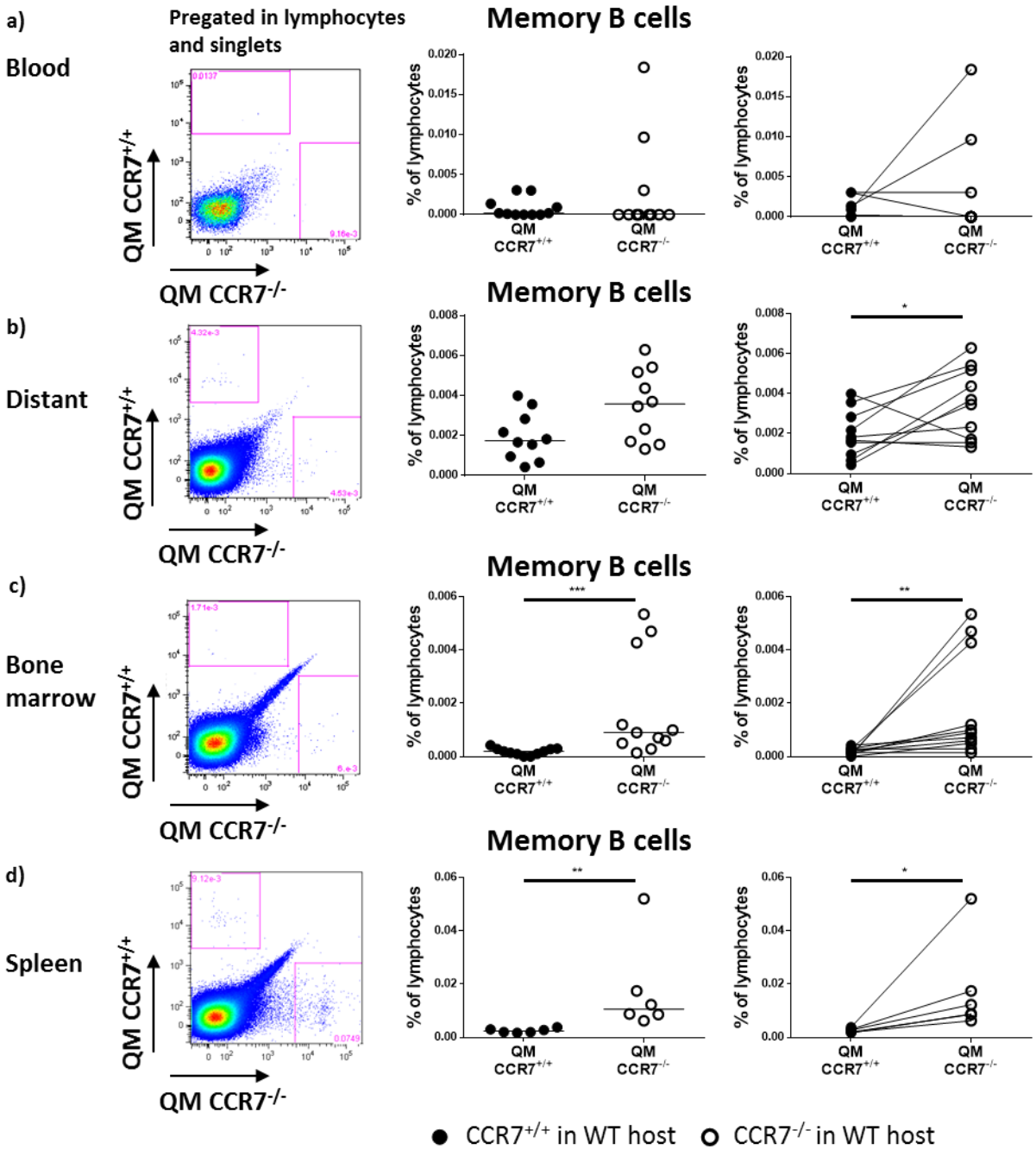

Figure 4.30: CCR7$^{-/-}$ MBCs appear in higher proportion in distant lymphoid sites. WT hosts were co-transferred with 1x10^5 NP$^+$B220$^+$ cells from QM CCR7$^{+/+}$ and same number from QM CCR7$^{-/-}$ i.v. and immunised 24 h later with NP-CGG s.c. in the rear feet. The response was studied 8 days post-immunisation in different secondary organs. a) Representative diagram for flow cytometry gating for memory B cells from distant LN for QM CCR7$^{+/+}$ and QM CCR7$^{-/-}$ MBCs (left). Flow cytometry data, as to the % of lymphocytes, for MBCs from distant LNs (right). b) Representative flow cytometry graph for MBCs from blood (left). Flow cytometry data, as to the % of lymphocytes, of MBCs from blood (right). c) Representative flow cytometry graph for MBCs from the bone marrow (left). Flow cytometry data, as to the % of lymphocytes, of MBCs from bone marrow (right). d) Representative flow cytometry graph for MBCs from the spleen (left). Flow cytometry data, as to the % of lymphocytes, of MBCs from spleen (right).
Data were combined from 2 independent experiments with 5-6 mice per group. Each pair of symbols represents one mouse. Horizontal line represents the median.
Key: i.v: intravenously; s.c: subcutaneously; LN: lymph node; MBC: memory B cell.
Same host compared using Wilcoxon matched-pairs signed rank test **p<0.01; ***p<0.001

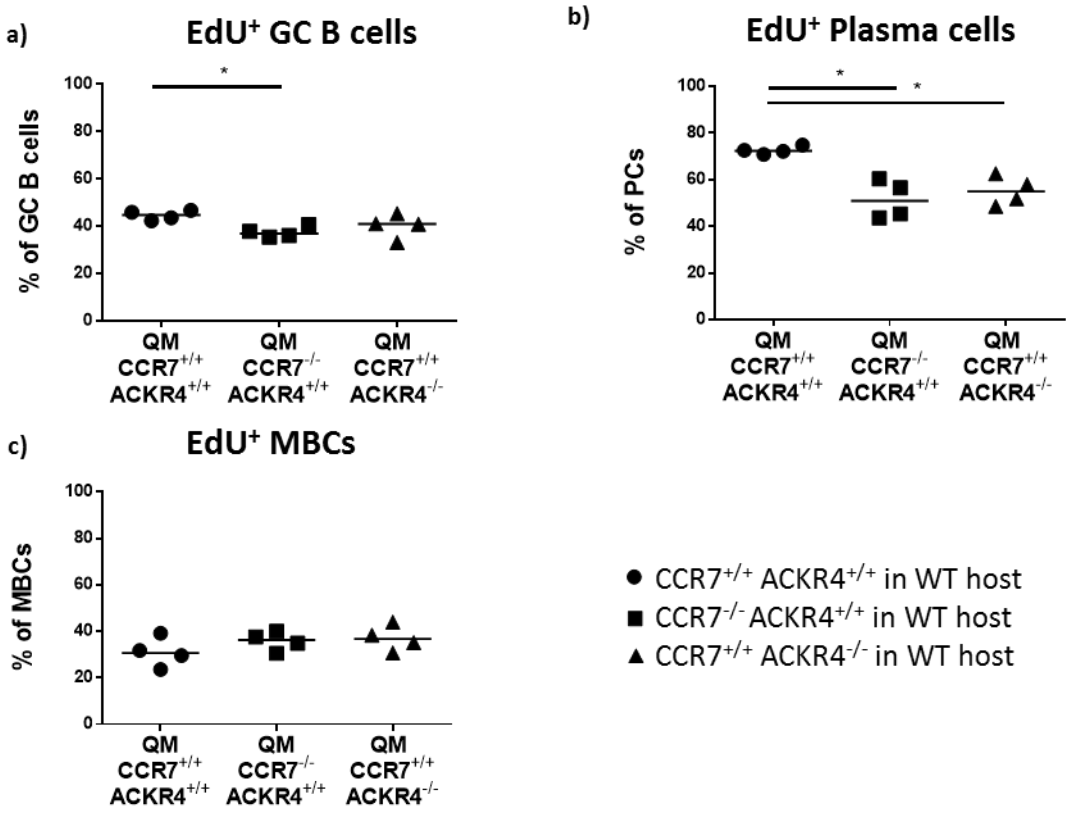

Figure 4.31: CCL19/21 does not have a major effect on memory B cell proliferation. WT hosts were separately transferred with $2x10^5$ NP^+B220^+ cells from QM $CCR7^{+/+}$ $ACKR4^{+/+}$ or QM $CCR7^{-/-}$ $ACKR4^{+/+}$ or QM $CCR7^{+/+}$ $ACKR4^{-/-}$ i.v. and immunised 24 h later with NP-CGG s.c. in the rear feet. The response was studied 8 days post-immunisation in the drLN. EdU was injected 1 h prior to sacrifice. a) Flow cytometry data, as to the % of GC B cells, for EdU^+ GC B cells. b) Flow cytometry data, as to the % of PCs, for EdU^+ PCs. c) Flow cytometry data, as to the % of MBCs, for EdU^+ MBCs.
1 independent experiment. Each symbol represents one mouse. Horizontal line represents the median.
Key: i.v: intravenously; s.c: subcutaneously; drLN: draining lymph node; GC: germinal centre; MBC: memory B cell; PC: plasma cell; EdU: 5-ethynyl-2′-deoxyuridine.
Non-parametric Mann-Whitney test *$p<0.05$

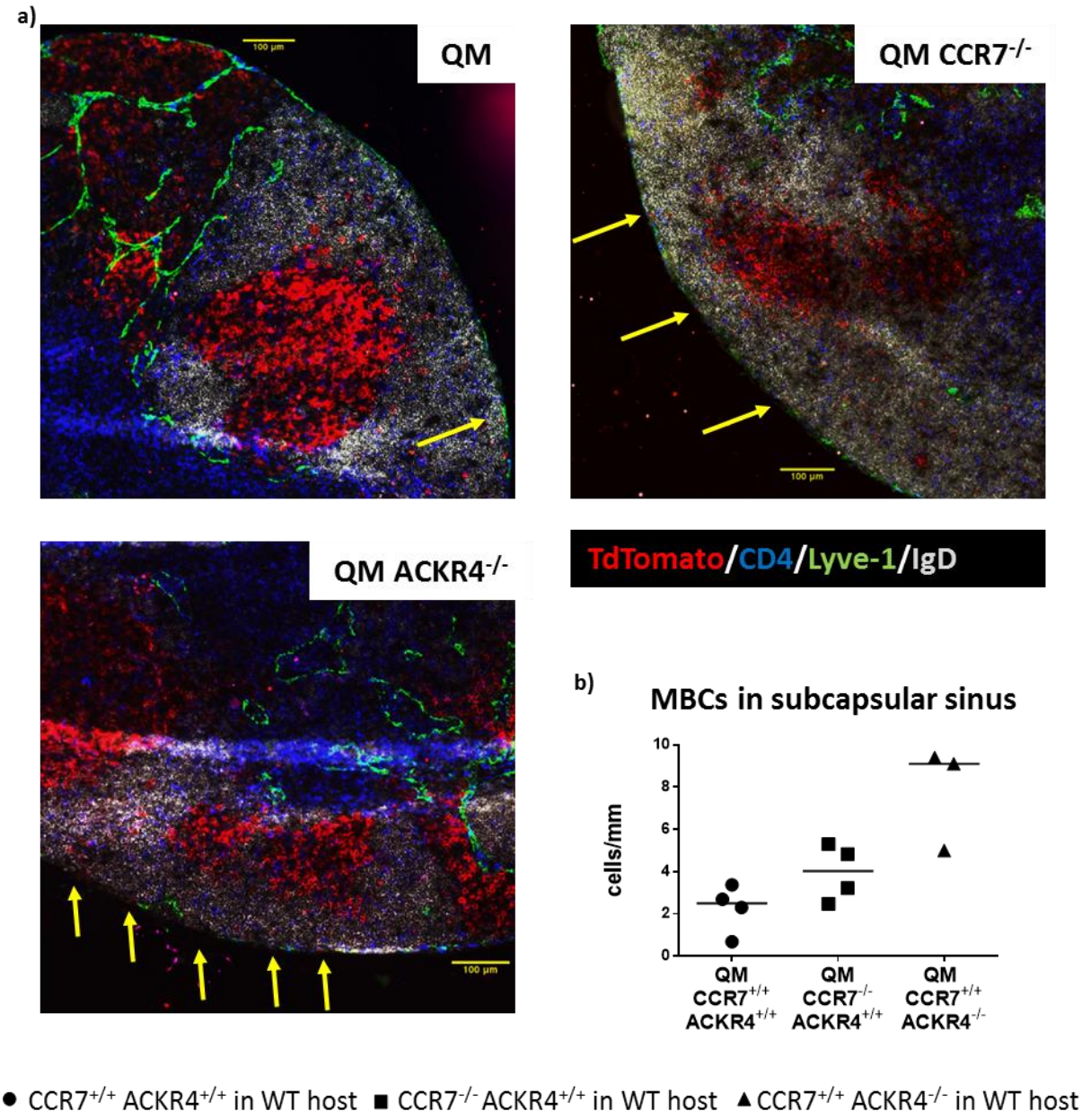

Figure 4.32: In the draining lymph node, CCR7$^{-/-}$ memory B cells appear in higher numbers than WT memory B cells in the subcapsular sinus. WT hosts were separately transferred with 2x10^5 NP$^+$B220$^+$ cells from QM CCR7$^{+/+}$ ACKR4$^{+/+}$ or QM CCR7$^{-/-}$ ACKR4$^{+/+}$ or QM CCR7$^{+/+}$ ACKR4$^{-/-}$ i.v. and immunised 24 h later with NP-CGG s.c. in the rear feet. The response was studied 8 days post-immunisation in the drLN. a) Representative example for immunofluorescence staining images of drLN for Lyve-1 (green), TdTomato (transferred cells) (red), IgD (grey) and CD4 (blue). Yellow arrows denote TdTomato$^+$ MBCs that have migrated to the subcapsular sinus. b) Quantification, as to the cells per mm of subcapsular sinus, of TdTomato$^+$ MBCs that have migrated to the subcapsular sinus.
1 independent experiment. Each symbol represents one mouse. Horizontal line represents the median.
Key: i.v: intravenously; s.c: subcutaneously; drLN: draining lymph node; MBC: memory B cell.

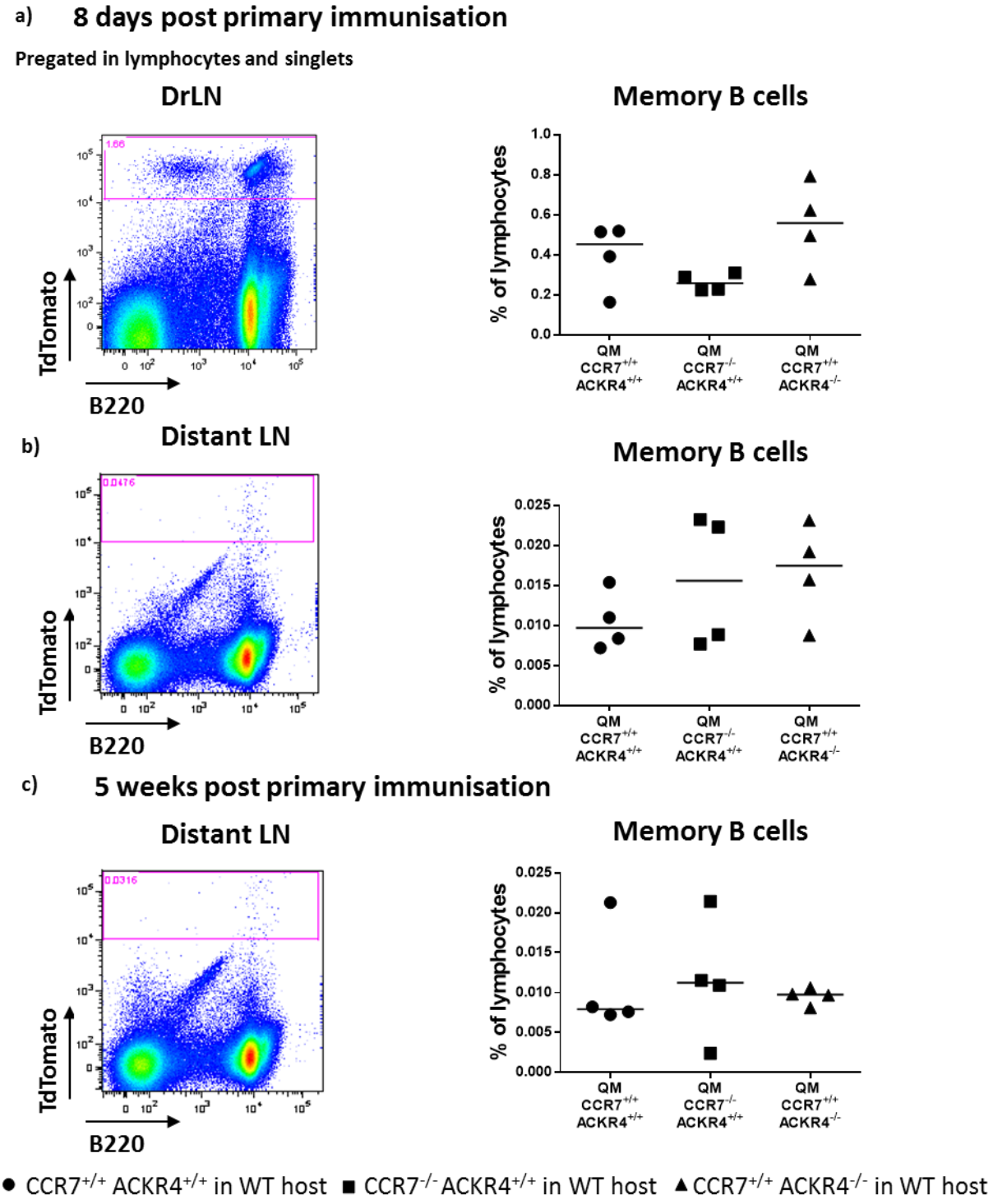

Figure 4.33: **5 weeks after primary immunisation CCR7$^{-/-}$ and ACKR4$^{-/-}$ MBCs are present in same numbers in distant LN.** WT hosts were separately transferred with 2x10^5 NP$^+$B220$^+$ cells from QM CCR7$^{+/+}$ ACKR4$^{+/+}$ or QM CCR7$^{-/-}$ ACKR4$^{+/+}$ or QM CCR7$^{+/+}$ ACKR4$^{-/-}$ i.v. and immunised 24 h later with NP-CGG s.c. in the rear feet. The response was studied at different times post-immunisation. a) The response was studied 8 days post-immunisation. Flow cytometry gating example and data, as to the % of lymphocytes, for MBCs from drLN. b) The response was studied 8 days post-immunisation. Flow cytometry gating example and data, as to the % of lymphocytes, for MBCs from distant LNs. c) The response was studied 5 weeks post primary immunisation. Flow cytometry gating example and data, as to the % of lymphocytes, for MBCs from distant LNs.
1 independent experiment. Each symbol represents one mouse. Horizontal line represents the median.
Key: i.v: intravenously; s.c: subcutaneously; drLN: draining lymph node; MBC: memory B cell.

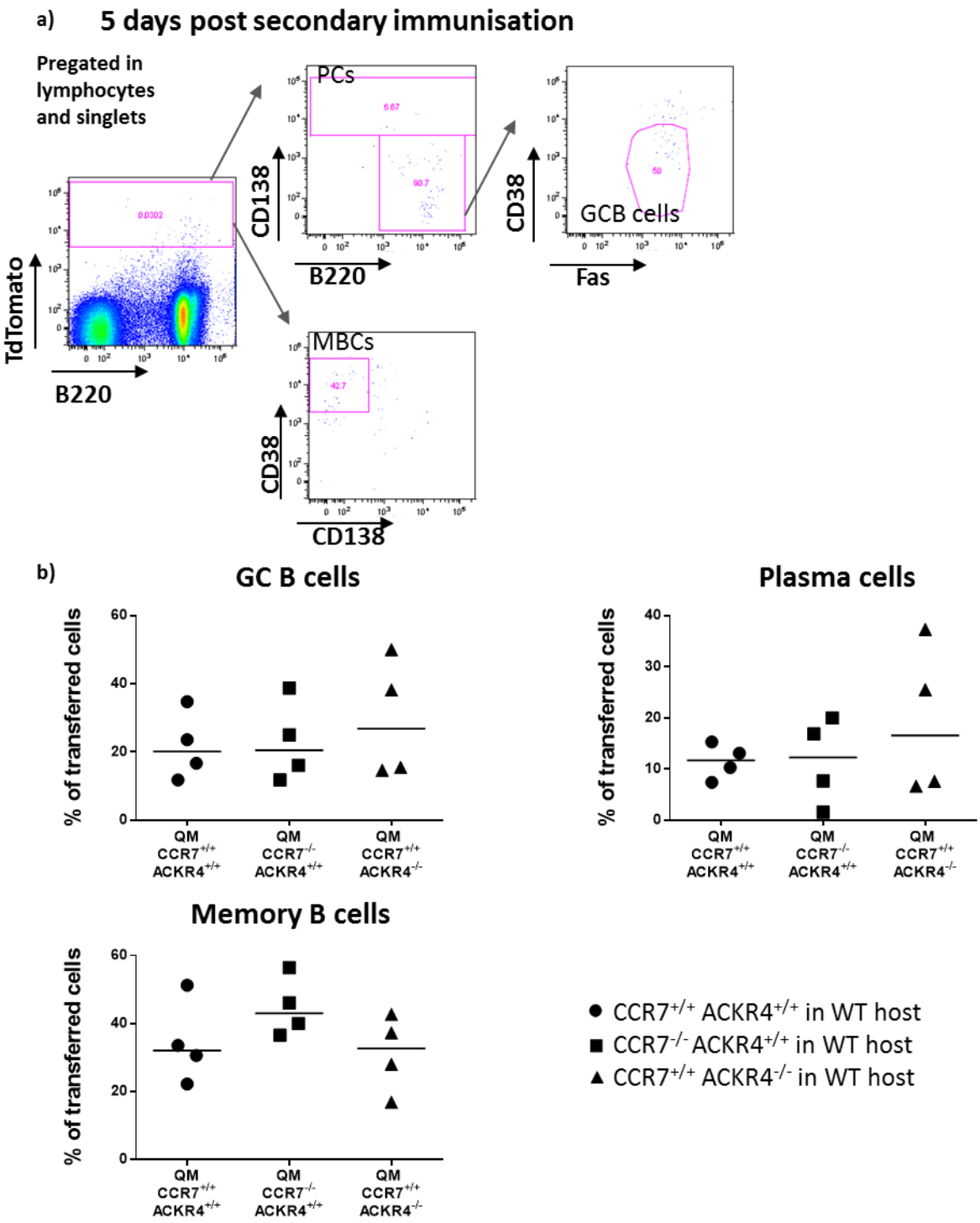

Figure 4.34: CCR7$^{-/-}$ and ACKR4$^{-/-}$ memory B cells mount normal secondary responses. WT hosts were separately transferred with 2x10^5 NP$^+$B220$^+$ cells from QM CCR7$^{+/+}$ ACKR4$^{+/+}$ or QM CCR7$^{-/-}$ ACKR4$^{+/+}$ or QM CCR7$^{+/+}$ ACKR4$^{-/-}$ and immunised 24 h later with NP-CGG s.c. in the rear feet. 5 weeks post primary immunisation, mice were boosted in the contralateral footpad with soluble NP-CGG and the response studied 5 days post-boosting. a) Representative diagram for flow cytometry gating of PCs, GC B cells and MBCs. b) Flow cytometry data, as to the % of transferred cells, for GC B cells, plasma cells and MBCs from draining LN.
1 independent experiment. Each symbol represents one mouse. Horizontal line represents the median.
Key: i.v: intravenously; s.c: subcutaneously; drLN: draining lymph node; GC: germinal centre; MBC: memory B cell; PC: plasma cell.

4.2.12 Disruption of CCL19/21 gradients in drLN by CCL19 injection causes increased MBC migration

The data shown above have indicated that the increased appearance of CCR7$^{-/-}$ MBCs in distant lymphoid sites may be caused through a lack of MBCs being attracted towards CCL19/21 gradients in the drLN. Similarly, disruption of the CCL19/21 gradient through ACKR4-deficiency in the host environment causes a similar effect. In order to further test the role of the CCL19/21 gradient in the drLN, chimeric mice for WT and CCR7$^{-/-}$ (described in 4.2.7) were immunised with NP-CGG in the rear feet. In order to disrupt the CCL19 gradient, mice were injected with 3 µg of CCL19 or PBS in the same feet of immunisation 6 h prior to sacrificing the mice on day 8 post-immunisation.

It has been shown previously that disruption of the CCL19/21 gradient by CCL21-overexpression disturbs T cell migration, T cell subpopulations and lymph node microarchitecture, demonstrating that chemotaxis caused by CCL19/21 is firmly regulated and can be altered easily (Christopherson, Campbell et al. 2001). Injection of 3 µg of CCL19 is enough to disturb the gradient. Injection of 1 µg of CCL19 s.c. altered the regular distribution of CCR7 ligands in the pLN and was enough to modify basal CD4^{+} T cell motility from T zones to subcapsular areas (Worbs, Mempel et al. 2007).

Preliminary experiments showed that the injection of CCL19 24 h prior to sacrifice had a profound effect in the GC B cell differentiation and differentiation of PCs and MBCs. Both WT and CCR7$^{-/-}$ GC B cell numbers were reduced after CCL19 incubation for 24h (Fig. 4.35a). Interestingly, CCL19 injection had an effect in the differentiation of cells and after 24 h, PC numbers are increased (Fig. 4.35b) while MBC numbers are reduced (Fig. 4.35c) both from the WT and CCR7$^{-/-}$ genotype. Therefore, it is difficult to distinguish if the effects observed in appearance of MBCs in distant sites were caused

by differences in the migration or in the generation of MBCs. In order to minimise the effects of output of MBCs from GCs, a short incubation of 6 h with CCL19 was chosen.

When the drLNs were analysed by flow cytometry, it could be observed that short term administration of CCL19 had no major effects on the number of GC B cells as to the percentage of transferred cells (Fig. 4.36a). $CCR7^{-/-}$ GC B cell numbers were reduced in both conditions as previously observed (Fig. 4.28). PCs and MBC numbers as to the percentage of transferred cells were comparable between genotypes and in both conditions (Fig. 4.36b, 4.36c). The expression of Fas by MBCs is a matter of controversy in the literature. Fas has been shown to be required for MBC generation (Takahashi, Ohta et al. 2001) and in humans, Fas is expressed in activated MBCs (Jacobi, Reiter et al. 2008). For this reason, MBCs were gated only in basis of their expression of CD38 and negative expression for CD138. As MBCs were not gated according to their Fas expression, this gate included also some cells that were previously included in the GC B cell gate, making the total of transferred cells higher than 100% when GC B cells, PCs and MBCs were added together.

However, in this particular experiment lower numbers of $CCR7^{-/-}$ NP-specific B cells than $CCR7^{+/+}$ NP-specific B cells were transferred. When antigen-differentiated cells were analysed as to the percentage of lymphocytes, it was observed that WT B cell numbers were at least 5 times higher than $CCR7^{-/-}$ B cells, including GC B cells (Fig. 4.37a), PCs (4.37b) and MBCs (Fig. 4.37c), while in previous experiments the ratio between WT and $CCR7^{-/-}$ B cells in the same host was only double (Fig. 4.28). This explains why $CCR7^{-/-}$ appeared in lower numbers than WT MBCs in distLN in control conditions (Fig. 4.38). In this experiment, injection of CCL19 led to a strong appearance of WT MBCs in the blood (Fig. 4.38a) and in the distLN (Fig. 4.38b), confirming that

the disruption of the gradient facilitates the exit of WT MBCs from the drLN. Further, the gradient disruption did not have an effect in the CCR7$^{-/-}$ population. However, in the spleen (Fig. 4.38c left) and in the bone marrow (Fig. 4.38d right), the effect of the CCL19 injection was not detectable. This may be due to an inefficient inhibition by CCL19, for example, because higher concentrations are necessary, a different route of injection should have been chosen or the incubation period was too short.

When MBCs that have migrated to the SCS were quantified in immunofluorescence images from drLN (Fig. 4.38e), it could be observed that in control conditions, CCR7$^{-/-}$ MBCs appeared in the SCS to the same extent as WT MBCs or even in higher numbers. However, when CCL19 was injected and the gradient disturbed, this scenario was reversed and more WT than CCR7$^{-/-}$ MBCs migrated to the SCS. This result supports the idea that the body, specifically the drLNs and the SCS, have a limited capacity to sustain MBCs and that is why the injection of CCL19 reverses the migration towards the SCS.

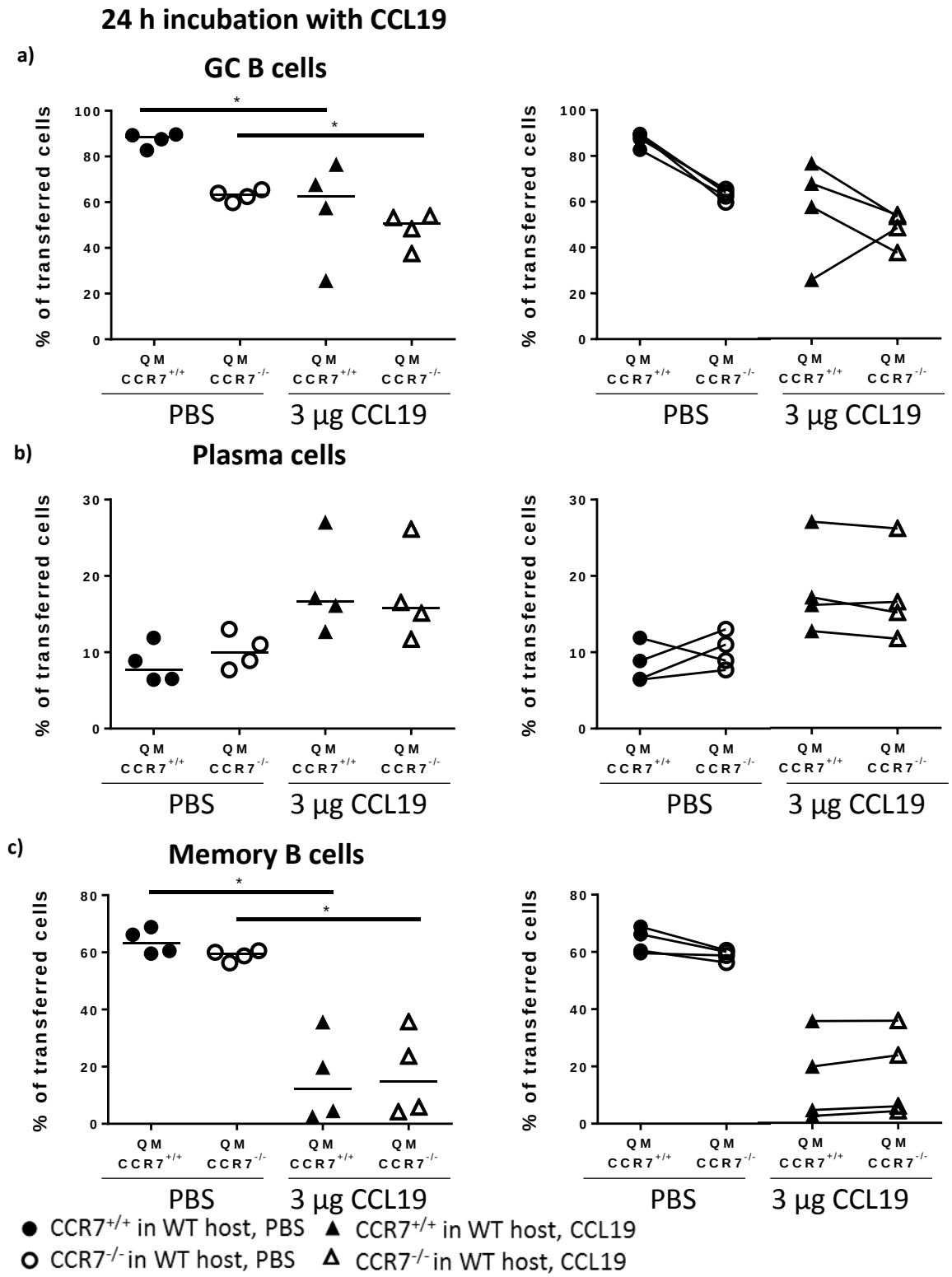

Figure 4.35: CCL19 injection in the drLN for 24 h affects antigen-stimulated B cell differentiation. WT hosts were co-transferred with $1x10^5$ NP^+B220^+ cells from QM $CCR7^{+/+}$ and same number from QM $CCR7^{-/-}$ i.v. and immunised 24 h later with NP-CGG s.c. in the rear feet. The response was studied 8 days post-immunisation in the drLN. 3 µg of CCL19 were injected in the same foot 24 h prior to sacrifice. a) Flow cytometry data, as to the % of transferred cells, for GC B cells. b) Flow cytometry data, as to the % of transferred cells, for PCs. c) Flow cytometry data, as to the % of transferred cells, for MBCs. 1 independent experiment. Each pair of symbols represents one mouse. Horizontal line represents the median.

Key: i.v: intravenously; s.c: subcutaneously; drLN: draining lymph node; GC: germinal centre; MBC: memory B cell; PC: plasma cell; PBS: phosphate buffer saline.

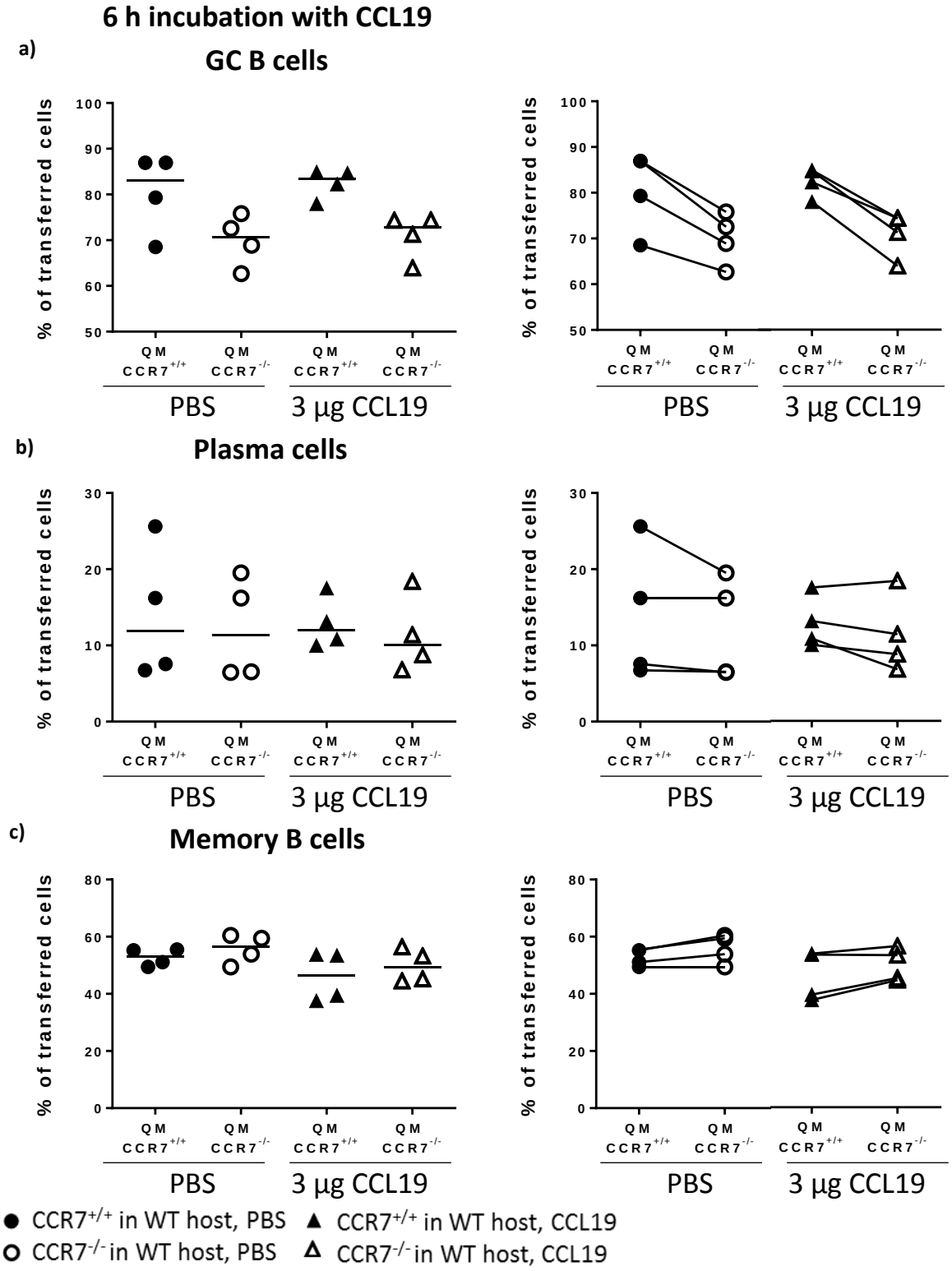

Figure 4.36: CCL19 injection in the drLN for 6 h has no effect in antigen-stimulated B cell differentiation. WT hosts were WT hosts were co-transferred with $1x10^5$ NP^+B220^+ cells from QM $CCR7^{+/+}$ and same number from QM $CCR7^{-/-}$ i.v. and immunised 24 h later with NP-CGG s.c. in the rear feet. The response was studied 8 days post-immunisation in the drLN. 3 µg of CCL19 were injected in the same foot 6 h prior to sacrifice. a) Flow cytometry data, as to the % of transferred cells, for GC B cells. b) Flow cytometry data, as to the % of transferred cells, for PCs. c) Flow cytometry data, as to the % of transferred cells, for MBCs. 1 independent experiment. Each pair of symbols represents one mouse. Horizontal line represents the median.

Key: i.v: intravenously; s.c: subcutaneously; drLN: draining lymph node; GC: germinal centre; MBC: memory B cell; PC: plasma cell; PBS: phosphate buffer saline

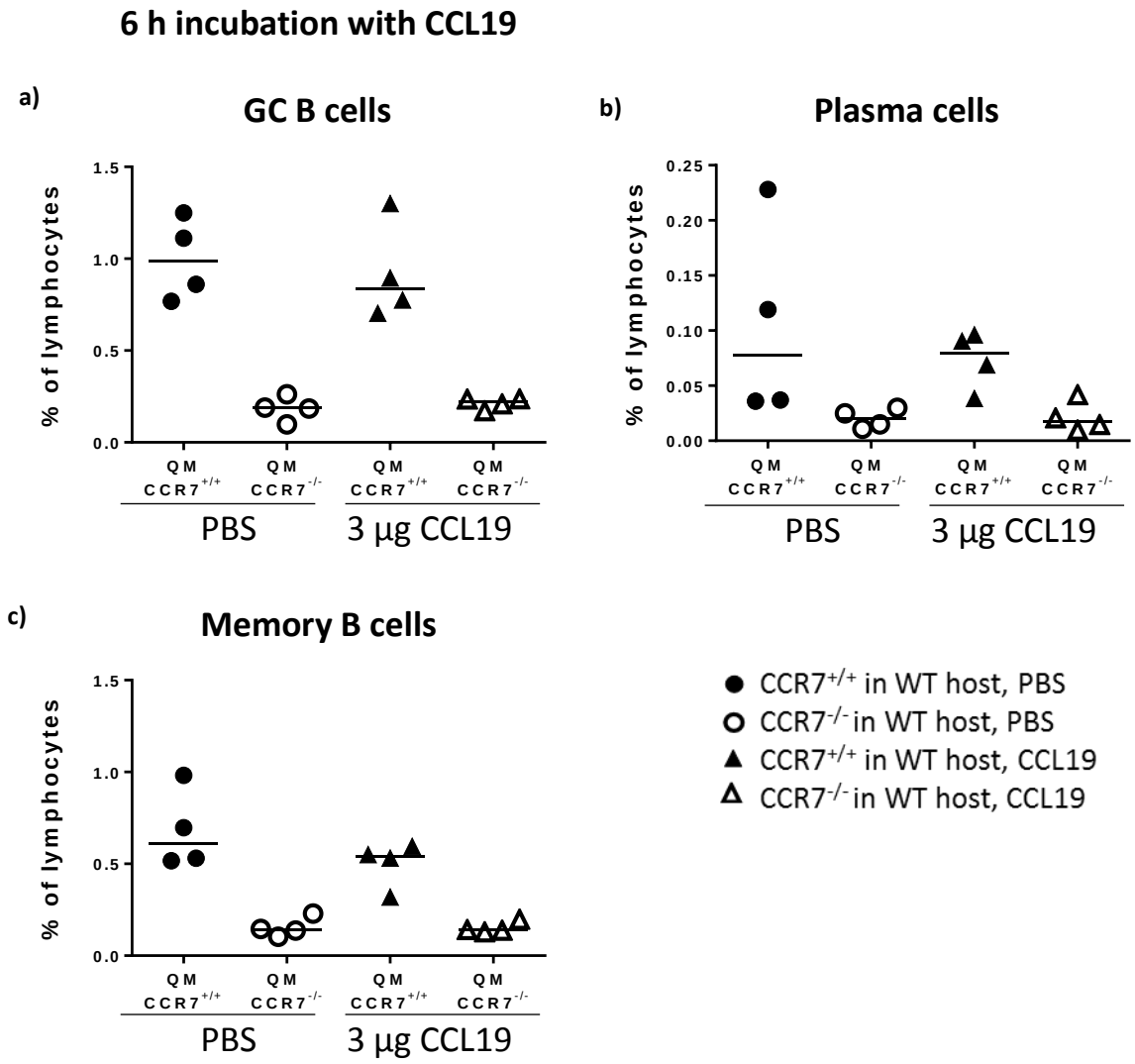

Figure 4.37: CCL19 injection in the drLN for 6 h has no effect in antigen-stimulated B cell differentiation (2). WT hosts were co-transferred with $NP^{+}B220^{+}$ cells from QM $CCR7^{+/+}$ and QM $CCR7^{-/-}$ and immunised 24 h later with NP-CGG s.c. in the rear feet. The response was studied 8 days post-immunisation in the drLN. 3 µg of CCL19 were injected in the same foot 6 h prior to sacrifice. a) Flow cytometry data, as to the % of lymphocytes, for GC B cells. b) Flow cytometry data, as to the % of lymphocytes, for PCs. c) Flow cytometry data, as to the % of lymphocytes, for MBCs.
1 independent experiment. Each pair of symbols represents one mouse. Horizontal line represents the median.
Key: i.v: intravenously; s.c: subcutaneously; drLN: draining lymph node; GC: germinal centre; MBC: memory B cell; PC: plasma cell; PBS: phosphate buffer saline

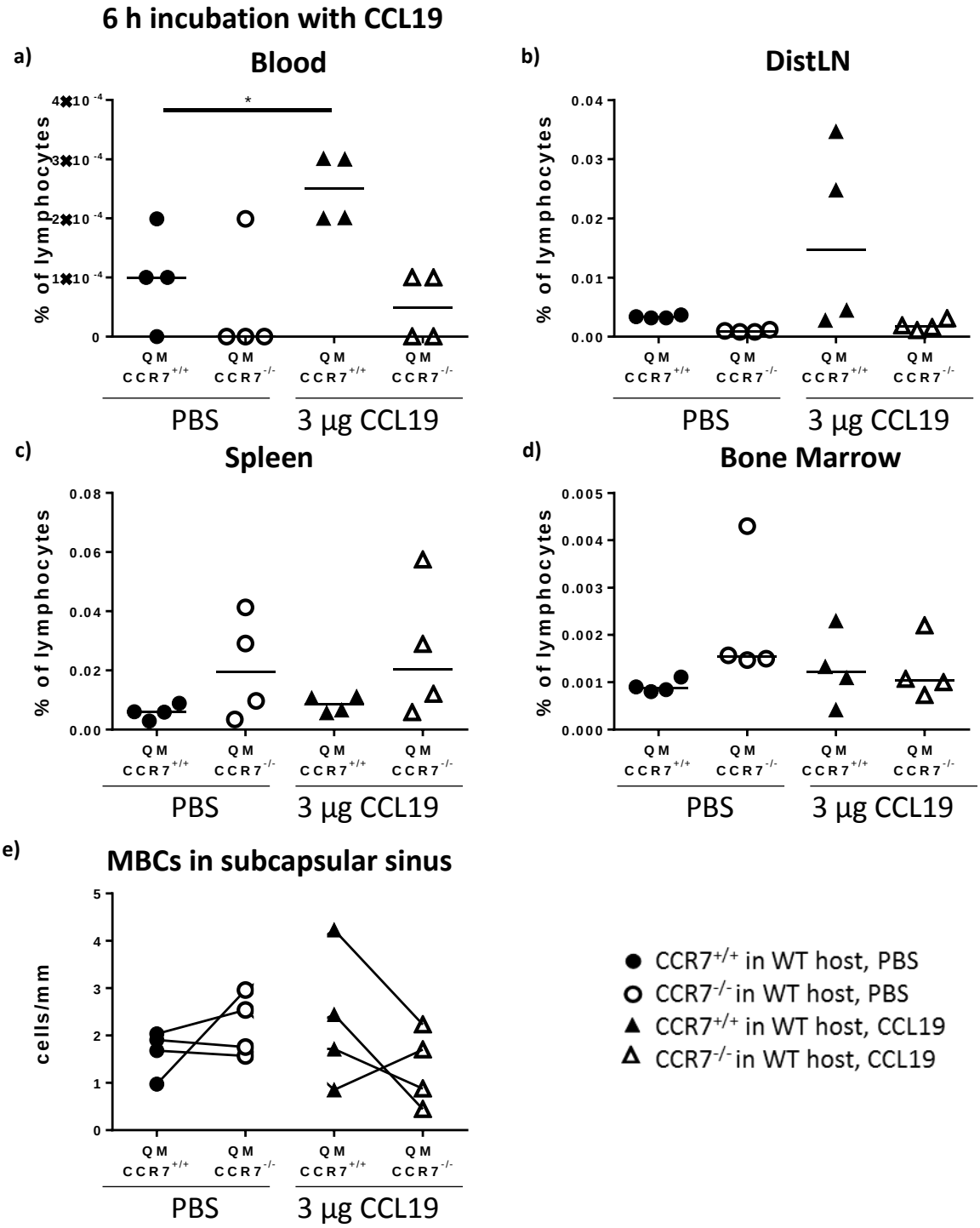

Figure 4.38: CCL19 injection in the drLN affects memory B cell migration to the distant sites. WT hosts were co-transferred with NP^+B220^+ cells from QM $CCR7^{+/+}$ and QM $CCR7^{-/-}$ and immunised 24 h later with NP-CGG s.c. in the rear feet. The response was studied 8 days post-immunisation in distant lymphoid organs. 3µg of CCL19 were injected in the same foot 6 h prior to sacrifice. a) Flow cytometry data, as to the % of lymphocytes, for MBCs in distLN. b) Flow cytometry data, as to the % of lymphocytes, for MBCs in blood. c) Flow cytometry data, as to the % of lymphocytes, for MBCs in the spleen. d) Flow cytometry data, as to the % of lymphocytes, for MBCs in the bone marrow. e) Quantification, as to cells per mm of SCS, of $TdTomato^+$ or $eYFP^+$ MBCs that have migrated to the subcapsular sinus. 1 independent experiment. Each pair of symbols represents one mouse. Horizontal line represents the median.

Key: i.v: intravenously; s.c: subcutaneously; distLN: distant lymph node; MBC: memory B cell; PBS: phosphate buffer saline

Non-parametric Mann-Whitney test *$p<0.05$

4.3 Discussion

4.3.1 Memory B cells appear in higher numbers in distant LNs of ACKR4$^{-/-}$ mice

The results presented in this chapter have shown that the distant LNs of ACKR4$^{-/-}$ mice have an elevated number of MBCs. While not obvious at the earliest stages of MBC generation (5 days post-immunisation), the effect is clear from day 8 post-immunisation. In order to track T-dependent MBC generation and migration, the Cγ1-Cre mTmG mouse model was used where B cells that have interacted with T cells express membrane-tethered GFP (Casola, Cattoretti et al. 2006). These include GC B cells, GC-derived PCs and MBCs, and also some of the PCs and MBCs that have been generated *via* GC-independent extrafollicular pathway (Y. Zhang, unpublished). Elevated numbers of MBCs in the distLNs may be caused by several reasons. Alternatives are: *(i)* increased differentiation into MBCs in ACKR4$^{-/-}$ mice leading to generally increased number of MBCs, *(ii)* increased exit from drLN leading to a larger number of circulating MBCs, *(iii)* increased entrance of recirculating MBCs into ACKR4$^{-/-}$ distLNs leading to elevated MBC numbers in distLNs, and *(iv)* increased retention of MBCs in ACKR4$^{-/-}$ distLN leading to higher frequencies of MBCs in ACKR4$^{-/-}$ distLNs.

Increased generation of MBCs in ACKR4$^{-/-}$ mice can be excluded due to the fact that drLN of ACKR4$^{-/-}$ mice have a similar number of MBCs to WT mice. An increase in exit from the drLN into the recirculating pool is compatible with the observation that in the drLN of ACKR4$^{-/-}$ mice, MBCs appear in the SCS at a higher frequency than in WT mice. Increased entrance into the distLN is also compatible with the data obtained in complete ACKR4$^{-/-}$ mice. Increased retention in ACKR4$^{-/-}$ distLN can be excluded because MBCs distributed similarly in the distLNs of WT and ACKR4$^{-/-}$ mice.

4.3.2 The expression of ACKR4 in the environment retains memory B cells in drLN

In order to determine if the increased appearance of MBCs in the distLNs of ACKR4$^{-/-}$ mice was caused by the expression of ACKR4 on the MBCs or on the environment, double transfers of NP-specific WT or ACKR4$^{-/-}$ B cells into WT or ACKR4$^{-/-}$ hosts were performed.

Strikingly, MBC numbers were greatly reduced in the draining LN when the host was ACKR4$^{-/-}$. In the blood of ACKR4$^{-/-}$ hosts, MBC numbers were increased. Reduced numbers in the drLN and increased numbers of MBCs in the blood indicate that when ACKR4 is absent from the environment of antigen-specific B cells, MBCs are able to leave the drLN in higher number, leading to elevated number in blood and in distLNs.

Interestingly, deficiency of ACKR4 in antigen-specific B cells leads to a specific reduction of CD80^{+} MBCs. CD80^{+}PDL2^{+} MBCs are the most mutated subset of MBCs while CD80^{-}PDL2^{+} have an intermediate mutation level (Zuccarino-Catania, Sadanand et al. 2014). Reduced numbers of CD80^{+} MBCs may indicate that ACKR4$^{-/-}$ MBCs do not accumulate as many mutations as WT MBCs due to GC intrinsic effects, but this possibility needs to be investigated further.

On the other hand, in distLN the differences in the number of MBCs were linked to ACKR4 expression on antigen specific B cells, and not on the environment. ACKR4$^{-/-}$ MBCs were present in the distLN in higher number than ACKR4$^{+/+}$ MBCs, independently of the genotype of the host. The different ACKR4$^{-/-}$ MBC subpopulations migrated in the same percentages to the distLN as the WT MBC subpopulations. However, the frequencies of the different MBC subpopulations in the distLN did not correlate to those observed in the drLN. The frequency of CD80^{+} MBCs was increased and the frequency of PDL2^{+} MBCs was decreased in the distLN compared to the drLN.

It has been shown that, during recall responses, the more mutated $CD80^{+}PDL2^{+}$ MBCs differentiate more efficiently into plasma cells while the less mutated $CD80^{-}PDL2^{+}$ MBCs are better in seeding GCs (Zuccarino-Catania, Sadanand et al. 2014). This dichotomy may explain why in our model there were more $PDL2^{+}$ MBCs and less $CD80^{+}$ in the drLN than in the distLN, as $CD80^{+}$ MBCs are more prone to differentiate into PCs, so they have to distribute all over the body to fight secondary infections, while the more prone to seed GCs would be mainly needed to reconstitute the MBC population. This dichotomy may also indicate that the different MBC subpopulations have different migratory properties. It has been shown that without re-exposure to antigen MBCs do not transform into other subsets (Tomayko, Steinel et al. 2010) so it is unlikely that in their migration towards distLN, MBCs shifted their CD80 and PDL2 expression. $CD73^{+}$ MBCs correspond to the more naïve-like MBCs as they have a low level of mutation and are usually not switched (Tomayko, Steinel et al. 2010). In our model, $CD73^{+}$ MBCs appeared in distLN in the same frequencies as in the drLN.

In tumours, ACKR4 expression has been described as a marker with negative correlation for metastasis. In a model of breast cancer, ACKR4 expression has been linked with reduced metastasis to lymph node and lack of expression correlates with lower survival rates. Moreover, ACKR4 sequestrates homeostatic chemokines inhibiting intra-tumour neovascularity (Feng, Ou et al. 2009) (Cheng and Hung 2009) (Chew, Tan et al. 2013). In colorectal cancer, ACKR4 expression by the tumour correlates with reduced metastases and increased patient survival (Zhu, Tang et al. 2014). In addition, from an analysis of tissues from cervical squamous cell cancer a negative correlation between ACKR4 expression with metastases to lymph nodes was also observed, as to whether individually expressed or co-expressed with DARC, another atypical chemokine receptor (Hou, Liang et al. 2013). There are also

contradictory findings about the tumorigenicity of ACKR4-expressing tumours. In an *in vitro* model of mammary carcinoma overexpressing ACKR4 there was an increase in spontaneous metastases caused by an enhanced epithelial-mesenchymal transition due to their increased invasive and migrating abilities and lower adhesion to the matrix or to other tumour cells (Harata-Lee, Turvey et al. 2014).

Similar to what has been described for the role of ACKR4 in metastasis, our results indicate a role for ACKR4 in the emigration of MBCs from their origin of differentiation, the drLN. When ACKR4 is absent in the host environment, there is more migration leading to more MBCs appearing in distLN, similar to the finding that the absence of ACKR4 expression in tumours leads to more metastases. The observation that there are more metastases in lymph nodes is also interesting, as MBCs according to the experiments described here migrate preferentially to distLN. ACKR4$^{-/-}$ MBCs are also more prone to enter distLN compared to WT MBCs.

4.3.3 The CCL19/CCL21 gradient retains memory B cells in the follicle of the drLN

Complete ACKR4 deficiency causes the disruption of CCL19/21 functional gradients, as ACKR4 expression in the SCS scavenges CCL19/21, which are produced in the T zone creating a gradient from the T zone to the SCS (Ulvmar, Werth et al. 2014). This disruption is able to influence DC migration on their entrance from the afferent lymphatics towards the T zone. The data presented here are consistent with a role for the gradient of CCL19/21 in LNs in the emigration of MBCs from the drLN. Absence of the CCL19/21 gradient between the SCS and the follicle in ACKR4$^{-/-}$ mice may be affecting MBC positioning within the drLN and migration to the SCS, resulting in

increased appearance of MBCs in the SCS and in the blood of ACKR4$^{-/-}$ mice and, therefore, increased appearance in distLN.

Murine ACKR4 binds with high affinity to the homeostatic chemokines CCL19, CCL21 and CCL25 (Townson and Nibbs 2002). CCL25 binds canonically to CCR9 (Zaballos, Gutierrez et al. 1999). As CCR9 is expressed at a low level in lymph nodes (Zaballos, Gutierrez et al. 1999) and is not expressed in B cells according to Immgen (Fig. 4.39), it was decided to focus on the behaviour of CCR7$^{-/-}$ MBCs to see if CCR7 deficiency in antigen-specific B cells results in effects comparable to ACKR4-deficiency. As mice completely deficient for CCR7 present profound effects on lymphoid architecture, such as lack of defined lymph nodes and mixed white pulps (Forster, Schubel et al. 1999), it is impossible to use these CCR7- deficient mice as recipients. Experiments using adoptive transfers of NP-specific WT and CCR7$^{-/-}$ B cells competing in WT hosts were performed. Eight days post-immunisation, there were fewer CCR7$^{-/-}$ antigen-specific B cells in the drLNs, but these cells differentiated to effector cells to the same extent, indicating that CCR7-deficiency is unlikely to affect B cell differentiation post-activation. Intriguingly, in distant lymphoid sites such as distLN, spleen and bone marrow, CCR7$^{-/-}$ MBCs appeared in higher numbers than WT MBCs, even though in the drLN CCR7$^{-/-}$ MBCs were less abundant. This indicates that CCR7$^{-/-}$ MBCs escape from the drLN far better than WT MBCs. The effect is similar to the effect of ACKR4-deficiency in the B cell environment. Non-responsiveness to CCL19/21 gradients (CCR7-deficient B cells) leads to similar results as absence of the gradient (ACKR4-deficiency in the environment). As the effect of CCR7-deficiency on the emigration on MBCs from the drLN has similar effects as ACKR4-deficiency in the B cell environment, it is unlikely that the axis ACKR4/CCR9-CCL25 has a major effect on MBC emigration from drLNs.

This is the first time, to our knowledge, that CCR7 has been shown to be involved in cell exit from LNs. In the lung, egress of $CD8^+$ T cells has been shown to occur in a CCR7-dependent manner. After antigen encounter in a model of influenza virus, CCR7 is downregulated and $CD8^+$ T cell egress is reduced (Jennrich, Lee et al. 2012). CCR7 has also been linked to the exit of lymphocytes from peripheral tissues and its deficiency leads to accumulation of B and T cells in the peritoneal cavities (Hopken, Winter et al. 2010). CCR7 deficiency also causes an accumulation of T cells in the asthmatic lungs and impaired exit of cells towards the afferent lymphatics (Bromley, Thomas et al. 2005) and a defect in $CD4^+$ T cell emigration from the skin (Debes, Arnold et al. 2005). Our results agree to some extent with these, as CCR7-deficient MBCs accumulate in distant sites, although their egress from these locations has not been studied. Five weeks post-primary response $CCR7^{-/-}$ MBCs and $ACKR4^{-/-}$ MBCs are contained in the distLNs in the same frequencies than WT MBCs, indicating that either secondary lymphoid organs have a limited capacity to sustain MBC survival or $CCR7^{-/-}$ MBCs and $ACKR4^{-/-}$ MBCs have intrinsic defects for long-term survival. The secondary response of $CCR7^{-/-}$ MBCs and $ACKR4^{-/-}$ MBCs is comparable to WT MBCs.

The results described here support the hypothesis of the existence of a MBC niche that is only able to maintain up to a certain number of MBCs. In a system where the total number of cells is limited, the ability of cells to survive will depend on their interactions with ligands and availability of other resources, which are limited (Agenes, Rosado et al. 2000). MBCs have been shown to reside long-term in the spleen as their frequency in humans is about 4 times higher than in peripheral blood several decades after vaccination (Mamani-Matsuda, Cosma et al. 2008). Some factors have been identified as essential for MBC long-term survival, such as Cadherin-17, an adhesion molecule

which is expressed in splenic BECs (blood endothelial cells) (Funakoshi, Shimizu et al. 2015). MBCs express TACI but not BCMA or BAFF-R while their survival and function are independent from BAFF and APRIL (Benson, Dillon et al. 2008). On the other hand, long-lived PCs downregulate TACI and BR3 expression and upregulate BCMA (Goenka, Scholz et al. 2014), which supports the idea that the MBC pool, the long-lived PC pool and the naïve pool are maintained in independent niches, as BCMA uses APRIL as its primary ligand (Goenka, Scholz et al. 2014). Syk and, therefore, BCR, have also been shown to be required for MBC survival (Ackermann, Nys et al. 2015). PLC-γ2 (phospholipase C γ2), another component of the BCR signalling, has also been reported to be essential for MBC generation and maintenance (Hikida, Casola et al. 2009). As antigen engagement to the BCR is not necessary for MBC survival (Maruyama, Lam et al. 2000), PLC-γ2 and Syk role should be activated through signalling to a different cytokine receptor that also signals through BCR-Syk survival path (Ackermann, Nys et al. 2015). $ACKR4^{-/-}$ and $CCR7^{-/-}$ MBCs survive at least 5 weeks post-immunisation, so signalling through the CCL19/21-CCR7 pathway does not seem essential for MBC survival. The chemokine receptor CXCR3 has been shown to be expressed differentially in IgG^{+} human MBCs, and this expression is maintained when these cells differentiate into PCs (Muehlinghaus, Cigliano et al. 2005), exemplifying the role of other chemokine receptors in the maintenance of immunological B cell memory.

Mice were injected with CCL19 to test the hypothesis that the presence of the CCL19/21 gradient, which is generated by the expression of ACKR4 on the SCS, organises MBC emigration from the drLN. The injection of large amounts of chemokine in the feet s.c. will drain into the SCS of the pLN and, therefore, increase the chemokine concentration in the whole LN, destroying any gradient. CCL19 and CCL21 have

similar affinity to CCR7 and there are signalling redundancies when these chemokines bind to CCR7, but they can also drive some biased signalling (Hauser and Legler 2016). Both CCL19 and CCL21 are able to polarise the actomyosin cytoskeleton, therefore, causing cells to migrate along chemokine gradients (Hauser and Legler 2016). CCL19 causes CCR7 phosphorylation and internalization, which will lead to receptor desensitization, while CCL21 does not (Forster, Davalos-Misslitz et al. 2008). CCL21 is immobilised to GAGs, *via* its C-terminus extension of 40 highly charged amino acids, induces integrin activation and cell adhesion (Hauser and Legler 2016). The main effect we were interested in is cellular migration; CCL19 because of its better solubility was chosen to disrupt gradients.

The presence of large amounts of CCL19 given 8 days post-immunisation did not have a noticeable effect on the differentiated B cell populations (GC B cells, PCs, MBCs) from WT and $CCR7^{-/-}$ NP-specific B cells in the drLN. Disruption of the gradient had a profound effect on the numbers of WT MBCs in the distLN and blood. WT MBCs appeared in higher numbers in the blood and in distLN, when the gradient was disrupted, while $CCR7^{-/-}$ MBC migration was unaltered. However, no differences were observed in the spleen and in the bone marrow. These results correlated and confirmed the hypothesis that the gradient of CCL19/21 influences MBC migration towards the SCS of the drLN and, therefore, the appearance of MBCs in other lymphoid sites.

Attempts to bypass the effect of the SCS gradient on the retention of MBCs in the drLNs by placing MBCs directly in the blood stream did not produce significant results. MBCs were sorted from drLN of WT mice transferred with WT and $ACKR4^{-/-}$ NP-specific B cells and injected i.v. into naïve WT recipients which were then immunised. However, 5 days post-immunisation, barely any transferred cell could be detected by

flow cytometry. There are several reasons for this outcome. It is possible that the number of MBC transferred into the new recipients (~4-8x10^3 $B220^+CD38^+CD138^-Fas^-$ MBCs) was not large enough to cause a strong secondary response. As to other examples of attempts to transfer MBCs, investigators have managed to transfer around 10 times more MBCs per mouse than in our experiments (Zuccarino-Catania, Sadanand et al. 2014). It is also possible that the sorting process affected the MBCs negatively, making them unable to respond adequately to a secondary stimulus. In addition, it is possible that there may be insufficient T cell help for MBC re-stimulation. The recipients were not antigen-primed and, therefore, there may not have sufficient numbers of pre-stimulated memory T cells available, essential for the induction of a secondary response to a TD antigen (Kurosaki, Kometani et al. 2015). Finally, loss of the expression of fluorescent proteins is an unlikely explanation, as when MBCs were re-stimulated in the same hosts they still expressed comparable levels of fluorescent protein than naïve B cells.

Future experiments should confirm MBC migration *in vitro.* The migration properties *in vitro* of WT and $CCR7^{-/-}$ MBCs generated *in vivo* in WT hosts will be studied. Cell suspension from drLNs can be stained for GC and PC markers in order to negatively distinguish MBCs and their migration pattern is being compared in the presence and absence of CCL19 in the medium to further confirm the model for MBC emigration from the drLN.

In summary, the experiments presented here have shown that MBC emigration from drLN is dependent on the ability to respond to CCL19/21 gradients. In standard conditions there is a CCL19/21 gradient from T zones to the SCS that is generated by ACKR4-expression in the SCS. This gradient retains MBCs closer to the GCs in the

follicles, while irresponsive MBCs, such as ACKR4$^{-/-}$ and CCR7$^{-/-}$ MBCs, are able to migrate to a higher extent to the SCS leading to higher number of MBCs at distant sites.

When the CCL19/21 gradient is absent, either due to ACKR4-deficiency in the environment or due to artificial CCL19-injection, the anchor that was retaining MBCs is lost and MBCs migrate to the SCS in a higher frequency, independently of their genotype.

It has also been demonstrated that the entrance of MBCs into distLN is also ACKR4-dependent. In this situation ACKR4-deficiency in B cells correlates with a higher entrance into distLN, probably due to an increased adhesion to CCL21-expressing HEV (Carlsen, Haraldsen et al. 2005).

CCR7-expression is essential for B and T lymphocyte entry into lymph nodes in homeostatic conditions (Okada, Ngo et al. 2002). Therefore, it is plausible that in order to leave drLNs as a MBC these cells need to loose responsiveness to CCR7-ligands. CCL21 has been shown to act as a homing chemokine for lymphocytes from tissues into draining lymphatics through its expression in lymphatic endothelium (Gunn, Tangemann et al. 1998). Moreover, cytokine-activated lymphatic endothelial cells (LECs) bind lymphocytes *in vitro* so they may be capable of influencing cell entry into the lymph (Young, Marston et al. 2000). Therefore, MBCs may be able to bind LECs on their way out of drLN, which is comparable to naïve lymphocytes binding LECs on their way in. Chemokinesis to certain locations in tissues is the result of a balance of attractive and retentive signals. The factors that attract MBCs to the SCS, counteracting the retentive signals from CCL19/21 gradients described here have still to be identified.

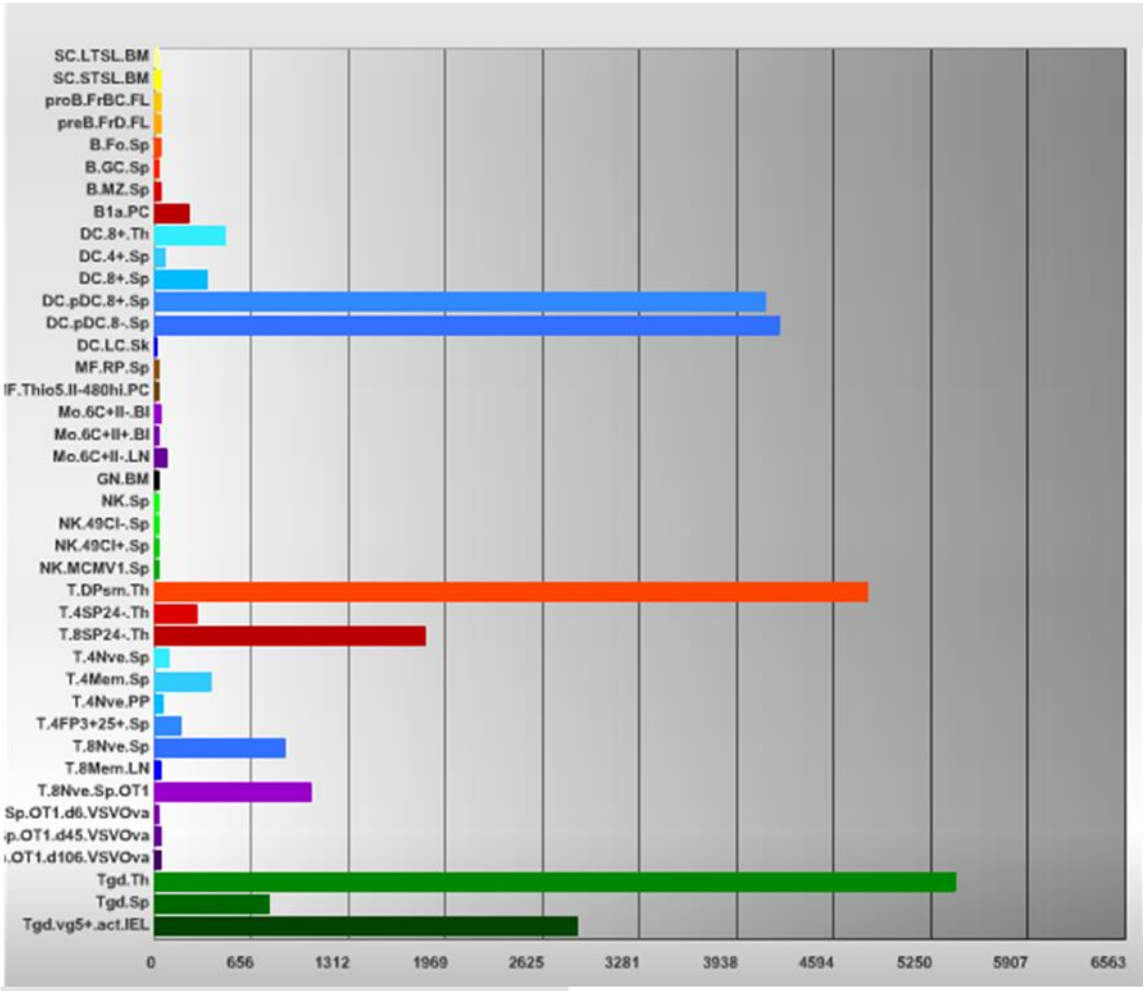

Probe Set:	10590620	Same Gene in Other Datagroup
Gene Symbol:	Ccr9	
Title:	chemokine (C-C motif) receptor 9	
Aliases:	CMKBR10 /// GPR-9-6	
Chromosome:	9	
Location:	123587557	
NCBI:	12769	
Unigene:	Mm.440604	
Ensembl:		
KEGG:	Cytokine-cytokine receptor interaction (mn	
GO:	signal transducer activity (4871) receptor activity (4872) G-protein coupled receptor activity (4930)	
SignatureDB: (human only)	SignatureDB (12769)	

Figure 4.39: **CCR9 is not expressed in B cells.** Ccr9 gene expression in the haematopoietic cells as revealed from the Immgen database.

Chapter 5. Conclusions

Activated B cells migrate to the T zone – B follicle interphase, where they receive positive signals from antigen-specific $CD4^+$ T cells (MacLennan, Toellner et al. 2003). These activated B cells will follow one of three pathways (Sagaert, Sprangers et al. 2007). Some will join the extrafollicular plasma cell foci, which will secret non-mutated low-affinity antibody. Others will become GC-independent MBCs. Some activated B cells will re-enter the follicle to form germinal centres and undergo extensive proliferation. The GC is the hallmark of a TD response and is divided into two distinct zones: the light zone and the dark zone. In the LZ, Tfh-dependent selection occurs and in the DZ, GC B cells proliferate and diversify their Ig variable genes, through somatic hypermutation (MacLennan 1994) (Victora and Nussenzweig 2012). GC B cells recirculate between the DZ and LZ in a chemokine-dependent manner. GC B cells in the DZ express more CXCR4 while LZ GC B cells tend to express more CXCR5 (Allen, Ansel et al. 2004). The responsiveness of GC B cells to chemokines and other factors needs to be tightly regulated in order to coordinate proliferation, selection and further differentiation into high-affinity plasma cells or memory B cells. The signals that regulate the differentiation of PCs and MBCs from GC B cells are far from being fully understood.

The data presented here identify a role for the chemokines CCL19/CCL21 in the later stages of the GC response. Deficiency of the CCL19/CCL21-scavenging receptor ACKR4, which is specifically expressed on GC B cells, causes dysregulation in the LZ/DZ distribution, with smaller DZ and larger LZ areas. This dysregulation is caused by increased activation of the downstream signalling components of CCR7, as there is more ligand binding to this receptor when ACKR4 is absent (Fig. 5.1). Downstream

signalling components include p-Akt and c-Myc. The role of c-Myc in the GC has been controversial, as GCs express a low level of c-Myc in comparison to the surrounding tissues (Klein, Tu et al. 2003). However, c-Myc is essential for the formation and maintenance of GCs. GCs have a cyclic dependence on c-Myc for proliferation; LZ GC B cells transiently express c-Myc when they interact with T cells and this expression triggers proliferation and re-entry into the DZ (Calado, Sasaki et al. 2012) (Dominguez-Sola, Victora et al. 2012). ACKR4-deficiency specifically in the GC B cells increases their expression of c-Myc and retains GC B cells in the LZ, preventing them from accessing the DZ. These data correlate with a low expression of ACKR4 in the c-Myc^{+} GC B cells, while the c-Myc^{-} population expresses higher levels of ACKR4. Upregulation of ACKR4 expression after c-Myc trigger would facilitate c-Myc downregulation and therefore, re-entry into the DZ area (see Figure 5.1).

On the other hand, ACKR4 is also expressed in a layer of stromal cells that surrounds the marginal zone in the spleen and in LECs that are present in the subcapsular sinus of the lymph node (Ulvmar, Werth et al. 2014). ACKR4 expression at this location creates a gradient of CCL19/21 from the T zone to the SCS and helps to maintain GC shape, as mice deficient for ACKR4 present GCs with fuzzy perimeters and infiltration of naïve B cells into the GC area. Uniform concentrations of CCL19/21 in the GC may attract naïve B cells into the GC area and therefore increase their infiltration (Fig. 5.1).

The skewed LZ/DZ distribution, with enlarged LZ in ACKR4$^{-/-}$ mice, appears to have consequences on the differentiation of GC B cells into MBCs as ACKR4-deficient antigen-specific B cells form reduced numbers of CD80^{+} MBCs within the drLN. CD80 is a marker for MBCs that have been longer in the GC and, therefore, accumulated more mutations (Zuccarino-Catania, Sadanand et al. 2014). Although overall MBC numbers

are not changed by ACKR4-deficiency, an inability of ACKR4-deficient GC B cells to cycle back into the DZ should prevent the accumulation of mutations and, therefore, the appearance of $CD80^{+}$ MBCs.

When GC B cells differentiate to MBCs and PCs, they need to change their responsiveness to chemokines in order to be able to leave the GC and home to their respective niches. While PC migration to the bone marrow is well-understood, MBC migration is less clear. MBCs have shown to appear in blood and remote LNs from one week post-immunisation (Blink, Light et al. 2005), although the route they follow within the LN and from the LN into the circulation is not clear. Data first produced by Y. Zhang (Fig. 4.13) have led to the proposal that MBCs migrate to the SCS from where they are able to distribute through lymph and blood to other lymphoid organs. The results presented in this thesis show that this migration towards the SCS is dependent on the ability to overcome the attraction of CCL19/CCL21 generated in the centre of the LN and are consistent with a role for this gradient in the exit of MBCs from the drLN. CCL19/CCL21 are produced in the T zone and ACKR4 expression in the SCS causes a gradient of CCL19/CCL21 from the T zone to the SCS that can influence cell migration (Ulvmar, Werth et al. 2014). ACKR4-deficient mice have elevated numbers of MBCs in the distant LNs. This is due to two steps during the migration of MBCs: the exit of MBC from the drLN is governed by the expression of ACKR4 in the LECs of the SCS. $ACKR4^{-/-}$ mice have less MBCs in the drLN and more in the blood, indicating that MBCs are able to escape the LN easier when ACKR4 is absent from the SCS. Accordingly, MBCs reach the SCS of reactive LN more easily. The second step is the entrance of MBCs into the distLN, which is governed by the expression of ACKR4 on the MBCs themselves. $ACKR4^{-/-}$ MBCs enter into the distLN better than WT MBCs independent on the expression of ACKR4 in the LN environment. Further evidence for

the role of CCL19/CCL21 in the migration of MBCs from reactive LNs is provided by $CCR7^{-/-}$ MBCs. $CCR7^{-/-}$ MBCs also appear in higher frequencies than WT MBCs in the distant lymphoid sites, including bone marrow and spleen. Artificial disruption of the CCL19/CCL21 by injection of an antagonistic amount of CCL19 in the drLN affects the migration of WT MBCs whilst migration of $CCR7^{-/-}$ MBCs is unaffected.

Chemokinesis in a specific direction is the response to a balance of signals coming from different directions. While it has been shown here that responsiveness to CCL19/CCL21 retains MBCs closer to the GCs in the drLN, there must be other signals that actively attract migrating MBCs to the drLN periphery and the SCS. These chemotactic factors able to override the retention signals from CCL19/CCL21 gradients on MBCs are not understood as yet and need to be defined in future studies.

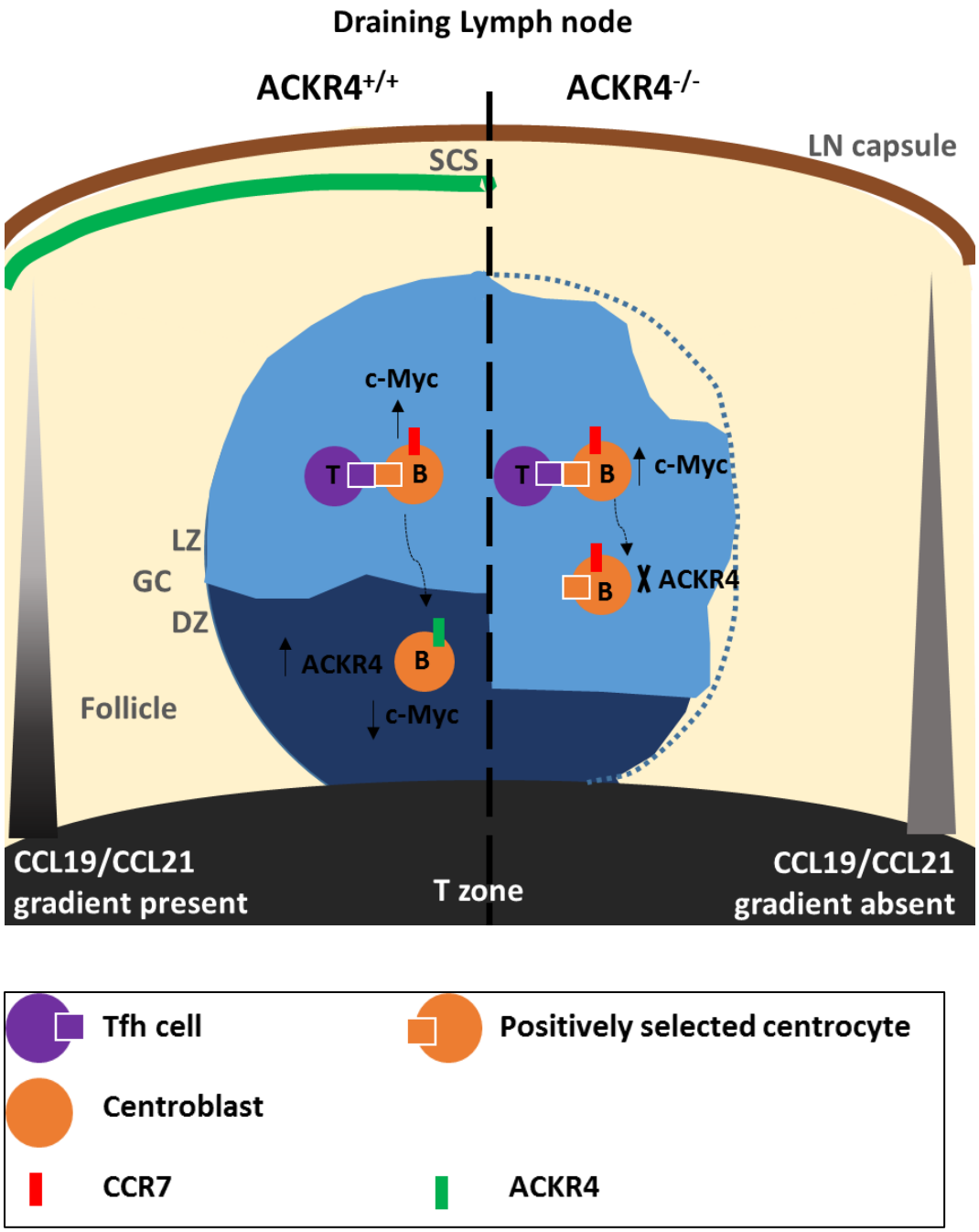

Figure 5.1: Graphic representation for the effects of ACKR4 on the GC response. The left side of the figure shows a GC in a drLN of an immunised ACKR4$^{+/+}$ mice. The right side shows an ACKR4$^{-/-}$ GC. After Tfh selection, centrocytes upregulate c-Myc, which triggers proliferation and migration back to the DZ. In WT mice, ACKR4 is upregulated in centroblasts and facilitates c-Myc downregulation by reducing the signalling through CCR7-p-Akt-c-Myc signalling pathway. In ACKR4$^{-/-}$ mice, the deficiency of ACKR4 prevents the downregulation of c-Myc and therefore, centrocyte recirculation into the DZ, leading to enlarged LZ areas and reduced DZ areas. ACKR4$^{-/-}$ GCs show fuzzy perimeters due to infiltration of IgD^{+} B cells in to the GC area. This effect is dependent on the expression of ACKR4 by the GC environment.
Key: LN: lymph node; SCS: subcapsular sinus; GC: germinal centre; LZ: light zone; DZ: dark zone.

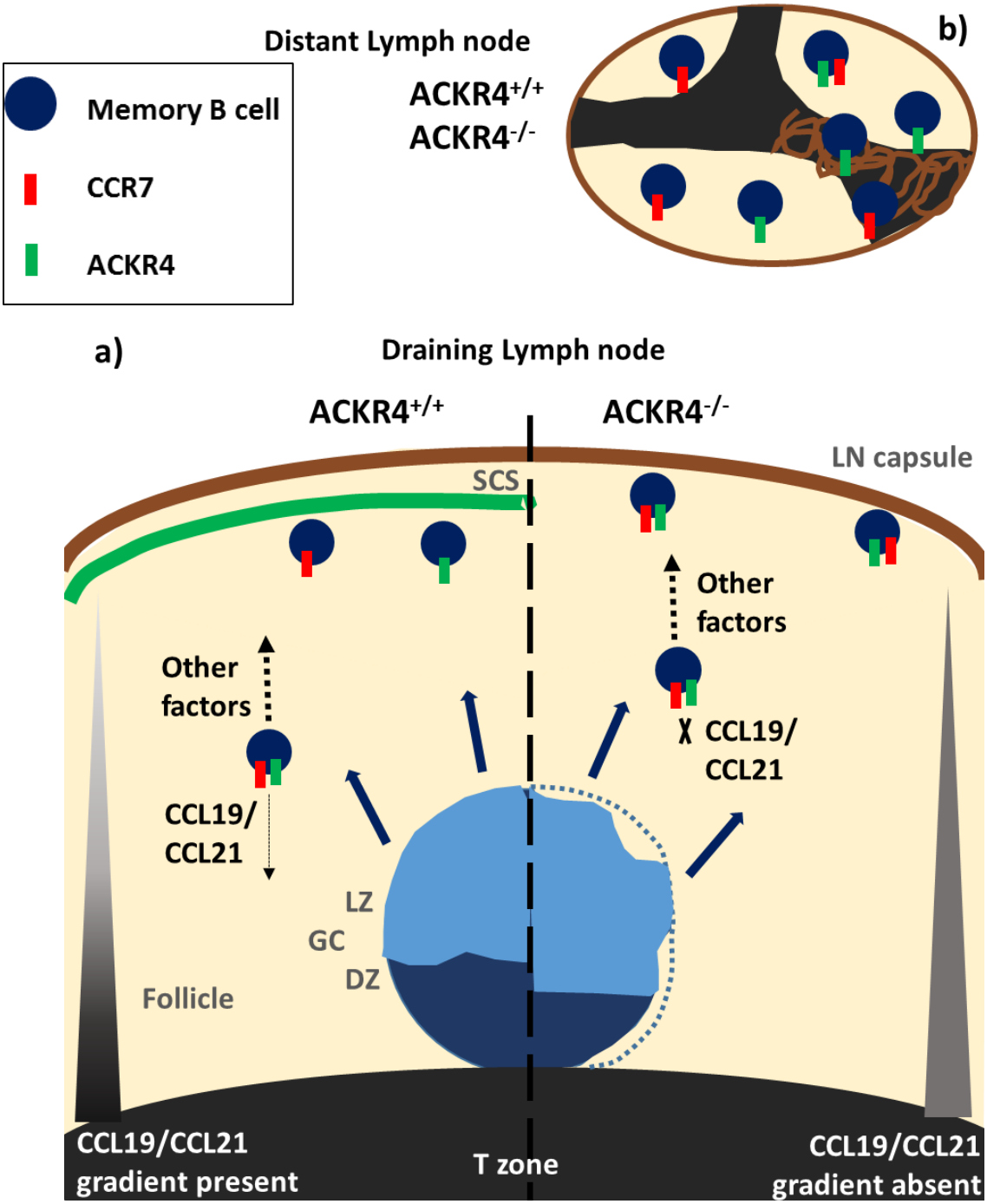

Figure 5.2: Graphic representation for the effects of ACKR4 on MBC migration. The main part of the figure (a) represents the drLN, the upper (b) part shows a distLN. a) The left side of the figure represents a drLN from an immunised ACKR4$^{+/+}$ mice, the right side shows an ACKR4$^{-/-}$ drLN. Blue arrows indicate that MBCs leave the GC from the LZ and migrate towards the SCS. ACKR4 expression in the SCS creates a gradient of CCL19/21. In WT mice, MBCs are retained in the follicles due to the CCL19/21 gradient. ACKR4$^{-/-}$ and CCR7$^{-/-}$ MBCs are not retained because CCR7 as well as ACKR4 facilitate chemoattraction by CCL19/21. Also in complete ACKR4$^{-/-}$ mice, MBCs are not retained in follicles due to the absence of the CCL19/21 gradient letting MBCs reach the SCS more easily. b) Migration into distLN is dependent on the expression of ACKR4 by the MBCs. ACKR4$^{-/-}$ and CCR7$^{-/-}$ MBCs appear in higher numbers than WT MBCs, and this is independent of ACKR4 expression in the environment. MBCs distribute preferentially into the follicles and lymphatic vessels. Key: LN: lymph node; SCS: subcapsular sinus; GC: germinal centre; LZ: light zone; DZ: dark zone.

Chapter 6. References

Ackermann, J. A., J. Nys, E. Schweighoffer, S. McCleary, N. Smithers and V. L. Tybulewicz (2015). "Syk tyrosine kinase is critical for B cell antibody responses and memory B cell survival." J Immunol **194**(10): 4650-4656.

Achtman, A. H., U. E. Hopken, C. Bernert and M. Lipp (2009). "CCR7-deficient mice develop atypically persistent germinal centers in response to thymus-independent type 2 antigens." J Leukoc Biol **85**(3): 409-417.

Agenes, F., M. M. Rosado and A. A. Freitas (2000). "Peripheral B cell survival." Cell Mol Life Sci **57**(8-9): 1220-1228.

Aiba, Y., K. Kometani, M. Hamadate, S. Moriyama, A. Sakaue-Sawano, M. Tomura, H. Luche, H. J. Fehling, R. Casellas, O. Kanagawa, A. Miyawaki and T. Kurosaki (2010). "Preferential localization of IgG memory B cells adjacent to contracted germinal centers." Proc Natl Acad Sci U S A **107**(27): 12192-12197.

Allen, C. D., K. M. Ansel, C. Low, R. Lesley, H. Tamamura, N. Fujii and J. G. Cyster (2004). "Germinal center dark and light zone organization is mediated by CXCR4 and CXCR5." Nat Immunol **5**(9): 943-952.

Allen, C. D., T. Okada and J. G. Cyster (2007). "Germinal-center organization and cellular dynamics." Immunity **27**(2): 190-202.

Allen, C. D., T. Okada, H. L. Tang and J. G. Cyster (2007). "Imaging of germinal center selection events during affinity maturation." Science **315**(5811): 528-531.

Anderson, S. M., M. M. Tomayko, A. Ahuja, A. M. Haberman and M. J. Shlomchik (2007). "New markers for murine memory B cells that define mutated and unmutated subsets." J Exp Med **204**(9): 2103-2114.

Ansel, K. M., V. N. Ngo, P. L. Hyman, S. A. Luther, R. Forster, J. D. Sedgwick, J. L. Browning, M. Lipp and J. G. Cyster (2000). "A chemokine-driven positive feedback loop organizes lymphoid follicles." Nature **406**(6793): 309-314.

Bachelerie, F., G. J. Graham, M. Locati, A. Mantovani, P. M. Murphy, R. Nibbs, A. Rot, S. Sozzani and M. Thelen (2014). "New nomenclature for atypical chemokine receptors." Nat Immunol **15**(3): 207-208.

Baggiolini, M., B. Dewald and B. Moser (1997). "Human chemokines: an update." Annu Rev Immunol **15**: 675-705.

Bajoghli, B. (2013). "Evolution and function of chemokine receptors in the immune system of lower vertebrates." Eur J Immunol **43**(7): 1686-1692.

Bannard, O., R. M. Horton, C. D. Allen, J. An, T. Nagasawa and J. G. Cyster (2013). "Germinal center centroblasts transition to a centrocyte phenotype according to a timed program and depend on the dark zone for effective selection." Immunity **39**(5): 912-924.

Basso, K. and R. Dalla-Favera (2010). "BCL6: master regulator of the germinal center reaction and key oncogene in B cell lymphomagenesis." Adv Immunol **105**: 193-210.

Basso, K., M. Saito, P. Sumazin, A. A. Margolin, K. Wang, W. K. Lim, Y. Kitagawa, C. Schneider, M. J. Alvarez, A. Califano and R. Dalla-Favera (2010). "Integrated biochemical and computational approach identifies BCL6 direct target genes controlling multiple pathways in normal germinal center B cells." Blood **115**(5): 975-984.

Behjati, M., I. Torktaz, M. Mohammadpour, G. Ahmadian and A. J. Easton (2012). "Comparative modeling of CCRL1, a key protein in masked immune diseases and virtual screening for finding inhibitor of this protein." Bioinformation **8**(7): 336-340.

Bekeredjian-Ding, I. and G. Jego (2009). "Toll-like receptors--sentries in the B-cell response." Immunology **128**(3): 311-323.

Ben-Baruch, A. (2008). "Organ selectivity in metastasis: regulation by chemokines and their receptors." Clin Exp Metastasis **25**(4): 345-356.

Benson, M. J., S. R. Dillon, E. Castigli, R. S. Geha, S. Xu, K. P. Lam and R. J. Noelle (2008). "Cutting edge: the dependence of plasma cells and independence of memory B cells on BAFF and APRIL." J Immunol **180**(6): 3655-3659.

Berkowska, M. A., G. J. Driessen, V. Bikos, C. Grosserichter-Wagener, K. Stamatopoulos, A. Cerutti, B. He, K. Biermann, J. F. Lange, M. van der Burg, J. J. van Dongen and M. C. van Zelm (2011). "Human memory B cells originate from three distinct germinal center-dependent and -independent maturation pathways." Blood **118**(8): 2150-2158.

Birkenbach, M., K. Josefsen, R. Yalamanchili, G. Lenoir and E. Kieff (1993). "Epstein-Barr virus-induced genes: first lymphocyte-specific G protein-coupled peptide receptors." J Virol **67**(4): 2209-2220.

Bleul, C. C., J. L. Schultze and T. A. Springer (1998). "B lymphocyte chemotaxis regulated in association with microanatomic localization, differentiation state, and B cell receptor engagement." J Exp Med **187**(5): 753-762.

Blink, E. J., A. Light, A. Kallies, S. L. Nutt, P. D. Hodgkin and D. M. Tarlinton (2005). "Early appearance of germinal center-derived memory B cells and plasma cells in blood after primary immunization." J Exp Med **201**(4): 545-554.

Bromley, S. K., S. Y. Thomas and A. D. Luster (2005). "Chemokine receptor CCR7 guides T cell exit from peripheral tissues and entry into afferent lymphatics." Nat Immunol **6**(9): 895-901.

Bryce, S. A., R. A. Wilson, E. M. Tiplady, D. L. Asquith, S. K. Bromley, A. D. Luster, G. J. Graham and R. J. Nibbs (2016). "ACKR4 on Stromal Cells Scavenges CCL19 To Enable CCR7-Dependent Trafficking of APCs from Inflamed Skin to Lymph Nodes." J Immunol **196**(8): 3341-3353.

Bunting, M. D., I. Comerford, N. Seach, M. V. Hammett, D. L. Asquith, H. Korner, R. L. Boyd, R. J. Nibbs and S. R. McColl (2013). "CCX-CKR deficiency alters thymic stroma impairing thymocyte development and promoting autoimmunity." Blood **121**(1): 118-128.

Butcher, E. C., M. Williams, K. Youngman, L. Rott and M. Briskin (1999). "Lymphocyte trafficking and regional immunity." Adv Immunol **72**: 209-253.

Calado, D. P., Y. Sasaki, S. A. Godinho, A. Pellerin, K. Kochert, B. P. Sleckman, I. M. de Alboran, M. Janz, S. Rodig and K. Rajewsky (2012). "The cell-cycle regulator c-Myc is essential for the formation and maintenance of germinal centers." Nat Immunol **13**(11): 1092-1100.

Cancro, M. P. and J. F. Kearney (2004). "B cell positive selection: road map to the primary repertoire?" J Immunol **173**(1): 15-19.

Cannons, J. L., H. Qi, K. T. Lu, M. Dutta, J. Gomez-Rodriguez, J. Cheng, E. K. Wakeland, R. N. Germain and P. L. Schwartzberg (2010). "Optimal germinal center responses require a multistage T cell:B cell adhesion process involving integrins, SLAM-associated protein, and CD84." Immunity **32**(2): 253-265.

Carlsen, H. S., G. Haraldsen, P. Brandtzaeg and E. S. Baekkevold (2005). "Disparate lymphoid chemokine expression in mice and men: no evidence of CCL21 synthesis by human high endothelial venules." Blood **106**(2): 444-446.

Casamayor-Palleja, M., J. Feuillard, J. Ball, M. Drew and I. C. MacLennan (1996). "Centrocytes rapidly adopt a memory B cell phenotype on co-culture with autologous germinal centre T cell-enriched preparations." Int Immunol **8**(5): 737-744.

Cascalho, M., A. Ma, S. Lee, L. Masat and M. Wabl (1996). "A quasi-monoclonal mouse." Science **272**(5268): 1649-1652.

Casola, S., G. Cattoretti, N. Uyttersprot, S. B. Koralov, J. Seagal, Z. Hao, A. Waisman, A. Egert, D. Ghitza and K. Rajewsky (2006). "Tracking germinal center B cells expressing germ-line immunoglobulin gamma1 transcripts by conditional gene targeting." Proc Natl Acad Sci U S A **103**(19): 7396-7401.

Cesta, M. F. (2006). "Normal structure, function, and histology of the spleen." Toxicol Pathol **34**(5): 455-465.

Coffey, F., B. Alabyev and T. Manser (2009). "Initial clonal expansion of germinal center B cells takes place at the perimeter of follicles." Immunity **30**(4): 599-609.

Comerford, I., Y. Harata-Lee, M. D. Bunting, C. Gregor, E. E. Kara and S. R. McColl (2013). "A myriad of functions and complex regulation of the CCR7/CCL19/CCL21 chemokine axis in the adaptive immune system." Cytokine Growth Factor Rev **24**(3): 269-283.

Comerford, I., S. Milasta, V. Morrow, G. Milligan and R. Nibbs (2006). "The chemokine receptor CCX-CKR mediates effective scavenging of CCL19 in vitro." Eur J Immunol **36**(7): 1904-1916.

Comerford, I., R. J. Nibbs, W. Litchfield, M. Bunting, Y. Harata-Lee, S. Haylock-Jacobs, S. Forrow, H. Korner and S. R. McColl (2010). "The atypical chemokine receptor CCX-CKR scavenges homeostatic chemokines in circulation and tissues and suppresses Th17 responses." Blood **116**(20): 4130-4140.

Crotty, S. (2011). "Follicular helper CD4 T cells (TFH)." Annu Rev Immunol **29**: 621-663.

Cunningham, A. F., K. Serre, E. Mohr, M. Khan and K. M. Toellner (2004). "Loss of CD154 impairs the Th2 extrafollicular plasma cell response but not early T cell proliferation and interleukin-4 induction." Immunology **113**(2): 187-193.

Chan, C., M. Billard, S. A. Ramirez, H. Schmidl, E. Monson and T. B. Kepler (2013). "A model for migratory B cell oscillations from receptor down-regulation induced by external chemokine fields." Bull Math Biol **75**(1): 185-205.

Chan, T. D., D. Gatto, K. Wood, T. Camidge, A. Basten and R. Brink (2009). "Antigen affinity controls rapid T-dependent antibody production by driving the expansion rather than the differentiation or extrafollicular migration of early plasmablasts." J Immunol **183**(5): 3139-3149.

Cheng, X. and M. C. Hung (2009). "Regulation of breast cancer metastasis by atypical chemokine receptors." Clin Cancer Res **15**(9): 2951-2953.

Chew, A. L., W. Y. Tan and B. Y. Khoo (2013). "Potential combinatorial effects of recombinant atypical chemokine receptors in breast cancer cell invasion: A research perspective." Biomed Rep **1**(2): 185-192.

Christopherson, K. W., 2nd, J. J. Campbell and R. A. Hromas (2001). "Transgenic overexpression of the CC chemokine CCL21 disrupts T-cell migration." Blood **98**(13): 3562-3568.

Davalos-Misslitz, A. C., J. Rieckenberg, S. Willenzon, T. Worbs, E. Kremmer, G. Bernhardt and R. Forster (2007). "Generalized multi-organ autoimmunity in CCR7-deficient mice." Eur J Immunol **37**(3): 613-622.

de Alboran, I. M., E. Baena and A. C. Martinez (2004). "c-Myc-deficient B lymphocytes are resistant to spontaneous and induced cell death." Cell Death Differ **11**(1): 61-68.

de Alboran, I. M., R. C. O'Hagan, F. Gartner, B. Malynn, L. Davidson, R. Rickert, K. Rajewsky, R. A. DePinho and F. W. Alt (2001). "Analysis of C-MYC function in normal cells via conditional gene-targeted mutation." Immunity **14**(1): 45-55.

de Vinuesa, C. G., M. C. Cook, J. Ball, M. Drew, Y. Sunners, M. Cascalho, M. Wabl, G. G. Klaus and I. C. MacLennan (2000). "Germinal centers without T cells." J Exp Med **191**(3): 485-494.

Debes, G. F., C. N. Arnold, A. J. Young, S. Krautwald, M. Lipp, J. B. Hay and E. C. Butcher (2005). "Chemokine receptor CCR7 required for T lymphocyte exit from peripheral tissues." Nat Immunol **6**(9): 889-894.

Debes, G. F., U. E. Hopken and A. Hamann (2002). "In vivo differentiated cytokine-producing CD4(+) T cells express functional CCR7." J Immunol **168**(11): 5441-5447.

Dogan, I., B. Bertocci, V. Vilmont, F. Delbos, J. Megret, S. Storck, C. A. Reynaud and J. C. Weill (2009). "Multiple layers of B cell memory with different effector functions." Nat Immunol **10**(12): 1292-1299.

Dominguez-Sola, D., G. D. Victora, C. Y. Ying, R. T. Phan, M. Saito, M. C. Nussenzweig and R. Dalla-Favera (2012). "The proto-oncogene MYC is required for selection in the germinal center and cyclic reentry." Nat Immunol **13**(11): 1083-1091.

Dona, E., J. D. Barry, G. Valentin, C. Quirin, A. Khmelinskii, A. Kunze, S. Durdu, L. R. Newton, A. Fernandez-Minan, W. Huber, M. Knop and D. Gilmour (2013). "Directional tissue migration through a self-generated chemokine gradient." Nature **503**(7475): 285-289.

Erickson, L. D., B. G. Durell, L. A. Vogel, B. P. O'Connor, M. Cascalho, T. Yasui, H. Kikutani and R. J. Noelle (2002). "Short-circuiting long-lived humoral immunity by the heightened engagement of CD40." J Clin Invest **109**(5): 613-620.

Fagarasan, S., N. Watanabe and T. Honjo (2000). "Generation, expansion, migration and activation of mouse B1 cells." Immunol Rev **176**: 205-215.

Feldmann, M. and A. Easten (1971). "The relationship between antigenic structure and the requirement for thymus-derived cells in the immune response." J Exp Med **134**(1): 103-119.

Feng, L. Y., Z. L. Ou, F. Y. Wu, Z. Z. Shen and Z. M. Shao (2009). "Involvement of a novel chemokine decoy receptor CCX-CKR in breast cancer growth, metastasis and patient survival." Clin Cancer Res **15**(9): 2962-2970.

Fernandez, D., M. Ortiz, L. Rodriguez, A. Garcia, D. Martinez and I. Moreno de Alboran (2013). "The proto-oncogene c-myc regulates antibody secretion and Ig class switch recombination." J Immunol **190**(12): 6135-6144.

Figge, M. T., A. Garin, M. Gunzer, M. Kosco-Vilbois, K. M. Toellner and M. Meyer-Hermann (2008). "Deriving a germinal center lymphocyte migration model from two-photon data." J Exp Med **205**(13): 3019-3029.

Fischer, S. F., P. Bouillet, K. O'Donnell, A. Light, D. M. Tarlinton and A. Strasser (2007). "Proapoptotic BH3-only protein Bim is essential for developmentally programmed death of germinal center-derived memory B cells and antibody-forming cells." Blood **110**(12): 3978-3984.

Forster, R., A. C. Davalos-Misslitz and A. Rot (2008). "CCR7 and its ligands: balancing immunity and tolerance." Nat Rev Immunol **8**(5): 362-371.

Forster, R., A. E. Mattis, E. Kremmer, E. Wolf, G. Brem and M. Lipp (1996). "A putative chemokine receptor, BLR1, directs B cell migration to defined lymphoid organs and specific anatomic compartments of the spleen." Cell **87**(6): 1037-1047.

Forster, R., A. Schubel, D. Breitfeld, E. Kremmer, I. Renner-Muller, E. Wolf and M. Lipp (1999). "CCR7 coordinates the primary immune response by establishing functional microenvironments in secondary lymphoid organs." Cell **99**(1): 23-33.

Funakoshi, S., T. Shimizu, O. Numata, M. Ato, F. Melchers and K. Ohnishi (2015). "BILL-cadherin/cadherin-17 contributes to the survival of memory B cells." PLoS One **10**(1): e0117566.

Garcia de Vinuesa, C., P. O'Leary, D. M. Sze, K. M. Toellner and I. C. MacLennan (1999). "T-independent type 2 antigens induce B cell proliferation in multiple splenic sites, but exponential growth is confined to extrafollicular foci." Eur J Immunol **29**(4): 1314-1323.

Garside, P., E. Ingulli, R. R. Merica, J. G. Johnson, R. J. Noelle and M. K. Jenkins (1998). "Visualization of specific B and T lymphocyte interactions in the lymph node." Science **281**(5373): 96-99.

Gatto, D., K. Wood and R. Brink (2011). "EBI2 operates independently of but in cooperation with CXCR5 and CCR7 to direct B cell migration and organization in follicles and the germinal center." J Immunol **187**(9): 4621-4628.

Gershon, R. K. and K. Kondo (1970). "Cell interactions in the induction of tolerance: the role of thymic lymphocytes." Immunology **18**(5): 723-737.

Girard, J. P., C. Moussion and R. Forster (2012). "HEVs, lymphatics and homeostatic immune cell trafficking in lymph nodes." Nat Rev Immunol **12**(11): 762-773.

Gitlin, A. D., L. von Boehmer, A. Gazumyan, Z. Shulman, T. Y. Oliveira and M. C. Nussenzweig (2016). "Independent Roles of Switching and Hypermutation in the Development and Persistence of B Lymphocyte Memory." Immunity **44**(4): 769-781.

Goenka, R., J. L. Scholz, M. S. Naradikian and M. P. Cancro (2014). "Memory B cells form in aged mice despite impaired affinity maturation and germinal center kinetics." Exp Gerontol **54**: 109-115.

Good-Jacobson, K. L., E. Song, S. Anderson, A. H. Sharpe and M. J. Shlomchik (2012). "CD80 expression on B cells regulates murine T follicular helper development, germinal center B cell survival, and plasma cell generation." J Immunol **188**(9): 4217-4225.

Good-Jacobson, K. L. and D. M. Tarlinton (2012). "Multiple routes to B-cell memory." Int Immunol **24**(7): 403-408.

Gosling, J., D. J. Dairaghi, Y. Wang, M. Hanley, D. Talbot, Z. Miao and T. J. Schall (2000). "Cutting edge: identification of a novel chemokine receptor that binds dendritic cell- and T cell-active chemokines including ELC, SLC, and TECK." J Immunol **164**(6): 2851-2856.

Green, J. A. and J. G. Cyster (2012). "S1PR2 links germinal center confinement and growth regulation." Immunol Rev **247**(1): 36-51.

Green, J. A., K. Suzuki, B. Cho, L. D. Willison, D. Palmer, C. D. Allen, T. H. Schmidt, Y. Xu, R. L. Proia, S. R. Coughlin and J. G. Cyster (2011). "The sphingosine 1-phosphate receptor S1P(2) maintains the homeostasis of germinal center B cells and promotes niche confinement." Nat Immunol **12**(7): 672-680.

Gunn, M. D., S. Kyuwa, C. Tam, T. Kakiuchi, A. Matsuzawa, L. T. Williams and H. Nakano (1999). "Mice lacking expression of secondary lymphoid organ chemokine have defects in lymphocyte homing and dendritic cell localization." J Exp Med **189**(3): 451-460.

Gunn, M. D., K. Tangemann, C. Tam, J. G. Cyster, S. D. Rosen and L. T. Williams (1998). "A chemokine expressed in lymphoid high endothelial venules promotes the adhesion and chemotaxis of naive T lymphocytes." Proc Natl Acad Sci U S A **95**(1): 258-263.

Habib, T., H. Park, M. Tsang, I. M. de Alboran, A. Nicks, L. Wilson, P. S. Knoepfler, S. Andrews, D. J. Rawlings, R. N. Eisenman and B. M. Iritani (2007). "Myc stimulates B lymphocyte differentiation and amplifies calcium signaling." J Cell Biol **179**(4): 717-731.

Harata-Lee, Y., M. E. Turvey, J. A. Brazzatti, C. E. Gregor, M. P. Brown, M. J. Smyth, I. Comerford and S. R. McColl (2014). "The atypical chemokine receptor CCX-CKR regulates metastasis of mammary carcinoma via an effect on EMT." Immunol Cell Biol **92**(10): 815-824.

Hardtke, S., L. Ohl and R. Forster (2005). "Balanced expression of CXCR5 and CCR7 on follicular T helper cells determines their transient positioning to lymph node follicles and is essential for efficient B-cell help." Blood **106**(6): 1924-1931.

Hardy, R. R. and K. Hayakawa (2001). "B cell development pathways." Annu Rev Immunol **19**: 595-621.

Hargreaves, D. C., P. L. Hyman, T. T. Lu, V. N. Ngo, A. Bidgol, G. Suzuki, Y. R. Zou, D. R. Littman and J. G. Cyster (2001). "A coordinated change in chemokine responsiveness guides plasma cell movements." J Exp Med **194**(1): 45-56.

Harrell, M. I., B. M. Iritani and A. Ruddell (2008). "Lymph node mapping in the mouse." J Immunol Methods **332**(1-2): 170-174.

Hauser, A. E., T. Junt, T. R. Mempel, M. W. Sneddon, S. H. Kleinstein, S. E. Henrickson, U. H. von Andrian, M. J. Shlomchik and A. M. Haberman (2007). "Definition of germinal-center B cell migration in vivo reveals predominant intrazonal circulation patterns." Immunity **26**(5): 655-667.

Hauser, A. E., M. J. Shlomchik and A. M. Haberman (2007). "In vivo imaging studies shed light on germinal-centre development." Nat Rev Immunol **7**(7): 499-504.

Hauser, M. A., I. Kindinger, J. M. Laufer, A. K. Spate, D. Bucher, S. L. Vanes, W. A. Krueger, V. Wittmann and D. F. Legler (2016). "Distinct CCR7 glycosylation pattern shapes receptor signaling and endocytosis to modulate chemotactic responses." J Leukoc Biol **99**(6): 993-1007.

Hauser, M. A. and D. F. Legler (2016). "Common and biased signaling pathways of the chemokine receptor CCR7 elicited by its ligands CCL19 and CCL21 in leukocytes." J Leukoc Biol **99**(6): 869-882.

Heinzel, K., C. Benz and C. C. Bleul (2007). "A silent chemokine receptor regulates steady-state leukocyte homing in vivo." Proc Natl Acad Sci U S A **104**(20): 8421-8426.

Heng, T. S. and M. W. Painter (2008). "The Immunological Genome Project: networks of gene expression in immune cells." Nat Immunol **9**(10): 1091-1094.

Hikida, M., S. Casola, N. Takahashi, T. Kaji, T. Takemori, K. Rajewsky and T. Kurosaki (2009). "PLC-gamma2 is essential for formation and maintenance of memory B cells." J Exp Med **206**(3): 681-689.

Hintzen, G., L. Ohl, M. L. del Rio, J. I. Rodriguez-Barbosa, O. Pabst, J. R. Kocks, J. Krege, S. Hardtke and R. Forster (2006). "Induction of tolerance to innocuous inhaled antigen relies on a CCR7-dependent dendritic cell-mediated antigen transport to the bronchial lymph node." J Immunol **177**(10): 7346-7354.

Hopken, U. E., S. Winter, A. H. Achtman, K. Kruger and M. Lipp (2010). "CCR7 regulates lymphocyte egress and recirculation through body cavities." J Leukoc Biol **87**(4): 671-682.

Hou, T., D. Liang, L. Xu, X. Huang, Y. Huang and Y. Zhang (2013). "Atypical chemokine receptors predict lymph node metastasis and prognosis in patients with cervical squamous cell cancer." Gynecol Oncol **130**(1): 181-187.

Hsu, M. C., K. M. Toellner, C. G. Vinuesa and I. C. Maclennan (2006). "B cell clones that sustain long-term plasmablast growth in T-independent extrafollicular antibody responses." Proc Natl Acad Sci U S A **103**(15): 5905-5910.

Humpert, M. L., D. Pinto, D. Jarrossay and M. Thelen (2014). "CXCR7 influences the migration of B cells during maturation." Eur J Immunol **44**(3): 694-705.

Inamine, A., Y. Takahashi, N. Baba, K. Miyake, T. Tokuhisa, T. Takemori and R. Abe (2005). "Two waves of memory B-cell generation in the primary immune response." Int Immunol **17**(5): 581-589.

Jacob, J., J. Przylepa, C. Miller and G. Kelsoe (1993). "In situ studies of the primary immune response to (4-hydroxy-3-nitrophenyl)acetyl. III. The kinetics of V region mutation and selection in germinal center B cells." J Exp Med **178**(4): 1293-1307.

Jacobi, A. M., K. Reiter, M. Mackay, C. Aranow, F. Hiepe, A. Radbruch, A. Hansen, G. R. Burmester, B. Diamond, P. E. Lipsky and T. Dorner (2008). "Activated memory B cell subsets correlate with disease activity in systemic lupus erythematosus: delineation by expression of CD27, IgD, and CD95." Arthritis Rheum **58**(6): 1762-1773.

Jennrich, S., M. H. Lee, R. C. Lynn, K. Dewberry and G. F. Debes (2012). "Tissue exit: a novel control point in the accumulation of antigen-specific CD8 T cells in the influenza a virus-infected lung." J Virol **86**(7): 3436-3445.

Jones, D. D., J. R. Wilmore and D. Allman (2015). "Cellular Dynamics of Memory B Cell Populations: IgM+ and IgG+ Memory B Cells Persist Indefinitely as Quiescent Cells." J Immunol **195**(10): 4753-4759.

Junt, T., K. Fink, R. Forster, B. Senn, M. Lipp, M. Muramatsu, R. M. Zinkernagel, B. Ludewig and H. Hengartner (2005). "CXCR5-dependent seeding of follicular niches by B and Th cells augments antiviral B cell responses." J Immunol **175**(11): 7109-7116.

Kaji, T., A. Ishige, M. Hikida, J. Taka, A. Hijikata, M. Kubo, T. Nagashima, Y. Takahashi, T. Kurosaki, M. Okada, O. Ohara, K. Rajewsky and T. Takemori (2012). "Distinct cellular pathways select germline-encoded and somatically mutated antibodies into immunological memory." J Exp Med **209**(11): 2079-2097.

Khoja, H., G. Wang, C. T. Ng, J. Tucker, T. Brown and V. Shyamala (2000). "Cloning of CCRL1, an orphan seven transmembrane receptor related to chemokine receptors, expressed abundantly in the heart." Gene **246**(1-2): 229-238.

Klein, U., S. Casola, G. Cattoretti, Q. Shen, M. Lia, T. Mo, T. Ludwig, K. Rajewsky and R. Dalla-Favera (2006). "Transcription factor IRF4 controls plasma cell differentiation and class-switch recombination." Nat Immunol **7**(7): 773-782.

Klein, U. and R. Dalla-Favera (2008). "Germinal centres: role in B-cell physiology and malignancy." Nat Rev Immunol **8**(1): 22-33.

Klein, U., Y. Tu, G. A. Stolovitzky, J. L. Keller, J. Haddad, Jr., V. Miljkovic, G. Cattoretti, A. Califano and R. Dalla-Favera (2003). "Transcriptional analysis of the B cell germinal center reaction." Proc Natl Acad Sci U S A **100**(5): 2639-2644.

Kohout, T. A., S. L. Nicholas, S. J. Perry, G. Reinhart, S. Junger and R. S. Struthers (2004). "Differential desensitization, receptor phosphorylation, beta-arrestin recruitment, and ERK1/2 activation by the two endogenous ligands for the CC chemokine receptor 7." J Biol Chem **279**(22): 23214-23222.

Kraal, G., I. L. Weissman and E. C. Butcher (1988). "Memory B cells express a phenotype consistent with migratory competence after secondary but not short-term primary immunization." Cell Immunol **115**(1): 78-87.

Krishnamurty, A. T., C. D. Thouvenel, S. Portugal, G. J. Keitany, K. S. Kim, A. Holder, P. D. Crompton, D. J. Rawlings and M. Pepper (2016). "Somatically Hypermutated Plasmodium-Specific IgM(+) Memory B Cells Are Rapid, Plastic, Early Responders upon Malaria Rechallenge." Immunity **45**(2): 402-414.

Kuraoka, M., A. G. Schmidt, T. Nojima, F. Feng, A. Watanabe, D. Kitamura, S. C. Harrison, T. B. Kepler and G. Kelsoe (2016). "Complex Antigens Drive Permissive Clonal Selection in Germinal Centers." Immunity **44**(3): 542-552.

Kurosaki, T., K. Kometani and W. Ise (2015). "Memory B cells." Nat Rev Immunol **15**(3): 149-159.

Le Gros, G., N. Schultze, S. Walti, K. Einsle, F. Finkelman, M. H. Kosco-Vilbois and C. Heusser (1996). "The development of IgE+ memory B cells following primary IgE immune responses." Eur J Immunol **26**(12): 3042-3047.

Lentz, V. M. and T. Manser (2001). "Cutting edge: germinal centers can be induced in the absence of T cells." J Immunol **167**(1): 15-20.

Lewis, G. K., R. Ranken, D. E. Nitecki and J. W. Goodman (1976). "Murine B-cell subpopulations responsive to T-dependent and T-independent antigens." J Exp Med **144**(2): 382-397.

Li, Y. F., X. Ou, S. Xu, Z. B. Jin, N. Iwai and K. P. Lam (2016). "Loss of miR-182 affects B-cell extrafollicular antibody response." Immunology **148**(2): 140-149.

Liu, Y. J., F. Malisan, O. de Bouteiller, C. Guret, S. Lebecque, J. Banchereau, F. C. Mills, E. E. Max and H. Martinez-Valdez (1996). "Within germinal centers, isotype switching of immunoglobulin genes occurs after the onset of somatic mutation." Immunity **4**(3): 241-250.

Livak, K. J. and T. D. Schmittgen (2001). "Analysis of relative gene expression data using real-time quantitative PCR and the 2(-Delta Delta C(T)) Method." Methods **25**(4): 402-408.

Loder, F., B. Mutschler, R. J. Ray, C. J. Paige, P. Sideras, R. Torres, M. C. Lamers and R. Carsetti (1999). "B cell development in the spleen takes place in discrete steps and is determined by the quality of B cell receptor-derived signals." J Exp Med **190**(1): 75-89.

Lucas, B., A. J. White, M. H. Ulvmar, R. J. Nibbs, K. M. Sitnik, W. W. Agace, W. E. Jenkinson, G. Anderson and A. Rot (2015). "CCRL1/ACKR4 is expressed in key thymic microenvironments but is dispensable for T lymphopoiesis at steady state in adult mice." Eur J Immunol **45**(2): 574-583.

Luther, S. A., H. L. Tang, P. L. Hyman, A. G. Farr and J. G. Cyster (2000). "Coexpression of the chemokines ELC and SLC by T zone stromal cells and deletion of the ELC gene in the plt/plt mouse." Proc Natl Acad Sci U S A **97**(23): 12694-12699.

MacLennan, I. C. (1994). "Germinal centers." Annu Rev Immunol **12**: 117-139.

MacLennan, I. C., Y. L. Liu and N. R. Ling (1988). "B cell proliferation in follicles, germinal centre formation and the site of neoplastic transformation in Burkitt's lymphoma." Curr Top Microbiol Immunol **141**: 138-148.

MacLennan, I. C., K. M. Toellner, A. F. Cunningham, K. Serre, D. M. Sze, E. Zuniga, M. C. Cook and C. G. Vinuesa (2003). "Extrafollicular antibody responses." Immunol Rev **194**: 8-18.

Malhotra, D., A. L. Fletcher and S. J. Turley (2013). "Stromal and hematopoietic cells in secondary lymphoid organs: partners in immunity." Immunol Rev **251**(1): 160-176.

Mamani-Matsuda, M., A. Cosma, S. Weller, A. Faili, C. Staib, L. Garcon, O. Hermine, O. Beyne-Rauzy, C. Fieschi, J. O. Pers, N. Arakelyan, B. Varet, A. Sauvanet, A. Berger, F. Paye, J. M. Andrieu, M. Michel, B. Godeau, P. Buffet, C. A. Reynaud and J. C. Weill (2008). "The human spleen is a major reservoir for long-lived vaccinia virus-specific memory B cells." Blood **111**(9): 4653-4659.

Mantovani, A., R. Bonecchi and M. Locati (2006). "Tuning inflammation and immunity by chemokine sequestration: decoys and more." Nat Rev Immunol **6**(12): 907-918.

Marshall, J. L., Y. Zhang, L. Pallan, M. C. Hsu, M. Khan, A. F. Cunningham, I. C. MacLennan and K. M. Toellner (2011). "Early B blasts acquire a capacity for Ig class switch recombination that is lost as they become plasmablasts." Eur J Immunol **41**(12): 3506-3512.

Martin, F., A. M. Oliver and J. F. Kearney (2001). "Marginal zone and B1 B cells unite in the early response against T-independent blood-borne particulate antigens." Immunity **14**(5): 617-629.

Martinez, M. R., A. Corradin, U. Klein, M. J. Alvarez, G. M. Toffolo, B. di Camillo, A. Califano and G. A. Stolovitzky (2012). "Quantitative modeling of the terminal differentiation of B cells and mechanisms of lymphomagenesis." Proc Natl Acad Sci U S A **109**(7): 2672-2677.

Maruyama, M., K. P. Lam and K. Rajewsky (2000). "Memory B-cell persistence is independent of persisting immunizing antigen." Nature **407**(6804): 636-642.

Mburu, Y. K., J. Wang, M. A. Wood, W. H. Walker and R. L. Ferris (2006). "CCR7 mediates inflammation-associated tumor progression." Immunol Res **36**(1-3): 61-72.

McHeyzer-Williams, L. J. and M. G. McHeyzer-Williams (2005). "Antigen-specific memory B cell development." Annu Rev Immunol **23**: 487-513.

McHeyzer-Williams, L. J., P. J. Milpied, S. L. Okitsu and M. G. McHeyzer-Williams (2015). "Class-switched memory B cells remodel BCRs within secondary germinal centers." Nat Immunol **16**(3): 296-305.

McHeyzer-Williams, M., S. Okitsu, N. Wang and L. McHeyzer-Williams (2012). "Molecular programming of B cell memory." Nat Rev Immunol **12**(1): 24-34.

Mebius, R. E. and G. Kraal (2005). "Structure and function of the spleen." Nat Rev Immunol **5**(8): 606-616.

Meurens, F., M. Berri, G. Auray, S. Melo, B. Levast, I. Virlogeux-Payant, C. Chevaleyre, V. Gerdts and H. Salmon (2009). "Early immune response following Salmonella enterica subspecies enterica serovar Typhimurium infection in porcine jejunal gut loops." Vet Res **40**(1): 5.

Meyer-Hermann, M., M. T. Figge and K. M. Toellner (2009). "Germinal centres seen through the mathematical eye: B-cell models on the catwalk." Trends Immunol **30**(4): 157-164.

Meyer-Hermann, M., E. Mohr, N. Pelletier, Y. Zhang, G. D. Victora and K. M. Toellner (2012). "A theory of germinal center B cell selection, division, and exit." Cell Rep **2**(1): 162-174.

Moratz, C., J. R. Hayman, H. Gu and J. H. Kehrl (2004). "Abnormal B-cell responses to chemokines, disturbed plasma cell localization, and distorted immune tissue architecture in Rgs1-/- mice." Mol Cell Biol **24**(13): 5767-5775.

Mosier, D. E., J. J. Mond and E. A. Goldings (1977). "The ontogeny of thymic independent antibody responses in vitro in normal mice and mice with an X-linked B cell defect." J Immunol **119**(6): 1874-1878.

Mountz, J. D., J. H. Wang, S. Xie and H. C. Hsu (2011). "Cytokine regulation of B-cell migratory behavior favors formation of germinal centers in autoimmune disease." Discov Med **11**(56): 76-85.

Muehlinghaus, G., L. Cigliano, S. Huehn, A. Peddinghaus, H. Leyendeckers, A. E. Hauser, F. Hiepe, A. Radbruch, S. Arce and R. A. Manz (2005). "Regulation of CXCR3 and CXCR4 expression during terminal differentiation of memory B cells into plasma cells." Blood **105**(10): 3965-3971.

Mueller, S. N., T. Gebhardt, F. R. Carbone and W. R. Heath (2013). "Memory T cell subsets, migration patterns, and tissue residence." Annu Rev Immunol **31**: 137-161.

Muramatsu, M., K. Kinoshita, S. Fagarasan, S. Yamada, Y. Shinkai and T. Honjo (2000). "Class switch recombination and hypermutation require activation-induced cytidine deaminase (AID), a potential RNA editing enzyme." Cell **102**(5): 553-563.

Muzumdar, M. D., B. Tasic, K. Miyamichi, L. Li and L. Luo (2007). "A global double-fluorescent Cre reporter mouse." Genesis **45**(9): 593-605.

Nagira, M., T. Imai, K. Hieshima, J. Kusuda, M. Ridanpaa, S. Takagi, M. Nishimura, M. Kakizaki, H. Nomiyama and O. Yoshie (1997). "Molecular cloning of a novel human CC chemokine secondary lymphoid-tissue chemokine that is a potent chemoattractant for lymphocytes and mapped to chromosome 9p13." J Biol Chem **272**(31): 19518-19524.

Nakano, H. and M. D. Gunn (2001). "Gene duplications at the chemokine locus on mouse chromosome 4: multiple strain-specific haplotypes and the deletion of secondary

lymphoid-organ chemokine and EBI-1 ligand chemokine genes in the plt mutation." J Immunol **166**(1): 361-369.

Nibbs, R. J. and G. J. Graham (2013). "Immune regulation by atypical chemokine receptors." Nat Rev Immunol **13**(11): 815-829.

Nie, Z., G. Hu, G. Wei, K. Cui, A. Yamane, W. Resch, R. Wang, D. R. Green, L. Tessarollo, R. Casellas, K. Zhao and D. Levens (2012). "c-Myc is a universal amplifier of expressed genes in lymphocytes and embryonic stem cells." Cell **151**(1): 68-79.

Nieuwenhuis, P. and D. Opstelten (1984). "Functional anatomy of germinal centers." Am J Anat **170**(3): 421-435.

Noelle, R. J. and E. C. Snow (1990). "Cognate interactions between helper T cells and B cells." Immunol Today **11**(10): 361-368.

Nutt, S. L., B. Heavey, A. G. Rolink and M. Busslinger (1999). "Commitment to the B-lymphoid lineage depends on the transcription factor Pax5." Nature **401**(6753): 556-562.

O'Connor, M. J., A. E. Hauser, A. M. Haberman and S. H. Kleinstein (2011). "Activated germinal centre B cells undergo directed migration." Int J Data Min Bioinform **5**(3): 321-331.

Ohl, L., G. Henning, S. Krautwald, M. Lipp, S. Hardtke, G. Bernhardt, O. Pabst and R. Forster (2003). "Cooperating mechanisms of CXCR5 and CCR7 in development and organization of secondary lymphoid organs." J Exp Med **197**(9): 1199-1204.

Okada, T. and J. G. Cyster (2006). "B cell migration and interactions in the early phase of antibody responses." Curr Opin Immunol **18**(3): 278-285.

Okada, T., M. J. Miller, I. Parker, M. F. Krummel, M. Neighbors, S. B. Hartley, A. O'Garra, M. D. Cahalan and J. G. Cyster (2005). "Antigen-engaged B cells undergo chemotaxis toward the T zone and form motile conjugates with helper T cells." PLoS Biol **3**(6): e150.

Okada, T., V. N. Ngo, E. H. Ekland, R. Forster, M. Lipp, D. R. Littman and J. G. Cyster (2002). "Chemokine requirements for B cell entry to lymph nodes and Peyer's patches." J Exp Med **196**(1): 65-75.

Okumura, K., C. M. Metzler, T. T. Tsu, L. A. Herzenberg and L. A. Herzenberg (1976). "Two stages of B-cell memory development with different T-cell requirements." J Exp Med **144**(2): 345-357.

Ott, T. R., F. M. Lio, D. Olshefski, X. J. Liu, N. Ling and R. S. Struthers (2006). "The N-terminal domain of CCL21 reconstitutes high affinity binding, G protein activation, and chemotactic activity, to the C-terminal domain of CCL19." Biochem Biophys Res Commun **348**(3): 1089-1093.

Papavasiliou, F. N. and D. G. Schatz (2000). "Cell-cycle-regulated DNA double-stranded breaks in somatic hypermutation of immunoglobulin genes." Nature **408**(6809): 216-221.

Pape, K. A., J. J. Taylor, R. W. Maul, P. J. Gearhart and M. K. Jenkins (2011). "Different B cell populations mediate early and late memory during an endogenous immune response." Science **331**(6021): 1203-1207.

Park, C., I. Y. Hwang, R. K. Sinha, O. Kamenyeva, M. D. Davis and J. H. Kehrl (2012). "Lymph node B lymphocyte trafficking is constrained by anatomy and highly dependent upon chemoattractant desensitization." Blood **119**(4): 978-989.

Paus, D., T. G. Phan, T. D. Chan, S. Gardam, A. Basten and R. Brink (2006). "Antigen recognition strength regulates the choice between extrafollicular plasma cell and germinal center B cell differentiation." J Exp Med **203**(4): 1081-1091.

Peperzak, V., I. B. Vikstrom and D. M. Tarlinton (2012). "Through a glass less darkly: apoptosis and the germinal center response to antigen." Immunol Rev **247**(1): 93-106.

Pereira, J. P., L. M. Kelly, Y. Xu and J. G. Cyster (2009). "EBI2 mediates B cell segregation between the outer and centre follicle." Nature **460**(7259): 1122-1126.

Perez-Roger, I., S. H. Kim, B. Griffiths, A. Sewing and H. Land (1999). "Cyclins D1 and D2 mediate myc-induced proliferation via sequestration of p27(Kip1) and p21(Cip1)." Embo j **18**(19): 5310-5320.

Pfeifer, M., M. Grau, D. Lenze, S. S. Wenzel, A. Wolf, B. Wollert-Wulf, K. Dietze, H. Nogai, B. Storek, H. Madle, B. Dorken, M. Janz, S. Dirnhofer, P. Lenz, M. Hummel, A. Tzankov and G. Lenz (2013). "PTEN loss defines a PI3K/AKT pathway-dependent germinal center subtype of diffuse large B-cell lymphoma." Proc Natl Acad Sci U S A **110**(30): 12420-12425.

Phan, R. T., M. Saito, K. Basso, H. Niu and R. Dalla-Favera (2005). "BCL6 interacts with the transcription factor Miz-1 to suppress the cyclin-dependent kinase inhibitor p21 and cell cycle arrest in germinal center B cells." Nat Immunol **6**(10): 1054-1060.

Phan, T. G., D. Paus, T. D. Chan, M. L. Turner, S. L. Nutt, A. Basten and R. Brink (2006). "High affinity germinal center B cells are actively selected into the plasma cell compartment." J Exp Med **203**(11): 2419-2424.

Pillai, S. and A. Cariappa (2009). "The bone marrow perisinusoidal niche for recirculating B cells and the positive selection of bone marrow-derived B lymphocytes." Immunol Cell Biol **87**(1): 16-19.

Pillai, S. and A. Cariappa (2009). "The follicular versus marginal zone B lymphocyte cell fate decision." Nat Rev Immunol **9**(11): 767-777.

Rahman, Z. S. (2011). "Impaired clearance of apoptotic cells in germinal centers: implications for loss of B cell tolerance and induction of autoimmunity." Immunol Res **51**(2-3): 125-133.

Rasmussen, T., M. Lodahl, S. Hancke and H. E. Johnsen (2004). "In multiple myeloma clonotypic CD38- /CD19+ / CD27+ memory B cells recirculate through bone marrow, peripheral blood and lymph nodes." Leuk Lymphoma **45**(7): 1413-1417.

Reichert, R. A., W. M. Gallatin, I. L. Weissman and E. C. Butcher (1983). "Germinal center B cells lack homing receptors necessary for normal lymphocyte recirculation." J Exp Med **157**(3): 813-827.

Reif, K., E. H. Ekland, L. Ohl, H. Nakano, M. Lipp, R. Forster and J. G. Cyster (2002). "Balanced responsiveness to chemoattractants from adjacent zones determines B-cell position." Nature **416**(6876): 94-99.

Revy, P., T. Muto, Y. Levy, F. Geissmann, A. Plebani, O. Sanal, N. Catalan, M. Forveille, R. Dufourcq-Labelouse, A. Gennery, I. Tezcan, F. Ersoy, H. Kayserili, A. G. Ugazio, N. Brousse, M. Muramatsu, L. D. Notarangelo, K. Kinoshita, T. Honjo, A. Fischer and A. Durandy (2000). "Activation-induced cytidine deaminase (AID) deficiency causes the autosomal recessive form of the Hyper-IgM syndrome (HIGM2)." Cell **102**(5): 565-575.

Ribeiro, A. R., C. Meireles, P. M. Rodrigues and N. L. Alves (2014). "Intermediate expression of CCRL1 reveals novel subpopulations of medullary thymic epithelial cells that emerge in the postnatal thymus." Eur J Immunol **44**(10): 2918-2924.

Rolink, A. G., C. Schaniel, J. Andersson and F. Melchers (2001). "Selection events operating at various stages in B cell development." Curr Opin Immunol **13**(2): 202-207.

Rollins, B. J. (1997). "Chemokines." Blood **90**(3): 909-928.

Rot, A. and U. H. von Andrian (2004). "Chemokines in innate and adaptive host defense: basic chemokinese grammar for immune cells." Annu Rev Immunol **22**: 891-928.

Roth, K., L. Oehme, S. Zehentmeier, Y. Zhang, R. Niesner and A. E. Hauser (2014). "Tracking plasma cell differentiation and survival." Cytometry A **85**(1): 15-24.

Roy, M. P., C. H. Kim and E. C. Butcher (2002). "Cytokine control of memory B cell homing machinery." J Immunol **169**(4): 1676-1682.

Sabo, A., T. R. Kress, M. Pelizzola, S. de Pretis, M. M. Gorski, A. Tesi, M. J. Morelli, P. Bora, M. Doni, A. Verrecchia, C. Tonelli, G. Faga, V. Bianchi, A. Ronchi, D. Low, H. Muller, E. Guccione, S. Campaner and B. Amati (2014). "Selective transcriptional regulation by Myc in cellular growth control and lymphomagenesis." Nature **511**(7510): 488-492.

Sagaert, X., B. Sprangers and C. De Wolf-Peeters (2007). "The dynamics of the B follicle: understanding the normal counterpart of B-cell-derived malignancies." Leukemia **21**(7): 1378-1386.

Sage, P. T., C. L. Tan, G. J. Freeman, M. Haigis and A. H. Sharpe (2015). "Defective TFH Cell Function and Increased TFR Cells Contribute to Defective Antibody Production in Aging." Cell Rep **12**(2): 163-171.

Sallusto, F., A. Langenkamp, J. Geginat and A. Lanzavecchia (2000). "Functional subsets of memory T cells identified by CCR7 expression." Curr Top Microbiol Immunol **251**: 167-171.

Sander, S. and K. Rajewsky (2012). "Burkitt lymphomagenesis linked to MYC plus PI3K in germinal center B cells." Oncotarget **3**(10): 1066-1067.

Scandella, E., K. Fink, T. Junt, B. M. Senn, E. Lattmann, R. Forster, H. Hengartner and B. Ludewig (2007). "Dendritic cell-independent B cell activation during acute virus infection: a role for early CCR7-driven B-T helper cell collaboration." J Immunol **178**(3): 1468-1476.

Schaeuble, K., M. A. Hauser, A. V. Rippl, R. Bruderer, C. Otero, M. Groettrup and D. F. Legler (2012). "Ubiquitylation of the chemokine receptor CCR7 enables efficient receptor recycling and cell migration." J Cell Sci **125**(Pt 19): 4463-4474.

Schittek, B. and K. Rajewsky (1990). "Maintenance of B-cell memory by long-lived cells generated from proliferating precursors." Nature **346**(6286): 749-751.

Schneider, P., H. Takatsuka, A. Wilson, F. Mackay, A. Tardivel, S. Lens, T. G. Cachero, D. Finke, F. Beermann and J. Tschopp (2001). "Maturation of marginal zone and follicular B cells requires B cell activating factor of the tumor necrosis factor family and is independent of B cell maturation antigen." J Exp Med **194**(11): 1691-1697.

Schumann, K., T. Lammermann, M. Bruckner, D. F. Legler, J. Polleux, J. P. Spatz, G. Schuler, R. Forster, M. B. Lutz, L. Sorokin and M. Sixt (2010). "Immobilized chemokine fields and soluble chemokine gradients cooperatively shape migration patterns of dendritic cells." Immunity **32**(5): 703-713.

Schweickart, V. L., A. Epp, C. J. Raport and P. W. Gray (2001). "CCR11 is a functional receptor for the monocyte chemoaattractant protein family of chemokines." J Biol Chem **276**(1): 856.

Schweickart, V. L., C. J. Raport, R. Godiska, M. G. Byers, R. L. Eddy, Jr., T. B. Shows and P. W. Gray (1994). "Cloning of human and mouse EBI1, a lymphoid-specific G-protein-coupled receptor encoded on human chromosome 17q12-q21.2." Genomics **23**(3): 643-650.

Schwickert, T. A., R. L. Lindquist, G. Shakhar, G. Livshits, D. Skokos, M. H. Kosco-Vilbois, M. L. Dustin and M. C. Nussenzweig (2007). "In vivo imaging of germinal centres reveals a dynamic open structure." Nature **446**(7131): 83-87.

Schwickert, T. A., G. D. Victora, D. R. Fooksman, A. O. Kamphorst, M. R. Mugnier, A. D. Gitlin, M. L. Dustin and M. C. Nussenzweig (2011). "A dynamic T cell-limited checkpoint regulates affinity-dependent B cell entry into the germinal center." J Exp Med **208**(6): 1243-1252.

Seifert, M., M. Przekopowitz, S. Taudien, A. Lollies, V. Ronge, B. Drees, M. Lindemann, U. Hillen, H. Engler, B. B. Singer and R. Kuppers (2015). "Functional capacities of human IgM memory B cells in early inflammatory responses and secondary germinal center reactions." Proc Natl Acad Sci U S A **112**(6): E546-555.

Shaffer, A. L., 3rd, R. M. Young and L. M. Staudt (2012). "Pathogenesis of human B cell lymphomas." Annu Rev Immunol **30**: 565-610.

Shaffer, A. L., K. I. Lin, T. C. Kuo, X. Yu, E. M. Hurt, A. Rosenwald, J. M. Giltnane, L. Yang, H. Zhao, K. Calame and L. M. Staudt (2002). "Blimp-1 orchestrates plasma cell differentiation by extinguishing the mature B cell gene expression program." Immunity **17**(1): 51-62.

Shaffer, A. L., X. Yu, Y. He, J. Boldrick, E. P. Chan and L. M. Staudt (2000). "BCL-6 represses genes that function in lymphocyte differentiation, inflammation, and cell cycle control." Immunity **13**(2): 199-212.

Shi, G. X., K. Harrison, G. L. Wilson, C. Moratz and J. H. Kehrl (2002). "RGS13 regulates germinal center B lymphocytes responsiveness to CXC chemokine ligand (CXCL)12 and CXCL13." J Immunol **169**(5): 2507-2515.

Shi, J. Y., L. X. Yang, Z. C. Wang, L. Y. Wang, J. Zhou, X. Y. Wang, G. M. Shi, Z. B. Ding, A. W. Ke, Z. Dai, S. J. Qiu, Q. Q. Tang, Q. Gao and J. Fan (2015). "CC chemokine receptor-like 1 functions as a tumour suppressor by impairing CCR7-related chemotaxis in hepatocellular carcinoma." J Pathol **235**(4): 546-558.

Shinnakasu, R., T. Inoue, K. Kometani, S. Moriyama, Y. Adachi, M. Nakayama, Y. Takahashi, H. Fukuyama, T. Okada and T. Kurosaki (2016). "Regulated selection of germinal-center cells into the memory B cell compartment." Nat Immunol **17**(7): 861-869.

Siepmann, K., J. Skok, D. van Essen, M. Harnett and D. Gray (2001). "Rewiring of CD40 is necessary for delivery of rescue signals to B cells in germinal centres and subsequent entry into the memory pool." Immunology **102**(3): 263-272.

Smith, K. G., T. D. Hewitson, G. J. Nossal and D. M. Tarlinton (1996). "The phenotype and fate of the antibody-forming cells of the splenic foci." Eur J Immunol **26**(2): 444-448.

Spender, L. C. and G. J. Inman (2014). "Developments in Burkitt's lymphoma: novel cooperations in oncogenic MYC signaling." Cancer Manag Res **6**: 27-38.

Su, M. L., T. M. Chang, C. H. Chiang, H. C. Chang, M. F. Hou, W. S. Li and W. C. Hung (2014). "Inhibition of chemokine (C-C motif) receptor 7 sialylation suppresses CCL19-stimulated proliferation, invasion and anti-anoikis." PLoS One **9**(6): e98823.

Sweet, R. A., M. L. Ols, J. L. Cullen, A. V. Milam, H. Yagita and M. J. Shlomchik (2011). "Facultative role for T cells in extrafollicular Toll-like receptor-dependent autoreactive B-cell responses in vivo." Proc Natl Acad Sci U S A **108**(19): 7932-7937.

Sze, D. M., K. M. Toellner, C. Garcia de Vinuesa, D. R. Taylor and I. C. MacLennan (2000). "Intrinsic constraint on plasmablast growth and extrinsic limits of plasma cell survival." J Exp Med **192**(6): 813-821.

Takahashi, Y., H. Ohta and T. Takemori (2001). "Fas Is Required for Clonal Selection in Germinal Centers and the Subsequent Establishment of the Memory B Cell Repertoire." Immunity **14**(2): 181-192.

Takemori, T., T. Kaji, Y. Takahashi, M. Shimoda and K. Rajewsky (2014). "Generation of memory B cells inside and outside germinal centers." Eur J Immunol **44**(5): 1258-1264.

Tangye, S. G., D. T. Avery, E. K. Deenick and P. D. Hodgkin (2003). "Intrinsic differences in the proliferation of naive and memory human B cells as a mechanism for enhanced secondary immune responses." J Immunol **170**(2): 686-694.

Taylor, J. J., K. A. Pape and M. K. Jenkins (2012). "A germinal center-independent pathway generates unswitched memory B cells early in the primary response." J Exp Med **209**(3): 597-606.

Tellier, J. and A. Kallies (2014). "Finding a home for plasma cells--a niche to survive." Eur J Immunol **44**(8): 2243-2246.

Toellner, K. M. (2014). "Cognate interactions: extrafollicular IL-4 drives germinal-center reactions, a new role for an old cytokine." Eur J Immunol **44**(7): 1917-1920.

Toellner, K. M., A. Gulbranson-Judge, D. R. Taylor, D. M. Sze and I. C. MacLennan (1996). "Immunoglobulin switch transcript production in vivo related to the site and time of antigen-specific B cell activation." J Exp Med **183**(5): 2303-2312.

Toellner, K. M., S. A. Luther, D. M. Sze, R. K. Choy, D. R. Taylor, I. C. MacLennan and H. Acha-Orbea (1998). "T helper 1 (Th1) and Th2 characteristics start to develop during T cell priming and are associated with an immediate ability to induce immunoglobulin class switching." J Exp Med **187**(8): 1193-1204.

Tokoyoda, K., A. E. Hauser, T. Nakayama and A. Radbruch (2010). "Organization of immunological memory by bone marrow stroma." Nat Rev Immunol **10**(3): 193-200.

Tomayko, M. M., N. C. Steinel, S. M. Anderson and M. J. Shlomchik (2010). "Cutting edge: Hierarchy of maturity of murine memory B cell subsets." J Immunol **185**(12): 7146-7150.

Tomura, M., N. Yoshida, J. Tanaka, S. Karasawa, Y. Miwa, A. Miyawaki and O. Kanagawa (2008). "Monitoring cellular movement in vivo with photoconvertible fluorescence protein "Kaede" transgenic mice." Proc Natl Acad Sci U S A **105**(31): 10871-10876.

Townson, J. R. and R. J. Nibbs (2002). "Characterization of mouse CCX-CKR, a receptor for the lymphocyte-attracting chemokines TECK/mCCL25, SLC/mCCL21 and MIP-3beta/mCCL19: comparison to human CCX-CKR." Eur J Immunol **32**(5): 1230-1241.

Ulvmar, M. H., E. Hub and A. Rot (2011). "Atypical chemokine receptors." Exp Cell Res **317**(5): 556-568.

Ulvmar, M. H., K. Werth, A. Braun, P. Kelay, E. Hub, K. Eller, L. Chan, B. Lucas, I. Novitzky-Basso, K. Nakamura and T. Rulicke (2014). "The atypical chemokine receptor CCRL1 shapes functional CCL21 gradients in lymph nodes."

Vallespinos, M., D. Fernandez, L. Rodriguez, J. Alvaro-Blanco, E. Baena, M. Ortiz, D. Dukovska, D. Martinez, A. Rojas, M. R. Campanero and I. Moreno de Alboran (2011). "B Lymphocyte commitment program is driven by the proto-oncogene c-Myc." J Immunol **186**(12): 6726-6736.

van Ewijk, W. and P. Nieuwenhuis (1985). "Compartments, domains and migration pathways of lymphoid cells in the splenic pulp." Experientia **41**(2): 199-208.

Vander Lugt, B., N. J. Tubo, S. T. Nizza, M. Boes, B. Malissen, R. C. Fuhlbrigge, T. S. Kupper and J. J. Campbell (2013). "CCR7 plays no appreciable role in trafficking of central memory CD4 T cells to lymph nodes." J Immunol **191**(6): 3119-3127.

Vassileva, G., H. Soto, A. Zlotnik, H. Nakano, T. Kakiuchi, J. A. Hedrick and S. A. Lira (1999). "The reduced expression of 6Ckine in the plt mouse results from the deletion of one of two 6Ckine genes." J Exp Med **190**(8): 1183-1188.

Venkiteswaran, G., S. W. Lewellis, J. Wang, E. Reynolds, C. Nicholson and H. Knaut (2013). "Generation and dynamics of an endogenous, self-generated signaling gradient across a migrating tissue." Cell **155**(3): 674-687.

Victora, G. D., D. Dominguez-Sola, A. B. Holmes, S. Deroubaix, R. Dalla-Favera and M. C. Nussenzweig (2012). "Identification of human germinal center light and dark zone cells and their relationship to human B-cell lymphomas." Blood **120**(11): 2240-2248.

Victora, G. D. and M. C. Nussenzweig (2012). "Germinal centers." Annu Rev Immunol **30**: 429-457.

Victora, G. D., T. A. Schwickert, D. R. Fooksman, A. O. Kamphorst, M. Meyer-Hermann, M. L. Dustin and M. C. Nussenzweig (2010). "Germinal center dynamics revealed by multiphoton microscopy with a photoactivatable fluorescent reporter." Cell **143**(4): 592-605.

Vieira, P. and K. Rajewsky (1990). "Persistence of memory B cells in mice deprived of T cell help." Int Immunol **2**(6): 487-494.

Vinuesa, C. G. and P. P. Chang (2013). "Innate B cell helpers reveal novel types of antibody responses." Nat Immunol **14**(2): 119-126.

Voigt, I., S. A. Camacho, B. A. de Boer, M. Lipp, R. Forster and C. Berek (2000). "CXCR5-deficient mice develop functional germinal centers in the splenic T cell zone." Eur J Immunol **30**(2): 560-567.

von Andrian, U. H. and T. R. Mempel (2003). "Homing and cellular traffic in lymph nodes." Nat Rev Immunol **3**(11): 867-878.

Watts, A. O., F. Verkaar, M. M. van der Lee, C. A. Timmerman, M. Kuijer, J. van Offenbeek, L. H. van Lith, M. J. Smit, R. Leurs, G. J. Zaman and H. F. Vischer (2013). "beta-Arrestin recruitment and G protein signaling by the atypical human chemokine decoy receptor CCX-CKR." J Biol Chem **288**(10): 7169-7181.

Weisel, F. J., G. V. Zuccarino-Catania, M. Chikina and M. J. Shlomchik (2016). "A Temporal Switch in the Germinal Center Determines Differential Output of Memory B and Plasma Cells." Immunity **44**(1): 116-130.

Westermann, J., E. M. Ehlers, M. S. Exton, M. Kaiser and U. Bode (2001). "Migration of naive, effector and memory T cells: implications for the regulation of immune responses." Immunol Rev **184**: 20-37.

Willard-Mack, C. L. (2006). "Normal structure, function, and histology of lymph nodes." Toxicol Pathol **34**(5): 409-424.

Worbs, T., U. Bode, S. Yan, M. W. Hoffmann, G. Hintzen, G. Bernhardt, R. Forster and O. Pabst (2006). "Oral tolerance originates in the intestinal immune system and relies on antigen carriage by dendritic cells." J Exp Med **203**(3): 519-527.

Worbs, T., T. R. Mempel, J. Bolter, U. H. von Andrian and R. Forster (2007). "CCR7 ligands stimulate the intranodal motility of T lymphocytes in vivo." J Exp Med **204**(3): 489-495.

Wu, M., M. Arsura, R. E. Bellas, M. J. FitzGerald, H. Lee, S. L. Schauer, D. H. Sherr and G. E. Sonenshein (1996). "Inhibition of c-myc expression induces apoptosis of WEHI 231 murine B cells." Mol Cell Biol **16**(9): 5015-5025.

Yanagihara, S., E. Komura, J. Nagafune, H. Watarai and Y. Yamaguchi (1998). "EBI1/CCR7 is a new member of dendritic cell chemokine receptor that is up-regulated upon maturation." J Immunol **161**(6): 3096-3102.

Yates, J. L., R. Racine, K. M. McBride and G. M. Winslow (2013). "T cell-dependent IgM memory B cells generated during bacterial infection are required for IgG responses to antigen challenge." J Immunol **191**(3): 1240-1249.

Yoshida, R., T. Imai, K. Hieshima, J. Kusuda, M. Baba, M. Kitaura, M. Nishimura, M. Kakizaki, H. Nomiyama and O. Yoshie (1997). "Molecular cloning of a novel human CC chemokine EBI1-ligand chemokine that is a specific functional ligand for EBI1, CCR7." J Biol Chem **272**(21): 13803-13809.

Yoshida, R., M. Nagira, M. Kitaura, N. Imagawa, T. Imai and O. Yoshie (1998). "Secondary lymphoid-tissue chemokine is a functional ligand for the CC chemokine receptor CCR7." J Biol Chem **273**(12): 7118-7122.

Young, A. J., W. L. Marston and L. Dudler (2000). "Subset-specific regulation of the lymphatic exit of recirculating lymphocytes in vivo." J Immunol **165**(6): 3168-3174.

Zaballos, A., J. Gutierrez, R. Varona, C. Ardavin and G. Marquez (1999). "Cutting edge: identification of the orphan chemokine receptor GPR-9-6 as CCR9, the receptor for the chemokine TECK." J Immunol **162**(10): 5671-5675.

Zabel, F., D. Mohanan, J. Bessa, A. Link, A. Fettelschoss, P. Saudan, T. M. Kundig and M. F. Bachmann (2014). "Viral particles drive rapid differentiation of memory B cells into secondary plasma cells producing increased levels of antibodies." J Immunol **192**(12): 5499-5508.

Zhang, Y., L. Garcia-Ibanez and K. M. Toellner (2016). "Regulation of germinal center B-cell differentiation." Immunol Rev **270**(1): 8-19.

Zhang, Y., M. Meyer-Hermann, L. A. George, M. T. Figge, M. Khan, M. Goodall, S. P. Young, A. Reynolds, F. Falciani, A. Waisman, C. A. Notley, M. R. Ehrenstein, M.

Kosco-Vilbois and K. M. Toellner (2013). "Germinal center B cells govern their own fate via antibody feedback." J Exp Med **210**(3): 457-464.

Zhu, Y., W. Tang, Y. Liu, G. Wang, Z. Liang and L. Cui (2014). "CCX-CKR expression in colorectal cancer and patient survival." Int J Biol Markers **29**(1): e40-48.

Zlotnik, A. and O. Yoshie (2000). "Chemokines: a new classification system and their role in immunity." Immunity **12**(2): 121-127.

Zuccarino-Catania, G. V., S. Sadanand, F. J. Weisel, M. M. Tomayko, H. Meng, S. H. Kleinstein, K. L. Good-Jacobson and M. J. Shlomchik (2014). "CD80 and PD-L2 define functionally distinct memory B cell subsets that are independent of antibody isotype." Nat Immunol **15**(7): 631-637.